Mecanismos de muerte celular inducidos por nuevas terapias antitumorales

Cell death mechanisms induced by new anti-tumour therapies

TESIS DOCTORAL

Santiago Rello Varona

Unidad de Citología, Departamento de Biología

Facultad de Ciencias, Universidad Autónoma de Madrid

Memoria presentada por Santiago Rello Varona

para optar al grado de Doctor

por la Universidad Autónoma de Madrid.

Proyecto de Tesis dirigido por la

Dra. ÁNGELES VILLANUEVA OROQUIETA

Profesora Titular de Biología Celular

de la Universidad Autónoma de Madrid.

Madrid, 2007

La presente Tesis Doctoral ha sido posible gracias a la financiación otorgada por las siguientes Instituciones:

- MEC (PB98 017-C02-01)

Mecanismos de la muerte celular inducida por fotosensibilizadores con características fotofísicas adecuadas para la terapia del cáncer.

- MCYT (SAF 2002-04034-C02-01)

Identificación morfológica y molecular de los mecanismos de inactivación tumoral por nuevos agentes fotoquimioterapeúticos.

- NIH (grant CA 91027)

MEC (HI2004-0029)

Photothermal sensitization of biological systems: a novel therapeutic modality for tumours.

- CAM (GR/SAL/0213/2004)

Análisis comparativo de la eficacia para inactivar células tumorales mediante Terapia Fotodinámica con ALA y su derivado metilado Me-ALA.

- CAM (S-0505 MAT-0194)

Nanoestructuras magnéticas: Fabricación, propiedades y aplicaciones Biomédicas y Tecnológicas.

- MEC (CTQ2007-67763-C03-02/BQU)

Evaluación de la eficacia de fotosensibilizadores de nueva síntesis para inactivar células tumorales en cultivo: influencia de su vehiculización e identificación de los mecanismos de muerte celular.

The tragedies reside in you

The secret sights hide in you

The lonely nights divide you in two

All my blisters now revealed

In the darkness of my dreams

In the spaces in between us

But no bodies ever knew

Nobodys

No bodies felt like you

Nobodys

Love is suicide

Love is all

The Smashing Pumpkins "Bodies"

Agradecimientos

Hubo un tiempo en el que los estudiantes que habían conseguido *licencia docenti* se planteaban sus propias preguntas y se enfrascaban en sus propias investigaciones. En la actualidad globalizada, la Ciencia es una actividad burocrática en la que el "licenciado" no sólo no está autorizado a enseñar sino que, por lo general, tampoco está autorizado a plantearse preguntas. Debe plegarse, como "obrero del conocimiento", al plan de trabajo de un grupo de investigación dependiente de la voluntad financiera de los poderes (públicos o privados). Si esta Tesis Doctoral se ha permitido realizar alguna pregunta más allá de los objetivos del proyecto científico registrado ha sido en dura pugna con la actual costumbre. Si esas preguntas han quedado en vacío por no haber sido convenientemente contestadas, se deberá en exclusiva a la incapacidad de este doctorando.

Para mi Directora, **Dra. Ángeles Villanueva** y para sus compañeros en el grupo de investigación del que han salido los fondos económicos (**Dres. Magdalena Cañete y Juan Carlos Stockert**) mi profundo reconocimiento por los años pasados, los conocimientos adquiridos y las lecciones aprendidas en su compañía.

Un recuerdo agradecido a todo el **personal de la Unidad de Citología del Departamento de Biología de la UAM** que me han permitido compatibilizar mi labor investigadora con mi trabajo docente como Ayudante. De igual manera, esta Tesis no habría sido posible sin el trabajo de una serie de técnicos, fantásticos profesionales y mejores personas: **Miguel Ángel y Pilar** del Departamento de Biología; **Esperanza, Marta y Laura** de los microscopios de barrido de la UAM y del MNCN; **Sylvia y Lola** de los microscopios confocales del CNB y la UAM y un saludo también a las secretarias del Departamento de Biología que tantas veces me han aguantado.

Llegar a este punto, en la lluviosa mañana en la que escribo estas líneas, ha implicado un largo viaje. Un viaje que se hace en solitario, pero que se comparte con mucha gente que lo hace no sólo posible, sino que lo determina en los más pequeños detalles. A todos ellos quiero dedicar estas páginas.

En primer lugar a los que me hicieron ser. A mi **madre,** que me da su cariño y de la que me siento muy orgulloso por su carácter determinado y valiente. Ella me ha hecho ver el Madrid de antaño, convirtiendo el monstruo urbano en un espacio tranquilo donde respirar y pasear, una ciudad de la que no se puede estar muy lejos. A mi **padre,** que, con mucha serenidad de ánimo y un sentido práctico que siempre he admirado, nunca ha cejado en animarme para ir siempre hacia delante. Él es la tierra oscura y los árboles centenarios de Palazuelos, el amarillo de las aliagas y el verde de la hierba en época de setas.

Desde que nací estaban ellos, pero sobre todo estaban ellas: mis hermanas. Una relación de quiero y no puedo, de la que simplemente no podría prescindir ni por un segundo. Mi siempre admirada **Marta** ("la Megue"), que me señaló el camino de la Ciencia y a caminar con un pasito por delante. Y mi siempre envidiada **Cristi** ("mi hermana diabólica") que me enseña continuamente a sobrevivir en este alocado mundo aplicando un puntillo de picardía. Las dos están ahí (generalmente al otro lado del teléfono) cuando las necesito y eso es simplemente impagable. Vaya también un saludo a las personas que las acompañan en sus viajes vitales (**Pablo** como soporte informático, **y Javi** como vigía de las partes en inglés) y un muy especialmente querido recuerdo a mis pequeñas **Sofía** e **Inés** (que garantizan con su risa la continuidad de la familia).

Un beso también a toda la diáspora familiar: tío-abuelos, tíos y primos en diferentes grados que se distribuyen por Madrid y Sevilla. Ellos forman parte de lo que soy, y yo soy parte de ellos también.

Uno nace dentro de una familia y con el tiempo se desgaja para acabar formando su propia familia. En el mundo del siglo XXI eso empieza a convertirse en una utopía y la persona debe darse por dichosa si consigue, al menos, mantenerse cerca de sus amigos. Yo no sé si conseguiré formar una familia, aunque por ahora no pienso rendirme (un saludo a aquellas que desistieron), pero me siento muy dichoso en la vida al saberme arropado por un buen número de amigos (aunque, a veces, no pueda dedicarles el tiempo necesario, absorbido por el estrés y la melancolía). Todos ellos constituyen mi tribu y sin ellos yo no soy nada. Cada uno de ellos me aporta distintas vitaminas que necesito para sobrellevar el día a día. Los siguientes párrafos no pretenden describirles, sino simplemente aportar un boceto de lo que representan para mi.

Por empezar de alguna manera, están todos ellos con los que comparto el día a día entre estos muros de ladrillo. Sin su apoyo constante esta Tesis no se habría terminado. Vaya pues mi agradecimiento extremo para **Óscar** (un científico excepcional, un artista impactante y gran persona que, tal vez por ello, engrosa las amplias listas de "rebotados" del sistema) y **Jose** (que también salió "rebotada" pero en progresión geométrica, creciendo, y sin permitir nada que la aleje de sus objetivos). Ellos me han enseñado a hipotizar, a ser científico y no dar nada ni por creído ni mucho menos por demostrado. A **Alicia** que, a pesar de haber salido con éxito del mundo de la Ciencia para disfrutar de lo que una buena empresa puede hacer por ti, nunca nos ha olvidado y es la primera en insistir para que nos veamos. A **Paloma** y **Josama** por su compañía diaría, por darme esa "visión dorsal" tan necesaría para desenvolverme con éxito en la jungla académica. A **Vero**, porque sabe que la vida es mucho más que trabajo, porque un buen libro con buena música tras algo de ejercicio es mano de santo para un "templo" agrietado. A **Bea, Ana Casadó, Esther "Kukada", Ana Peropadre, Óscar "Mosquis", Conchi, Nargisse, Montse, Fernando, Rosario, Cristina, Raquel, Lidia, Cris** y toda la gente de bien que ha pasado por el laboratorio A-115, por el soporte que proporcionan con un simple rato de conversación banal o con una sincera mirada de complicidad, por hacer que un mal rato se difumine bajando a cafetería.

Los años de la carrera me depararon la suerte de hacer muchos amigos, y el doctorado la desgracia de no tener mucho tiempo que dedicarles. La verdad es que yo sé exactamente qué me aportan ellos, porqué les necesito tanto… lo que no sé es lo qué ven ellos en mí. Cuando me agobio en vez de recurrir a ellos, les dedico menos tiempo. Pero, cuando reaparezco, ellos simplemente están ahí, dejando claro que no los perderé nunca, que cuando lleguen tiempos mejores nos veremos más (pero que no me agobie mientras tanto). Y en ese mientras tanto, hay tres que me dan continuidad a base de comida semanal con terapia de grupo. **Inma**, la que siempre tiene una ilusión, un plan o un viaje en la recámara, la única persona que sigue la "literatura" científica cómo si fuese una novela de aventuras por entregas. **David**, el hombre de las ochocientas facetas, el permanentemente enamorado, el optimista insomne, el guerrero wu-shu, el que hace posible mezclar arte y ciencia, que hace poesía con la genética porque lleva la poesía en los genes. **María**, la nueva incorporación, la que muestra que el fuerte no es el que no tiene miedo sino el que se enfrenta a las mañanas llevando consigo sus miedos en el maletero.

Curiosamente a los otros nunca he conseguido juntarlos en un restaurante. **Marga** es la inconstancia caótica de la vida, la conciencia que anida en un fotón, una mariposa que pone un toque de color mientras revolotea, aparentemente sin una dirección clara, pero que se te acerca cuando necesitas algo de magia. **MariCarmen** es la búsqueda, es la amiga que te acoge cuando no sabes bien qué te pasa y cuando no quieres en realidad saberlo: ella busca las causas para que las respuestas salgan solas. **Miguel** es la inducción callada, el que siempre tiene la casa abierta y el güisqui en el baúl, el que te conoce con sólo mirarte, el que te da un consejo útil sin abrir la boca. **Roberto** es la pasión decidida, un huracán, el pensamiento sincero, la voluntad de actuar, es capaz de animarte por su sola cabezonería. **Guillermo** no cierra jamás la boca: siempre te hace ver que hay algo por lo que hay que reír a carcajada limpia (y, si puede ser, mientras se salta de pura felicidad). Y hay muchos más que han ido apareciendo con el tiempo, gentes a las que todavía estoy conociendo pero que ya me han recompensado con su afecto: **Modesto** (la amistad hecha institución)**, Gilda** (la alegría en la mirada)**, Mariano** (siempre disponible para unas cañas)**, Larre** (porque la juerga no apaga la sed de "culturilla")**, Javi** (la palabra adecuada en el momento justo)**, Ernesto** (el optimista irredento), **Chico** (la locura), **Luis, Ana, Nani …**

De entre todos mis amigos hay un grupo de “resistentes” que llevan ahí desde los tiempos del colegio y que todavía siguen habitando mi antiguo barrio (la hermosa y vacía Mirasierra). Ellos me sufren a muerte sin que yo muestre ninguna compasión, de igual manera que yo estoy siempre dispuesto a sufrirlos (haciendo honor a la célebre máxima de “Donde hay confianza, da asco”). **Manu** es la incongruencia por antonomasia: con un ego hipertrofiado y pendenciero hasta la desesperación, cambia de chip en nanosegundos para revelarse como un compañero pendiente y abierto a escuchar durante horas o días (todo lo que sea necesario para que los problemas se difuminen). Cuando crees que lo que deberías hacer es matarle y disolver el cadáver, te demuestra porqué es a él al primero que llamas. **Bea** es la alegría en el agobio: siempre estresada, siempre falta de tiempo pero decididamente obstinada en ser feliz. Puede costarte años conseguir que libere media hora para un paseo, pero no tarda ni tres segundos en hacer acto de presencia para elevarte el ánimo de golpe cuando todo lo demás falla. Y si no tiene tiempo, te resume el problema (tu problema) en diez palabras, te da la solución en dos berridos y te manda un beso y te cuelga antes de que puedas siquiera sentirte estupefacto. **Miren** no sabe decirme que no, y yo me aprovecho de ello con asiduidad, pero sabe como nadie demostrar que un largo camino se hace a base de pasos pequeños. Como recién llegada, parece mostrar menores síntomas de psicopatía que el resto y eso es muy refrescante. Con ella vino **Gorka** quien, a pesar del nombre falso, es todo un ejemplo de sentido común (cosa de la que yo suelo carecer), un valiente que cambió de país por amor, un compañero resistente contra la biodanza… al que vamos maleando con tranquilidad, poquito a poco. Un besazo también a **Ana María,** a **Paula,** a tantos otros…

Seguro que me estoy dejando a mucha gente, personas que van y vienen pero que saben cómo situarse cerca en todo momento. Como **Isora**, “princesa de Anaga”, mujer de dulce reflexionar, que atraviesa la hora de diferencia de improviso cuando más te apetece verla.

Soy una persona tremendamente complicada, lo que no quiere decir que sea compleja sino que soy incapaz de mostrarme simple. Parte de esto se puede explicar porque soy dos personas en una. Hasta ahora casi todo se ha referido al *Santi* urbano, madrileño por los cuatro costados: cines, museos, compras en Gran Vía y copas en Malasaña. Mi otra alma es *el Santi* de Palazuelos: observación de aves, recogida de setas, gambas con gabardina en el Alameda y botellones con los amigotes. Ése es el yo que decidió estudiar Biológicas mientras paseaba por el Prao y el Monte escuchando el canto de los pájaros. Ése es el yo que no sabe porqué trabajo en un laboratorio habiendo tanto campo por recorrer.

Ese otro yo también tiene la suerte de contar con un buen montón de amigos, que conviven agrupados en la peña El Callejón (como debe ser en una villa que cuenta con más metros de muralla que habitantes). Estos amigos apenas coinciden con el Santi urbano, es más, a muchos tal vez no habría conocido nunca si yo sólo fuese el Santi urbano. Son mis particulares extraterrestres, son la gente que me enseña a ver el mundo con otros ojos. Y para un científico, la posibilidad de contar con otros puntos de vista es una ventaja incomparable. Con el paso del tiempo, la población de la peña se va incrementando de manera que se hace imposible poner algo sobre cada uno (espero que me lo sepan perdonar: a cambio de una pancetada), pero esto no sería un “Agradecimientos” si no constaran. **David, Víctor y Diana** son, además de amigos, parte inseparable de mi herencia genética. Mis compañeras de viaje, caminos y actos culturales (me habría matado sin ellas estos dos años), **Sole y Sandra**, siempre dispuestas a esforzarse y a superar cualquier dificultad. **MaryPaz y Rubén**, “los Morales”, forman el centro del universo palazueleño (a fuerza de no faltar ni a una juerga). **Pablo** y **Héctor** que comparten conmigo el gusto por la cháchara. “Los Cuencos”: **Rubén “Dos”, Moisés y Alberto**, personas elevadas a categoría de mito rural por méritos propios. **Conchi, Paloma, Silvia, Emma, Róber, Carlos, Isaac, Edu y Óscar:** los mayores (casi en retirada pero con impactantes reapariciones). **Laura “Moi”, Nerea, Marta y Laura:** las chicas (dulzura sin cursilería). **Ramón, Jorge, Rafa, Rafita, Fernando, Ricardo, Javi y Álex:** los chicos (que valen para unas risas, hacer cemento o desesperarte en plan futbolístico). Y por último (¿por ahora?), los pequeños: **Iván, David “Niño Baturro”, Sergio, David “Júber”, Jaime, Álvaro, Samu y Arturo**.

La presente Tesi di dottorato è stata realizzata grazie alla possibilità offerta dal gentile ***Prof. Giulio Jori*** *dell'Università degli Studi di Padova, di arrivare lì a convivere ed imparare della sua saggezza. A lui il mio profondo riconoscimento.*

Il tempo a Padova mi ha fatto diventare trino (che non é divino) e così da allora ho tre anime: madrilena, castigliana e padovana. Di nuovo sono stato grandemente fortunato e ho dei grandissimi amici nelle paludi venete. Il mio ringraziamento va a ***Monica*** *e* ***Folco****, che (mentre si urlano come cane e gatto) si assicurano sempre che tutto vada benissimo quando sono là.*

Un ringraziamento va a tutti nel lab Jori ed anzi nel semipiano sesto nord: ***Stefania, Benedetta, Ivan, Betta, Lara, Chiara, Michela, Clara, Marina,*** *etc. Grazie a tutti i miei amici di Tencarola (che sono sempre pronti per uscire a "pasta e birra"):* ***David "Mighe", Andrea, Roberta, Claudia, Carlo, Claudio, Dario*** *etc. Ed a tutti gli* ***ospiti dalla Fondazione Casa Virgilio Ducceschi*** *per farmi viaggiare in tutto il mondo senza uscire dalla cucina.*

Direi tante cose su tutti quelli con cui ho condiviso i miei mesi a Padova!! Ma non sono mai riuscito ad acquistare un buono stile per scrivere nella lingua di Dante, non ho un vocabolario abbastanza ampio per tutte le cose che ho nel cuore. Semplicemente grazie!!

Aunque estás lejos, tus rayos brillan sobre la Tierra.

Aunque cualquiera sienta tu presencia, tus rayos son invisibles.

Ajenatón "Himno a Atón"

In this phial is caught the light of Eärendil's star.

It will shine still brighter when night is about you.

May it be a light to you in dark places, when all other lights go out.

JRR Tolkien "The Lord Of The Rings"

Índice

Abreviaturas

- A-549: línea celular establecida derivada de un carcinoma de pulmón humano.
- ACA: antígeno anti-centromérico.
- ADN: ácido desoxirribonucleico.
- AIF: factor inductor de la apoptosis.
- ALA: ácido aminolevulínico.
- ATP: trifosfato de adenosina.
- B78H1: línea celular establecida derivada de un melanoma amelanótico murino.
- Bak: proteína asesina homóloga y antagonista de Bcl-2.
- Bax: proteína X asociada a Bcl-2.
- Bcl-2: proteína 2 del linfoma de células B.
- Bcl-x_L: isoforma larga de la proteína parecida a Bcl-2 número 1.
- Beclin-1: proteína parecida a la miosina y superenrollada que interactúa con Bcl-2.
- BH3-only: proteínas promotoras de la apoptosis que contienen sólo el dominio de homología de la familia Bcl-2 (BH) número 3.
- Bid: proteína con el dominio agonista de muerte que interactúa con BH3.
- Bok: proteína asesina del ovario relacionada con Bcl-2.
- C32: línea celular establecida derivada de un melanoma amelanótico humano.
- C57BL/6: grupo de ratones generado en 1921 por Miss Abbie Lathrop mediante cruzamientos endogámicos sucesivos (de manera que presentan una mínima diferencia genotípica entre ellos).
- Caspasas: proteasas de cisteinil-aspartato.
- CC: ciclo celular.
- CF3: 5-(4-*N*-(*N*-2′,6′-dinitro-4′-trifluorometilfenil)-aminofenil)-10,15,20-tris(2,4,6-trimetoxifenil) porfirina.
- Chk2: proteína 2 del *checkpoint* del huso mitótico.

- DISC: complejo de señalización inductor de muerte.
- DPPC: dipalmitoil-fosfatidilcolina.
- ECM: matriz extracelular.
- EGF: factor de crecimiento epidérmico.
- EMEA: Agencia Europea de los Medicamentos.
- ER: retículo endoplásmico.
- Fas: receptor 6 de la superfamilia del factor necrosador de tumores.
- FasL: ligando de Fas.
- FLICE: caspasa 8.
- FLIPs: proteínas inhibidoras parecidas a FLICE.
- H1975: línea celular derivada de un carcinoma de pulmón de células "no-pequeñas"
- H-33258: fluorocromo Hoechst 33258.
- HaCaT: línea celular establecida derivada de queratinocitos humanos espontáneamente inmortalizados.
- HCT116: línea celular establecida derivada de un carcinoma de colon humano.
- HeLa: línea celular establecida derivada de un adenocarcinoma de cérvix del útero humano.
- HPV-18: virus 18 del papiloma humano.
- HT-1080: línea celular establecida derivada de un fibrosarcoma humano.
- IAPs: proteínas inhibidoras de la apoptosis.
- LD_X: dosis letal del x %.
- LED: diodo emisor de luz.
- MAPKs: quinasas de la proteína activada por mitógenos.
- MCF7: línea celular establecida derivada de un adenocarcinoma de mama humano.
- MTs: microtúbulos.
- NBD-C_6-ceramida: marcador vital específico del aparato de Golgi.
- NiNc: níquel (II)-octabutoxi-naftalocianina.
- $^1O_2$: oxígeno singlete.
- Omi/HtrA2: proteína requerida en elevadas temperaturas A2.

- p21: inhibidor de la quinasa dependiente de ciclina.
- p53: proteína supresora de tumores de 53 kDa.
- PARP: poli-(ADP-ribosa) polimerasa.
- PCD: muerte celular programada.
- PDT: terapia fotodinámica.
- PI: yoduro de propidio.
- PIDD: proteína inducida por p53 con dominio de muerte.
- PS: fotosensibilizador.
- PTT: terapia fototérmica.
- Puma: proteína moduladora de la apoptosis sobrerregulada por p53.
- ROS: especies reactivas de oxígeno.
- SEM: microscopía electrónica de barrido.
- Smac/DIABLO: segundo activador de las caspasas derivado de la mitocondria.
- tBid: fragmento polipeptídico producido por la acción de caspasa 8 sobre Bid.
- TEM: microscopía electrónica de trasmisión.
- Topo II: topoisomerasa II del ADN.
- VP-16: etopósido.
- ZnPc: ftalocianina de zinc (II).
- **Δ**T: intervalo de tiempo transcurrido desde la finalización del tratamiento.
- **Δ**T^{a}: incremento de temperatura.

RESUMEN

Resumen

La muerte celular es un conjunto de procesos evolutivamente conservados. Los diferentes mecanismos de muerte celular han sido recientemente clasificados en una reducida lista atendiendo a criterios morfológicos (los criterios bioquímicos no presentan suficiente poder de discriminación) por el *Comité de nomenclatura de muerte celular*. La apoptosis (muerte celular de tipo 1) es el más conocido de todos. El número de rutas bioquímicas implicadas en el proceso apoptótico hace muy difícil dilucidar si existe alguna más relevante que las otras, aunque las caspasas están consideradas como las principales moléculas efectoras (a pesar de la identificación de otros efectores). Actualmente no es posible determinar si la muerte de tipo 2 lo es siempre *por* autofagia o *con* autofagia. La importancia de la necrosis (tipo 3) está siendo evaluada de nuevo, tras haber sido tradicionalmente considerada un mero subproducto de células con insuficiente energía para completar la apoptosis. De entre los otros procesos de muerte propuestos, la catástrofe mitótica se destaca por vincular la inestabilidad genómica con la muerte celular y la resistencia (con implicaciones fundamentales en los procesos de oncogénesis y de terapia antitumoral). El cáncer es un proceso patológico debido a la pérdida de la homeostasis tisular. Los tumores evolucionan mediante la adquisición de una serie de propiedades como la resistencia a las señales de muerte celular y la sobrexpresión de factores de supervivencia, entre otros. El tumor se comporta como una comunidad ecológica entre las células del hospedador y las tumorales. La proteína p53 tiene un papel capital en la supresión tumoral como “guardiana” de la integridad del genoma: desde el control del ciclo celular al disparo de la apoptosis. La investigación en terapia antitumoral no ha dejado de avanzar en el último medio siglo, aunque la mejora en los sistemas de prevención y detección precoz sigue siendo prioritaria. La mayoría de los tratamientos antineoplásicos autorizados o en fase de aprobación están dirigidos contra la capacidad de división incrementada de las células cancerígenas: son tanto fármacos genotóxicos como anti-mitóticos con otras dianas específicas. En esta Tesis Doctoral mostramos resultados acerca de la inducción de muerte celular con dos novedosas aproximaciones terapéuticas (terapias Fotodinámica y Fototérmica) y un bien conocido agente quimioterapéutico en nuevas condiciones experimentales (la genotoxina etopósido). Además de conseguir altos niveles de inactivación celular (particularmente interesantes en el caso de la terapia Fototérmica), nuestros resultados relacionan el tipo de muerte desencadenado con la intensidad del daño generado, independientemente de la naturaleza del agente causante. La necrosis es la respuesta ante los daños más intensos y la catástrofe mitótica representa la frontera entre las condiciones subletales y la aparición de resistencias. Analizados morfológicamente, los tipos de muerte celular consisten en una serie de eventos que se desarrollan en secuencias equivalentes, independientemente del agente causante. Estas secuencias presentan diferencias en cuanto al tiempo de respuesta, debidas a las distintas rutas estimuladas por cada modalidad terapéutica. Proponemos una detallada serie de acontecimientos definitorios del proceso necrótico en cultivos adherentes comenzando con la pérdida de la barrera osmótica de la membrana plasmática (que se materializa en la formación de burbujas en la superficie celular). Cuando las burbujas se desprenden la membrana pierde físicamente su integridad. Los restos insolubles de la célula muerta permanecen en la superficie de cultivo conformando un “fantasma celular”. Nuestros resultados nos han permitido también corroborar que las salidas hacia muerte del proceso de catástrofe mitótica presentan marcadores definitorios de la apoptosis (tanto morfológicos como bioquímicos), con una diferencia en el tamaño de las células aneuploides, encuadrándola dentro de este tipo de muerte celular.

Abstract

Cell death is an evolutionary conserved process present in almost all the eukaryotic clades (both single-cell or multicellular). Scientists have classified the number of different cell death mechanisms into a few types according to morphological characters (as biochemical markers are inefficient to discriminate between them). Apoptosis (cell death type 1) is the best-known of them. A number of biochemical pathways are implied in the development of the apoptotic phenotype, making rather difficult to elucidate which of them is prominent. Caspases are considered the main effectors of apoptosis, but there are others apoptototic effectors as well as caspases exert functions other than apoptosis triggering. The knowledge about type 2 is really not enough to determinate even if there is a always a death *through* autophagy or merely *with* autophagy. Necrosis (type 3) was considered a “sub-product” of cells without enough ATP to complete apoptosis; but nowadays its role is being re-evaluated. Other cell death processes have been proposed through time. One of the most highlightened in the last few years is mitotic catastrophe, a process that links genomic instability, cell death triggering and resistance and connected with oncogenesis and anti-tumour therapy. Cancer is a pathological process due to the loss of proper tissue homeostasis, often by cell death dysfunction. Tumours evolve by the acquisition of a series of hallmarks in which the resistance to the orders of death triggering and the overexpression of survival factors are important milestones. In the host, tumours behave as ecosystem of evolutionary-related cancer subclones (maybe derived from tumour stem cell populations) and host’s cells. As genome’s integrity keeper, the tumour suppressor protein p53 have a quite import role in tumour progression, comprising both cell cycle control and cell death triggering. Anti-tumour therapy research is in constant growing since the last fifty years, but the main factors that have contributed to reduce cancer’s mortality rates are the improvements in prevention and in cancer early detection. The vast majority of approved anti-tumour agents are targeted against the increased capacity of cancer cells to enter in mitosis; they are mainly genotoxic but also other anti-mitotic agents. In this PhD Thesis we present results concerning cell death triggering with two novel non-genotoxic therapeutic approaches (Photodynamic and Photothermal therapies) and a well-known chemotherapeutic compound (the genotoxic agent etoposide) in new experimental conditions. Besides to obtain high cell inactivation records with those approaches (specially interesting in the pioneer Photothermal therapy); our results show that cell death types can be successfully related with the intensity of the damage caused, independently of the nature of the agent employed. Necrosis represents the response of the most intense injures and mitotic catastrophe is the mechanism triggered in sub-lethal conditions and behaves as an open gate to the arising of resistant clones. Cell death types, under morphological analysis, consist in series of events that develop in equivalent sequences but can diverge in the response times in a fashion linked to the precise nature of the death pathway stimulated by each agent. We propose a detailed sequence of milestones that define the necrotic process in adherent cell cultures. It starts with loss of the osmotic barrier of the plasma membrane, leading in the conformation of hyaline bubbles in cell surface. When the bubbles detach, the plasma membrane is physically disrupted. The insoluble remnants of the death cell remains attached to surface forming a “cell phantom”. Our results also confirms that the death exits present in the mitotic catastrophe sequence show both morphological and biochemical characters of apoptosis (with a difference in size in the aneuploid cells) allowing to a definitive classification of this process as an apoptotic subtype.

INTRODUCCIÓN

La muerte celular está implicada en gran número de procesos relevantes: en los seres vivos unicelulares regula su dinámica de poblaciones; en los seres pluricelulares rige el desarrollo embrionario y el devenir de la vida adulta de los organismos. En las poblaciones humanas, la muerte celular (o más concretamente las alteraciones de los procesos de muerte celular) está implicada en numerosas patologías. Pero, al mismo tiempo, la muerte celular contiene las respuestas a muchas de las incógnitas que debemos despejar para poder combatirlas.

Evolución de la muerte celular

¿Qué implica en términos de Biología Evolutiva la inevitabilidad de la muerte? Al no poderse anular la probabilidad de morir por accidente (que aumenta con el paso de los años de vida), no tiene ningún sentido seleccionar características que permitan incrementar la longevidad. La evolución ha tendido a mejorar la "calidad" de la vida, en términos de *fitness* reproductivo fundamentalmente, frente al incremento de la longevidad de las formas de vida (Klarsfeld y Revah, 2002).

Cell Death in Evolution

- Cell death is involved in several life processes from population dynamics in single-cell living forms until embryonic development in multicellulars.
- Death is inevitable, and evolution is moving towards increase juvenile fitness rather than improving longevity.
- All the main components of cell death signalisation and execution pathways are spread in every eukaryotic clade.
- Not only apoptosis but also other cell death types are being positively identified even in protists.

Se considera habitualmente que las poblaciones unicelulares (tanto eucariotas como procariotas) son inmortales gracias a su capacidad de división ilimitada. Sin embargo las poblaciones de organismos unicelulares acuáticos son capaces de reaccionar, ante condiciones desfavorables del medio ambiente en el que viven, reduciendo su densidad: las poblaciones emiten señales que, en algunos individuos, desencadenan procesos de "suicidio" celular equivalentes a la apoptosis de los pluricelulares (Huettenbrenner y col., 2003; Ameisen, 2004). De esta manera, la muerte de parte de la población, inducida por la otra parte, permite al conjunto sobrevivir ante condiciones cambiantes.

Casi todos los componentes principales de las rutas bioquímicas que regulan los procesos de muerte celular se encuentran **presentes en todos los clados eucariotas** (Segovia y col., 2003; Boyce y col., 2004; van Doorn y Woltering, 2005). Dicha conservación indicaría que nos encontramos ante un mecanismo universal, ligado a un antiguo origen y a una importante función, de carácter vital, que no admite grandes posibilidades de cambio (Ameisen, 2004).

Las proteínas no se diseñan sólo para ejecutar los programas de muerte celular sino que ejercen importantes papeles en el normal funcionamiento celular (con la posible excepción de las proteínas de la familia Bcl-2) (Garrido y Kroemer, 2004). Pero las razones de esta universalidad están lejos de ser claras, manteniéndose vivo el debate sobre si esta maquinaria ha podido distribuirse como consecuencia de procesos de transferencia horizontal de genes (Leist y Jäättelä, 2001a; Segovia y col., 2003; Boyce y col., 2004).

En términos evolutivos hay que ser especialmente conscientes de que no hay que emplear el el concepto de muerte celular como sinónimo de apoptosis. La apoptosis constituye el ejemplo más paradigmático de "una muerte al servicio de la vida" (Klarsfeld y Revah, 2002), pero no es la única. Los mecanismos de muerte celular no apoptóticos han sido objeto de una atención reducida durante varios años (Okada y Mak, 2004). La muerte celular en plantas parece corresponderse, por lo general, más con mecanismos autofágicos que apoptóticos (van Doorn y Woltering, 2005). Existen referencias acerca de la capacidad de ciertos unicelulares de "envejecer" mediante la acumulación en la célula "madre" de todos los complejos proteicos que dan muestras de agotamiento o mal funcionamiento (Ameisen, 2004). El grupo de Laporte y colaboradores ha publicado recientemente la existencia de muerte celular autofágica en el género *Dyctiostelium* y que, si dicha muerte por autofagia es inhibida, se desencadena un proceso de necrosis (Laporte y col., 2007).

Las distintas caras de la muerte

The Faces of Death

- Since its characterization, by Kerr, Wyllie & Currie in 1972, apoptosis has been considered as a fundamental process for the accurate embryonic development and physiological behaviour of the living forms.
- As researchers focused their efforts in this process (150,000 papers in the last 20 years) different types, mechanisms and classifications have been proposed for cell death, causing misunderstandings and nomenclature conflicts.
- Arising nomenclature consensus is increased around the proposals of the Nomenclature Committee on Cell Death of the prestigious journal *Cell Death and Differentiation*.
- The committee strongly recommend using morphological data as main characters to define cell death as, nowadays, biochemical probes have not accurate capability to discriminate cell death types.

La evidencia de la existencia de un tipo activo y "programado" de muerte celular, con especial implicación en los fenómenos de desarrollo embrionario, surgió con la ya clásica publicación de Kerr, Wyllie y Currie en 1972. En las últimas décadas, la muerte celular se ha convertido en una estrella de la investigación en Biología, con más de 150.000 publicaciones científicas en los últimos 20 años (Galluzzi y col., 2007). Todo este esfuerzo investigador se ha traducido en un elevadísimo conjunto de datos sobre las sofisticadas cascadas de señalización responsables del disparo apoptótico, así como la proposición de distintos tipos de muerte celular no apoptótica. Tal conjunto de datos no siempre se presenta de una manera coherente y la proliferación de mecanismos alternativos ha contribuido a generar una cierta controversia.

En 2005 la prestigiosa revista *Cell Death and Differentiation* reunió a una serie de especialistas en un **Comité de nomenclatura de muerte celular**. Las propuestas acordadas fueron publicadas, en la sección “Noticias y Comentarios” de dicha revista, como una serie de recomendaciones a autores, revisores y editores de revistas científicas acerca de la manera más correcta y precisa de referirse a los procesos de muerte celular. Asimismo, el comité analizaba las distintas denominaciones tradicionales de los procesos de muerte más conocidos y marcaba una clara distinción entre apoptosis, autofagia y necrosis-oncosis y todos los demás (considerados variantes de la apoptosis o procesos muy específicos de ciertos tejidos) (Kroemer y col., 2005).

A principios de 2007, miembros de dicho comité publicaron una nueva revisión, en la que analizan la muerte celular en base a cuatro criterios generales: **morfológicos**, **enzimáticos** (en función de la implicación o no de una serie de nucleasas y proteasas), **funcionales** (programada/accidental, fisiológica/patológica) e **inmunológicos** (inmunogénica o no inmunogénica). Con este análisis establecen una clasificación más acotada, basada en el <u>empleo de caracteres morfológicos claros y definitorios</u> para cada uno de los mecanismos de muerte propuestos, ya que los posibles marcadores bioquímicos no permiten siempre un nivel de discriminación suficiente (**ver Tabla I y Figura 1**) (Galluzzi y col., 2007).

Table I (from Galluzzi *et al.*, 2007) Morphological aspects of different modes of cell death

Cell death mode	Characteristic morphological aspects	Notes
Apoptosis (Type 1)	● Rounding up of the cell ● Reduction of cellular and nuclear volume (pyknosis) ● Retraction of pseudopodes ● Nuclear fragmentation (karyorrhexis) ● Little modification of cytoplasmic organelles ● Plasma membrane blebbing	‘Apoptosis’ is the original term introduced by Kerr *et al.* to define a cell death with specific morphological features.
Autophagy (Type 2)	● Lack of chromatin condensation ● Massive vacuolization of the cytoplasm (double-membraned autophagic vacuoles)	‘Autophagic cell death’ defines cell death occurring *with* autophagy, though it may misleadingly suggest a form of death occurring *through* autophagy.
Necrosis (oncosis) (Type 3)	● Cytoplasmic swelling ● Rupture of plasma membrane ● Swelling of cytoplasmic organelles ● Moderate chromatin condensation	‘Necrosis’ identifies, in a negative fashion, cell death lacking the features of apoptosis or autophagy, and usually appears as oncosis.
Mitotic catastrophe	● Micronucleation ● Multinucleation	‘Mitotic catastrophe’ refers to a cell death occurring during or shortly after a failed mitosis.

o La muerte celular tipo 1

La **apoptosis** fue definida de acuerdo a criterios exclusivamente morfológicos: el desprendimiento de los llamados cuerpos apoptóticos se relacionó metafóricamente con la caída de las hojas en otoño (Kerr y col., 1972). La apoptosis está así ligada a una serie muy clara de fenómenos morfológicos (**ver Tabla I**): redondeamiento celular, condensación nuclear, reducción de volumen celular, compartimentalización de la célula en cuerpos apoptóticos y fagocitosis de los mismos por las células vecinas (Lawen, 2003; Okada y Mak, 2004). Las investigaciones siguientes, desde que Shalka publicase en 1976 la relación entre la condensación nuclear con la fragmentación internucleosomal de los cromosomas (tal y como se revisa en Robertson y col., 2000), se centraron en desentrañar las rutas bioquímicas que subyacen a los fenotipos descritos. En los últimos años se ha avanzado mucho en la identificación de dichos complejos de señalización, llegándose a esquemas generales que muestran un elevado nivel de redundancia e interrelación entre las distintas señales (**ver Figura 2**).

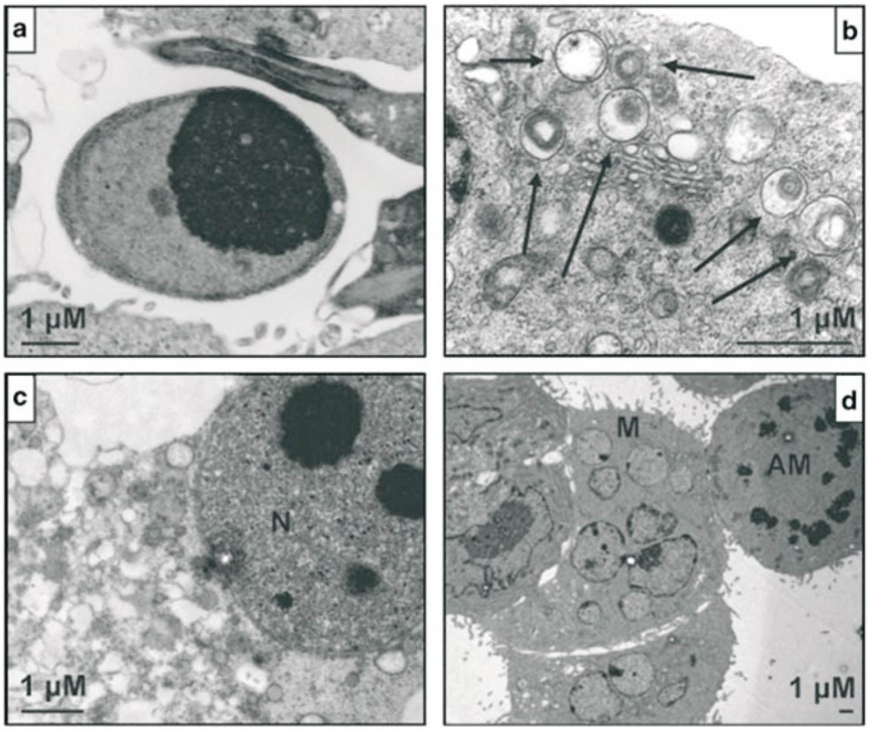

Figure 1 (from Galluzzi et al., 2007) Morphological ultrastructural features of cell death by transmission electron microscopy. (a) Human non-small cell lung cancer (H1975) cell undergoing apoptosis induced by the treatment with an inhibitor of the epidermal growth factor receptor (EGFR). Note the cell's shrinkage and complete nuclear condensation (pyknosis). (b) Human epithelial cancer (HeLa) cell treated with the endoplasmic reticulum toxin thapsigargin. The cell is succumbing from autophagic cell death, as witnessed by the massive accumulation of double-membraned cytoplasmic vacuoles (arrows) containing organelles or parts of the cytosol. (c) Human colon carcinoma (HCT116) cell responding to a necrotic stimulus. Whereas the nucleus (N) is still intact and presents clearly defined nucleoli, the plasma membrane and the cytoplasm are extensively dismantled. (d) HCT116 cells treated with substances that alter the microtubule dynamics (e.g. taxanes) exhibit the hallmarks of mitotic catastrophe, including aberrant multipolar mitotic figures (AM) as well as multinucleation (M) phenomena. Scale bars represent 1 μm.

Los procesos bioquímicos implicados en la apoptosis habitualmente se agrupan en dos rutas principales: la de los **receptores de muerte** (o extrínseca) y la **mitocondrial** (o intrínseca). Ambas rutas son mutuamente interdependientes y acaban convergiendo en sus pasos finales (**ver Figura 2**). La transducción de la señal apoptótica se da a través de un balanceo de inhibiciones (Huang, 2002), llegándose como resultado a un "punto de no retorno". La naturaleza de ese punto se considera comúnmente marcada por la activación de proteasas específicas de los procesos de muerte celular (Danial y Korsmeyer, 2004; Galluzzi y col., 2007).

Las **caspasas** (proteasas de cisteinil-aspartato) han sido consideradas generalmente como representativas de dicho punto en la apoptosis (Kumar, 2007; Rupinder y col., 2007). Son las enzimas que se encargan de degradar los sustratos clave, para que se desarrollen los caracteres morfológicos que definen a la apoptosis. Las caspasas son un grupo de proteasas muy conservadas evolutivamente tanto en su estructura como en su función (Danial y Korsmeyer, 2004). En seres humanos se han identificado 14 miembros de la familia de las caspasas y su actividad está regulada por sofisticados mecanismos que impiden su activación no deseada (Kumar, 2007). Estas proteasas son producidas como cimógenos inactivos y necesitan ser digeridas por ellas mismas, u otras caspasas, para su activación. Complejos multiproteicos se encargan de reclutar series de subunidades de procaspasa para permitir esa autocatálisis cruzada. Estos complejos son conocidos como **apoptosomas** (por la denominación del primero en caracterizarse: el apoptosoma para caspasa-9) (Adams y Cory, 2002; Bao y Shi, 2007).

Cell Death Type 1

- Apoptosis was defined only from morphological features: cell rounding, nuclear condensation, shrinkage and cell compartmentalisation followed by final phagocytosis by surrounding cells.
- Much literature is published about biochemical signalisation pathways of apoptosis but signalisation networks have such levels of redundancy and imbrications that make difficult to clarify the more relevant steps.
- There is a consensus for organising the signalisation network in two main routes: the death receptors and the mitochondrial pathways. Both finished in protease activation.
- Caspases are the main proteases involved in apoptosis, but there is also caspase-independent apoptosis and caspases have non-apoptotic functions.
- IAPs are the main regulators of active caspases. FLIPs (in the death receptors pathway) and the Bcl-2 family of proteins (in the mitochondrial pathway) regulate the activation of initiator pro-caspases (meanwhile apoptosome configuration).

El mecanismo activador de las caspasas se encuentra ya presente en organismos sencillos, como el nematodo *C. elegans*; en organismos más complejos, la activación de las caspasas se realiza en cascada y se ha producido la separación física de los procesos de activación regulada y de ejecución del programa apoptótico. De esta manera, las primeras en activarse (empleando el sistema de apoptosomas) son simplemente **iniciadoras** (caspasas 8 y 9 en las dos rutas principales, aunque se están identificando otras). La responsabilidad de la morfología apoptótica se debe al más reducido grupo de caspasas **efectoras** (entre las que destaca la caspasa 3) que son activadas por la catálisis de su correspondiente procaspasa por parte de las caspasas iniciadoras (Chang y Yang, 2000; Kumar, 2007).

La activación de las caspasas se debe a juegos de interacciones de inhibición con reguladores específicos, que afectan a todas las rutas de señalización. La familia de las **IAPs** (*Inhibitor of apoptosis proteins*) se encargan de la inhibición directa de las caspasas activas gracias a dominios de interacción específicos (Deveraux y Reed, 1999; Schimmer, 2004). Las IAPs, en interacción con otras proteínas, son las máximas reguladoras de la apoptosis en organismos como *Drosophila melanogaster*, por encima de otros sistemas (Danial y Korsmeyer, 2004). Las **FLIPs** (*FLICE-like inhibitory proteins*) son las encargadas de controlar la activación de la ruta de los receptores de muerte. Son proteínas estructuralmente muy similares a la caspasa 8 (pero sin capacidad catalítica) y compiten con ella en la unión al centro activador (DISC, *Death-inducing signalling complex*) que conforman los receptores y proteínas adaptadoras (Fulda y Debatin, 2004). Por último, la **familia de proteínas Bcl-2** (*B-cell lymphoma protein 2*) ha sido la que más interés ha recibido por corresponderse al mecanismo regulatorio descrito primariamente en nemátodos (Festjens y col., 2004; H. Kim y col., 2006). El resultado del desplazamiento del equilibrio de las proteínas Bcl-2 hacia la apoptosis es la liberación de proteínas solubles del espacio intermembranal (citocromo c, Smac/DIABLO, Omi/HtrA2, AIF o endonucleasa G) que son las encargadas de la activación de las caspasas, la inhibición de las IAPs o son efectores directos de muerte (Festjens y col., 2004; Garrido y Kroemer, 2004; Garrido y col., 2006).

Las proteínas de la familia Bcl-2 poseen funciones tanto anti como proapoptóticas. Se caracterizan por una serie de dominios conservados, conocidos como BH, de los que se han descrito cuatro variantes. Los miembros antiapoptóticos (Bcl-2, Bcl-x_L etc.) poseen los cuatro dominios. Los proapotóticos del tipo Bax (*Bcl-2-associated X protein*): Bax, Bak y Bok, sólo tienen los tres primeros. Un último subgrupo lo forman los miembros proapoptóticos que sólo poseen el dominio BH3 (*BH3-only*): Bid, Puma, etc. Las proteínas *BH3-only* actúan cómo sensores de distintas vías de señalización y las proapoptóticas del tipo Bax son los ejecutores de la orden de muerte. La actividad de las proteínas *BH3-only* se mantiene bajo control por toda

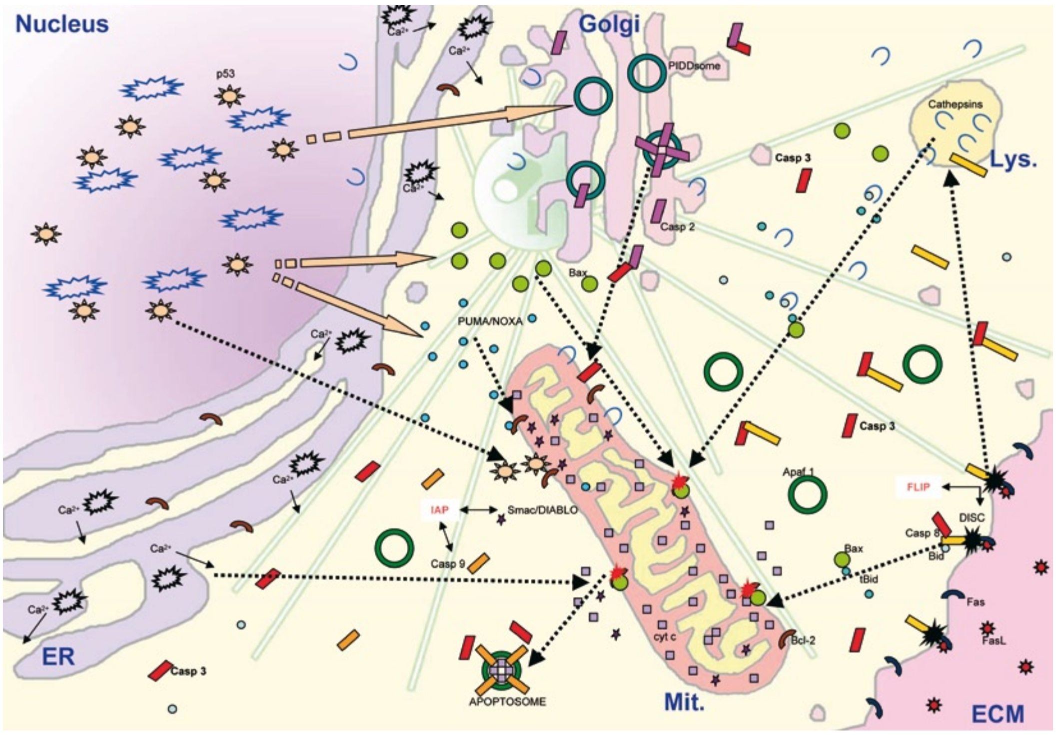

Figure 2 Schematic overview of some of the main pathways for caspase activation and apoptosis triggering. The death receptors pathway is based in Extra-Cellular Matrix (ECM) signals recognition by specific receptors (like the pair FasL and Fas). Activation of receptors leads on DISC complex formation and Caspase 8 recruitment (the process could be inhibited by FLIPs). The process links with the mitochondrial pathway by Bax activation due to tBid activity (tBid is produced by cleavage of Bid from Casp. 8). Pro-apoptotic activity of Bax leads in anti-apoptotic Bcl-2 inhibition and mitochondrial membranes permeabilization for cytochrome c and other proteins. Cytochrome c promotes Apoptosome recruitment and activation of Caspase 9. Both Casp. 8 and Casp. 9 can activate effector Caspase 3 (responsible of apoptotic phenotype). Smac/DIABLO in the cytosol blocks the IAP inhibition of caspases. Mitochondrial pathway can be stimulated from the nucleus after injures, by p53 activity (both promoting pro-apoptotic Puma and Bax or meanwhile translocation and direct inhibition of Bcl-2). p53 also promotes Caspase 2 activation in the Golgi apparatus by PIDDsome formation. Lysosomes and the Endoplasmic Reticulum (ER) can also trigger apoptosis upon stimulation by cathepsin liberation or Ca^{2+} signalling. Note that the above representation only includes few of the described pathways and links that lead in apoptosis. The figure neither includes the described molecular crosslinks among the pathways that are active in type 2 (autophagic) death and those represented.

una serie de mecanismos, tanto transcripcionales como post-transcripcionales, y la ejecución de la orden proapoptótica se hace mediante un sistema jerarquizado de regulación entre las distintas subfamilias de las Bcl-2 (Borner, 2003; Willis y Adams, 2005; H. Kim y col., 2006).

A medida que el tiempo pasa, este esquema se sofistica y se complica más y más (**ver Figura 2**), incluyendo: el **papel protector de la integridad genómica de p53** (Johnstone y col., 2002; Rozan y El-Deiry, 2007), que la apoptosis puede ser **iniciada por otros orgánulos subcelulares** (Ferri y Kroemer, 2001), que la **caspasa 2** funciona como una verdadera caspasa iniciadora (con su propio apoptosoma) de regulación incierta (Bao y Shi, 2007), la inducción de la apoptosis mediante **rutas más genéricas como la de las MAPKs** (Almeida y col., 2004), o que se puede tener **apoptosis sin la concurrencia de las caspasas** (Leist y Jäättelä, 2001b; Kim y col., 2005).

Este último punto es el que más polémica científica sigue suscitando. Las caspasas no son las únicas responsables de la aparición del fenotipo apoptótico (en especial de la fragmentación cromatínica a través de la liberación de endonucleasas), sino que otras proteínas liberadas del espacio intermembrana de la mitocondria (como el *Apoptosis inducing factor*, AIF) pueden inducir la fragmentación nuclear independientemente de las caspasas (Robertson y col., 2000). De esta manera, ciertos investigadores han puesto en entredicho a las caspasas como "punto de no retorno" y han propuesto, en su lugar, a la pérdida de la integridad de la membrana mitocondrial (Kim y col., 2005). Otros investigadores han defendido que la participación de las caspasas debe ser considerada cómo un carácter diagnóstico de la apoptosis (definiendo nuevos modelos de muerte para los casos en los que no participan las caspasas) (Bröker y col., 2005). Contra ambas opiniones se ha situado el comité de *Cell Death and Differentiation* (Kroemer y col., 2005). En su revisión de este mismo año, el grupo dirigido por Kroemer ha definido dicho "punto de no retorno" (aunque no le guste el término) como de activación de proteasas en general (incluyendo así a catepsinas lisosomales etc.), insistiendo siempre en la aplicación de criterios morfológicos, mientras las rutas bioquímicas no esten completamente esclarecidas (Galluzzi y col., 2007).

La apoptosis puede, por tanto, ser ejecutada por efectores que dependen o no de la activación de las caspasas. Asimismo, las caspasas pueden activarse en numerosos ejemplos de procesos no relacionados con la muerte celular: diferenciación, activación, proliferación y citoprotección (Danial y Korsmeyer, 2004). Funciones importantes en procesos vitales del metabolismo también se han descrito para otros efectores de la apoptosis (endonucleasa G u Omi/HtrA2) (Garrido y Kroemer, 2004).

o La muerte celular tipo 2

Cell Death Type 2
- Autophagy could lead in cell death in some occasions.
- There is no consensus about type 2 is a death "with" or "through" autophagy.
- Morphologically, cell death type 2 presents several cell vacuolisation joined with delayed or absent chromatin condensation.
- Autophagy also can act as an anti-apoptotic process isolating and degrading apoptotically activated mitochondria.

La **autofagia** es un proceso celular que, de manera normal y regular, se encarga de la remodelación del citoplasma celular con la remoción de orgánulos o grandes complejos multiproteicos en la célula (de forma complementaria al funcionamiento de los proteasomas). Los procesos de autofagia están atrayendo un creciente interés por su vinculación con los mecanismos de inmunidad innata, tumorigénesis y terapia anticancerígena (Klionsky, 2007).

Sin embargo, a gran escala, la autofagia puede acabar "autodigiriendo" a la propia célula (**ver Figura 1**) (Okada y Mak, 2004; Gozuacik y Kimchi, 2007). Pero aún no está cerrado el debate sobre si la muerte celular de tipo 2 es verdaderamente una muerte "por" autofagia o una muerte "con" autofagia (Galluzzi y col., 2007). En este sentido, la autofagia está siendo reinterpretada en la actualidad, más como un mecanismo de resistencia a la muerte apoptótica (en la que se retirarían mitocondrias dañadas y/o que hubiesen sufrido la pérdida de la integridad de membrana por activación de la familia Bcl-2) (Gozuacik y Kimchi, 2007; Klionsky, 2007).

Morfológicamente, la autofagia se caracteriza por la masiva vacuolización del citoplasma y una falta de condensación cromatínica (Gozuacik y Kimchi, 2007). A nivel bioquímico, la autofagia se considera dependiente de miembros antiapoptóticos de las Bcl-2, con localización en las membranas de retículo endoplásmico que regularían la actividad del principal producto proteico identificado hasta el momento: Beclin-1 (Edinger y Thompson, 2003; Kim y col., 2005).

Diversos estímulos se han identificado para el desarrollo de la muerte celular tipo 2, pero todos ellos inciden en el estrés del retículo endoplásmico (ER): acumulación de proteínas defectuosas, especies reactivas de oxígeno etc. (Edinger y Thompson, 2003; Liu y Lenardo, 2007). Asimismo se considera que el tipo 2 sería el mayoritario al referirnos a la muerte celular en plantas (van Doorn y Woltering, 2005). Las últimas revisiones parecen indicar que podría haber algún tipo de diferencia metabólica entre una autofagia "pro-supervivencia" y otra "pro-muerte", pero el nivel de imbricación de estas dos posibles rutas y sus numerosos puntos de relación con las rutas apoptóticas lo hacen muy difícil de comprobar (Galluzzi y col., 2007; Gozuacik y Kimchi, 2007).

- La muerte celular tipo 3

Cell Death Type 3

- Necrosis was traditionally considered as a simply product of cells with not enough energy to complete the apoptotic program, causing nomenclature controversy.
- Nowadays is considered as cell death type with its own morphological features, compressing cellular swelling (oncosis) and loss of plasma membrane integrity.

El éxito investigador de la apoptosis hizo minusvalorar durante años el concepto clásico de **necrosis** como forma de muerte celular. Tradicionalmente, la necrosis ha sido considerada un mero subproducto de células con insuficiente energía para completar el proceso apoptótico (Desagher y Martinou, 2000; Nieminen, 2003).

Se ha generado ambigüedad terminológica al identificarse la necrosis con la pérdida de la integridad de la membrana (convirtiendo al término en sinónimo de muerte), de manera que las células apoptóticas acababan “necrosando” (Darzynkiewicz y col., 1997). Actualmente se considera que esta forma de muerte típicamente accidental no es tan simple como se pretendía y la secuencia de acontecimientos que se desarrollan en una célula en necrosis puede ser de gran importancia en ciertos procesos patológicos (Nieminen, 2003; Okada y Mak, 2004; Laporte y col., 2007). La necrosis presenta sus propias características morfológicas (como la oncosis o hinchamiento y la moderada condensación cromatínica, **ver Tabla I**) y, recientemente, se han propuesto candidatos a marcadores moleculares de este proceso (Galluzzi y col., 2007).

- ¿Otros tipos de muerte celular?

Other types of cell death?

- The controversial relationships among Programmed Cell Death, Accidental Cell Death, Apoptosis and Necrosis must be overcome as PCD could develop with the characteristics of the three types (meaning also that necrosis could occur in a programmed fashion).
- So-called mitotic catastrophe represents a process in which cell death occurs after several dysfunctions of the mitotic process (with the implication of proteins like p53, Chk2, p21 and caspase 2).
- As related with cell division, mitotic catastrophe has pointed researchers attention due to its possible links with both resistance and oncogenesis.
- Cellular senescence represents a process of complete avoidance of the entry into mitosis (reproductive death) without cellular death and degradation.

La clarificación de la nomenclatura ha permitido cerrar debates semánticos, como el que existía entre los términos apoptosis y muerte celular programada (PCD por *Programmed Cell Death*). Dichos términos no se consideran antagónicos al tener en cuenta que las características citológicas de la apoptosis se desarrollan igual, independientemente de si el programa se activa en respuesta a morfógenos durante el desarrollo o si se desencadena ante un fallo de índole interno (Lawen, 2003). Atendiendo a las últimas investigaciones tampoco han de ser considerados sinónimos, ya que la PCD se puede manifestar tanto como una muerte de tipo 1 como de tipo 2, e incluso se ha determinado PCD por necrosis (rompiendo con ello la sinonimia entre necrosis y muerte accidental) (Edinger y Thompson, 2004; Galluzzi y col., 2007).

El Comité de nomenclatura de muerte celular no se mostró partidario de considerar a la **catástrofe mitótica** merecedora de la denominación “muerte celular de tipo 4”, pero el grupo de Kroemer sí la incluye a la misma altura que los otros tres tipos anteriores en su revisión de este año (**ver Tabla I**) (Galluzzi y col., 2007). La catástrofe mitótica constituye una serie de procesos en los que la muerte celular se vincula estrechamente al proceso de división celular (Erenpreisa y Cragg, 2001). Se desencadena tras graves fallos en el proceso de división, relacionados con paradas en metafase, que hacen saltar los complejos proteicos del punto de control (*checkpoint*) del huso mitótico (que monitoriza el correcto anclaje de los cromosomas a los microtúbulos y su congregación en la placa metafásica) (Castedo y col., 2002; Sullivan y Morgan, 2007).

La catástrofe mitótica tiene claros puntos en común con la apoptosis, tanto en su desarrollo como en su regulación (Erenpreisa y col., 2000; Chen y col., 2003; Castedo y col., 2006). Pero a nivel experimental persiste cierta controversia sobre la caracterización final del tipo de muerte celular, debido a que en ciertos modelos se han descrito fenómenos distintos a la apoptosis (Michalakis y col., 2005; Mansilla y col., 2006).

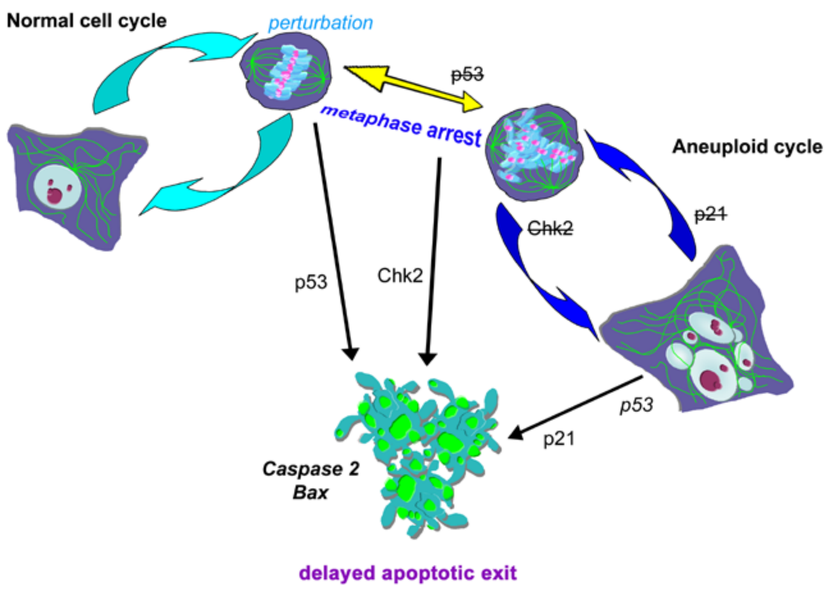

Figure 3 The process of mitotic catastrophe includes various end points depending on the activity of the different checkpoints involved. p53 dysfunction is required for metaphase arrest after a serious perturbation of the normal behaviour of the cell cycle (CC) process (p53 activity leads in CC arrest and apoptosis prior to enter into mitosis). Metaphase arrest could directly link to cell death upon the spindle checkpoint activation (controlled by the Chk2 protein). If the cell can avoid the spindle checkpoint regulation it will suffer restitution to an aneuploid/tetraploid interphase by mitotic slippage. In aneuploid G1 period, tumour suppressor p21 can became active (depending or not on p53 activity) and trigger a last exit to death. If p21 checkpoint doesn’t become active properly, the cell will start an aneuploid cycle.

Los fenómenos de catástrofe mitótica se deben a graves alteraciones en las rutas de señalización que normalmente disparan la apoptosis en la interfase (comúnmente vinculados al *checkpoint* de daño genético o de G2) permitiendo la entrada en mitosis (Vogel y col., 2007). Diversas familias proteicas se encuentran implicadas en los procesos de finalización de la mitosis y de inducción de la catástrofe mitótica: quinasas dependientes de ciclina, el factor promotor de la anafase, el complejo del *checkpoint* del huso mitótico, los supresores de tumores p21 y p53, la IAP survivina, la familia Bcl-2 y la caspasa 2 (Castedo y col., 2004; Castedo y col., 2006; Sullivan y Morgan, 2007).

La regulación bioquímica está todavía siendo investigada, pero ya tenemos información suficiente para señalar los que parecen ser puntos clave (**ver Figura 3**). Los procesos de catástrofe mitótica se inician con la aparición de importantes alteraciones (sea a nivel del material genético o del huso mitótico) que impiden una correcta mitosis (Castedo y col., 2004). Si los mecanismos de control (generalmente gobernados por la activación de p53) no funcionan adecuadamente, estas células desreguladas progresan hasta metafase donde el *checkpoint* del huso mitótico (independiente de p53) se pone en marcha y regula la activación de la caspasa 2 a través de la proteína Chk2 (Castedo y col., 2004; Kastan y Bartek, 2004). Pero la célula puede, en ocasiones, superar este punto tras una salida "en falso" de la mitosis (restitución) hacia una interfase aneuploide (Erenpreisa y Cragg, 2001; Castedo y col., 2004). En este instante se desencadena la segunda "salida" hacia la muerte celular (generalmente con características apoptóticas aunque también se ha visto senescencia) a través de una ruta en la que p21 (relacionada con p53) ejerce un papel fundamental (Andreassen y col., 2001; Castedo y col., 2002; Chen y col., 2003).

La catástrofe mitótica permite sobrevivir un tiempo crucial a células que portan graves daños, capacitándolas asimismo a entrar en mitosis; confiere, por tanto, una oportunidad a la aparición de mecanismos de resistencia (Erenpreisa y col., 2005).

En el extremo contrario se encontraría la llamada **senescencia**, que queda fuera de la clasificación de 2005 del panel de expertos de *Cell Death and Differentiation*. Por senescencia se conoce al fenómeno por el que una célula sufre una "muerte reproductiva", dejando de dividirse en respuesta a algún tipo de daño (Johnstone y col., 2002; Okada y Mak, 2004). La distinción entre los términos senescencia y diferenciación celular (que se emplea en Biología del Desarrollo) es meramente funcional, ya que, en la práctica, las dos hacen referencia a un mismo estado fisiológico. El término **quiescencia**, por el contrario, hace referencia a un estado de muerte reproductiva (parada en G0/G1) que es meramente transitorio (Aguirre-Ghiso, 2007). Las células senescentes siguen estado metabólicamente activas, pero tienen completamente abolida la posibilidad de entrar en mitosis (por lo que el riesgo de resistencias es más reducido) mediante mecanismos en los que intervendría p53 (Rozan y El-Deiry, 2007).

En resumen, la muerte celular depende de la naturaleza y de la intensidad del estrés que sufra la célula. El paradigma apoptosis-necrosis es demasiado simple para abarcar el amplio espectro de posibilidades de eliminación de células.

El cáncer

La integridad de los tejidos en los seres pluricelulares se basa en un delicado equilibrio entre las células que se dividen, las que se diferencian y las que mueren (**homeostasis tisular**). El conjunto de patologías que designamos con el nombre de **cáncer** constituyen un ejemplo paradigmático de defectos en la fina regulación que sostiene los tejidos (Greaves, 2002). Los principales modelos de cáncer aparecen en tejidos con una elevada tasa de recambio celular, en los que cualquier desviación del correcto equilibrio genera una patología (Eccles y Welch, 2007). El cáncer es la consecuencia indeseada de la apuesta de las formas de vida por el vigor reproductivo, sin preocuparse por los fallos que a largo plazo inducen dichas apuestas (Klarsfeld y Revah, 2002).

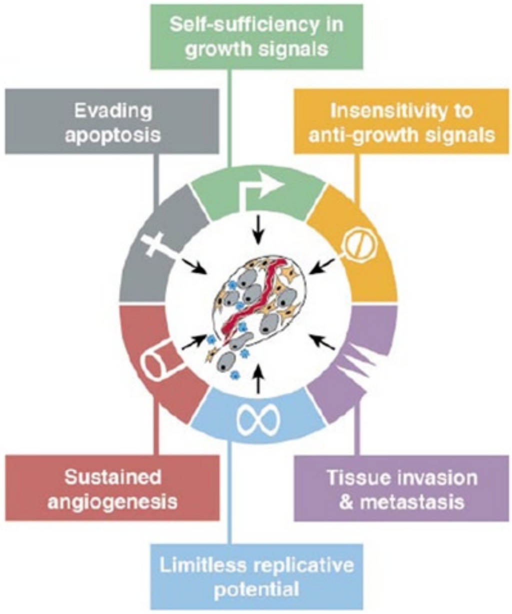

Figure 4 (from Hanahan and Weinberg, 2000) Acquired capabilities of cancer. Most, if not all, cancers have acquired the same set of functional capabilities during their development, albeit through various mechanistic strategies.

Las causas últimas de la progresión tumoral parecen residir en la existencia de un llamado **fenotipo mutador** derivado y favorecedor de la conocida como **inestabilidad genómica** (Greaves, 2002; Merlo y col., 2006). Esta noción de la progresión tumoral se ha desarrollado a través de la propuesta del llamado "póquer de ases": el tumor se desarrolla a través de una secuencia de subsiguientes mutaciones y reemplazos clonales (establecida en la ya clásica revisión de Hanahan y Weinberg, 2000). Estos "sellos del cáncer", desde la simple inmortalización hasta la metástasis, presentan cada vez una mayor agresividad (**ver Figura 4**) (Hanahan y Weinberg, 2000; Varmus, 2006). Este modelo se ha refinado mucho hasta la actualidad, mediante el empleo de herramientas informáticas para monitorizar los cambios producidos al variar distintos parámetros tisulares (Anderson y col., 2006).

Cancer

- Cancer is one of the most evident pathologies related with deficiencies in the normal cell death behaviour.
- It has been traditionally considered that tumour progression depends on the progressive acquisition of a series of properties (the hallmarks of cancer) including the insensibility to cell death stimulus.
- The so-called genomic instability by which a sub-population of clones develop the mutator phenotype is considered to allow cells to evolve into a tumour.
- Cancer stem cells could be the responsible for the resistance of tumours to therapy due to their low mitotic rate.
- Recent researches highlight the importance of considering tumours as a dynamic system of different sub-populations with specialised niches that interact between them and with the host, as an ecosystem, evolving continuously. This point of view has important consequences in order to programme the strategy to fight against tumours, as therapy could enhance cancer evolution.

El papel de la inestabilidad genómica como origen último del proceso tumoral presenta todavía algunos detractores, que defienden todavía el papel de la mutación azarosa en ciertos modelos (Sieber y col., 2003). Asimismo, el verdadero valor de la aneuploidía, como motor de la tumorigénesis *per se*, está aún evaluándose (Baker y col., 2005). Conexiones entre la acumulación de proteínas defectuosas (por fallos en la proteolisis o en las rutas autofágicas) y la progresión tumoral han sido igualmente señaladas, pero la evidencia es aún insuficiente para hacer conexiones causales precisas entre este fenómeno y la tumorigénesis (Edinger y Thompson, 2003). Una reciente publicación, que analiza un modelo de inestabilización genómica (mediante un proceso de aneuploidización sin riesgo de aparición de mutaciones adicionales), muestra una mayor resistencia al desarrollo de cierto tipo de tumores en ratones, aunque también se observe una buena correlación con la inducción de otros (Weaver y col., 2007).

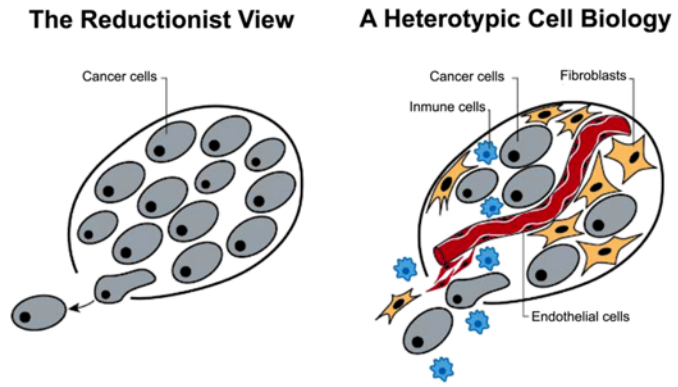

Figure 5 (from Hanahan and Weinberg, 2000) Tumours as complex tissues. The field of cancer research has largely been guided by a reductionist focus on cancer cells and the genes within them (left panel)—a focus that has produced an extraordinary body of knowledge. Looking forward in time, important new inroads will come from regarding tumours as complex tissues in which mutant cancer cells have conscripted and subverted normal cell types to serve as active collaborators in their neoplasic agenda (right panel). The interactions between the genetically altered malignant cells and these supporting co-conspirators will prove critical to understanding cancer pathogenesis and to the development of novel, effective therapies.

Lo que entendemos como **tumor** es un heterogéneo conjunto de subclones relacionados evolutivamente entre sí que comparten y compiten por el espacio y los recursos (de manera que llega a darse una cierta especialización de nicho) y que conviven con células sanas del hospedador (**ver Figura 5**) (Hanahan y Weinberg, 2000). El cáncer se comporta en ocasiones como un organismo patógeno, pero la visión más adecuada es entenderlo como toda una comunidad biológica con sus propias relaciones ecológicas internas (Merlo y col., 2006). Ciertos tumores, al menos, poseen una subpoblación de **células madre tumorales**: de larga vida, bajo índice de proliferación (quiescentes) y gran capacidad de resistencia a la terapia (Varmus, 2006; Aguirre-Ghiso, 2007; Eccles y Welch, 2007). Los subclones tumorales reclutan, por medio de señalizaciones específicas, ciertos tipos de células normales del organismo (preferentemente las relacionadas con la vascularización del tumor) (Hanahan y Weinberg, 2000; Merlo y col., 2006). La falta de recursos, la depredación a cargo del sistema inmunitario, la interrelación con el entorno, la metástasis y la terapia antitumoral constituyen las presiones selectivas que encauzan la continua evolución del tumor (Perona y Sánchez-Pérez, 2004; Merlo y col., 2006; Eccles y Welch, 2007).

Todos estos procesos condicionan el desarrollo histológico del cáncer (Merlo y col., 2006). Desde la célula tumoral originaria, tal vez una célula madre tumoral, los distintos subclones van creciendo dentro del tejido huésped a medida que se van verificando la adquisición de las distintas propiedades del cáncer (Hanahan y Weinberg, 2000). El crecimiento de un tumor es descontrolado y sólo la falta de nutrientes lo interfiere; de manera que el número de células observado es siempre una infrarrepresentación de las producidas, generándose en el interior de los tumores sólidos un área de elevada mortalidad celular (Hanahan y Weinberg, 2000; Merlo y col., 2006). La capacidad de reclutar células sanas del entorno, que quedan al servicio del tumor, es un factor esencial de la naturaleza de la progresión tumoral; un entorno permisivo es una característica común en los cánceres de peor prognosis (Hanahan y Weinberg, 2000; Eccles y Welch, 2007). Dentro de este proceso hay que destacar la capacidad angiogénica (es rara la linfogénesis) que precede a los procesos de **metástasis** (colonización y proliferación a larga distancia) y que supone un verdadero "cuello de botella" en la evolución clonal del tumor (de ahí la enorme importancia a efectos terapéuticos) (Merlo y col., 2006; Eccles y Welch, 2007).

- p53: muerte y resistencia

Por la importancia que se le da a la inestabilidad genómica, p53 siempre ha sido una de las proteínas más estudiadas a la hora de relacionar progresión tumoral, muerte celular y terapia anticancerígena (Hanahan y Weinberg, 2000; Vousden y Lane, 2007).

La **proteína supresora de tumores p53**, considerada la "guardiana del genoma", se encuentra ausente o alterada en aproximadamente la mitad de lo tumores humanos analizados (Perona y Sánchez-Pérez, 2004). El porcentaje sube hasta el 77 % si nos quedamos para los últimos resultados en cáncer de colon (Rozan y El-Deiry, 2007). Aquellos que no presentan mutaciones en *p53* suelen presentar mutaciones en los principales puntos de su ruta de actuación (Perona y Sánchez-Pérez, 2004).

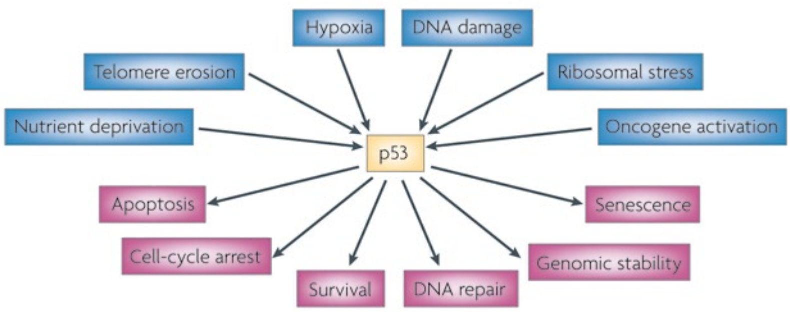

Figure 6 (from Vousden and Lane, 2007) Activation and functions of p53. p53 has a key role in integrating the cellular responses (pink boxes) to different types of stress (blue boxes). Activation of p53 can result in a number of cellular responses, and it is possible that different responses are induced by different stress signals. There is evidence that p53 can play a part in determining which response is induced through differential activation of target-gene expression. Although the importance of these responses to tumour suppression is clear, previously unanticipated contributions of these responses to other aspects of human health and disease are being uncovered. The role of p53 in tumour suppression, development and ageing is likely to depend on which cellular response is activated and on the context in which the activation occurs.

p53 es una de las proteínas más estudiadas de la historia, y aún así, es mucho aún lo que ignoramos sobre ella y su proteínas hermanas p63 y p73. Son proteínas presentes en todos los modelos animales estudiados hasta ahora y funcionan a múltiples niveles (**ver Figura 6**): regulación de la diferenciación, parada del ciclo celular ante la aparición de daños en el genoma, y promoción de la apoptosis si esos daños no se pueden reparar (Stiewe, 2007; Vousden y Lane, 2007). En general hay que tener en cuenta que, a nivel de terapia, p53 se relaciona más con la capacidad de inducir apoptosis *sensu strictu* que con la capacidad de la terapia para inactivar el tumor (Brown y Wouters, 1999; Vousden y Lane, 2007).

p53: death & resistance

- p53, the "genome keeper", is probably one of the most studied proteins but nowadays we ignore the majority of the interdependencies along the p53 pathway.
- p53 exerts functions at multiple levels in a normal cell that could be summarized as differentiation regulation, cell cycle arrest after damage and apoptosis triggering if no complete repair is possible.
- More than 50 % of human cancers analysed present p53 mutant or absent but rather than tumour progression or bad prognosis, this datum is more connected with a deficient response to apoptosis signalling.
- Dysfunctions in p53 not only cause insensibility to apoptosis but also inactivate the normal response against abnormal progression of mitosis (related with genomic instability), giving to the cells time for (by aneuploidy) developing resistant phenotypes.

Pese a ello, y en términos generales, la desaparición o alteración de p53 es un claro marcador de cáncer y un indicador, por lo general, de una mala prognosis (Kastan y Bartek, 2004; Perona y Sánchez-Pérez, 2004; Rozan y El-Deiry, 2007). Se considera que las mutaciones en *p53* otorgan a los subclones de cáncer un fenotipo de alto "*fitness* ecológico" (Merlo y col., 2006). Los fenómenos de la llamada catástrofe mitótica están íntimamente relacionados con mutaciones de *p53*, afectando a su capacidad de inducir paradas en el ciclo celular (Castedo y col., 2004).

La importancia de todos estos fenómenos es la constatación de cómo las mutaciones en *p53*, retrasan o inhiben la respuesta de muerte celular que debiera presentar la célula (que se vuelve resistente). Además, esta resistencia se realiza a través de mecanismos reproductivos y generadores de una mayor inestabilidad genómica propiciando la aparición de nuevos genotipos más agresivos (Erenpreisa y col., 2005; Vousden y Lane, 2007).

Gracias a que las rutas de señalización apoptóticas conforman una tupida malla de regulaciones y contrarregulaciones, disponemos de diversos puntos redundantes que permiten la estimulación independiente para garantizar el resultado final (la muerte) incluso en las células tumorales con p53 alterada o ausente (Johnstone y col., 2002; Castedo y col., 2006).

Nuevas terapias antitumorales

New anti-tumour therapies

- Despite the research efforts in the last years, we are nowadays at the same overall mortality rates than the 1950s.
- New anti-tumour drugs' development tries to go further from the traditional genotoxic damage.
- New therapies are highly variable in structure and mechanism of action, but mainly they are still being interfering agents of the mitotic process. Especially successful are the anti-microtubule agents (Taxol) and the tyrosine-kinase inhibitors (Gleevec).
- New delivery protocols for old well-known drugs and designed therapies against new targets are also needed.
- Genotoxic and anti-mitotic therapy could lead in an increase of genomic instability of tumours stimulating its evolution and allowing resistance.
- A new prospective in therapy development (considering the heterogenic nature of tumours, the different anti-neoplasic compounds to use and looking for patients wellness) is actually growing up.

La constante amenaza del cáncer (con un número de afectados en crecimiento en todo el mundo), ha impulsado a la industria farmacéutica a una continua lucha para generar nuevos agentes anticancerígenos que mejoren los resultados y puedan evitar la aparición de resistencias y de efectos secundarios (Greaves, 2002; Cozzi y col., 2004). En los últimos años se está avanzando mucho a nivel de identificación y desarrollo de nuevos fármacos anticancerígenos, pero seguimos en los mismos niveles de mortalidad general (salvo contadísimas excepciones) que hace más de medio siglo (Varmus, 2006). La supervivencia de los clones tumorales a través de la aparición de mecanismos de resistencia se da en la práctica totalidad de los modelos existentes en la literatura (Greaves, 2002; Johnstone y col., 2002; Merlo y col., 2006). En relación a los tipos de muerte celular inducidos por cada terapia anticancerígena, es en los procesos que conllevan la inducción de catástrofe mitótica donde mejor se ha documentado, *in vitro*, como las células supervivientes se convierten en mutantes aneuploides con capacidades de resistencia aumentadas (Erenpreisa y Cragg, 2001; Castedo y col., 2004). El incremento observado en las tasas de supervivencia de los afectados por cáncer se debe, fundamentalmente, a la mejora de los criterios de diagnosis y a la extensión de los procedimientos de detección temprana (Cozzi y col., 2004).

Los nuevos agentes quimioterapéuticos son extremadamente variados en cuanto a su origen, estructura química y mecanismo de acción. El desarrollo de fármacos implica una amplia variedad de áreas de conocimiento, aunque la identificación de nuevos agentes (a través del estudio de las propiedades de distintos productos de origen animal o vegetal) sigue siendo la principal herramienta (Cozzi y col., 2004).

A principios de la década de los noventa se consideraba que los compuestos que se estaban empleando comúnmente en quimioterapia (en general **medicamentos genotóxicos**) estaban tocando techo de efectividad y que el futuro vendría dado a través de nuevos agentes mucho más dirigidos. La realidad está demostrando que el desarrollo de estos nuevos "fármacos moleculares" está siendo más lento de lo esperado, mientras que los medicamentos más clásicos (como el metotrexato, el cisplatino, el etopósido o las camptotecinas) presentan todavía un más que aceptable balance de resultados al emplearse en las condiciones adecuadas (Nicholson, 2000; Cozzi y col., 2004; Varmus, 2006).

Los nuevos fármacos moleculares presentan más una capacidad citostática que citotóxica, haciendo incluso que se replanteen los criterios de evaluación de los ensayos clínicos (Cozzi y col., 2004). Esta nueva generación de agentes anticancerígenos abarca una amplia variedad de compuestos: desde **anticuerpos** contra antígenos específicos hasta **oligonucleótidos con capacidad de interferir** en la síntesis de ciertas proteínas, pasando por **imitadores** sintéticos de distintas proteínas clave en la transducción de señales de muerte celular (Ricci y Zong, 2006; Stone, 2007). La quimioterapia se está reenfocando para no depender exclusivamente de los procesos apoptóticos, y así se están desarrollando terapias específicas que afecten a los procesos de autofagia (como la rapamicina o el tamoxifeno) o que inducen necrosis, catástrofe mitótica o senescencia (R. Kim y col., 2006; Ricci y Zong, 2006). Por último, se trabaja en **mejorar el transporte de los medicamentos** (nuevos y tradicionales) de manera específica, usando distintos tipos de vehículos (Harrington y col., 2002).

Los esfuerzos en búsqueda de las nuevas dianas se han venido centrando en otros procesos que permiten la proliferación celular, yendo más allá del daño al ADN. En este sentido, los llamados **agentes anti-microtúbulos** (tanto hiperpolimerizadores como despolimerizadores) siguen despertando especial interés. Estos agentes se han ido desarrollando en la estela marcada por los taxoles, entre otros, y están mostrando gran capacidad para inactivar células tumorales mediante alteraciones en el ciclo celular y apoptosis (Mollinedo y Gajate, 2003; Jordan y Wilson, 2004; Cortes y Baselga, 2007). Relacionados con los anteriores se encuentran los **compuestos anti-mitóticos,** que no interfieren con la tubulina sino que atacan directamente a los componentes de los *checkpoints* mitóticos (Jackson y col., 2007). Hay, igualmente, un gran desarrollo en el campo de los **inhibidores para los receptores tirosina-quinasa de factores de crecimiento**, especialmente en el caso del factor de crecimiento epidérmico (EGF), desde el gran éxito médico que ha supuesto la autorización final de la imatiniba (Gleevec™) para la leucemia mieloide crónica (Cozzi y col., 2004; Varmus, 2006). Otras muchas dianas se encuentran actualmente en estudio (Nicholson, 2000; Varmus, 2006).

Los fármacos diseñados para **reponer o restaurar funciones proteicas,** perdidas en el proceso tumoral, proporcionan una nueva perspectiva terapéutica. Especialmente se trabaja sobre p53 pretendiendo ayudar a las proteínas mutantes mal plegadas a recuperar (aunque sea parcialmente) su función (Vousden y Lane, 2007).

Los que están experimentando una progresión menor de lo esperado son los medicamentos de la llamada **terapia antiangiogénica** (fundamentalmente los inhibidores de las metaloproteasas) que pretenden acabar con los tumores privándoles de los recursos energéticos y de las vías de desarrollo de la metástasis (Varmus, 2006; Eccles y Welch, 2007). Las pruebas preclínicas que se van realizando no están dando los resultados esperados y se está incluso replanteando la importancia de estas enzimas como posibles dianas antitumorales (Cozzi y col., 2004).

Por el momento, casi todos los agentes desarrollados o en ensayo se basan en el mismo principio que los primeros compuestos genotóxicos: impedir la capacidad proliferativa de los clones tumorales al introducir trabas en el sistema. Casi todos los fármacos aquí revisados presentan el mismo punto débil: incrementan la inestabilidad genómica del tumor, pudiendo inducir la aparición de cepas resistentes (Perona y Sánchez-Pérez, 2004; Jackson y col., 2007).

Una nueva perspectiva mucho más integradora, de los procesos subyacentes al cáncer se está abriendo paso, sugiriendo cambios (en los protocolos de aplicación de la quimioterapia) para conseguir incrementar su efectividad al emplearla de un modo que no se convierta en una fuerza motora que guíe el desarrollo de resistencias (Merlo y col., 2006). Estas nuevas perspectivas se materializan en nuevos protocolos de aplicación de fármacos ya conocidos (cócteles, combinaciones etc.), así cómo en el desarrollo de nuevas terapias (no dirigidas hacia los mecanismos de proliferación, sino directamente hacia la maquinaria energética de la célula).

De igual manera, se está trabajando en la manera de mejorar la calidad de vida de los pacientes a través de la reducción en lo posible de los efectos secundarios generados por las terapias citotóxicas. Curiosamente, estos trabajos pretenden desarrollar fármacos que inactiven la respuesta de las células sanas a la terapia (inhibiendo p53) para conseguir su supervivencia (Varmus, 2006; Vousden y Lane, 2007).

En el ámbito de la presente Tesis Doctoral hemos investigado las posibilidades de dos nuevas aproximaciones terapéuticas y hemos probado variaciones en los protocolos de tratamiento en cultivos celulares de otra; en los siguientes párrafos procederemos a introducirlos.

- La Terapia Fotodinámica del cáncer

La Terapia Fotodinámica (PDT por *Photodynamic Therapy*) del cáncer constituye una modalidad terapéutica alternativa, adecuada para el tratamiento de tumores pequeños y superficiales, tanto con fines paliativos como curativos. Se basa en el uso de compuestos fotosensibilizadores (PSs por *photosensitizers*) exógenos que se acumulan preferentemente en tejidos tumorales. La irradiación del área tumoral con luz visible de longitud de onda apropiada, ocasiona la formación de especies reactivas de oxígeno (*reactive oxygen species*, ROS), principalmente **oxígeno singlete** ($^1O_2$), con efectos citotóxicos que llevan a la muerte selectiva de las células en el tejido tumoral (**ver Figura 7**) (Dougherty, 2002; Dolmans y col., 2003; Triesscheijn y col., 2006).

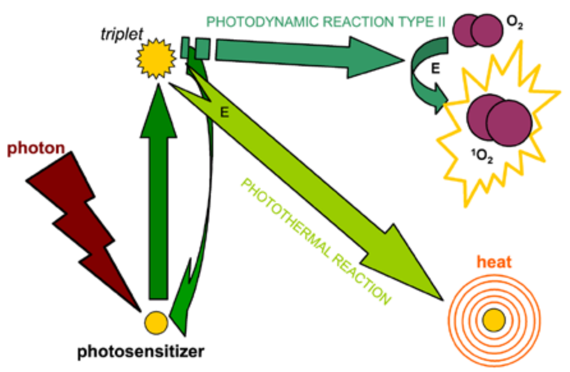

Figure 7 Photodynamic (PDT) and Photothermal (PTT) therapies are based in the same principle. In both cases a substance with proper physico-chemical characteristics for being a photosensitizer (PS) is excited with light of the appropriate wavelength. The PS takes the energy from the photons changing its electron configuration and reaching the triplet state. In the photodynamic reaction type II, the PS stays in the triplet state for milliseconds and, in the presence of molecular oxygen, the energy of the photon is transferred to it, becoming cytotoxic singlet oxygen (a reactive oxygen species) and the PS returns to the basal state. In the photothermal reaction, the triplet state takes only few nanoseconds. As there is no time to transfer it to oxygen, the energy is finally dissipated as heat when the PS returns to the basal state.

En relación con terapias convencionales, la PDT presenta mayor selectividad, ya que el daño celular queda restringido a la zona tumoral irradiada donde se reúnen los tres agentes responsables del efecto fotodinámico (PS, luz y oxígeno), lo que conlleva una importante disminución de efectos secundarios en el organismo. Además, la PDT puede repetirse sin afectar a los tejidos normales, se puede usar sola o en combinación con otros tratamientos (quimio o radioterapia) y no induce efectos mutagénicos (Dolmans y col., 2003; Triesscheijn y col., 2006). La PDT se está utilizando también para el diagnóstico y localización de las lesiones neoplásicas gracias a la detección de la fluorescencia del PS (Dolmans y col., 2003).

Photodynamic therapy of cancer

- PDT is based on the use of photosensitisers (PSs) that become only active in conjunction with appropriate wavelength light and oxygen, leading in ROS production
- The PS is include is several sub-cellular structures leading in focalised damage by ROS that finish in a metabolic failure. PDT is not a genotoxic therapy.
- PDT is more selective than other therapies due to the use of light that allow targeting the therapy only against the tumour area. PDT can also be used in repeated dosages.
- The EMEA has already approved six PDT protocols and the new prospective is the development of new light delivery systems as well the new "second generation" PSs and PS carriers more selective for cancer cells.

La primera aprobación de un medicamento para PDT, la fotofrina (Photofrin®: una mezcla purificada de oligómeros del llamado derivado hematoporfirínico), en cánceres humanos tuvo lugar en Canadá en 1999 (seguida de los EEUU) (Dougherty, 2002; Dolmans y col., 2003). En la actualidad, se han ido incrementando lentamente los protocolos de PDT aprobados para cáncer (por la *European Medicines Agency*, EMEA) hasta llegar a tres medicamentos en seis procedimientos de empleo distintos: el Photofrin®, el ácido amino-levulínico (ALA, Levulan®) y su formulación metilada (Metvix®) y la temoporfina (Foscan®, un derivado de la clorina) para distintos cánceres superficiales o de diversos tractos (Triesscheijn y col., 2006).

Las perspectivas futuras de la PDT se ven acrecentadas por el desarrollo de nuevos equipos de fibra óptica capaces de introducir la luz requerida en cualquier punto del organismo, rompiendo la vinculación de esta terapia a los tumores superficiales (Dolmans y col., 2003). Actualmente se están llevando a cabo varios ensayos clínicos que están probando la utilidad de la PDT en ciertos tumores no operables o en pacientes terminales, con significativas mejoras en cuanto al tiempo y a la calidad de vida (Triesscheijn y col., 2006). Asimismo se están perfeccionando los protocolos para conseguir más autorizaciones para tratamientos basados en el empleo de los llamados "fotosensibilizadores de segunda generación" con propiedades mejoradas con respecto al Photofrin® (Morgan y Oseroff, 2001; Dolmans y col., 2003; Triesscheijn y col., 2006).

Los estudios realizados en cultivos celulares muestran que muchos de los orgánulos y estructuras celulares pueden verse afectados, bien directa o indirectamente, por el proceso fotodinámico: mitocondrias, lisosomas, aparato de Golgi, retículo endoplásmico (ER), la membrana plasmática y el citoesqueleto (Oleinick y Evans, 1998; Villanueva y col., 2003; Stockert y col., 2007). El daño a estas estructuras subcelulares está relacionado con la localización del PS, dado que el oxígeno singlete generado durante la PDT tiene una vida media muy corta (menos de 0,04 μs) y, por consiguiente, su radio de acción no excede de las 0,02 μm (Moan y Berg, 1991). En este contexto, los estudios sobre el lugar de acumulación de los PSs dentro de la célula resultan de especial interés, ya que permiten determinar las dianas primarias del tratamiento fotodinámico (Oleinick y Evans, 1998; Villanueva y col., 2003; Stockert y col., 2007).

El estrés oxidativo generado por la PDT induce un **fallo metabólico**, ligado al punto de acumulación del PS, que activa las rutas de señalización que conducen al disparo apoptótico (Moor, 2000; Srivastava y col., 2001; Oleinick y col., 2002; Almeida y col., 2004). Como se ha comentado, la mitocondria es el punto de acumulación más común de los PSs pero no el único, ya que se ha documentado el disparo apoptótico con PS que se acumulan en los lisosomas (Reiners y col., 2002), ER (Kessel y col., 2005) o Golgi (Cristóbal y col., 2006). De igual manera se ha documentado el daño a estructuras del citoesqueleto (Juarranz y col., 2001; Galaz y col., 2005). Por tanto, las rutas implicadas, aunque tienden a confluir en la llamada vía mitocondrial, abarcan una gran variedad de eventos de señalización (incluyendo la ruta de los receptores de muerte) en función del punto primario de daño (Almeida y col., 2004; Castano y col., 2006; Ricci y Zong, 2006).

En los últimos años se está abriendo paso una serie de datos que relacionan a la PDT con la capacidad de estimular al sistema inmune a reconocer y luchar contra el tumor; de esta manera, se está empezando a trabajar en el empleo de la PDT para obtener lisados tumorales con capacidad de vacunación al ser inyectados en otro organismo (Dolmans y col., 2003; Castano y col., 2006).

o La Terapia Fototérmica

La Terapia Fototérmica (PTT por *Photothermal Therapy*) representa una auténtica aproximación novedosa a la eliminación de células tumorales empleando la luz y un PS que, incapaz de completar la reacción fotodinámica, desprende el exceso de energía absorbida en forma de calor (**ver Figura 7**). La PTT es capaz de aprovechar esa incapacidad de generar ROS al decaer rápidamente la energía captada por la irradiación. Esa energía se disipa mediante un aumento en cascada de la energía cinética de las moléculas adyacentes al PS, produciendo un aumento de la temperatura. Empleando láseres de pulso de alta frecuencia se consigue hacer secuencial este fenómeno (induciendo un nuevo pico de temperatura antes de que el previo se pierda) generando una onda de choque térmico por la vaporización de las moléculas de agua (Jori y Spikes, 1990).

Photothermal therapy of cancer

- Branched of PDT, PTT is a novel therapeutic approach that uses PSs that are not capable to generate ROS instead of producing heat as a consequence of photoactivation.
- PTT does not need oxygen and uses wavelengths in the far red and infrared areas, characteristic that makes it so attractive in treatment of solid poor-vascularised tumours.
- There is a growing interest in hyperthermal reactions as anti-tumour approaches, but nowadays are still little references in literature.

Existe muy poca literatura aún sobre el empleo de reacciones que procedan a la eliminación del cáncer mediante la inducción de fenómenos de hipertermia, aunque sí existen varias aproximaciones al concepto (últimamente empleando nanopartículas como mediadores) (Marchal y col., 1986; Ito y col., 2005). En lo poco existente se advierte un creciente interés por el uso de estas tecnologías (basadas en el empleo de potentes láseres) en base a la especial susceptibilidad de las células neoplásicas a los cambios de temperatura (Diven y col., 1996; Liu y col., 2002).

La PDT se distingue de la hipertermia inducida clásica en que el desprendimiento de calor, que produce el daño celular, no es un efecto general sino muy localizado en el lugar donde se encuentra el PS (Soncin y col., 1999). El desprendimiento de energía al retornar al estado fundamental se traduce en un incremento de temperatura (ΔT^a) calculado de unos 130 ºC en un volumen esférico de agua de 5 Å de diámetro alrededor de la molécula fotoexcitada por un fotón de 700 nm que trasmite una energía de sólo $284 \cdot 10^{-21}$ J (Soncin, 1999). A 2 mm del PS, el ΔT^a será ya sólo de 2 ºC, generando un grave desequilibrio térmico en la célula diana. Este ΔT^a se extiende por la célula como una onda de choque térmico, causando a su paso importantes daños tanto químicos (desnaturalización y ruptura de enlaces) como físicos (ruptura y disgregación de las membranas celulares) que determinan la respuesta al tratamiento (Soncin y col., 1999).

Los escasos experimentos publicados con este tipo de terapia, incluyendo los de la presente Tesis Doctoral, han demostrado unos excelentes resultados de fotoinactivación tanto *in vitro* como *in vivo*, augurando unas buenas perspectivas de futuro conforme se vaya desarrollando esta terapia (Chen y col., 1996; Busetti y col., 1999; Diddens y col., 2003).

Las ventajas de la PTT inciden y desarrollan las de la PDT. De esta manera, la PTT, al requerir irradiaciones en la longitud de onda del rojo lejano y del infrarrojo, presenta mayor capacidad de penetración en los tejidos que la PDT (con irradiaciones en el espectro visible). Como en la PDT, muchos de los PS empleados requieren vehiculización específica para su administración en el torrente sanguíneo y esto asegura una buena acumulación en los tejidos neoplásicos en comparación con el tejido circundante. Por último, la PTT es totalmente independiente del oxígeno, lo que elimina la principal desventaja de la PDT en el tratamiento de tumores sólidos de un tamaño relevante (Jori y Spikes, 1990; Camerin y col., 2005).

o El agente genotóxico VP-16

The genotoxic agent etoposide

- VP-16 is well-known and widely used chemotherapeutic drug.
- It acts as a DNA topoisomerase II poison, leading in genotoxicity by DNA double-strain breaking.
- Cell death by VP-16 treatment is described as apoptotic and is used in Cell Biology research for obtaining pure apoptotic populations.

Las células neoplásicas se dividen mucho más rápidamente que las células normales del organismo (Varmus, 2006), pero eso no es indicativo de la viabilidad reproductiva de los clones y de la capacidad de expansión del tumor: si fuese así, los tumores crecerían hasta igualar la masa corporal en unos pocos ciclos (Hanahan y Weinberg, 2000; Weaver y col., 2007). Son muchas las razones que determinan la alta mortalidad de las células en un tumor, razones que se vuelven presiones selectivas que conducen a un mayor desarrollo del cáncer (Anderson y col., 2006; Merlo y col., 2006).

La capacidad de dividirse con éxito (a pesar de las mutaciones acumuladas) es una de ellas, y es precisamente la que ha sido objeto de diana por parte de los agentes quimioterapéuticos clásicos (Perona y Sánchez-Pérez, 2004; Varmus, 2006).

El etopósido, también conocido por sus siglas VP-16, es un derivado semisintético de la podofilotoxina y actúa como un veneno catalítico de la topoisomerasa II del ADN (topo II). La topo II es una enzima estructural de las células, se encarga del mantenimiento del superenrollamiento de la doble hélice del ADN, con funciones especialmente delicadas en los procesos de copia de los cromosomas durante la fase S del ciclo celular. La inhibición causada por el etopósido impide la función de la topo II (**ver Figura 8**), bloqueando la finalización del proceso catalítico y generando roturas de la doble cadena del ADN que desembocan en fragmentación cromosómica (Burden y col., 1996; Meresse y col., 2004; Schellens y col., 2005).

El etopósido se emplea en clínica desde los años 1970s, estando autorizado para el tratamiento de distintos tipos de cánceres (pulmón, testículo, leucemias, etc.) con buenos resultados y se plantea su aplicación a otros tipos (como el ovárico) donde hasta ahora no se consideraba tan efectivo (Schellens y col., 2005; Markman, 2007). En la investigación básica en Biología Celular, el etopósido es muy conocido y utilizado como inductor de la apoptosis, ya que, en condiciones determinadas, produce dicho tipo de muerte de forma exclusiva (Castedo y col., 2006). Sin embargo, su capacidad mutagénica, y la relación de ésta con recidivas y resistencias, determinan que actualmente se emplee de manera más prudente y en combinación con otros agentes quimioterapéuticos (Meresse y col., 2004).

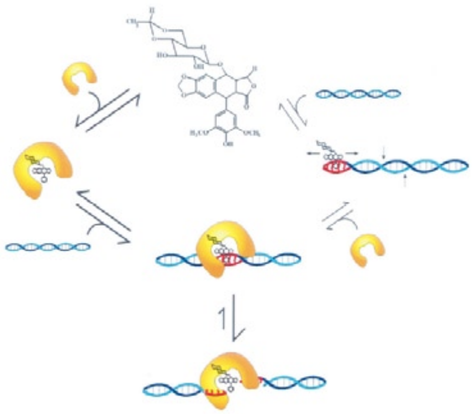

Figure 8 (from Burden et al., 1996) Pathway of etoposide-induced DNA cleavage complex formation. A pathway is shown depicting the formation of topoisomerase II-DNA cleavage complexes in the presence of etoposide (the structure of which is shown at the top). It is based on the premise that drugs enhance topoisomerase II-mediated nucleic acid scission predominately by altering the structure of DNA (shown in red) within the cleavage overhang (indicated by vertical arrows). It is proposed that the primary pathway for the formation of the noncovalent enzyme·drug·DNA ternary complex is through etoposide·topoisomerase II interactions (left side). Although etoposide may bind DNA prior to ternary complex formation (right side), these non-specific interactions are proposed to be repository in nature. Finally, once the ternary complex is formed at specific sites, enhanced cleavage complex formation results from the ability of etoposide to inhibit DNA religation at those sequences (bottom).

HIPÓTESIS Y OBJETIVOS

Hipótesis de partida y Objetivos

Teniendo en cuenta los conceptos acerca de la muerte celular que se han presentado en la Introducción, nos planteamos el diseño del trabajo experimental de la presente Tesis Doctoral a través de la siguiente Hipótesis de partida.

Las distintas terapias antineoplásicas están basadas en la inducción de toxicidad en las células tumorales. Los daños generados son reconocidos por una compleja red de señalización que los traduce en distintos fenotipos y, aunque presentan cierta variabilidad en cuanto a las distintas rutas de señalización activadas, los fenotipos se pueden agrupar en una serie reducida de tipos de muerte celular. Con un adecuado diseño de los protocolos de inducción del daño, sería posible conseguir patrones similares de muerte celular, empleando distintos agentes antitumorales.

Partiendo de esta premisa, decidimos realizar una serie de procedimientos experimentales con los siguientes Objetivos específicos:

A) Cuantificar el potencial citotóxico (sobre líneas celulares en cultivo) de tratamientos antitumorales de distinta naturaleza.

B) Relacionar el tipo de muerte celular inducida en función de la intensidad del estímulo aplicado.

C) Ampliar los criterios (morfológicos y/o bioquímicos) existentes para identificar los distintos tipos de muerte celular observados, profundizando en aquellos que están menos clarificados.

D) Analizar las diferencias que puedan presentarse entre los patrones de muerte observados, con particular atención a los intervalos de tiempo post-tratamiento en que se manifiestan los eventos que conforman la respuesta a los tratamientos.

Hypothesis

Different anti-tumour therapies are based on cytotoxicity induction. Damage is recognised by a complex signalisation network that drives the response to different phenotypes of death that could be classified (despite minor variations in the signalling pathways triggered) in a reduced number of cell death types. With an appropriate design of the damage induction protocols, it could be possible to obtain similar patterns of cell death using different anti-tumour agents.

Main Objectives

A) To quantify the cytotoxic potential in cell cultures of a number of different anti-tumour treatments.

B) To establish relationships between cell death types triggered by the intensity of the caused injure.

C) To widen the criteria (morphological, biochemical) currently in use for identifying cell death types, specially on those processes not completely understood at the moment.

D) To analyse the differences that death patterns could show, specifically at the response times (after treatment) of the events that configure the processes.

RESULTADOS

Artículo 1:

Fotoinactivación de células tumorales en cultivo mediante el derivado porfirínico CF3

Anti-Cancer Drug Design 16: 279-290 (2001)

El avance en las últimas décadas de la Terapia Fotodinámica del cáncer está directamente ligado a la síntesis de nuevos compuestos con características físico-químicas que les confieren una mayor actividad biológica. En este artículo se presentan los resultados obtenidos sobre la capacidad fotoinactivadora de la 5-(4-*N*-(*N*-2',6'-dinitro-4'-trifluorometilfenil)-aminofenil)-10,15,20-tris(2,4,6-trimetoxifenil) porfirina (CF3). Este derivado profirínico es una molécula de nueva síntesis química, configurada como un compuesto de distribución de carga asimétrica (lo que se considera una cualidad, al suponerse que mejora su capacidad de ser incorporado por las células tumorales) sobre la que se pretende incrementar su potencial terapéutico al ser suministrada dentro de liposomas de dipalmitoil-fosfatidilcolina (DPPC), ya que CF3 es un compuesto muy hidrofóbico.

CF3 es incorporado por las células y se observa su acumulación en estructuras discretas del citoplasma que parecen corresponder, al menos en parte, al conjunto de lisosomas. Esta incorporación se demuestra inocua para el cultivo, siempre que se mantenga en condiciones de oscuridad.

La irradiación se efectuó con una lámpara de 8 mW/cm^2 de potencia, cuya luz debe atravesar un filtro azul antes de incidir sobre las células, con el fin de aprovechar la máxima intensidad de absorción lumínica del compuesto (λ= 420 nm). Las condiciones experimentales determinadas para los primeros experimentos fueron de 18 h de incubación con $[CF3]=5\times10^{-6}$ M, empleándose distintos tiempos de irradiación, para evaluar la supervivencia 24 h después de haberse efectuado la exposición a la luz.

Se determinó que la mínima supervivencia se daba con 15 min de irradiación (LD_{96}). Las células sometidas a este tratamiento presentaban, inmediatamente después de la irradiación, deformaciones muy notables de la membrana plasmática. Estas deformaciones comienzan como pequeñas burbujas (hialinas y basófilas) que al cabo del tiempo convergen y se desprenden provocando la ruptura de la integridad de membrana (proceso característico de la necrosis). Con tiempos menores de irradiación se observa la aparición de muerte celular apoptótica (caracterizada por el redondeamiento y división de la célula en cuerpos, al tiempo que se da el desprendimiento de la superficie de adhesión). La muerte celular apoptótica alcanza su máximo porcentaje (75,8 %) con 7 min de irradiación (LD_{85}).

Ambos tipos de muerte (apoptosis y necrosis), determinados por estudios morfológicos, fueron confirmados mediante el análisis electroforético del ADN.

Se comprobó, asimismo, que el mecanismo de muerte celular que se desencadenaba tras el tratamiento era claramente dependiente del tiempo de irradiación. De esta manera, el porcentaje de células muertas por necrosis se incrementa con el tiempo de irradiación: los porcentajes son mínimos en tiempos cortos pero se llega rápidamente al máximo, alcanzado en LD_{96}, con tiempos de irradiación superiores a los 7 min. Por el contrario, el porcentaje de células identificadas como apoptóticas alcanza su máximo con 7 min de irradiación, decreciendo posteriormente a medida que aumenta el porcentaje de células necróticas. Con 10 min de irradiación se consigue prácticamente igualar la proporción apoptosis *vs.* necrosis, con una mortalidad total muy próxima a LD_{96}.

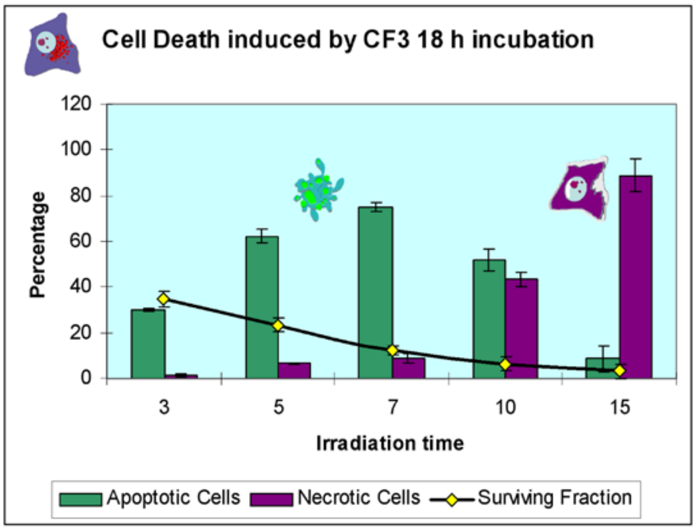

Figure 9 Dose-dependent induction of cell death types by CF3-PDT. Photodynamic therapy protocols allow a high control of the damage levels generated into the cells. As it is clearly seen in the graphic, minimal changes in the light irradiation time induced major changes in the cell death type triggered, with minor affection to the overall mortality caused by the therapy. This characteristic provides the power to select type-specific cell death conditions.

También se ensayaron tiempos de incubación inferiores (sólo 3 h de incubación frente a 18 h). Sin llegar a los valores anteriores, sí se observó que tiempos largos de irradiación eran bastante eficaces para inactivar el cultivo tumoral. El dato más interesante a nuestro juicio era, sin embargo, el derivado de la condición subletal LD_{38} (correspondiente a 7 min de irradiación en estas condiciones). 18 h después de realizada la irradiación bajo estos parámetros, se verificó la existencia de una parada del ciclo celular caracterizada por la acumulación de células en metafase (con un índice mitótico del 25,1 % frente al valor de referencia 4,6 % de las HeLa control). Una gran parte de esas metafases presentaban graves y evidentes anomalías en la disposición del huso mitótico (aproximadamente un 32 % del total de células en división), pero no se pudieron verificar alteraciones significativas en las redes de MTs interfásicos. Unas 24 h más tarde se confirmó que el 76,8 % de las células del cultivo se desprendía del sustrato (la mayoría de esas células despegadas fueron identificadas como apoptóticas empleando criterios morfológicos).

Este trabajo refleja cómo variaciones en los protocolos experimentales de PDT generan respuestas significativamente diferentes, en los mecanismos de muerte celular implicados, y cómo existe entre ellos una graduación en lo referente al nivel de daño que inducen.

Anti-Cancer Drug Design (2001), 16, 279–290

Photokilling of cultured tumour cells by the porphyrin derivative CF3

A. Villanueva, E.N. Durantini[1], J.C. Stockert, S. Rello, R. Vidania[2], M. Cañete, A. Juarranz, R. Arranz and V. Rivarola[3]

Departamento de Biología, Facultad de Ciencias, Universidad Autónoma de Madrid, Canto Blanco, E-28049 Madrid, Spain, [1]Departamento de Química y Física, Facultad de Ciencias Exactas y Naturales, Universidad Nacional de Río Cuarto, 5800 Río Cuarto, Argentina, [2]Centro de Investigaciones Energéticas Medioambientales y Tecnológicas (CIEMAT), E-28040 Madrid, Spain and [3]Departamento de Biología Molecular, Facultad de Ciencias Exactas y Naturales, Universidad Nacional de Río Cuarto, 5800 Río Cuarto, Argentina

Summary

We have analysed the photosensitizing properties of the new porphyrin 5-(4-*N*-(*N*-2′,6′-dinitro-4′-trifluoromethylphenyl)-aminophenyl)-10,15,20-tris(2,4,6-trimethoxyphenyl) porphyrin (CF3) on HeLa cells. The fluorescence and singlet oxygen quantum yield for CF3 were, respectively, $\phi_F = 0.032$ and $\phi\Delta = 0.25$. Cell treatments were done with 5×10^{-6} M CF3 incorporated into liposome vesicles. Under violet-blue exciting light, the red fluorescence of CF3 was mainly detected in lysosome-like granules. No dark cytotoxicity was observed using high concentration (5×10^{-6} M) and long incubation time (18 h). Cell cultures treated for 18 h with CF3 and exposed to light ($360 < \lambda < 460$ nm; 8 mW/cm^2) for 7 min revealed a great amount of apoptotic (75.8%) and detached cells (62%) 8 h later, leading to a cell lethality of 85% (LD_{85}). Apoptosis was identified by chromatin fragmentation and DNA ladder in gel electrophoresis. Necrotic cells were found using 15 min irradiation (LD_{96}) and showed first small and then giant bubbles at the cell surface, with homogeneous nuclear condensation. Incubation with CF3 for 3 h followed by 7 min irradiation (LD_{38}) produced a mitotic arrest 18 h later (mitotic index: 25.1%). Forty-eight hours after this metaphase blockage, cultures showed a great number of apoptotic cells. Taking into account these results, CF3 could be a valuable photosensitizer for the photodynamic therapy of cancer.

Key words

apoptosis/metaphase blockage/liposomes/necrosis/photodynamic therapy/photosensitizing agents/porphyrin derivatives/singlet oxygen

Introduction

Photodynamic therapy (PDT) constitutes a relatively new and attractive therapeutic modality for the treatment of small and superficial solid tumours. Recent reviews on the results of clinical trials emphasize the great potential of PDT for the treatment of esophagus (Greenwald, 2000) and lung tumours (Ost, 2000). PDT relies on the preferential accumulation of a photosensitizing drug in neoplastic tissue, followed by the formation of cytotoxic products generated by irradiation with light of suitable wavelength in the presence of molecular oxygen. Although the precise mechanism of PDT is not yet fully understood, it is accepted that the highly reactive singlet oxygen, O_2 ($^1\Delta_g$) (hereafter simply $^1O_2$), is the main photoproduct responsible for cell death. The advantages of PDT over other conventional cancer treatments are its low systemic toxicity and its ability to destroy tumours selectively.

The most widely applied photosensitizers (PSs) for PDT (such as the hematoporphyrin derivative, HpD, or its partially purified version, Photofrin®) are far from ideal because of their chemical heterogeneity and variable composition, poor optical properties, reduced capacity for tumour targeting and long-lasting side-effects (skin phototoxicity). Therefore, there has been increasing interest in the search for second-generation PSs with improved physical, chemical and therapeutic properties. Some examples of new sensitizers are synthetic porphyrins, chlorins, phthalocyanines and porphycenes. A detailed review on several of these second-generation PSs has been published (Ali and van Lier, 1999).

It is worth noting that the growing research on new PSs and their application for cancer therapy has also extended PDT to other medical fields such as ophthalmology and dermatology. Thus, the benzoporphyrin derivative verteporfin has been used for the treatment of age-related macular degeneration (Harding, 2001). Likewise, both tumoral and other proliferative skin diseases can be treated with 5-aminolevulinic acid (ALA), which is a precursor of the endogenous PS protoporphyrin IX (Kalka *et al*., 2000).

Methoxyphenyl-porphyrins have shown effective photo-

Correspondence to: Prof. Angeles Villanueva, Departamento de Biología, Facultad de Ciencias, Universidad Autónoma de Madrid, Canto Blanco, E-28049 Madrid, Spain. e-mail: angeles.villanueva@uam.es. Received 1 March 2002; accepted 24 April 2002

sensitizing properties (Yslas *et al.*, 2000) and the presence of methoxy groups appears to be beneficial from the standpoint of tumour localization (Faustino *et al.*, 2000). On the other hand, the influence of the trifluoromethyl group in biologically active molecules is often associated with the increased lipophilicity that this substituent imparts (McClinton and McClinton, 1992). Fluorine analogs of natural porphyrins containing trifluoromethyl and difluorovinyl groups have been found to localize selectively in tumour tissues (Ando and Kumadaki, 1999). Similarly, hexadecafluorinated zinc-phthalocyanine offers some advantages over zinc-phthalocyanine as a PS for clinical applications (Boyle *et al.*, 1996).

Recently, several porphyrin derivatives covalently linked to other active molecules (resulting in asymmetric porphyrin dyads showing two moieties with different electron donor-acceptor properties) have been described and proposed for potential use in PDT (Tatman *et al.*, 1998; Durantini, 2000). Taking into account that one of the basic objectives in PDT research is the characterization of new and more efficient drugs, we have synthesized the porphyrin dyad 5-(4-*N*-(*N*-2′, 6′-dinitro-4′-trifluoromethylphenyl)aminophenyl)-10,15,20-tris(2,4,6-trimethoxyphenyl)porphyrin (Milanesio *et al.*, 2001) or CF3 (Figure 1). The presence of an asymmetric substitution on the macrocycle ring should produce a better accumulation in subcellular compartments, which is a prerequisite for effective photosensitization (Moser, 1998).

In the present work we describe the photophysical and photobiological properties of the asymmetric porphyrin CF3. This compound was incorporated into liposomes and, following administration to HeLa cells, the dark toxicity and cellular localization were analysed. After incubation with liposomal CF3 and violet-blue light irradiation, photosensitization kinetics and morphological changes induced by the drug were studied. Depending on the incubation time and light dose, massive apoptotic or necrotic mechanisms of cell death were observed. In addition, a striking increase of the mitotic index with metaphase arrest followed by apoptosis was found after sublethal photodynamic treatments with CF3.

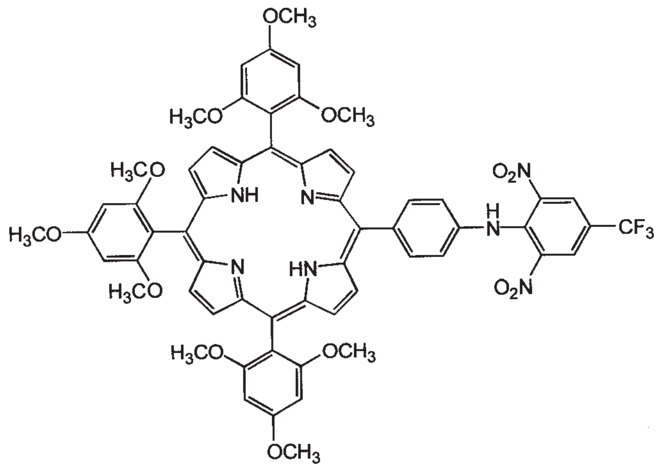

Figure 1

Chemical structure of the porphyrin CF3 [5-(4-*N*-(*N*-2′,6′-dinitro-4′-trifluoromethylphenyl) aminophenyl)-10,15,20-tris(2,4,6-trimethoxyphenyl) porphyrin].

Materials and methods

Cell cultures

The human HeLa carcinoma cell line was routinely grown either in 35 mm culture dishes (Costar) or on 22 mm square coverslips placed into the dishes, using Dulbecco's modified Eagle's medium (DMEM) containing 10% (v/v) fetal calf serum (FCS), 50 units/ml penicillin, 50 μg/ml streptomycin and 1% (v/v) 0.2 M L-glutamine (all from Imperial Laboratories, UK). Cell cultures were carried out at 37°C in a humidified atmosphere containing 5% CO_2.

Chemicals and preparation of liposomes

CF3 was synthesized according to the previously described procedure (Milanesio *et al.*, 2001). Briefly, the acid-catalyzed condensation of 2,4,6-trimethoxybenzaldehyde with a large excess of pyrrole formed *m*-(2,4,6-trimethoxyphenyl)dipyrromethane which, in the presence of both 2,4,6-trimethoxybenzaldehyde and 4-acetamidobenzaldehyde, yielded the corresponding 5-(4-acetamidophenyl)-10,15,20-tris(2,4,6-trimethoxyphenyl)porphyrin. After purification by flash column chromatography, basic hydrolysis of this acetamidoporphyrin produced the amino derivative (5-(4-aminophenyl)-10,15,20-tris(2,4,6-trimethoxyphenyl)porphyrin) and then potassium hydroxide activated the amino group for the coupling reaction with 1-chloro-2,6-dinitro-4-trifluoromethylbenzene to form the porphyrin dyad CF3. The absorption spectrum of CF3 is nearly identical to the previous amino derivative, indicating that both chromophores retain their individual identities in the ground state. Fluorescence emission of porphyrin in CF3 is diminished with a quenching efficiency of 0.48 by the attachment of the 2,6-dinitro-4-(trifluoromethylphenyl) group. Thus, a possible competitive excited singlet-state deactivation pathway occurs in CF3, which might involve a charge separation state.

Since CF3 is not soluble in aqueous solvents, the drug was incorporated into dipalmitoyl-phosphatidylcholine (DPPC) liposomes according to the injection procedure at 55°C (Ginevra *et al.*, 1990). CF3 was first dissolved in tetrahydrofuran (THF; Merck) at a concentration of 0.5 mg/ml and then mixed with DPPC (Sigma) in ethanol. CF3-liposomes in phosphate buffered saline (PBS) solution were dialyzed for 4 h in PBS, sterilized through a Millipore® filter (diameter 0.22 μm), diluted with DMEM–1% FCS to obtain adequate concentrations of CF3 and used within 48 h after preparation. The resulting concentration of the drug was estimated by absorbance at 420 nm (ε = 216 950 M^{-1} cm^{-1} in THF; FW = 1133). Thiazolyl blue [MTT; 3-(4,5-dimethylthiazol-

[2-yl])-2,5-diphenyl-tetrazolium bromide; Sigma] was used for cell viability studies. Other chemicals used were: *meso*-tetraphenylporphyrin (TPP), 9,10-dimethylanthracene (DMA) and Mowiol 40-88 (Aldrich); toluidine blue (TB), sodium dodecyl sulfate (SDS), glycerol and isopropanol (Merck); Hoechst 33258 (H-33258; Riedel-de Haën); paraformaldehyde (BDH); proteinase K (Sigma); DPX (Serva); and agarose, bromophenol blue and xylene cyanole (Bio-Rad).

Spectroscopy

Spectroscopic studies were performed to characterize photophysical properties of CF3 in THF. UV-visible and fluorescence spectra were recorded on a Shimadzu UV-2401PC spectrometer and on a Spex FluoroMax fluorometer, respectively. The fluorescence quantum yield (ϕ_F) of CF3 was calculated by comparison of the area below the corrected emission spectrum with that of TPP as a fluorescence standard under excitation at 550 nm. A value of $\phi_F = 0.10$ for TPP in THF was calculated by comparison with the fluorescence spectrum in toluene using $\phi_F = 0.11$ and taking into account the refractive index of the solvents. Photo-oxidation of DMA (which quenches $^1O_2$ by an exclusively chemical reaction) was used to determine the quantum yield ($\phi\Delta$) of $^1O_2$ production by CF3. Solutions of DMA (45 µM) and CF3 (absorbance 0.1, λ = 515 nm) in THF were irradiated with monochromatic light at λ = 515 nm. DMA photo-oxidation was measured by the decrease in absorbance at λ_{max} = 378 nm. The observed rate constants were obtained by a linear least-squares fit of the semilogarithmic plot of Ln A_0/A versus time. TPP in THF was used as the standard ($\phi\Delta$ = 0.62). Measurements of sample and reference under similar conditions afforded $\phi\Delta$ for CF3 by direct comparison of the slopes in the linear region of the plots.

Treatments

Hela cells were treated with either 5×10^{-7}, 10^{-6} or 5×10^{-6} M solutions of CF3 in liposomes and DMEM–1% FCS (hereafter simply CF3), for 3 or 18 h in the darkness. After washing, cells were allowed to grow in complete DMEM or subjected to light irradiation. Cell survival was assessed for CF3-treated and untreated (control) cultures. The surviving fraction of cells (*SF*) was evaluated 24 h after treatments using the MTT method. Briefly, MTT in DMEM was added to cell cultures at a final concentration of 50 µg/ml for 3 h; the reduced formazan was then extracted with DMSO and absorption measured at 540 nm.

Irradiation

Irradiation was performed using a Reflecta slide projector equipped with a 150 W lamp. The light was filtered through a 3 cm water layer to absorb heat and a violet-blue filter (360 < λ < 460 nm; light intensity at the irradiation site, 8 mW/cm^2). Measurements of light intensity were made with an M8 Spectrum Power energymeter. HeLa cells were irradiated for variable times immediately after CF3 treatments and *SF* values were evaluated by the MTT method 24 h after irradiation. The efficiency of photodynamic treatments was expressed as the cell lethality for each experimental condition, represented by the lethal dose (*LD*, in %; *LD* = 100 – *SF*). All the photodynamic treatments were repeated at least three times.

Microscopy and cell counting

Microscopic observations and photography were performed with an Olympus IMT2-RFA epifluorescence photomicroscope equipped with a HBO 100 W mercury lamp and ultraviolet (UV; 365 nm), violet-blue (436 nm) and blue (450–490 nm) excitation filters. Colour photomicrographs were taken on Ektachrome 160 ASA tungsten-balanced film (Kodak) and processed using Adobe Photoshop 5.0 (Adobe Systems) and PowerPoint 2000 software (Microsoft).

The localization of the drug in HeLa cells was analysed after 18 h incubation in culture medium (DMEM–1% FCS) containing 5×10^{-6} M CF3. Cells were washed and mounted with PBS and then observed under violet-blue exciting light. Changes in cell morphology were analysed using bright-field illumination, phase contrast and fluorescence microscopy. After fixation either with 3% (w/v) paraformaldehyde in PBS for 30 min or methanol at –20°C for 10 min, cells were stained with TB (0.5 mg/ml in distilled water, 0.5 min) for general morphology, or with H-33258 (10 µg/ml in distilled water, 5 min) for visualization of chromatin DNA. After washing and air drying, preparations were mounted in DPX and observed under bright-field (TB) or UV excitation (H-33258).

Mitotic index (MI) was determined using coverslips processed for immunofluorescence of microtubules (MT). Cells were fixed in methanol at –20°C for 5 min, followed by acetone (1 min) at room temperature and hydrated in graded ethanol–PBS solutions. Cells were incubated with mouse monoclonal antibody against α-tubulin (Sigma) for 1 h at 37°C, washed in PBS for 15 min and subjected to fluorescein isothiocyanate (FITC)-labelled rabbit anti-mouse IgG (Southern Biotechnology Associates) for 1 h at 37°C. After washing in PBS, preparations were mounted in 8% Mowiol–25% glycerol. Cells in mitosis were divided into prophase, metaphase and anaphase–telophase steps. Metaphases were also divided into normal and abnormal figures, depending on whether or not the spindle apparatus was clearly disturbed. About 3000 cells were counted for each MI value and 100 cells in division for distribution of phases within mitosis.

For evaluation of the proportion of cell detachment after photodynamic treatments, detached cells were obtained directly from the culture supernatants, whereas the remaining (attached) cells were scraped from the dishes. After centrifugation (1200 r.p.m.; rotor radius, 7 cm), each fraction was resuspended in 75 µl of PBS and cell counting was carried out using a hemocytometer.

DNA gel electrophoresis

For genomic DNA isolation, total or detached cells were collected from dishes as described above and washed twice with PBS. Cell pellets were resuspended in 0.5 ml of the lysis buffer (10 mM Tris–HCl, 10 mM EDTA, 200 mM NaCl, 0.2% SDS and 0.1 μg/μl of proteinase K) and incubated overnight at 37ºC. One volume of isopropanol was added to the lysate and the samples were mixed until DNA precipitation was complete (10–20 min). DNA samples were resuspended in TE buffer (10 mM Tris–HCl, 0.1 mM EDTA, pH 7.5) and electrophoresed for 3 h at 40 V using 1.5% agarose gels and TAE [40 mM Tris base (pH 7.6), 20 mM acetic acid, 1 mM EDTA] as electrophoresis buffer. Loading dyes were 0.25% bromophenol blue and 0.25% xylene cyanole in TAE containing 10% glycerol. After electrophoresis, gels were stained with ethidium bromide (2.5 μg/ml). The Bio-Rad size standards No. 170-3470 (λcI857 *Sam*7/*Hin*dIII) and No. 170-3465 (a mixture of pBR322/*Ava*I and pBR322/*Eco*RI/*Ava*II) were mixed (0.16 μg of each) and used as DNA mol. wt markers.

Results

Spectroscopy

CF3 showed a characteristic absorption spectrum which makes it suitable for irradiation with visible light, particularly at the intense Soret band (420 nm). Its absorption spectrum in THF was [λ_{max} (ε, M^{-1} cm^{-1})] 420 (216 950), 515 (14 270), 550 (5770), 592 (5110), 650 (2470). On account of the low absorption in the red spectral region, irradiation with red light was not used for photosensitization. CF3 in THF also showed a characteristic fluorescence emission (λ_{max} = 652 and 719 nm), with a fluorescence quantum yield of ϕ_F = 0.032. The production of $^1O_2$ by CF3 in THF showed a quantum yield of $\phi\Delta$ = 0.25.

Microscopic localization

Cellular localization of CF3 was analysed, on account of its red emission under fluorescence microscopy, using violet-blue exciting light. HeLa cells incubated for 18 h with 5 × 10^{-6} M CF3 showed the bright red fluorescence of the porphyrin mainly located as a granular signal in the cytoplasm (Figure 2). A weaker and diffuse red emission was also observed in the remaining cytoplasm. After continuous observation for several minutes, considerable fading of the fluorescence was found. The fluorescent granular signal of CF3 was entirely similar to that observed after lysosome labeling of HeLa cells with acridine orange and very different from the filamentous pattern of mitochondria labelled by rhodamine 123 (Cañete *et al.*, 2001). Therefore, lysosomes could be the main site of CF3 accumulation.

Dark toxicity

Cultured HeLa cells treated with 5 × 10^{-6} M CF3 for a short (3 h) or prolonged time (18 h), as well as irradiation with violet-blue light alone for 15 min, revealed no cell toxicity (Table I). Lower CF3 concentrations (5 × 10^{-7} and 10^{-6} M) used for 3 or 18 h in the absence of light were also non-toxic. Likewise, maintaining cells for 18 h in DMEM–1% FCS (the culture medium during incubation with CF3) did not affect cell viability.

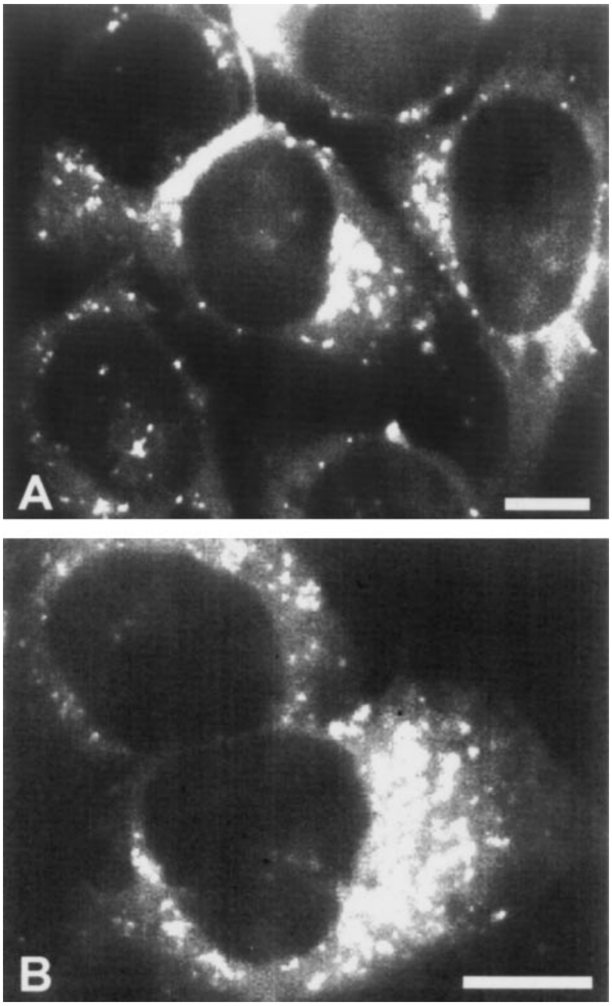

Figure 2

(A, B) Fluorescence micrographs of living HeLa cells showing the microscopic localization of CF3 immediately after incubation with the drug (5 × 10^{-6} M for 18 h). The fluorescent signal in lysosome-like granules and background cytoplasm is clearly observed. Violet-blue exciting light. Scale bars = 5 μm.

Photosensitization kinetics

Photosensitization of HeLa cells was analysed using 5 × 10^{-6} M CF3 for 3 or 18 h, followed by violet-blue light irradiation for variable times (3, 5, 7, 10 and 15 min; Figure 3). Photokilling and morphological changes were found to be mainly dependent on CF3 incubation and irradiation times. After 18 h incubation with 5 × 10^{-6} M CF3 and irradiation for 15 min, the surviving fraction of cells was very low (*SF* = 4%),

Table I

Dark toxicity and irradiation control

CF3 concentration	*Incubation time (h)*	*Violet-blue light irradiation (min)*	*Surviving fraction (% ± SD)*
–	–	–	100.0 ± 2.6
–	–	15	93.8 ± 5.2
5×10^{-6} M	3	–	98.8 ± 3.9
5×10^{-6} M	18	–	98.5 ± 3.3

Surviving fractions correspond to mean ± SD values from at least three different experiments.

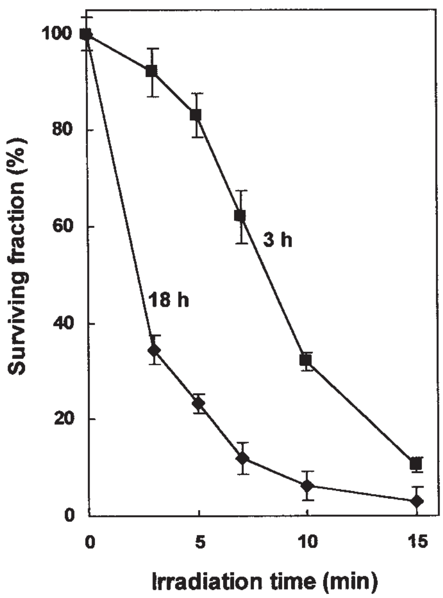

Figure 3

HeLa cell photosensitization by incubation in CF3 (5×10^{-6} M) for 3 h (■) or 18 h (◆), followed by irradiation with violet-blue light for variable times. Surviving fractions of cells (percentage of untreated controls) correspond to mean ± SD values from at least three different experiments.

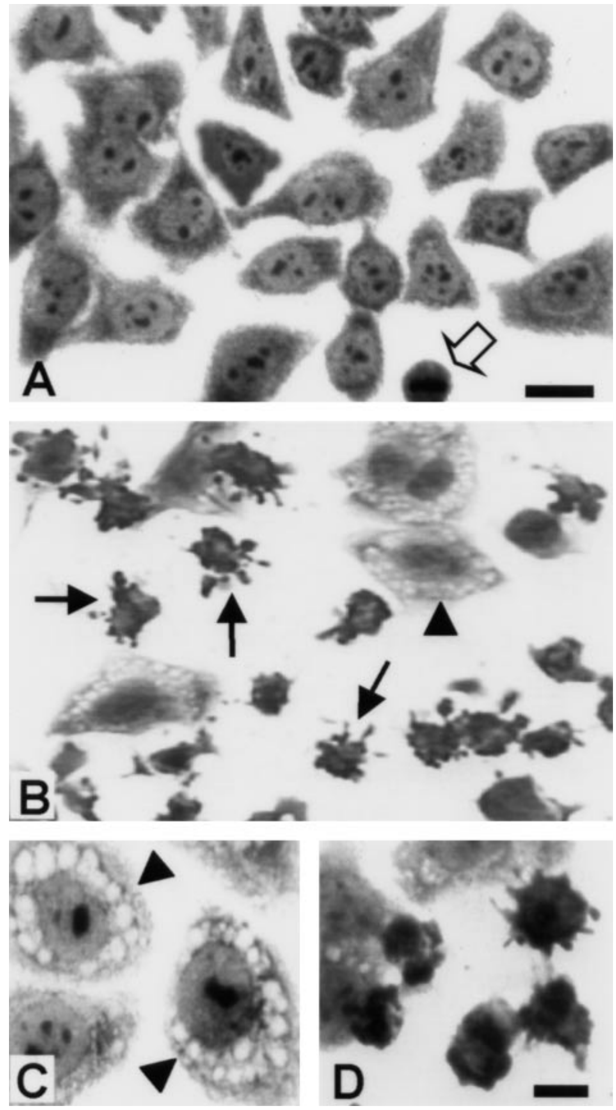

Figure 4

Morphology of HeLa cells after methanol fixation and TB staining. (A) Untreated (control) culture showing a mitotic figure (white arrow). (B–D) Cells incubated for 18 h with 5×10^{-6} M CF3 followed by 7 min of violet-blue light irradiation and observed 3 h later. Note the great amount of cells with a clear apoptotic morphology (D and arrows in B), as well as cytoplasmic vacuoles in other cells (arrowheads in B and C). Scale bars = 10 μm (A and B) and 5 μm (C and D).

thus resulting in a high cell lethality (LD_{96}). Irradiation for 5 or 7 min produced more cell survival (LD_{77} and LD_{85}, respectively), whereas cells incubated for only 3 h with 5×10^{-6} M CF3 and irradiated for 7 min showed high survival (sublethal treatment, LD_{38}).

When stained with TB or H-33258, characteristic morphological changes were found in photosensitized cells by incubation with 5×10^{-6} M CF3 for 18 h, revealing different cell death mechanisms depending on the irradiation time. Analysed 8 h after photodynamic treatments with 7 min irradiation, a great number of apoptotic cells (75.8 ± 8.3%) were obtained. This treatment resulted in an 85 ± 3% of cell lethality (LD_{85}; 'apoptotic' treatment). On the other hand, necrotic cells (89.2 ± 3.8%) were observed using the same drug concentration and incubation time, but with 15 min irradiation (LD_{96}; 'necrotic' treatment).

Apoptotic cell death was identified by the occurrence of cell rounding and shrinkage, projecting basophilic blebs (Figure 4B,D) and a typical chromatin fragmentation (Figure 6B,D). DNA fragmentation was confirmed by gel electrophoresis (see below). In addition to apoptotic cells, the remaining population corresponded to cells with an overall morphology very similar to controls, as well as cells with a variable number of perinuclear vacuoles (Figure 4B,C). HeLa cells subjected to LD_{96} conditions using 15 min irradiation immediately revealed deformations of the plasma membrane and massive production of small bubbles on the cell surface

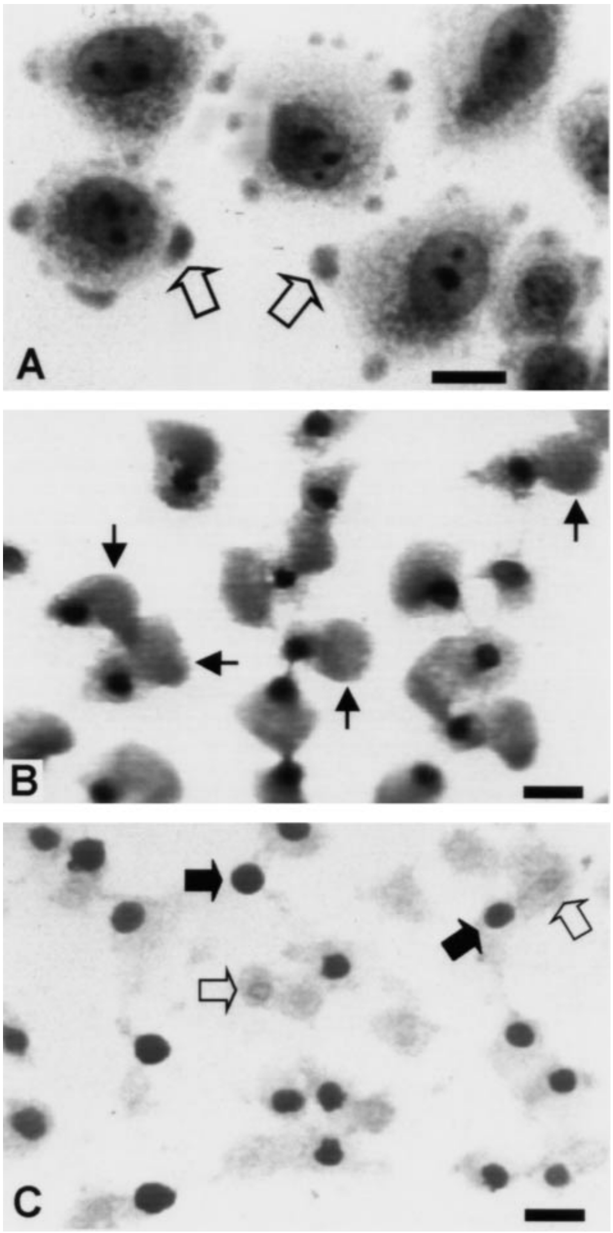

Figure 5

TB-stained HeLa cells previously subjected to CF3 (5×10^{-6} M, 18 h) and 15 min of violet-blue light irradiation. (A) Cells observed immediately after the photodynamic treatment (*LD*$_{96}$), showing numerous small bubbles (arrows). (B) Cells observed 1 h after the *LD*$_{96}$ treatment. Note the presence of giant bubbles (arrows). (C) Homogeneous nuclear condensation (black arrows) and nuclear ghosts (open arrows) 8 h after the *LD*$_{96}$ treatment. Scale bars = 10 μm.

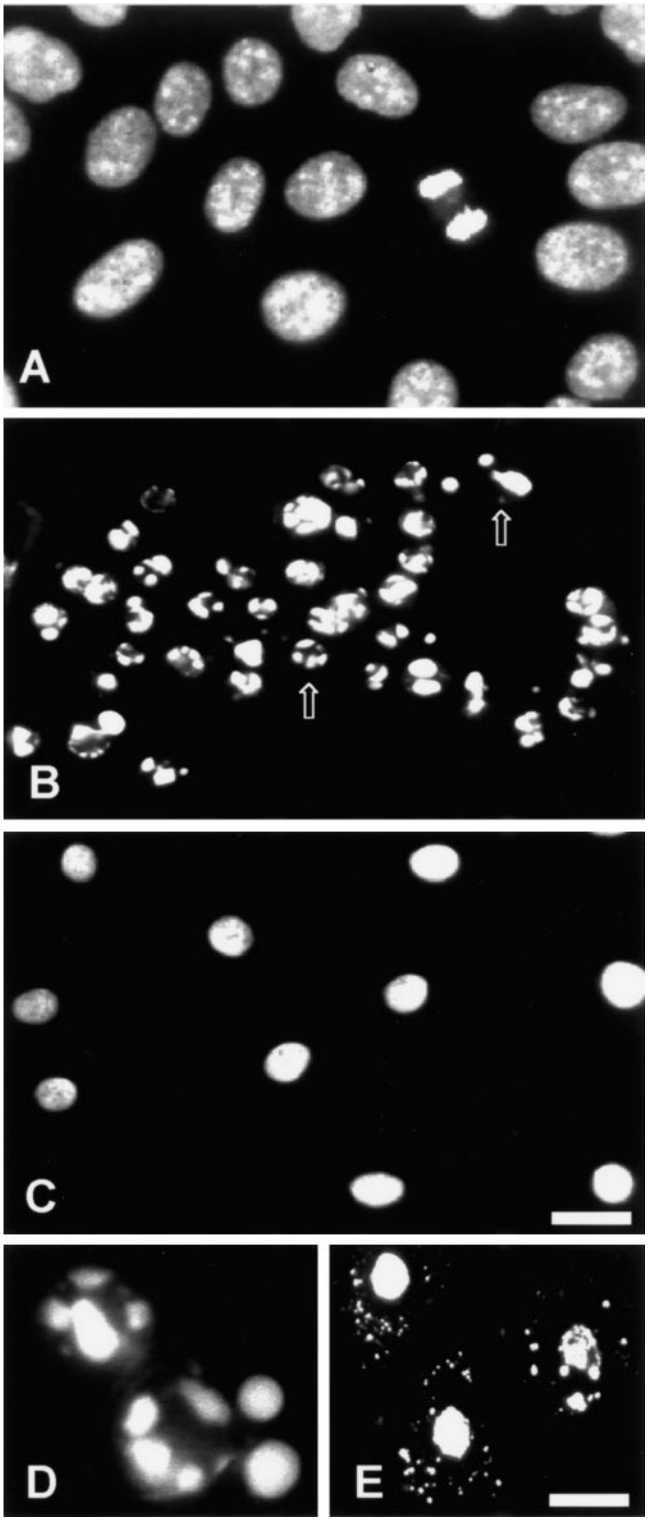

Figure 6

Fluorescence micrographs of HeLa cells stained with H-33258, showing characteristic morphological features. (A) Untreated (control) cells. (B, D) Detached cells showing apoptosis (arrows) 8 and 3 h, respectively, after an 'apoptotic' treatment (5×10^{-6} M for 18 h and 7 min of violet-blue light irradiation). (C, E) Necrotic cells 3 and 24 h, respectively, after an *LD*$_{96}$ treatment (5×10^{-6} M for 18 h and 15 min of violet-blue light irradiation). Scale bars = 10 μm.

(Figure 5A). These round cytoplasmic evaginations appeared dense and hyaline under phase-contrast optics and considerably basophilic after TB staining. After 1–3 h they fused into a giant bubble (Figure 5B) which finally detached from the cell.

The nuclear morphology was not affected immediately after *LD*$_{96}$ photodynamic treatments, but 1–3 h later nuclei

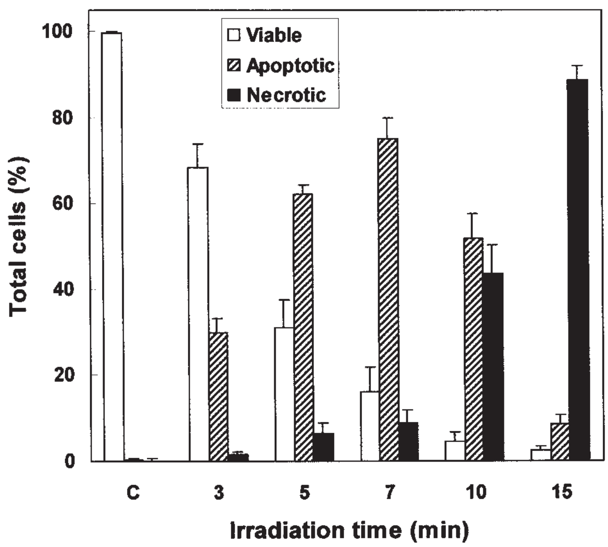

Figure 7

Evaluation of lethality mechanisms after incubation of HeLa cells with CF3 (5×10^{-6} M, 18 h) followed by different irradiation times with violet-blue light. Eight hours after photodynamic treatments, the numbers of viable, apoptotic and necrotic cells were determined according to morphological criteria in preparations stained with H-33258. Mean ± SD values from three different experiments are shown.

became homogeneously condensed (Figures 5B and 6C). The morphology of cells from a 'necrotic' treatment remained severely modified when they were additionally maintained in culture for some hours and then examined. Cell remnants with pycnotic nuclei, as well as cell ghosts, were predominantly observed 8 h later (Figure 5C). After 24 h, some necrotic cells stained with H-33258 showed variable numbers of small and brightly fluorescing chromatin-like bodies in the disorganized cytoplasm (Figure 6E).

In order to evaluate the kinetics of apoptotic and necrotic mechanisms for cell death, cultures were incubated for 18 h with 5×10^{-6} M CF3 and different irradiation times were then applied. Eight hours after photodynamic treatments, the proportions of viable, apoptotic and necrotic cells were determined by morphological criteria. As can be observed in Figure 7, the numbers of apoptotic and necrotic cells were clearly related to the irradiation time, with the maximum for apoptosis and necrosis being produced by 7 and 15 min irradiation, respectively. Both cell death mechanisms were present in similar proportions using 10 min irradiation. Interestingly, a growing number of detached cells were found from 3 to 7 min of irradiation, reaching with 7 min (the maximum for apoptosis) a value of 62 ± 6.5%, whereas the control value for detached cells in untreated cultures was 1%.

Mitotic arrest

As observed using immunofluorescent detection of tubulin, control interphase cells presented a wide MT network and a well-organized spindle apparatus in mitosis (Figure 8A).

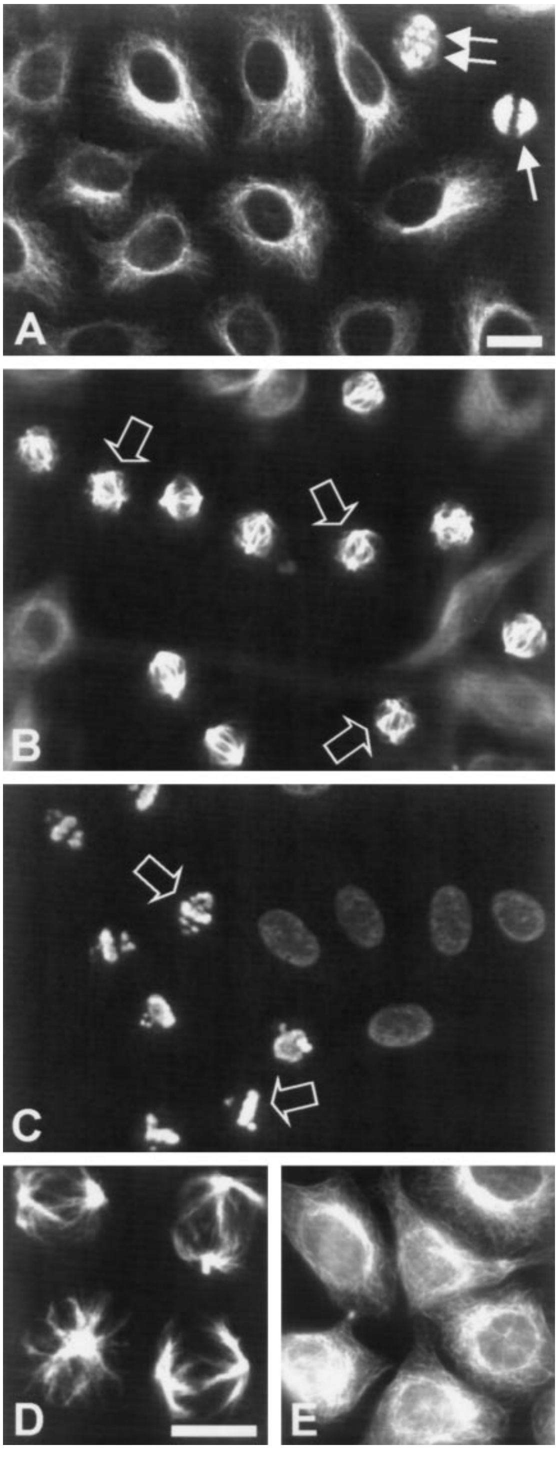

Figure 8

Immunofluorescent visualization of microtubules (A, B, D, E) and H-33258 staining of chromatin DNA (C) in HeLa cells. (A) Control culture showing metaphase (arrow) and anaphase cells (double arrow). (B, C) Metaphase blockage 18 h after incubation with CF3 (5×10^{-6} M for 3 h) followed by 7 min irradiation with violet-blue light. Arrows indicate abnormal metaphases observed either by immunofluorescence (B) or H-33258 staining (C). (D, E) Metaphase and interphase cells, respectively, from the same treatment as in (B), showing (D) abnormal mitotic spindles and (E) interphase cells with an apparently normal distribution of microtubules. Scale bars = 10 μm.

Incubation of cells with 5×10^{-6} M CF3 for 3 h followed by 5 or 7 min irradiation (LD_{17} and LD_{38}, respectively) produced a striking mitotic arrest 18 h later. The MI reached values of 21.3 ± 2.7 and 25.1 ± 1.8% using 5 and 7 min irradiation, respectively, the normal value of MI in control cultures being 4.6 ± 0.1%. The increase of mitotic cells following these sublethal treatments corresponded mainly to a metaphase blockage (Figure 8B,C). MT immunofluorescence allowed the identification of a great number of abnormal metaphases (i.e. cells with a disorganized mitotic spindle; Figure 8D), but the distribution of interphase MT was apparently not affected (Figure 8E). Under LD_{38} conditions, 51.5 ± 8.5 and 32 ± 8.9% of mitotic cells were normal and abnormal metaphases, respectively, whereas prophases, anaphases and telophases corresponded to 9.5 ± 2.7, 1.3 ± 0.6, and 5.7 ± 1.9%, respectively.

It is worth noting that 48 h after this metaphase blockage induced by LD_{38} treatments, cultures showed a great proportion of detached cells (76.8 ± 3.7%), with 83 ± 5.1, 16.8 ± 2.3 and 0.2 ± 3.4% of them being apoptotic, viable and necrotic cells, respectively. The remaining attached cells were viable.

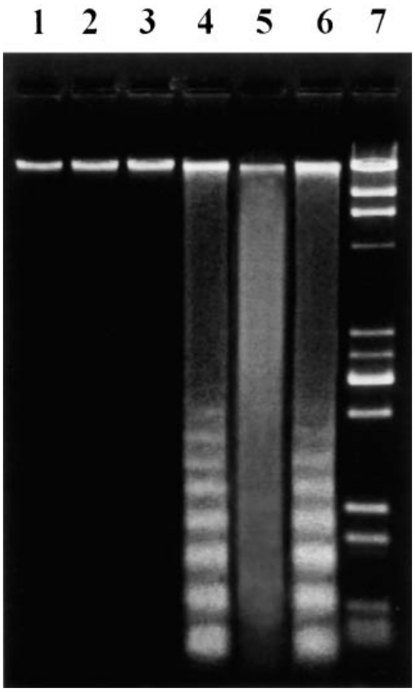

Figure 9

Gel electrophoresis of DNA from total cells (lanes 1–5) and detached cells (lane 6). Lane 1: untreated (control) cells. Lane 2: cells treated for 18 h with 5×10^{-6} M CF3 alone. Lane 3: cells exposed for 15 min to violet-blue light alone. Lane 4: cells 8 h after an 'apoptoptic' photodynamic treatment (5×10^{-6} M CF3 for 18 h and violet-blue light for 7 min). Lane 5: cells 24 h after a 'necrotic' photodynamic treatment (5×10^{-6} M CF3 for 18 h and violet-blue light for 15 min). Lane 6: cells 48 h after 3 h incubation with 5×10^{-6} M CF3 followed by violet-blue light for 7 min. Lane 7: DNA bands from the mol. wt marker.

DNA electrophoresis

As revealed by electrophoretic analysis, no DNA fragmentation was present in total cells from control cultures or in those subjected to treatments either with CF3 or violet-blue light alone (Figure 9, lanes 1–3). On the other hand, the fractions of detached cells collected either 8 h after an 'apoptoptic' (LD_{85}) treatment or 48 h after a sublethal (LD_{38}) treatment clearly showed the typical ladder pattern which characterizes the apoptotic (oligonucleosomal) DNA fragmentation (Figure 9, lanes 4 and 6). A homogeneous DNA smear was found from total cells 24 h after a 'necrotic' (LD_{96}) photodynamic treatment (Figure 9, lane 5).

Discussion

In the last few years, numerous research works concerning PDT have been centered in the study of new PSs with improved therapeutic efficiency. Among the analysed compounds, porphyrin derivatives have shown interesting photodynamic properties (Durantini, 2000; Yslas *et al.*, 2000; Harding, 2001). In the present work we show the results of photodynamic treatments with the recently described porphyrin derivative CF3 (Milanesio *et al.*, 2001) on cultured human tumour cells.

Dark toxicity of CF3 was not found even after long incubation (18 h) with the highest drug concentration used (5×10^{-6} M). The intracellular localization of CF3 was studied by fluorescence microscopy. A short incubation time (3 h) with CF3 (5×10^{-6} M) did not allow us to observe the intracellular localization of the drug, possibly because of its relatively low fluorescence quantum yield ($\phi_F = 0.032$). However, after 18 h incubation of HeLa cells with CF3, the red fluorescence was mainly localized in lysosome-like granules, although weak and diffuse red fluorescence was also found in the background cytoplasm. On account of this localization and the hydrophobic character of CF3, it is tempting to assume that the main photodamage induced by this porphyrin could take place at the level of lysosomes. In this respect, lysosomes have been described as targets for the photodynamic action of porphyrins and other PSs (Berg and Moan, 1994; Kessel *et al.*, 2000).

When incorporated into liposomes and in combination with light, CF3 was able to photoinactivate HeLa cells. The efficiency of photokilling was high and appeared related to both the porphyrin incubation time and light dose. The efficiency for HeLa cell photokilling by CF3 (LD_{96}) was similar to that of TPP (LD_{93}) (Cañete *et al.*, 1998), using for both PSs a concentration of 5×10^{-6} M in DPPC liposomes, 18 h incubation and 15 min irradiation with 8 mW/cm^2 violet-blue light (CF3) or 21 mW/cm^2 red light (TPP).

It is worth noting that using the same CF3 concentration (5×10^{-6} M) and incubation time (18 h), different photokilling mechanisms were observed, depending on the irradiation time. Thus, very high yields of apoptotic (75.8%) or necrotic (89.2%) cells were found using 7 or 15 min irradiation, respectively.

It is known that different cell damaging factors lead to cell death by means of apoptotic or necrotic mechanisms. Apoptosis is a regulated process which requires the active participation of specific molecules (e.g. caspases, Apaf-1). This type of cell death is characterized by shrinkage, deformation and external projections of the cell surface, integrity of the plasma membrane in the early stages, typical internucleosomal fragmentation of DNA and formation of apoptotic bodies. On the other hand, necrosis is produced as a cell response to severe and immediate damage, with disorganization and loss of the cell content (Villanueva *et al.*, 1999).

There are numerous publications concerning apoptotic cell death after PDT *in vivo* (Whitacre *et al.*, 2000; McGarrity *et al.*, 2001), contributing to an increasing interest in this therapeutic modality. Studies on the photodynamic induction of apoptosis in cultured cells are also abundant, but results are rather difficult to compare because of the heterogeneity of the experimental protocols (e.g. different cell lines, PSs and treatment doses).

It is accepted that the subcellular localization of the PS can influence the mechanism of cell death induced by PDT (Kessel *et al.* 1997; Kessel and Luo, 1998). PSs accumulated in mitochondria often produce rapid apoptotic responses (generally <4 h). This is an expected result, taking into account that (i) mitochondria play an important role in apoptosis and (ii) the action radius of $^1O_2$ is very short (~0.1 μm) and, therefore, cell targets must be close enough to the generation site. At present, several research groups on PDT are working on the identification of apoptotic pathways induced by photodynamic treatments with PSs with mitochondrial localization, such as silicon phthalocyanine (Pc 4) (Ahmad *et al.*, 1998), aluminum phthalocyanine (AlPc) (Kim *et al.*, 1999) and verteporfin (Granville *et al.*, 1998; Belzacq *et al.*, 2001). Detailed reviews of PDT-induced apoptotic signals, including the liberation of cytochrome *c* into the cytosol, the subsequent activation of caspases and the role of the Bcl-2 protein family, have been published (Oleinick and Evans, 1998; Granville *et al.*, 2001; Morgan and Oseroff, 2001).

It is worth noting that although the accumulation of PSs in other organelles (e.g. lysosomes) was at first considered to show lesser ability to trigger apoptotic responses (Kessel *et al.*, 1997), it is now accepted that PSs that localize in lysosomes are also efficient inductors of apoptosis, although in this case it occurs later (Noodt *et al.*, 1999; Villanueva *et al.*, 1999; Kessel and Poretz, 2000; Matroule *et al.*, 2001). Proteases released from the lysosomes, such as cathepsin B, could activate caspases directly or indirectly as a consequence of mitochondrial damage (Kessel *et al.*, 2000).

In this context, the new compound CF3, which shows a lysosome-like localization, would belong to the group of PSs with delayed apoptotic response. Morphological studies using TB and H-33258 staining (Figures 4 and 6) 8 h after LD_{85} treatments with CF3 revealed the alterations which are characteristic of apoptosis, such as cell shrinkage and rounding, nuclear fragmentation and loss of adhesion to the substrate (Villanueva *et al.*, 1999). It must be emphasized that cell counting after CF3 photodynamic treatments was performed on the whole culture and also included detached cells, an important strategy for the evaluation of apoptosis-inducing treatments. The detection of oligonucleosomal DNA fragments ('ladder' pattern) by gel electrophoresis (Figure 9) confirmed the occurrence of apoptosis 24 h after PDT with CF3 in HeLa cells.

Many PSs are able to induce apoptosis using only sublethal (~LD_{50}) photodynamic treatments (Luo *et al.*, 1996; Dahle *et al.*, 1999; Villanueva *et al.*, 1999). Interestingly, CF3 shows high efficiency for inducing cell death (85%) by apoptosis (75.8%) after LD_{85} treatments. This photodynamic property has also been described for other PSs such as Pc 4 (Ahmad *et al.*, 1998), ALA (Noodt *et al.*, 1996) and hypericin (Vantieghem *et al.*, 1998).

In contrast, photodynamic treatments with CF3 using longer irradiation times (15 min) result in a decrease of cell survival to 4% (LD_{96}). In this case, cell death occurs almost exclusively by a necrotic mechanism, in which the immediate alteration of the plasma membrane is the most conspicuous microscopical feature (Figure 5). Furthermore, DNA electrophoresis from cells subjected to LD_{96} treatments shows the homogeneous degradation ('smear' pattern) which characterizes cell death by necrosis (Figure 9).

Cell death by apoptosis or necrosis provoked by PDT seems to be dependent on several parameters, including drug concentration, incubation time, light dose and cell density (Vantieghem *et al.*, 1998; Villanueva *et al.*, 1999; Kessel and Poretz, 2000; Di Stefano *et al.*, 2001). Apoptosis or necrosis can be encountered following a similar initial insult (radiation, temperature, cytotoxic drugs, etc.) and the balance between both cell death mechanisms appears to depend upon the intensity of the injury. When the insult is applied at high intensity, immediate and irreversible damage which leads to cell necrosis is provoked. In this case, the rapid degradation of cell components is incompatible with the activation of biomolecules involved in the apoptotic pathway (Samali *et al.*, 1996).

On the other hand, short incubation times (3 h) with CF3 showed that 6 h after photodynamic treatments the cell cycle was blocked at the metaphase stage. The normal MI of untreated cells (4.6%) increased to reach a maximum value of 25.1% (mostly metaphase cells) 6 h after 7 min of irradiation. An abnormal mitotic spindle (Figure 8D) was observed in 32% of these metaphases. Some accumulation of CF3 in the background cytoplasm could be responsible for the photo-effects on MTs of the mitotic spindle, leading to striking changes in the MI. It is well known that MTs are cytoskeletal elements of great importance in the proliferation of cancer cells and that they are affected by photodynamic treatments (Berg and Moan, 1997; Juarranz *et al.*, 2001).

In this connection, Sporn and Foster (Sporn and Foster, 1992) have described the reversible or irreversible depolymerization of MTs induced by Photofrin in dependence on the light dose. Other PSs, such as some carbocyanine and thiazine dyes, zinc-phthalocyanine and tetraphenylporphycene, give a granular lysosome-like localization and also induce photodamage to MTs (Berg and Moan, 1997; Juarranz *et al*., 2001). For the porphyrin $TPPS_4$ it has been proposed (Berg and Moan, 1997) that free (non-polymerized) tubulin could be the cell target for cytotoxic actions induced by this lysosomal PS, but the precise mechanisms by which MTs are damaged by PDT are not yet known.

On the other hand, mitotic arrest is also related to cell death. MT-targeted drugs (e.g. taxols) are used as antitumour drugs and are associated with the triggering of apoptosis. Biochemical events leading to apoptosis are complex and vary among cell types (Jordan *et al.*, 1996; Blagosklonny, 1999; Wang *et al.*, 2000). In this respect, 48 h after the metaphase blockage induced by LD_{38} treatments with CF3, a great number of cells (76.8%) lost their adhesion to the substrate, with 83% of detached cells showing the characteristic apoptotic morphology. The typical ladder pattern observed by DNA electrophoresis confirmed the development of apoptosis in these cells. In agreement with our results, photodynamic treatments with the antitumour antibiotic cryptophycin 52 induced metaphase arrest and apoptosis 18 and 36 h later, respectively (Kessel and Luo, 2000).

From the results shown here, it can be concluded that the porphyrin derivative CF3 is a very promising PS. An attractive photobiological feature is its ability to inactivate cultured tumour cells with high efficiency by apoptotic or necrotic modes depending on the light dose. In addition, short incubation times are also able to block the cell cycle with metaphase arrest and posterior activation of apoptotic pathways. Taking into account that apoptosis, necrosis and MT photodamage are important aspects to be understood in relation to the biochemical mechanisms which lead to cell photokilling, it is obvious that CF3 photosensitization can constitute a useful tool for future research in PDT and tumour cell biology.

Acknowledgements

We thank G. Solarz for their valuable collaboration. This work was supported by a grant (PM98-0017-C0201) from the Dirección General de Investigación Científica y Técnica, Spain. J.C.S. is a scientific member of the Consejo Superior de Investigaciones Científicas (CSIC), Spain. E.N.D. and V.R. are researchers at the Consejo Nacional de Investigaciones Científicas y Técnicas, (CONICET), Argentina.

References

Ahmad N., Feyes D.K., Agarwal R., Mukhtar H. (1998) Photodynamic therapy results in induction of WAF1/CIP1/P21 leading to cell cycle arrest and apoptosis. *Proceedings of the National Academy of Sciences, USA*, **95**, 6977.

Ali H., Van Lier J.E. (1999) Metal complexes as photo- and radiosensitizers. *Chemical Reviews*, **99,** 2379.

Ando A., Kumadaki I. (1999) Progress on the syntheses of fluorine analogs of natural porphyrins potentially useful for the diagnosis and therapy of certain cancers. *Journal of Fluorine Chemistry*, **100**, 135.

Belzacq A.S., Jacotot E., Vieira H.L., Mistro D., Granville D.J., Xie Z., Reed J.C., Kroemer G., Brenner C. (2001) Apoptosis induction by the photosensitizer verteporfin: identification of mitochondrial adenine nucleotide translocator as a critical target. *Cancer Research*, **61**, 1260.

Berg K., Moan J. (1994) Lysosomes as photochemical targets. *International Journal of Cancer*, **59**, 814.

Berg K., Moan J. (1997) Lysosomes and microtubules as targets for photochemotherapy of cancer. *Photochemistry and Photobiology*, **65**, 403.

Blagosklonny M.V. (1999) A node between proliferation, apoptosis, and growth arrest. *Bioessays*, **21**, 704.

Boyle R.W., Rousseau J., Kudrevich S.V., Obochi M., Van Lier J.E. (1996) Hexadecafluorinated zinc phthalocyanine: photodynamic properties against the EMT-6 tumour in mice and pharmacokinetics using 65Zn as a radiotracer. *British Journal of Cancer*, **73**, 49.

Cañete M., Villanueva A., Dominguez V., Polo S., Juarranz A., Stockert J.C. (1998) Meso-tetraphenylporphyrin: photosensitizing properties and cytotoxic effects on cultured tumor cells. *International Journal of Oncology*, **13**, 497.

Cañete M., Juarranz A., Lopez-Nieva P., Alonso-Torcal C., Villanueva A., Stockert J.C. (2001) Fixation and permanent mounting of fluorescent probes after vital labelling of cultured cells. *Acta Histochemica*, **103**, 117.

Dahle J., Steen H.B., Moan J. (1999) The mode of cell death induced by photodynamic therapy treatment depends on cell density. *Photochemistry and Photobiology*, **70**, 363.

Di Stefano A., Ettorre A., Sbrana S., Giovani C., Neri P. (2001) Purpurin-18 in combination with light leads to apoptosis or necrosis in HL60 leukemia cells. *Photochemistry and Photobiology*, **73**, 290.

Durantini E.N. (2000) Synthesis of *meso*-nitrophenylporphyrins covalently linked to a polyphenylene chain bearing methoxy groups. *Journal of Porphyrins and Phthalocyanines*, **4**, 233.

Faustino M.A., Neves M.G., Cavaleiro J.A., Neumann M., Brauer H.D., Jori G. (2000) Meso-tetraphenylporphyrin dimer derivatives as potential photosensitizers in photodynamic therapy. Part 2. *Photochemistry and Photobiology*, **72**, 217.

Ginevra F., Biffanti S., Pagnan A., Biolo R., Reddi E., Jori G. (1990) Delivery of the tumour photosensitizer zinc(II)-phthalocyanine to serum proteins by different liposomes: studies *in vitro* and *in vivo*. *Cancer Letters*, **49**, 59.

Granville D.J., Carthy C.M., Jiang H., Shore G.C., McManus B.M., Hunt D.W. (1998) Rapid cytochrome *c* release, activation of caspases 3, 6, 7 and 8 followed by *Bap*31 cleavage in HeLa cells treated with photodynamic therapy. *FEBS Letters*, **437**, 5.

Granville D.J., McManus B.M., Hunt D.W. (2001) Photodynamic therapy: shedding light on the biochemical pathways regulating porphyrin-mediated cell death. *Histology and Histopathology*, **16**, 309.

Greenwald B.D. (2000) Photodynamic therapy for esophageal cancer. Update. *Chest Surgery Clinics of North America*, **10**, 625.

Harding S. (2001) Photodynamic therapy in the treatment of subfoveal choroidal neovascularisation. *Eye*, **15**, 407.

Jordan M.A., Wendell K., Gardiner S., Derry W.B., Copp H., Wilson L. (1996) Mitotic block induced in HeLa cells by low concentrations of paclitaxel (taxol) results in abnormal mitotic exit and apoptotic cell death. *Cancer Research*, **56**, 816.

Juarranz A., Espada J., Stockert J.C., Villanueva A., Polo S., Domínguez V., Cañete M. (2001) Photodamage induced by zinc(II)-phthalocyanine to microtubules, actin, α-actinin and keratin of HeLa cells. *Photochemistry and Photobiology*, **73**, 283.

Kalka K., Merk H., Mukhtar H. (2000) Photodynamic therapy in dermatology. *Journal of the American Academy of Dermatology*, **42**, 389.

Kessel D., Luo Y. (1998) Mitochondrial photodamage and PDT-induced apoptosis. *Journal of Photochemistry and Photobiology B: Biology*, **42**, 89.

Kessel D., Luo Y. (2000) Cells in cryptophycin-induced cell-cycle arrest are susceptible to apoptosis. *Cancer Letters*, **151**, 25.

Kessel D., Poretz R.D. (2000) Sites of photodamage induced by photodynamic therapy with a chlorine6 triacetoxymethyl ester (CAME). *Photochemistry and Photobiology*, **71**, 94.

Kessel D., Luo Y., Deng Y., Chang C.K. (1997) The role of subcellular localization in initiation of apoptosis by photodynamic therapy. *Photochemistry and Photobiology*, **65**, 422.

Kessel D., Luo Y., Mathieu P., Reiners J.J. Jr (2000) Determinants of the apoptotic response to lysosomal photodamage. *Photochemistry and Photobiology*, **71**, 196.

Kim H.R., Luo Y., Li G., Kessel D. (1999) Enhanced apoptotic response to photodynamic therapy after bcl-2 transfection. *Cancer Research*, **59**, 3429.

Luo Y., Chang C.K., Kessel D. (1996) Rapid initiation of apoptosis by photodynamic therapy. *Photochemistry and Photobiology*, **63**, 528.

McClinton M.A, McClinton D.A. (1992) Trifluoromethylations and related reactions in organic chemistry. *Tetrahedron*, **48**, 6555.

McGarrity T.J., Peiffer L.P., Granville D.J., Carthy C.M., Levy J.G., Khandelwal M., Hunt D.W. (2001) Apoptosis associated with esophageal adenocarcinoma: influence of photodynamic therapy. *Cancer Letters*, **163**, 33.

Matroule J.Y., Carthy C.M., Granville D.J., Jolois O., Hunt D.W., Piette J. (2001) Mechanism of colon cancer cell apoptosis mediated by pyropheophorbide-α methylester photosensitization. *Oncogene*, **20**, 4070.

Milanesio M.E., Moran F.S., Yslas E.I., Alvarez M.G., Rivarola V., Durantini E.N. (2001) Synthesis and biological evaluation of methoxyphenyl porphyrin derivatives as potential photodynamic agents. *Bioorganic and Medicinal Chemistry*, **9**, 1943.

Morgan J., Oseroff A.R. (2001) Mitochondria-based photodynamic anti-cancer therapy. *Advanced Drug Delivery Reviews*, **49**, 71.

Moser J.G. (ed.) (1998) *Photodynamic Tumor Therapy, 2nd and 3rd Generation Photosensitizers*. Harwood Academic: Amsterdam.

Noodt B.B., Berg K., Stokke T., Peng Q., Nesland J.M. (1996) Apoptosis and necrosis induced with light and 5-aminolaevulinic acid-derived protoporphyrin IX. *British Journal of Cancer*, **74**, 22.

Noodt B.B., Berg K., Stokke T., Peng Q., Nesland J.M. (1999) Different apoptotic pathways are induced from various intracellular sites by tetraphenylporphyrins and light. *British Journal of Cancer*, **79**, 72.

Oleinick N.L., Evans H.H. (1998) The photobiology of photodynamic therapy: cellular targets and mechanisms. *Radiation Research*, **150**, S146.

Ost D. (2000) Photodynamic therapy in lung cancer. *Oncology*, **14**, 379.

Samali A., Gorman A.M., Cotter T.G. (1996) Apoptosis—the story so far . . . *Experientia*, **52**, 933.

Sporn L.A., Foster T.H. (1992). Photofrin and light induces microtubule depolymerization in cultured human endothelial cells. *Cancer Research*, **52**, 3443.

Tatman D., Liddell P.A., Moore T.A., Gust D., Moore A.L. (1998) Carotenohematoporphyrins as tumor-imaging dyes. Synthesis and *in vitro* photophysical characterization. *Photochemistry and Photobiology*, **68**, 59.

Vantieghem A., Assefa Z., Vandenabeele P., Declercq W., Courtois S., Vandenheede J.R., Merlevede W., De Witte P., Agostinis P. (1998) Hypericin-induced photosensitization of HeLa cells leads to apoptosis or necrosis. *FEBS Letters*, **440**, 19.

Villanueva A., Domínguez V., Polo S., Vendrell V., Sanz C., Cañete M., Juarranz A., Stockert J.C. (1999) Photokilling mechanisms induced by Zinc (II)-phthalocyanine on cultured tumor cells. *Oncology Research*, **11**, 447.

Wang T.H., Wang H.S., Soong Y.K. (2000) Paclitaxel-induced cell death: where the cell cycle and apoptosis come together. *Cancer*, **88**, 2619.

Whitacre C.M., Feyes D.K., Satoh T., Grossmann J., Mulvihill J.W., Mukhtar H., Oleinick N.L. (2000) Photodynamic therapy with the phthalocyanine photosensitizer Pc 4 of SW480 human colon cancer xenografts in athymic mice. *Clinical Cancer Research*, **6**, 2021.

Yslas I., Alvarez M.G., Marty C., Mori G., Durantini E.N., Rivarola V. (2000) Expression of Fas antigen and apoptosis caused by 5,10,15,20-tetra(4-methoxyphenyl)porphyrin (TMP) on carcinoma cells: implication for photodynamic therapy. *Toxicology*, **149**, 69.

Artículo 2:

La sensibilización fototérmica como nueva herramienta terapéutica contra tumores: estudios a nivel celular y animal

European Journal of Cancer 41: 1203-1212 (2005)

La Terapia Fototérmica del cáncer (PTT) ha sido recientemente propuesta como herramienta terapéutica. El presente estudio ha supuesto el primer análisis en profundidad de sus capacidades frente a células tumorales en cultivo y a tumores *in vivo*. Se empleó el cromóforo naftalocianina de níquel, NiNc, que reúne todas las características de un fotosensibilizador fototérmico (no produce $^1O_2$, absorbe en el infrarrojo, es capaz de agregarse etc.) que se administra en un preparado de liposomas de DPPC, por ser altamente hidrófoba.

La primera fase de estudio se realizó en distintos tipos celulares en cultivo, tanto tumorales como no tumorales, derivadas de ratón y de seres humanos (líneas B78H1, C32, HT-1080 y HaCaT). Los estudios de incorporación del PS mostraron un incremento en función de la concentración y del tiempo de incubación. A partir de estos datos se seleccionaron dos protocolos de incubación (7,7 µM durante 18 h y 5,1 µM durante 48 h) que permiten acumulaciones intracelulares de NiNc similares, para cada línea celular individualmente, de manera que se revelasen los efectos debidos exclusivamente al tiempo de incubación en la localización y el estado de agregación del fármaco. Con este procedimiento se observó la agregación de la droga a tiempos de incubación largos en la línea B78H1. Este proceso se corresponde con la relocalización de la droga en una gran área concreta, cercana al núcleo, desde el conjunto de vesículas que se observaban a tiempos cortos. En C32 la droga se muestra siempre agregada y concentrada en dicha estructura próxima al núcleo (y que podría corresponderse con el aparato de Golgi). En las otras dos líneas celulares la NiNc no mostraba agregación ni relocalización a lo largo del tiempo de incubación, distribuyéndose en pequeñas vesículas dispersas por todo el citoplasma.

La irradiación (de 1 a 20 min) se realizó con las células tripsinazadas y mantenidas en suero fetal bovino dentro de una cubeta de cuarzo, bajo agitación magnética, empleando un láser de Ti:zafiro en un régimen de pulsos de 30 ns (10 Hz) con una energía de 120 mJ/pulso. La supervivencia al tratamiento se evaluó una hora después de realizada la irradiación, por el test de exclusión del Azul Tripán. Los estudios de supervivencia confirmaron que las máximas cotas de mortalidad (que alcanzan la práctica totalidad del cultivo) se correspondían a las líneas y condiciones en las que el agente fototérmico se encontraba agregado en una única gran estructura, sin que la concentración intracelular de NiNc pareciera intervenir decisivamente.

Asimismo, se realizaron observaciones al microscopio electrónico de barrido (SEM) de las células tratadas (y de los correspondientes controles: absoluto, incubado en oscuridad e irradiado sin cromóforo) que mostraron que las células muertas presentan profundas cavidades en su interior. Estas cavidades son producidas por la eyección de grandes masas citoplasmáticas como resultado del tratamiento. Dichas lesiones se corresponden con las descritas previamente como definitorias de la necrosis (ya que la muerte se verifica mediante una drástica rotura de la membrana plasmática). Entre las células sometidas a menores tiempos de irradiación se pueden encontrar ejemplos de dicha expulsión de material que, al ser observados en microscopía óptica de campo claro, evidenciaban que entre los materiales eyectados se encontraba el área donde se acumulaba la NiNc. Este fenómeno sugiere que la eyección es el resultado de la onda de choque térmico producida por la reacción fototérmica.

La segunda fase del estudio consistió en inducir tumores subcutáneos en ratones C57BL/6 mediante la inyección de un millón de células de melanoma amelanótico murino B78H1. Una vez desarrollado el tumor, unas dos semanas tras la inyección, se procedió a inyectar la NiNc en una concentración de 1,8 mg/Kg de masa corporal. Transcurridas 24 h para permitir la incorporación de la NiNc por el tumor, se procedió a anestesiar a los animales con ketamina antes de someterlos a irradiación durante 140 s (con pulsos de 30 ns y una energía de 100 mJ/pulso). Mediante una cámara térmica se midió un incremento de la temperatura en el área irradiada, que alcanzó los 105 ºC, en presencia del cromóforo (en su ausencia sólo hasta los 48 ºC); la temperatura se recuperaba un minuto después de la irradiación. La irradiación provocaba una herida necrosada que generaba una costra, la cual se curaba en aproximadamente en una semana (demostrando que las áreas adyacentes al tumor sólo se ven afectadas de manera colateral). Tras aproximadamente 20 días, en los cuales no se apreciaba recrecimiento tumoral, éste volvió a ser visible (no se verificó ningún caso de regresión total).

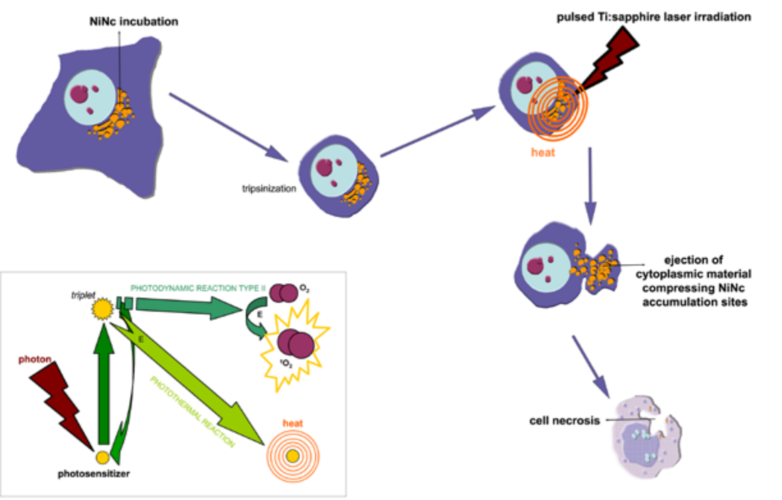

Figure 10 NiNc-linked photothermal killing. Albeit PDT and PTT are based on the same physico-chemical principle, the final outcome is clearly different as thermal PSs don't transfer the photon energy to oxygen and returns to the basal state by dissipation as heat *(box)*. Photothermal killing induced by intracellular NiNc laser irradiation could be seen as a necrotic process, as a large amount of cytoplasmic material (compressing the areas with the PS) is ejected by the thermal shockwave, causing plasma membrane disruption.

Tomados en conjunto, estos experimentos apoyan las posibilidades antitumorales de la PTT, tanto de forma aislada como combinada con otras terapias.

ELSEVIER

European Journal of Cancer 41 (2005) 1203–1212

European Journal of Cancer

www.ejconline.com

Photothermal sensitisation as a novel therapeutic approach for tumours: Studies at the cellular and animal level

Monica Camerin [a], Santiago Rello [b], Angeles Villanueva [b], Xinzhan Ping [c], Malcolm E. Kenney [c], Michael A.J. Rodgers [d], Giulio Jori [a,*]

[a] Department of Biology, University of Padova, Via Ugo Bassi 58 B, 35121 Padova, Italy
[b] Department of Biology, University of Madrid, Spain
[c] Department of Chemistry, Case Western Reserve University, Cleveland, OH, USA
[d] Department of Chemistry, Bowling Green State University, Bowling Green, OH, USA

Received 16 December 2004; received in revised form 27 January 2005; accepted 2 February 2005
Available online 18 April 2005

Abstract

Irradiation of B78H1 murine amelanotic melanoma cells with 850 nm light emitted from a Ti:sapphire laser, operated in a pulsed mode at high fluence rates and in the presence of Ni(II)-octabutoxy-naphthalocyanine (NiNc), promoted a photothermally sensitised process leading to fast and irreversible cell death. This resulted in the ejection of a consistent mass of cytoplasmic material from the irradiated cells that was detected by scanning electron microscopy. The extensive chemical and mechanical damage was probably caused by the photoinduced generation of an acoustic shock wave. The efficiency of the photoprocess was modulated by intracellular concentration of NiNc and maximally by the formation of aggregated naphthalocyanine clusters in specific subcellular areas. Very similar results were obtained upon irradiation of NiNc-loaded C32 human amelanotic melanoma cells and transformed murine HT-1080 and HaCaT fibroblasts. From these results, photothermal sensitisation appears to be a general phenomenon and preliminary studies with mice bearing subcutaneously transplanted amelanotic melanomas, irradiated with 850 nm light 24 h after intravenous injection of NiNc, suggest that this approach has potential for the therapy of some types of skin tumours.

Keywords: Phototherapy; Photothermal; Photosensitisation; Pulsed irradiation; Lasers; Naphthalocyanines; Tumours; Amelanotic melanoma

1. Introduction

Photodynamic therapy (PDT) is becoming an established treatment for selected neoplastic lesions, especially after the recent approval by the Food and Drugs Administration USA, of Photofrin-based PDT [1] and the advent of 5-amino-levulinic acid (ALA). ALA is a prodrug that generates the photosensitising agent protoporphyrin IX in tumour cells through the stimulation of endogenous metabolic processes [2]. So far, the majority of thousands of patients that have been treated with PDT have objectively benefited from the therapy [3]. At the same time, PDT is also being considered as a treatment tool for several cutaneous diseases [4], microbial infections [5], and the prevention of restenosis after balloon angioplasty [6]. The introduction of second-generation photosensitising agents, with superior photophysical and pharmacokinetic properties compared with porphyrins, is also increasing the potential of PDT as a treatment choice [7]. In spite of these positive features, some limitations appear to be associated with PDT [1,2], which can be partially overcome by

* Corresponding author. Tel.: +39 049 8276333; fax: +39 049 8276344.
E-mail address: jori@bio.unipd.it (G. Jori).

0959-8049/$ - see front matter
doi:10.1016/j.ejca.2005.02.021

combining it with other therapeutics such as chemotherapy [8] or radiotherapy [9].

Recently, we proposed a variant of PDT, namely photothermal therapy (PTT), as a novel approach for the treatment of tumours [10]. The approach is based on the promotion of photothermally sensitised processes in tumour cells or tissues. In general, photothermal processes reflect the tendency of a light-absorbing species to dissipate electronic excitation energy via a rapid cascade through vibrational modes resulting in increased kinetic energy of the matrix species around the chromophore, i.e., to heat the local environment. The temperature rise can reach 130 °C above the basal value [11]. Under these conditions, water molecules tend to vaporize setting up an acoustic shock wave that propagates through the medium causing both mechanical and chemical alterations in the system. In some molecular absorbers, radiationless decay to the ground state and heat generation occur on a picosecond time scale [12]. Using laser pulses of high fluence rates (e.g., 1 J cm^{-2} in 10 ns) allows the possibility of absorption of other photons in the same volume before the first temperature spike has suffered much dissipation. This then creates the conditions for increased shock wave activity and subsequent damage to cell/tissue components. These effects could be further potentiated in biological systems when suitable chromophores are present at high local concentrations due to aggregation or compartmentalisation. Simultaneous photoexcitation events could lead to two or more thermal spikes in close proximity with concomitant generation of more vigorous shock waves and greater damage. A few endogenous constituents of cells and tissues, such as melanin and oxyhemoglobin, can act as starting points for the promotion of photothermal processes, and this property has been used in clinical practice for the fading of cutaneous lesions such as nevi or *café-au-lait* macules [13] or the removal of port-wine stains [14]. However, the scope of photothermal sensitisation is not necessarily limited to the treatment of diseased tissues containing natural chromophores. Dyes such as cyanines, azo-dyes, triphenylmethane derivatives and porphyrins coordinated with transition metal ions exhibit photophysical features that are suitable for photothermal sensitisation [15]. The introduction of exogenous photothermally acting chromophores that localise preferentially in diseased tissues could provide a novel therapeutic approach. Indeed, photothermal therapy of cancer lesions using a combination of *in situ* administered indocyanine green and a near-infrared laser has been previously described [16,17].

The available lines of evidence suggest that PTT [10,15] could have either specific applications or act synergistically with PDT. In PDT, where photogenerated hyper-reactive oxygen species are the main cytotoxic intermediates, cell death is less efficient in tumours that are poorly vascularised, owing to insufficient oxygen levels in the neoplastic tissue [18]. However, in PDT photothermal sensitisers appear to efficiently induce malignant cell death even in the absence of oxygen [19]. Furthermore, PTT can also be usefully applied [20] in cases of highly pigmented tumours, such as melanotic melanoma, where PDT yields unsatisfactory results due to light-filtration by melanin [1,3]. In view of the clinical potential for PTT, it is important to investigate the mechanisms by which photothermal sensitisation acts at the cellular and tissue level. In this paper, we present the first set of observations on the processes involved in the photothermal inactivation of tumour cells sensitised by Ni(II)-octabutoxy-naphthalocyanine (NiNc) *in vitro* and *in vivo*. This naphthalocyanine (Fig. 1) is endowed with favourable properties to act as a photothermal sensitizer [15], including a large molar extinction coefficient in the 800–850 nm spectral region where most human tissues exhibit a high relative transparency to light [21], a very short lifetime of the electronically excited states, an efficient conversion of electronic into thermal energy and a high affinity for tumour cells that is typical of several phthalo- and naphthalo-cyanines [22].

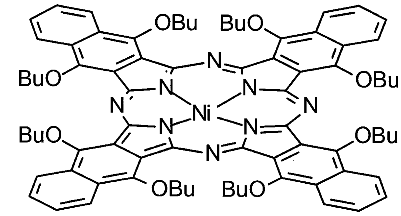

Fig. 1. Chemical structure of Ni(II)-5,9,14,18,23,27,32,36-octabutoxy-2,3-naphthalocyanine (NiNc).

2. Materials and methods

2.1. Photosensitizer and liposomal formulation

Ni(II)-5,9,14,18,23,27,32,36-octabutoxy-2,3-naphthalocyanine (NiNc) was prepared according to standard methods [23] and its purity was found to be greater than 98% by elemental analysis and NMR. The naphthalocyanine concentration was determined spectrophotometrically using an extinction coefficient of 280 000 M^{-1} cm^{-1} at 848 nm in tetrahydrofuran [24]. NiNc was added to the cells or injected *in vivo* after incorporation into small unilamellar vesicles of DL-α-dipalmitoyl-phosphatidyl-choline (DPPC, Sigma, 99% pure), which were prepared according to a modified protocol of the ethanol injection procedure developed by Kremer and colleagues [25]. Typically, 0.75 ml of an ethanol–tetrahydrofuran binary mixture (1:1, v/v), which was 9.56 mM in DPPC and 0.27 mM in NiNc, was injected into 10 ml of a 0.9% (w/v) aqueous solution of NaCl regulated at 55 °C. The NiNc appeared to be in a purely monomeric state inside the liposomes and the suspension thus obtained was stable for at least 24 h as judged by the lack of appreciable variations in the visible absorption spectrum.

2.2. Studies of cell accumulation and subcellular distribution

Four tumour cell lines, as shown in Table 1, were studied. B78H1, HT-1080 and HaCaT cells were grown in Dulbecco's modified minimal essential medium (D-MEM, Sigma) containing 10% heat-inactivated foetal calf serum (FCS, Boehringer, Mannheim, Germany) and supplemented with 100 units/ml penicillin, 100 μg/ml streptomycin and 0.25 μg/ml amphotericin. C32 cells were grown under identical conditions but using minimal essential medium containing non-essential amino acids (Gibco). The cell lines were routinely checked for the absence of mycoplasma contamination.

For photosensitizer accumulation studies, $2.5–5 \times 10^5$ cells after 24 h seeding in 25 cm^2 Falcon flasks (Falcon, Lincoln Park, NJ) were added with the incubation medium containing 3% FCS, as well as with predetermined NiNc concentrations in DPPC liposomes and incubated for 18 or 48 h at 37 °C in a dark humid atmosphere containing 5% CO_2. At the end of the incubation period, the medium was removed and the cell monolayer was carefully washed three times with cold phosphate-buffered saline (PBS). The trypsinised cells were centrifuged, resuspended in 0.5 ml of 2% aqueous sodium dodecyl sulphate (SDS, Prolabo, Fontenay-sous-Bois, France) and magnetically stirred for 1 h at room temperature. Each sample was subdivided into two portions: 0.2 ml was stored for protein determination by the bicinchoninic acid (BCA) assay [26], while 0.3 ml was analysed spectrophotometrically by recording the absorption spectrum in the 500–950 nm range. The naphthalocyanine recovery was expressed as nanomoles of photosensitizer per mg of protein after calculation from a calibration curve. Previous investigations [24] showed that this procedure yielded a quantitative extraction of the naphthalocyanine into the surfactant micelles.

In order to investigate the subcellular distribution of NiNc, the naphthalocyanine-loaded cells were layered on a cover glass and observed by an optical microscope (Zeiss) in a clear field. The analysis was performed with cell samples that had been incubated with NiNc for 18 or 48 h. The location of NiNc was identified by the appearance of yellowish-brown spots. The spots were attributed to NiNc since (a) no such spots were detectable in cells that had not been incubated with the naphthalocyanine and (b) the colour intensity and number of spots increased with increasing intracellular NiNc concentration.

2.3. Cell photosensitisation studies

The photothermal sensitisation studies with NiNc-incubated and control unsensitised cells were performed by means of a Q-switched Ti:sapphire laser tuned at 850 nm and operated in a pulsed mode (30 ns pulses, 10 Hz) with an energy of 120 mJ/pulse. Typically, the cells were seeded and incubated in 25 cm^2 flasks as described above. After incubation with NiNc, the flasks were rinsed once with Ca^{2+}- and Mg^{2+}-free PBS and treated with an aqueous solution (0.6 ml) containing 0.05% trypsin and 0.02% EDTA (Seromed, Berlin). The action of trypsin was stopped by addition of FCS (0.6 ml) and the cell suspension was collected in a 1-cm quartz cuvette and irradiated under gentle magnetic stirring for different time intervals. At the end of irradiation, cell survival was determined by trypan blue exclusion test [27]. The control and photothermally sensitised cells were fixed in 3% glutaraldehyde, post-fixed in 1% osmium tetroxide and dehydrated by graded ethanol solutions. The specimens were gold-coated to improve the resolution and analysed with a scanning electron microscope (Phillips XL30/EDAX DX4i).

2.4. Studies on tumour-bearing mice

Female C57/BL6 mice (20–22 g body weight, supplied by Charles River, Como, Italy) were subcutaneously injected in the upper flank with 10^6 amelanotic melanoma cells (B78H1) suspended in 20 μl sterile D-MEM. At about 15 days after cell implantation, when the tumour diameter was in the 0.4–0.6 cm range, the mice (at least five mice per group) were injected in the caudal vein with DPPC liposome-incorporated NiNc (1.8 mg/kg body

Table 1
Accumulation and physical state of NiNc in selected cell lines under different incubation conditions

Cell line	Characteristics	Recovery		Predominant state	
		A	B	A	B
B78H1	Amelanotic melanoma, murine	3.06 ± 0.06	3.31 ± 0.19	Monomer	Aggregated
C32	Amelanotic melanoma, human	10.88 ± 0.97	11.74 ± 0.41	Aggregated	Aggregated
HT-1080	Transformed fibroblasts, murine	6.95 ± 0.56	8.14 ± 0.53	Monomer	Monomer
HaCaT	Transformed keratinocytes, murine	13.87 ± 0.40	6.02 ± 0.50	Monomer	Monomer

NiNc = Ni(II)-5,9,14,18,23,27,32,36-octabutoxy-2,3-naphthalocyanine.
Incubation conditions: A = NiNc 7.7 μM, 18 h; B = NiNc 5.1 μM, 48 h. Recoveries are expressed as nmol NiNc/mg of cell protein. The monomeric/aggregated state of the NiNc was probed by absorption spectroscopy of cell-bound naphthalocyanine (see Figs. 3(a) and (b)).

weight). In all cases, the mice were kept in standard cages with free access to tap water and normal dietary chow. At 24 h after injection, the tumour area was irradiated for 140 s by the Ti:sapphire laser (30 ns pulses, 10 Hz, 100 mJ/pulse). An identical irradiation protocol was used for a group of tumour-bearing mice that had not received NiNc. The tumour response was assessed by following the rate of amelanotic melanoma growth as a function of post-irradiation time using a calliper to measure the volume of the lesion at daily intervals. Individual tumour volumes were calculated assuming a hemiellipsoidal structure for the tumour nodule and measuring the two perpendicular axes (a and b) and the height (c). Tumour volume was obtained by the relationship $V = 4/3\pi(a/2 \times b/2 \times c/2)$. The mice were sacrificed when the tumour volume approached 20% of the mouse body weight in line with the rules established by the University of Padova ethical committee for humane treatment of experimental animals. No case had a spontaneous regression of the transplanted tumour.

2.5. Statistical analysis

All data are reported as means ± standard deviation (s.d).

3. Results

3.1. Naphthalocyanine uptake by cells

The uptake of NiNc by B78H1 amelanotic melanoma cells as a function of the naphthalocyanine concentration after 18 and 48 h incubation periods was tested. Clearly, the amount of cell-bound NiNc steadily increased up to at least 7.7 μM, which was the highest test concentration used at both incubation times (Fig. 2).

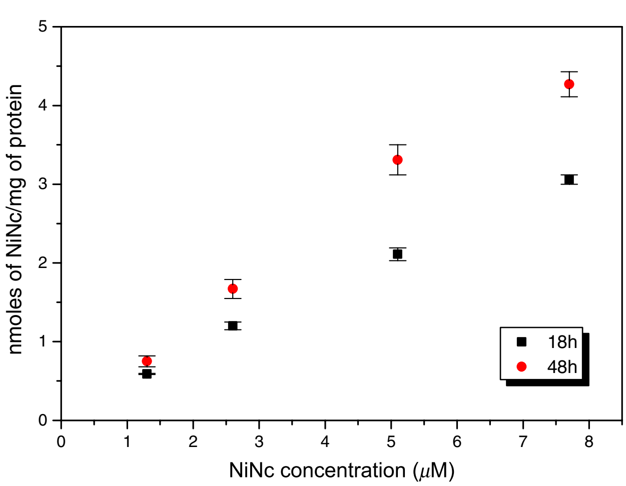

Fig. 2. Effect of NiNc concentration on the accumulation of the naphthalocyanine by B78H1 cells after 18 and 48 h incubation.

This behaviour was observed for several transformed murine (B78H1, HT-1080, HaCaT) or human (C32) cell lines and similar intracellular concentrations were obtained upon incubation of the different cells for 18/48 h with 5.1 or 7.7 μM NiNc. One notable exception was the results from HaCaT cells, where approximately 50% lower recovery of NiNc was obtained from the 48 h incubated sample (Table 1). In no sample did the naphthalocyanine-loaded cells undergo any appreciable decreases in survival and indicated that NiNc caused no toxic effects on the various cell types in the dark.

In 18 h incubated B78H1 cells, NiNc appeared to be largely monomeric, as shown by the clearly resolved Q-band in the visible absorption spectrum obtained from readings of the naphthalocyanine-loaded cells against a sample of non-incubated cells (Fig. 3(a)). This band underwent a bathochromic shift and a marked broadening after 48 h incubation period (Fig. 3(b)), which suggested a spectral pattern typical of aggregated naphthalocyanines [28]. The flat tetraaza-benzoisoindole macrocycle is known to favour the formation of stacked or pseudomicellar naphthalocyanine complexes as a result of hydrophobic and π–π interactions, especially in relatively polar microenvironments. The oligomerisation process can be further favoured by the trend of the cell-bound naphthalocyanine molecules to gradually partition to specific subcellular regions. This was clearly demonstrated by optical microscope analysis of NiNc-incubated B78H1 cells, where the pattern of photosensitiser distribution was identified by the presence of typical NiNc dark yellow spots that were absent in control cells (Fig. 4(a_1)). In 18 h incubated B78H1 cells, the spots were seen throughout the cell except the nucleus (Fig. 4(a_2)) and confirmed the observation that naphthalocyanines preferentially partitioned to subcellular membranes [29]. After 48 h incubation, the spots increased in size and were often concentrated in limited cellular areas for most detectable cells, a process that should facilitate the stacking of the photosensitizer molecules (Fig. 4(a_3)). The extent and kinetics of NiNc distribution differed for different cell types. For amelanotic melanoma C32 cells (Fig. 4(b)), a significant degree of NiNc compartmentalisation was already evident after 18 h incubation (Fig. 4(b_2)) and this pattern underwent minor changes upon prolonged incubation to 48 h (Fig. 4(b_3)). This finding was in good agreement with the predominantly aggregated shape of the NiNc absorption spectrum at 48 h incubation time for C32 cells (Fig. 3(c)). Peculiarly, in HaCaT keratinocytes (Fig. 4(c)) and HT1080 fibroblasts (data not shown), the cell-bound NiNc gave a monomeric-type absorption spectrum (Fig. 3(d)) and also appeared to remain finely dispersed at least up to 48 h incubation (Figs. 4(c_2) and (c_3)). The prevalent monomeric or aggregated feature of the visible absorption spectrum of cell-bound NiNc is summarised in Table 1.

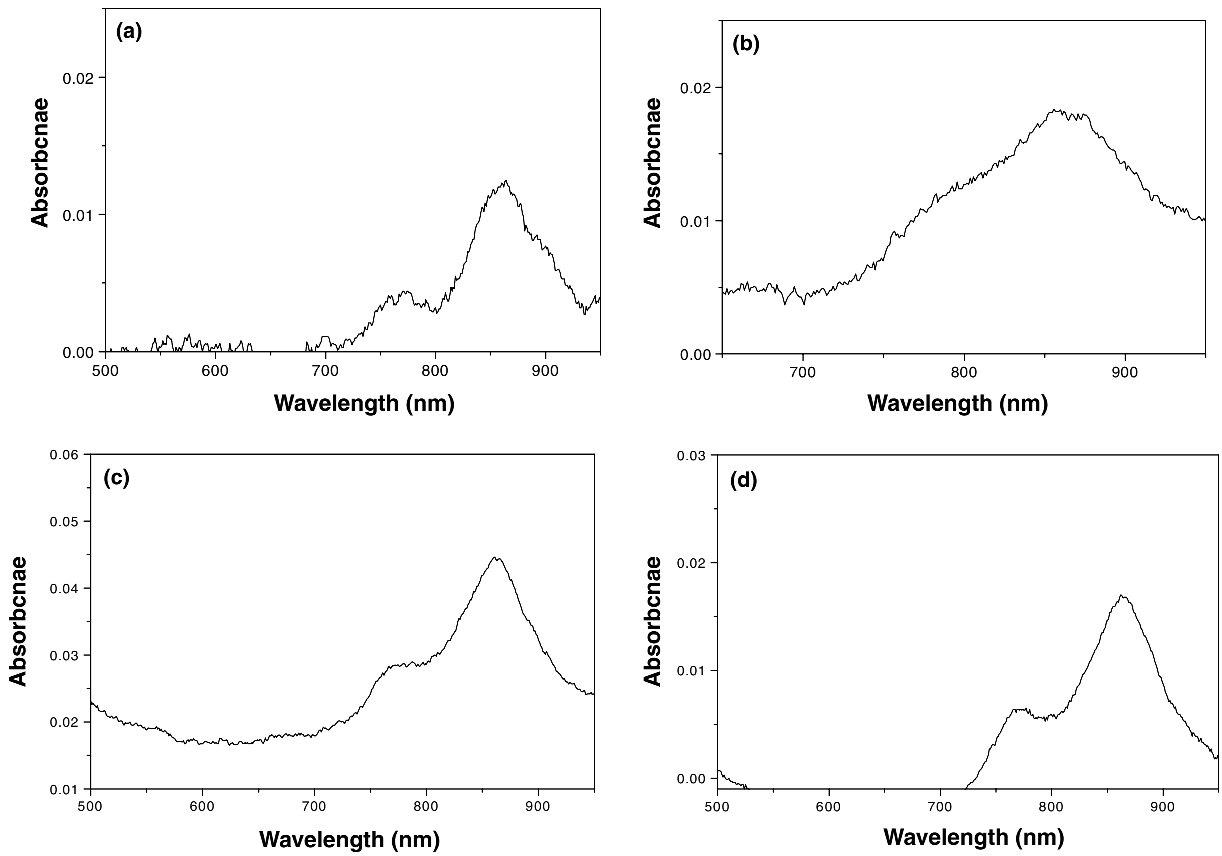

Fig. 3. Absorption spectrum in the visible range of cells incubated with 7.7 μM naphthalocyanine. NiNc bound to B78H1 cells after (a) 18 h, (b) 48 h and (c) C32 cells (d) HT1080 cells after 48 h.

3.2. Cell photosensitisation studies

On the basis of the binding/distribution studies, the cells were exposed to irradiation after incubation with 7.7 μM NiNc for 18 h and 5.1 μM NiNc for 48 h i.e., under experimental conditions yielding fairly similar intracellular molar concentrations of the photosensitizer (Table 1). Preliminary studies showed that irradiation of NiNc-loaded B78H1 amelanotic melanoma cells for 30 min with 850 nm from a c.w. operated Ti:sapphire laser caused no appreciable decrease in cell survival in spite of the efficient accumulation of the naphtalocyanine. Similarly, as a control, 20 min irradiation of the various cell lines with the Ti:sapphire operated in the pulsed regime (see Section 2) and in the absence of NiNc had no effect on cell survival. It seemed that no photodynamic process or thermal effects were induced by irradiation with pulsed high intensity 850 nm light under these experimental conditions. On the other hand, exposure of the cells, which had been incubated with NiNc, to pulsed 850 nm light invariably induced cytotoxic effects (Figs. 5(a) and (b)). The degree of cell mortality was particularly extensive for those samples (18 and 48 h C32 human amelanotic melanoma cells, 48 h B78H1 murine amelanotic melanoma cells) where the naphthalocyanine was aggregated and/or compartmentalised (Figs. 3 and 4). The photoprocess was very efficient since less than 10% residual survival was measured after 1 min exposure to light. The weight of these factors appears to be far greater than that of the intracellular naphthalocyanine concentration, since B78H1 cells (3.31 nmol NiNc/mg protein) were significantly more photosensitive than HaCaT cells (13.87 or 6.02 nmol) or HT-1080 cells (6.95 or 8.14 nmol).

Such a high level of cell photosensitivity could reflect the mechanisms controlling photothermal sensitization. Scanning electron microscopy analysis showed that control and unsensitised but irradiated C32 cells (Figs. 6(a) and (b)) exhibited a regular spherical shape. However, after 1 min of irradiation, in 18 h NiNc incubated C32 cells the outward separation of a consistent cellular mass (Fig. 6(c)) followed by formation of a deep hole (Fig. 6(d)) that can reach the cell nucleus was seen. A similar pattern was observed for 48 h incubated cells (Figs. 6(e) and (f)). It is tempting to propose that the images represent the photothermally induced ejection of cytoplasmic material subsequent to the photogeneration of shock waves. When the 1 min irradiated cells were observed by optical microscopy, the expelled material from C32 (Fig. 6(g)) and B78H1 (Fig. 6(h)) cells appeared to be

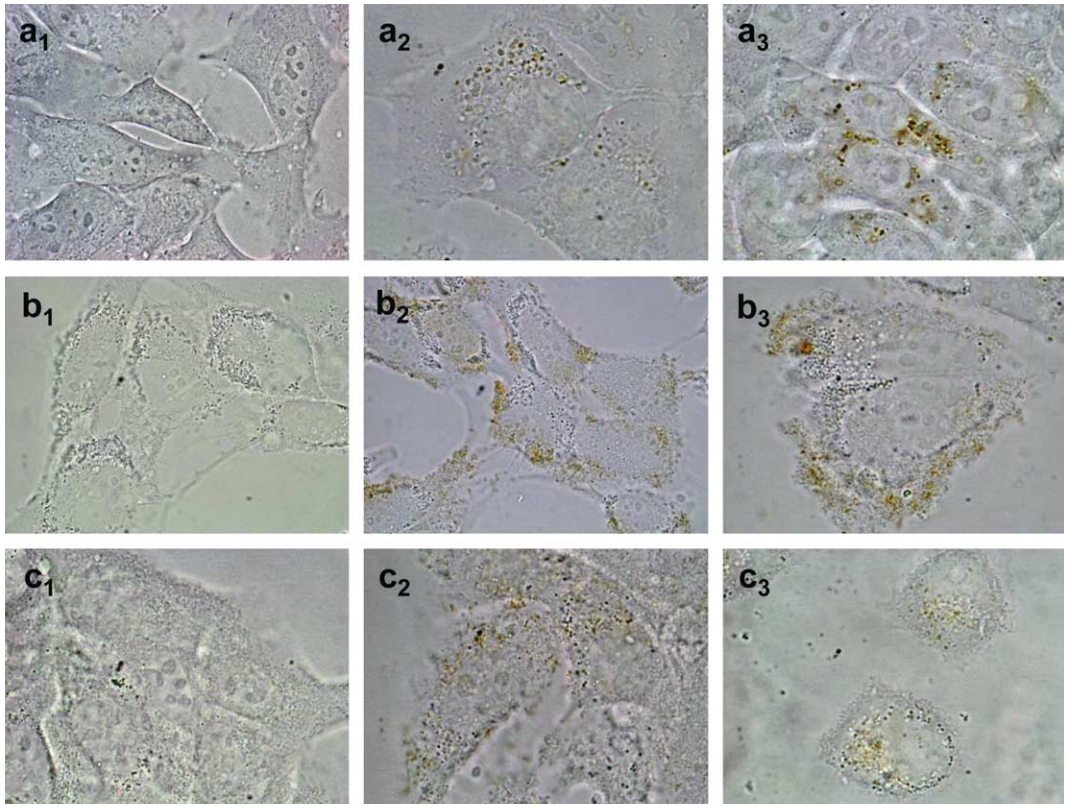

Fig. 4. Subcellular distribution of 7.7 μM NiNc was determined by optical microscope observations in clear field. Panels: (a_1) untreated controls, (a_2) 18 h incubated and (a_3) 48 h incubated B78H1 cells; (b_1) untreated controls, (b_2) 18 h incubated and (b_3) 48 h incubated C32 cells; (c_1) untreated controls, (c_2) 18 h incubated and (c_3) 48 h incubated HaCaT cells.

densely loaded with NiNc. It would appear then that the cytotoxic effects are maximal for cell regions with higher photosensitizer concentrations. Similar alterations of cell morphology were also noted for 48 h incubated and irradiated B78H1, HT-1080 and HaCaT cells (Figs. 6(i)–(n)).

NiNc appeared to be very photostable to pulsed laser irradiation, since the naphthalocyanine could be quantitatively recovered from B78H1 and C32 cells after 20 min irradiation.

3.3. *In vivo phototherapeutic studies*

Photothermal sensitisation of tumours is also effective *in vivo*. Mice bearing a subcutaneous amelanotic melanoma, which were irradiated by the pulsed Ti:sapphire laser 24 h after intravenous (i.v) injection of 1.8 mg/kg NiNc (the post-injection time interval corresponded to a large accumulation in skin tumours for various naphthalocyanines [30]), displayed an apparently complete disappearance of the lesions with initial eschar formation indicative of massive hemorrhagic necrosis (Fig. 7). Measurement of the intratumoural temperature by a thermocamera during pulsed Ti:sapphire irradiation indicated that the temperature of the NiNc-loaded neoplastic lesion rose to approximately 105 °C within 80 s, remained essentially stable until the end of irradiation (140 s) and returned to basal temperature (approximately 32 °C) within 1 min after tumour exposure to light was interrupted. The temperature spike obtained was markedly hotter than that measured for the same tumour (45–48 °C) when the irradiations were performed by the Ti:sapphire laser under identical experimental conditions in the absence of NiNc.

Complete healing of the NiNc-photosensisitised neoplastic lesion occurred in approximately seven days, suggesting that an extensive photothermally induced damage of the tumour tissue was not accompanied by irreversible damage of the peritumoural districts. Both the tumour-adjacent normal skin and the tissue layers underlying the neoplastic mass were spared, even though the average depth of the melanoma (0.4 cm) was smaller than the penetration depth of 850 nm light (approximately 1 cm in lightly pigmented tumours, see Ref. [31]). It is unlikely that important contributions to tumour response was provided by hyperthermal effects, since irradiation of NiNc-unsensitised mice caused only a minor delay of tumour growth. The photothermal process acted with an unusually high efficiency, since all the NiNc-injected phototreated mice remained tumour-free for about 20 days after irradiation times as short as 140 s. The regrowth of tumours can probably be

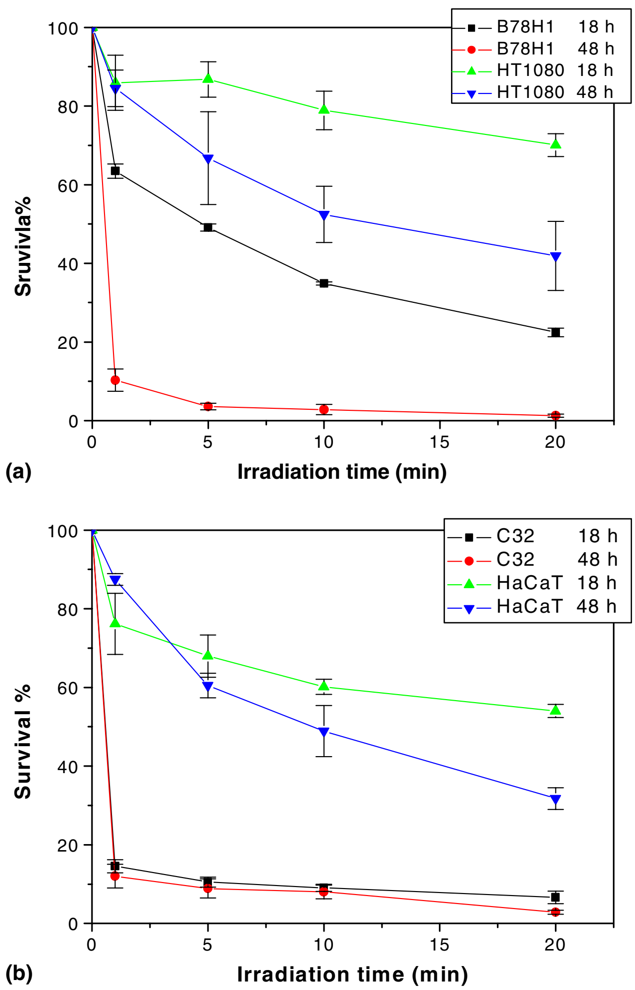

Fig. 5. Photothermal sensitisation of tumour cells *in vitro* by NiNc. Photosensitised inactivation of (a) murine (B78H1, HT-1080) and (b) human (C32, HaCaT) cells upon irradiation (850 nm, 120 mJ, 30 ns pulses) for different periods of time after incubation for 18 h with 7.7 μM NiNc and 48 h with 5.1 μM NiNc.

ascribed to the proliferation of small numbers of undamaged or sublethally damaged malignant cells. Normally, the implantation of a melanoma requires ca. 10^6 cells leading to visible detection of the tumour after 1 week.

4. Discussion

The present findings clearly underline that photothermal sensitisation is a very efficient process at both a cellular and animal level and can be usefully applied for the treatment of at least cutaneous tumours. An extensive and irreversible damage to neoplastic cells was achieved *in vitro* and *in vivo* after irradiation times as short as a few minutes with minimal and recoverable damage to the normal tissue surrounding the malignant lesion. The technique was highly selective in space and time and generated extensive and irreversible cell damage especially when the photosensitiser underwent significant compartmentalisation, which in turn promoted the formation of aggregated photosensitizer clusters. This type of process is especially facilitated in naphthalocyanines that are significantly hydrophobic and are known to localize to inner membranous districts [29,30]. These observations are also in agreement with theoretical predictions, namely the sudden temperature rise in the photosensitizer microenvironment leading to violent water evaporation and the consequent generation of a shock wave. The overall effect is obviously potentiated by the simultaneous development of more than one shock wave in the same subcellular space, as is likely to occur when aggregated derivatives of the photosensitizer are present. Examination of the irradiated cells even after short periods of exposure to light shows the NiNc-promoted release of a consistent mass of cytoplasmic material and related formation of large endocellular cavities (Fig. 6). The photothermal processes promoted under our experimental conditions appear to be markedly different from those typical of a traditional thermal interaction, as shown also by the lack of correlation between the amount of cell-bound naphthalocyanine and overall cell photosensitivity. The temperature rise induced by irradiation with high intensity light in the absence of naphthalocyanine, even though leading to values that are 15–20 °C higher than the basal temperature of the mouse, did not seem to cause a persistent or significant damage, possibly due to the short light exposure time.

To our knowledge, the images obtained with optical and scanning electron microscope are the first experimental demonstration of the mechanisms involved in photothermal sensitisation at a cellular level. The nature of the photodamage precludes the possibility of repair processes or selection of resistant cell clones. Photothermal sensitisation works through a different mode of action on cells compared to photodynamic or radiosensitised processes, where the chemical modification of specific targets is usually ultimately responsible for cell death, which may take place by a variety of apoptotic or random necrotic pathways [32]. The introduction of photothermal drugs would broaden the field of phototherapeutic applications. Photodynamic and radiosensitised therapy require the generation of reactive chemical intermediates and are only efficient in the presence of oxygen [33]. Importantly, photothermal therapy is independent of oxygen concentration in the irradiated system [19] and employs molecular vibrations that are much lower in energy than electronic levels and so even low-lying electronic states can initiate photothermal processes. In principle, polycyclic compounds absorbing far-red or near-infrared light could be used as photothermal sensitizers, whereas the choice of photodynamic sensitizers is limited by the requirement for them to possess sufficiently high-energy triplet states in order

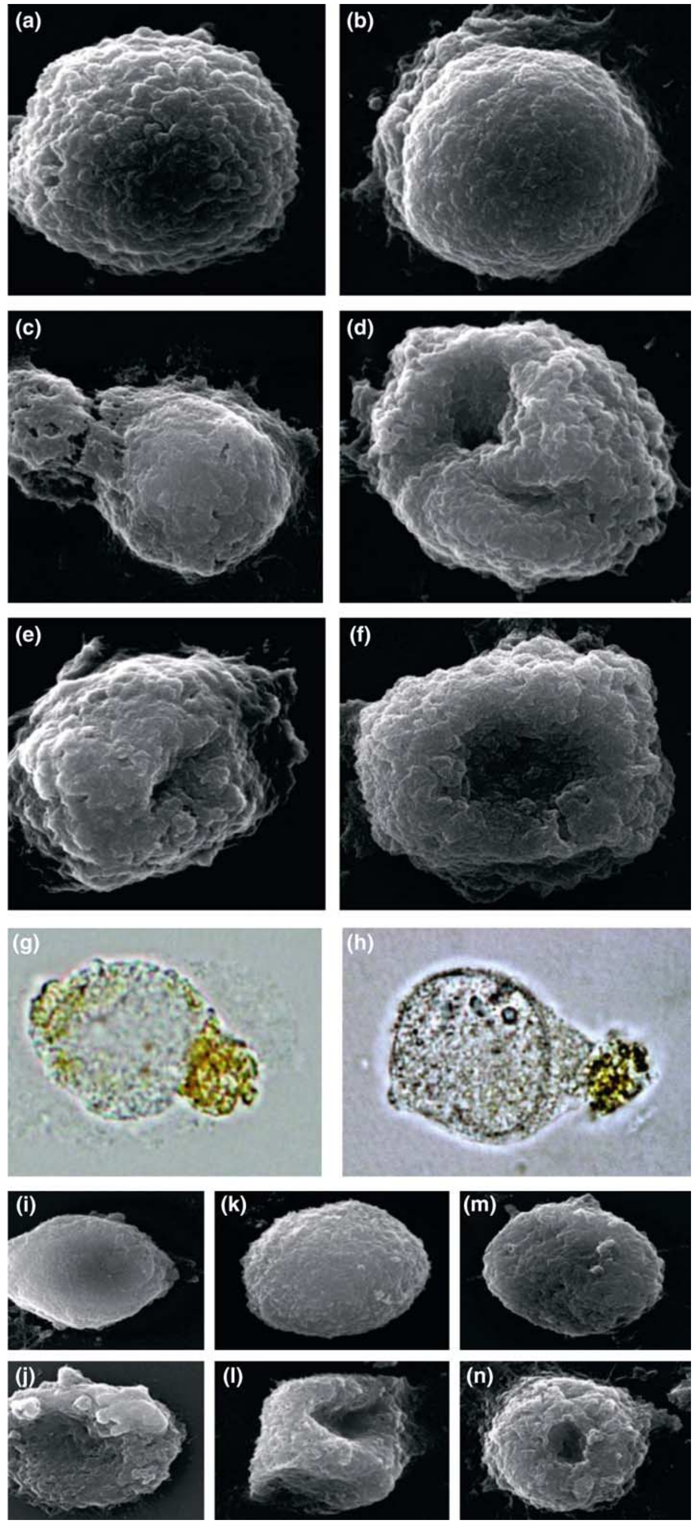

Fig. 6. Morphological alterations in photothermally sensitised tumour cells as studied by scanning electron microscopy (SEM) and optical microscopy (OM). First panel: SEM images of C32 cells (a) untreated controls; (b) irradiated controls in the absence of NiNc; 18 h incubated with 7.7 μM NiNc and (c) 1 min or (d) 20 min irradiated cells; 48 h incubated with 5.1 μM NiNc and (e) 1 min or (f) 20 min irradiated cells. Second panel: OM images in clear field of (g) C32 and (h) B78H1 cells irradiated for 1 min after 18 h incubation with 7.7 μM NiNc. Third panel: SEM images of (i) control and (j) 20 min irradiated B78H1 cells, (k) control and (1) 20 min irradiated HT1080 cells and (m) control and (n) 20 min irradiated HaCaT cells. In all cases, the irradiated cells had been incubated for 48 h with 5.1 μM NiNc.

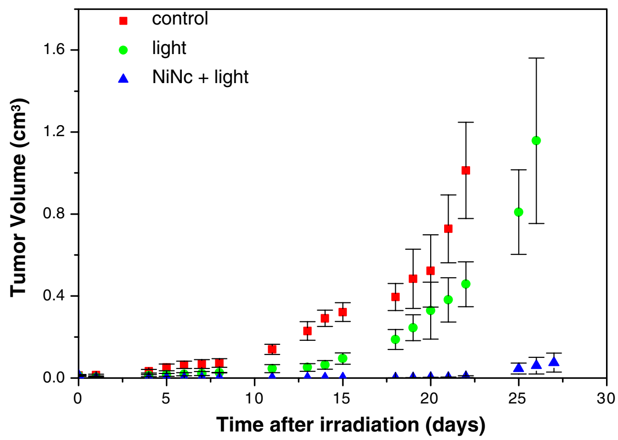

Fig. 7. Rate of tumour growth in C57BL/6 mice bearing a subcutaneously transplanted amelanotic melanoma, that were irradiated (850 nm, 100 mJ, 30 ns pulses) for 140 s in the absence and at 24 h after intravenous injection of NiNc (1.8 mg/kg); the growth rate is compared with that observed for control untreated mice.

to generate the cytotoxic singlet oxygen species via electronic energy transfer [33]. Lastly, the inertness of photothermal sensitizers to cw light (including sunlight) irradiation alleviates the problem of prolonged photosensitivity, which has been an undesired side effect of photodynamic therapy [1,4].

So far, we were unable to determine the pharmacokinetic behaviour of photothermal sensitizers. The lack of detectable fluorescence emission by these compounds makes it very difficult to measure their concentrations in tumours and healthy tissues by the traditional spectrophotofluorimetric analysis either directly *in vivo* [34] or after chemical extraction from tissue homogenates [30]. However, it appears reasonable to expect that the time-dependence of *in vivo* distribution of NiNc or other photothermally acting metallo-naphthalocyanines is very similar to other typical naphthalo- and phthalocyanines that have photodynamic properties (e.g., the Si(IV), Zn(II) or Ge(IV) derivatives), all of which exhibit essentially identical kinetics of accumulation and clearance from a variety of experimental tumours [35]. In our case, the irradiation of subcutaneously transplanted amelanotic melanoma at 24 h after i.v injection of NiNc, yielded a satisfactory tumour response as observed for several PDT treatments. Such a close similarity in the pharmacokinetic properties, coupled with the large differences in the photosensitisation mechanism, opens the possibility to develop a combined therapeutic protocol, involving the sequential treatment of a tumour by PDT and PTT. The simultaneous administration of a photothermal and photodynamic sensitiser differing only in the nature of the metal ion coordinated with the naphthalocyanine (or similar) macrocycle could be of therapeutic value. These approaches could complement other previously proposed techniques, such as indocyanine green-assisted laser therapy that share the use of near-infrared radiation as the photoactivating light [17].

Conflict of interest statement

None declared.

Acknowledgement

Partial support for this work was obtained from NIH Grant CA 91027.

References

1. Moor AC, Ortel B, Hasan T. Mechanisms of photodynamic therapy. In Patrice T, ed. *Photodynamic Therapy*. Cambridge, The Royal Society of Chemistry, 2003. pp. 19–57.
2. Peng Q, Warloe T, Berg K, *et al*. 5-Amino-levulinic acid-based photodynamic therapy: clinical research and future challenges. *Cancer* 1997, **79**, 2282–2308.
3. Dougherty TJ, Gomer CJ, Jori G, *et al*. Photodynamic therapy. *J Natl Cancer Inst* 1998, **90**, 889–905.
4. Calzavara PG, Szeimies RM, Ortel B. *Photodynamic Therapy and Fluorescence Diagnosis in Dermatology*. Cambridge, Royal Society of Chemistry, 2001.
5. Jori G, Brown SB. Photosensitised inactivation of microorganisms. *Photochem Photobiol Sci* 2004, **3**, 403–405.
6. Valassis G, Pragst I, Adolfs C, *et al*. Local photodynamic therapy reduces tissue hyperplasia after stenting in an experimental restenosis model. *Basic Res Cardiol* 2002, **97**, 132–136.
7. Boyle RW, Dolphin D. Structure and biodistribution relationships of photodynamic sensitisers. *Photochem Photobiol* 1996, **64**, 469–485.
8. Ma LW, Moan J, Steen HB, *et al*. Anti-tumour activity of photodynamic therapy in combination with mitomycin c in nude mice with human colon adenocarcinoma. *Br J Cancer* 1995, **71**, 950–956.
9. Schaffer M, Ertl-Wagner B, Kulka U, *et al*. Porphyrins as radiosensitising agents for solid neoplasms. *Curr Pharm Design* 2003, **9**, 2024–2035.
10. Soncin M, Busetti A, Fusi F, *et al*. Irradiation of amelanotic melanoma cells with 532 nm high peak power pulsed laser radiation in the presence of the photothermal sensitiser Cu (II)-haematoporphyrin: a new approach to cell photoinactivation. *Photochem Photobiol* 1999, **69**, 708–712.
11. Okazaki T, Hirota N, Nagata T, *et al*. High temporally and spatially resolved thermal energy detection after non-radiative transition in solution using a molecular heater-molecular thermometer integrated system. *J Am Chem Soc* 1999, **121**, 5079–5080.
12. Drain CM, Rockwell S, Cheng G, *et al*. Picosecond to microsecond photodynamics of a non-planar nickel-porphyrin: solvent dielectric and temperature effects. *J Am Chem Soc* 1998, **120**, 3781–3791.
13. Goldberg TJ. Laser treatment of pigmented lesions. *Dermatol Clin* 1997, **15**, 397–407.
14. Dierickx CC, Casparian JM, Venugopalan V, *et al*. Thermal relaxation of port-wine vessels probed *in vivo*: the need for 1–10 millisecond laser pulse treatment. *J Invest Dermatol* 1995, **105**, 709–714.
15. Jori G, Spikes JD. Photothermal sensitizers: possible use in tumour therapy. *J Photochem Photobiol B: Biol* 1990, **6**, 93–101.
16. Chen WR, Adams RL, Carubelli R, *et al*. Laser-photosensitiser assisted immunotherapy. A novel modality in cancer treatment. *Cancer Lett* 1997, **115**, 25–30.

17. Chen WR, Jeong SW, Lucroy MD, *et al*. Induced anti-tumour immunity against DMBA-4 metastatic mammary tumours in rats using a novel approach. *Int J Cancer* 2003, **107**, 1053–1057.
18. Moan J, Sommer S. Oxygen dependence of the photosensitising effect of haematoporphyrin derivative in NHIK 3025 cells. *Cancer Res* 1985, **45**, 1608–1610.
19. Camerin M, Rodgers MAJ, Kenney ME, *et al*. Photothermal sensitisation: evidence for the lack of oxygen effect on the photosensitizing activity. *Photochem Photobiol Sci* 2005, **4**, 251–253.
20. Busetti A, Soncin M, Jori G, *et al*. Treatment of malignant melanoma by high-peak-power 1064 nm irradiation followed by photodynamic therapy. *Photochem Photobiol* 1998, **68**, 377–381.
21. Star WM. Light dosimetry *in vivo*. *Phys Med Biol* 1997, **42**, 763–787.
22. Jori G, Schindl L, Schindl A, *et al*. Novel approaches towards a detailed control of the mechanism and efficiency of photosensitized processes *in vivo*. *J Photochem Photobiol A: Chem* 1996, **102**, 101–107.
23. Aoudia M, Cheng G, Kennedy VO, *et al*. Synthesis of a series of octabutoxy-benzophthalocyanines and photophysical properties of two members of the series. *J Am Chem Soc* 1997, **119**, 6029–6039.
24. Busetti A, Soncin M, Reddi E, *et al*. Photothermal sensitisation of amelonatic melanoma cells by Ni (II)-octabutoxy-naphthalocyanine. *J Photochem Photobiol B: Biol* 1999, **53**, 103–109.
25. Kremer JMH, Esker MWJ, Pathmanoharan C, *et al*. Vesicles of variable diameter prepared by a modified injection method. *Biochemistry* 1997, **16**, 3932–3935.
26. Smith PH, Krohn RI, Hermanson GT, *et al*. Measurement of protein using bicinchoninic acid. *Anal Biochem* 1985, **150**, 76–85.
27. Rockwell S. *In vivo* and *in vitro* tumour cell lines: characteristics and models for human cancer. *Br J Cancer* 1980, **41**, 118–126.
28. Reddi E, Jori G. Steady-state and time-resolved spectroscopic studies of photodynamic sensitizers: porphyrins and phthalocyanines. *Rev Chem Interm* 1988, **10**, 241–268.
29. Jori G. Tumour photosensitizers: approaches to enhance the selectivity and efficiency of photodynamic therapy. *J Photochem Photobiol B: Biol* 1996, **36**, 87–93.
30. Soncin M, Busetti A, Biolo R, *et al*. Photoinactivation of amelanotic and melanotic melanoma cells sensitized by axially substituted Si-naphthalocyanines. *J Photochem Photobiol B: Biol* 1998, **42**, 202–210.
31. Wilson BC. Technologies and biophysical techniques for PDT. In Patrice T, ed. *Photodynamic Therapy*. Cambridge, Royal Society of Chemistry, 2003. pp. 127–157.
32. Oleinick NL, Morris RL, Belichenko I. The role of apoptosis in response to photodynamic therapy: what, where, why, and how. *Photochem Photobiol Sci* 2002, **1**, 1–21.
33. Oleinick NL, Evans HH. The photobiology of photodynamic therapy: cellular targets and mechanisms. *Radiat Res* 1998, **150**, 146–156.
34. Sutedja G. Fluorescence bronchoscopy for early detection of lung cancer. In Patrice T, ed. *Photodynamic Therapy*. Cambridge, Royal Society of Chemistry, 2003. pp. 159–175.
35. Biolo R, Jori G, Soncin M, *et al*. Effect of photosensitizer delivery system and irradiation parameters on the efficiency of photodynamic therapy of B16 pigmented melanoma in mice. *Photochem Photobiol* 1996, **63**, 224–228.

Artículo 3:

Criterios morfológicos para distinguir la muerte celular inducida por tratamientos apoptóticos y necróticos

Apoptosis 10: 201-208 (2005)

¿Pueden la apoptosis y la necrosis ser definidas mediante el empleo de criterios morfológicos independientemente de la naturaleza de los agentes causantes del daño? Para realizar este análisis, se seleccionó de la literatura un abanico de protocolos capaces de causar apoptosis o necrosis de manera más o menos exclusiva. Los agentes elegidos fueron:

- Los fotosensibilizadores CF3 y ZnPc empleados en condiciones previamente descritas como inductoras de apoptosis y de necrosis.
- Deprivación de suero en el medio de cultivo para inducir apoptosis.
- El agente quimioterapéutico etopósido (VP-16), conocido inductor de apoptosis.
- Elevadas concentraciones de H_2O_2, para inducir necrosis.
- Ciclos repetidos de congelación y descongelación, que necrosan las células del cultivo.

Los criterios morfológicos que se emplearon se basaron en observaciones empleando microscopía de contraste de fase, complementadas con análisis de microscopía electrónica de barrido y con observaciones de la morfología nuclear empleando el fluorocromo Hoechst-33258 (H-33258).

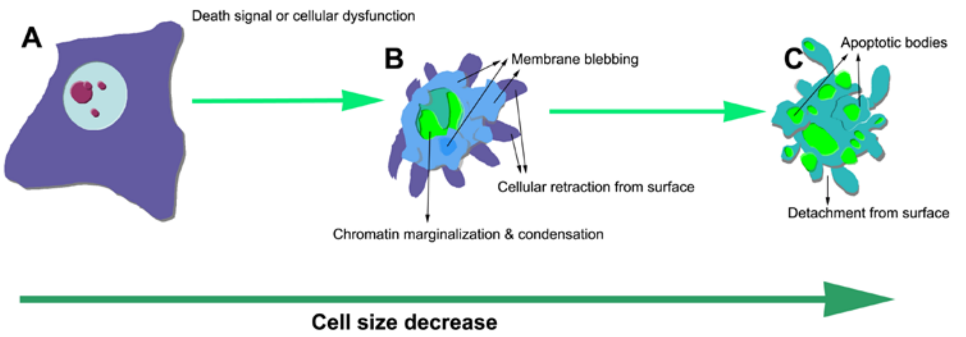

Figure 11 Apoptotic morphological development. Upon proper stimulation, cells trigger the apoptotic machinery without larger morphological alterations at the first minutes (A). The apoptotic commitment is evidenced later by the cellular retraction from surface (with lost of pseudopodes), membrane blebbing and chromatin condensation in a crescent-like disposition (B). Finally, in cell cultures, cells detach from surface and became packed into a number of apoptotic bodies compressing both cytoplasmic and nuclear masses (C).

Los resultados permitieron determinar que todos los tratamientos utilizados sobre células tumorales HeLa, inducían exactamente el mismo tipo de cambios morfológicos; pero dichos cambios no se daban en escalas de tiempo equivalentes, sino que ciertas fases se producían con grandes retrasos entre unos y otros tratamientos.

La apoptosis se reconoce fundamentalmente por los cambios dramáticos que sufre la superficie celular. La célula experimenta un proceso de redondeamiento y encogimiento, que se desarrolla sin pérdida de la integridad de membrana pero con la desaparición de las conexiones con las células vecinas. Mientras esto ocurre, en un proceso denominado *zeiosis*, la membrana sufre reorganizaciones dando lugar a los llamados *blebs* o evaginaciones macizas de la membrana y del citoplasma subyacente y que, al desprenderse, conforman los cuerpos apoptóticos. El núcleo sufre condensación, marginación y fragmentación de la cromatina. Al completarse toda esta secuencia de acontecimientos, la célula se desprende del sustrato al que estaba adherida.

La necrosis es un proceso mucho menos estudiado que la apoptosis, y el presente trabajo aporta la suficientes evidencias para establecer una serie de fases a través de las cuales el proceso de muerte necrótica se completa, y que permiten una fácil identificación.

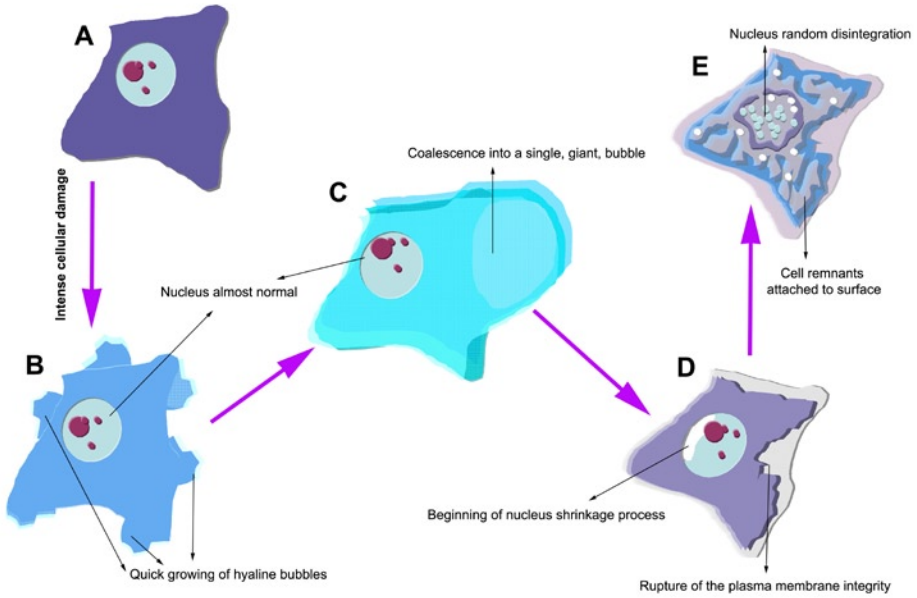

Figure 12 Proposed sequence of events in necrosis development. Living cells (A) quickly show the emergence of several hyaline bubbles into their surface after an intense injure (B). This bubbles converge into a single giant deformation of the plasma membrane (C). These processes occur without any evident morphological change at the nucleus. The water influx that causes cellular swelling (oncosis) finishes when the single giant bubble detaches, rupturing the plasma membrane. When the plasma membrane became holed, an incipient nuclear shrinkage is noticed (D). In our cell cultures, the necrosis process finished with the conformation of "phantoms" by the cell remnants that continue attached to surface. Nucleus shows random disintegration of the genomic material (E).

Inmediatamente después de actuar el agente lesivo se observan pequeñas evaginaciones (burbujas) en la superficie celular; estas burbujas no son macizas sino hialinas (al estar compuestas básicamente por agua, que entra descontroladamente en la célula y que se acumula justo por debajo de la membrana plasmática). Pasados unos minutos, las burbujas convergen en una única "macroburbuja" que acaba cerrándose sobre sí misma y desprendiéndose de la célula.

En el momento del desprendimiento de la macroburbuja, la célula sufre la pérdida de la integridad de la membrana plasmática. Sin embargo, el cuerpo celular no sufre redondeamiento ni se despega en ningún momento de la necrosis.

Hasta el momento de la ruptura de la macroburbuja, los núcleos de las células en necrosis no sufren ninguna alteración morfológica evidente. A medida que pasa el tiempo, la célula va perdiendo todo su contenido soluble a través de una membrana plasmática que está rota; mientras que los componentes insolubles precipitan generando un "fantasma" que retiene la morfología *premortem* de la célula. Los núcleos muestran una condensación y un encogimiento progresivos (muy evidente al contraste de fase); finalmente estos núcleos picnóticos sufren la ruptura azarosa de la cromatina que se distribuye como estructuras más o menos aisladas por toda la estructura del "fantasma celular".

Como se ha señalado previamente, todos los tratamientos inducen los mismos cambios morfológicos, variando sólo los tiempos postratamiento en los que se verifican. Así los tratamientos fotodinámicos son más rápidos inductores de apoptosis que la deprivación y el VP-16 (24-48 h *vs.* 72 h), pero son más lentos inductores de las fases finales de la necrosis (24 h *vs.* 3 h), ya que la aparición de las burbujas es inmediata al daño.

Con este artículo, en resumen, se defiende la validez de la observación morfológica como herramienta de estudio de la muerte celular frente a la proliferación de técnicas bioquímicas indirectas, asumiendo la necesidad de realizar siempre identificaciones combinadas, ya que ningún criterio o prueba por sí mismo alcanza un 100% de fiabilidad.

Apoptosis 2005; **10**: 201–208

Morphological criteria to distinguish cell death induced by apoptotic and necrotic treatments

S. Rello, J. C. Stockert, V. Moreno, A. Gámez, M. Pacheco, A. Juarranz, M. Cañete and A. Villanueva

Departamento de Biología, Facultad de Ciencias, Universidad Autónoma de Madrid, Ciudad Universitaria de Cantoblanco, E-28049 Madrid, Spain

We present a comparative study of apoptotic and necrotic morphology (light and scanning electron microscopy), induced by well known experimental conditions (photodynamic treatments, etoposide, hydrogen peroxide, freezing-thawing and serum deprivation) on cell cultures. Our results indicate that morphological criteria (apoptotic cell rounding and shrinkage, and appearance of membrane bubbles in early necrosis) allow to distinguish these cell death mechanisms, and also show that, independently of the damaging agents, the necrotic process occurs in a characteristic sequence (coalescence of membrane bubbles in a single big one that detaches from cells remaining on the substrate).

Keywords: apoptosis; cell morphology; necrosis; scanning electron microscopy.

Introduction

The objective of our study was to answer the following questions: (i) are the morphological changes, analysed by phase contrast, fluorescence, and scanning electron microscopy (SEM), capable of providing a precise assessment of the cell death mechanisms (necrosis or apoptosis) involved? (ii) are the morphological events exclusive of cell death induced by Photodynamic Therapy, or they also can be provoked by other damaging conditions? (iii) can apoptotic and necrotic processes be defined by morphological criteria independently of the damaging agent?

Using HeLa cells as a model system, the morphological alterations induced by necrotic and apoptotic photodynamic treatments with two selected photosensitisers, zinc(II)-phthalocyanine (ZnPc)[1] and 5-(4-*N*-(*N*-2′,6′-dinitro-4′-trifluoromethyl-phenyl)-aminophenyl)-10,15, 20-tris(2,4,6-trimethoxyphenyl) porphyrin (CF3),[2] have been compared to those induced by other experimental conditions which are known to cause either apoptosis or necrosis, preferentially. For apoptosis induction we used two widely applied procedures as positive controls for cultured cells. The first one is serum deprivation,[3,4] which simulates growth factors withdrawal and provokes apoptosis after several hours. The second method corresponds to a treatment with a well known chemotherapeutic agent: the topoisomerase II inhibitor etoposide (VP-16),[3,5] which induces DNA breaks followed by apoptosis. The induction of necrosis requires more severe cell damage. We applied cell freezing-thawing cycles to provoke plasma membrane disfunctions[6,7] and hydrogen peroxide (H_2O_2) incubation to generate an intracellular non-reversible oxidative stress. H_2O_2 is an important reactive oxygen species that triggers the apoptotic machinery when used at low doses, but high doses of H_2O_2 lead to cell death by necrosis.[8,9]

In the present study we show that all damaging treatments employed on cultured cells induced the morphological events characteristic of apoptosis or necrosis in a similar way. Therefore, the microscopical appearance of cell death is not an exclusive feature of photodynamic treatments. Thus, the morphological analysis under light (phase contrast, fluorescence) and scanning electron microscopy constitutes a very important and even decisive tool to identify the specific type of cell death unambiguously.

Material and methods

Cell culture

Human carcinoma HeLa cells were grown as monolayer in Dulbecco's modified Eagle's medium (DMEM) supplemented with 10% (v/v) foetal calf serum (FCS), 50 units/ml penicillin, 50 μg/ml streptomycin (all from Gibco, Paisley, Scotland, UK). Cell cultures were performed in an incubator with 5% CO_2 plus 95% air at 37°C. Cells were plated on 12 mm round coverslips within 35 mm culture dishes for photodynamic, freezing, H_2O_2 or etoposide treatments, or in 25 cm^2 flasks for serum

Correspondence to: A. Villanueva, Departamento de Biología, Facultad de Ciencias, Universidad Autónoma de Madrid, Ciudad Universitaria de Cantoblanco, E-28049 Madrid, Spain. Tel.: +34 914978236; Fax: +34 914978344; e-mail: angeles.villanueva@uam.es

deprivation treatment. In all cases, subconfluent cell cultures were used.

Induction of apoptosis

The following apoptotic treatments were applied: (i) previously described photodynamic treatments using the porphyrin derivative CF3 (5×10^{-6} M for 18 h plus 7 min irradiation with 8 mW/cm^2 blue light)[2], and ZnPc (10^{-7} M for 1 h plus 3 min irradiation with 21 mW/cm^2 red light)[1] (ii) pure population of apoptotic cells obtained by collection of detached (floating) cells after incubation in DMEM lacking FCS for 72 h, and (iii) cells treated with 50 μM VP-16 (Sigma, St. Louis, MO, USA) for 3 h and collected 72 h after treatment.

Induction of necrosis

Necrosis was induced with photodynamic treatments either by exposing cells to CF3 (5×10^{-6} M for 18 h plus 15 min irradiation with 8 mW/cm^2 blue light)[2] or ZnPc (5×10^{-6} M for 1 h plus 5 min irradiation with 21 mW/cm^2 red light)[1]. Likewise, to generate a population of necrotic cells, 35 mm culture dishes with HeLa cells (in DMEM) were subjected to three freezing-thawing cycles, as well as by 2 h incubation with 0.1 M H_2O_2 (Panreac Química SA, Montcada i Reixac, Spain). After all treatments, cells were washed for 3 times in phosphate buffered saline solution (PBS, Gibco) and maintained in the incubator until they were processed for observation.

Morphological characterisation of cell death mechanisms light and fluorescence microscopy

Control (without any treatment) and treated HeLa cells with the different necrotic and apoptotic protocols were directly visualised under phase contrast microscopy after mounting the coverslips on a drop of PBS. Apoptotic and necrotic nuclear morphology was assessed using fluorescence microscopy. Cells fixed with methanol at $-20°$C for 10 min were stained with Hoechst 33258 (H-33258, Sigma; 5 μl/ml in distilled water, 2 min). After washing and air drying, preparations were mounted in DPX and observed under UV excitation in an Olympus BX61 epifluorescence microscope equipped with an Olympus DP50 digital camera.

Scanning electron microscopy

For SEM analysis, cells on coverslips were fixed in 3% glutaraldehyde (Taab Laboratories, Aldermaston, England, UK) in PBS for one hour, washed in PBS for 3 times, and immediately postfixed in 1% osmium tetroxide (Taab) in the same buffer for another hour. After dehydration in graded ethanol solutions, the specimens were critical-point dried and sputter-coated with 10% gold using Emitech K850 and SC502 instruments. Observations were performed in a Phillips XL30 scanning electron microscope at an accelerating voltage of 20 kV. Detached cells after serum deprivation were centrifuged at 1200 rpm (rotor radius: 7 cm) during 5 min, placed into 12 mm coverslips previously covered with poly-L-lysine (Sigma), and then processed for SEM as above.

Results

SEM examination revealed that control interphase HeLa cells have a rather polygonal shape, showing the characteristic features of normal cell surface such as numerous microvilli and lamellipodia extensions, as well as plasma membrane connections (Figure 1A). On the contrary, mitotic cells are spherical in shape and present a smooth external surface (Figure 1A′). Under phase contrast, the oval form of the nucleus containing several nucleoli can be observed (Figure 1B). Metaphase cells with condensed chromosomes in the middle plane and a smooth cell surface are also well recognised (Figure 1B′). Untreated HeLa cells stained with H-33258 show an interphase nucleus with relaxed chromatin (Figure 1C, left). The aligned position of the chromosomes can be seen in the centre of a metaphase cell (Figure 1C, right).

Morphological apoptotic changes

The different apoptotic treatments applied to HeLa cells induced deep morphological alterations of the cellular surface (Figure 2), which were common to all of them, but at variable time intervals. Particularly, cells observed by SEM 72 h after etoposide treatment exhibited rounding, shrinkage and severe blebbing of the plasma membrane (Figure 2A); detached cells 72 h after serum deprivation also showed the same morphology. These surface alterations were easily visible by phase contrast microscopy (Figure 2B). Under these conditions, differences in cell shape and surface of apoptotic and mitotic cells are also clear (see Figure 1B′). The condensation and posterior fragmentation of the apoptotic chromatin are evident in fluorescence microscopy after H-33258 staining (Figure 2C).

After apoptotic photodynamic treatments with CF3 and ZnPc, HeLa cells showed structural alterations that characterise this type of death mechanism (Figure 2, right panel). Cells subjected to apoptotic photodynamic protocols suffered deep changes in the cell shape and

Figure 1. Control interphase and metaphase HeLa cells observed either by SEM (A, A′), phase contrast microscopy (B, B′); or fluorescence microscopy after staining with H-33258 (C). Scale bar: 5 μm.

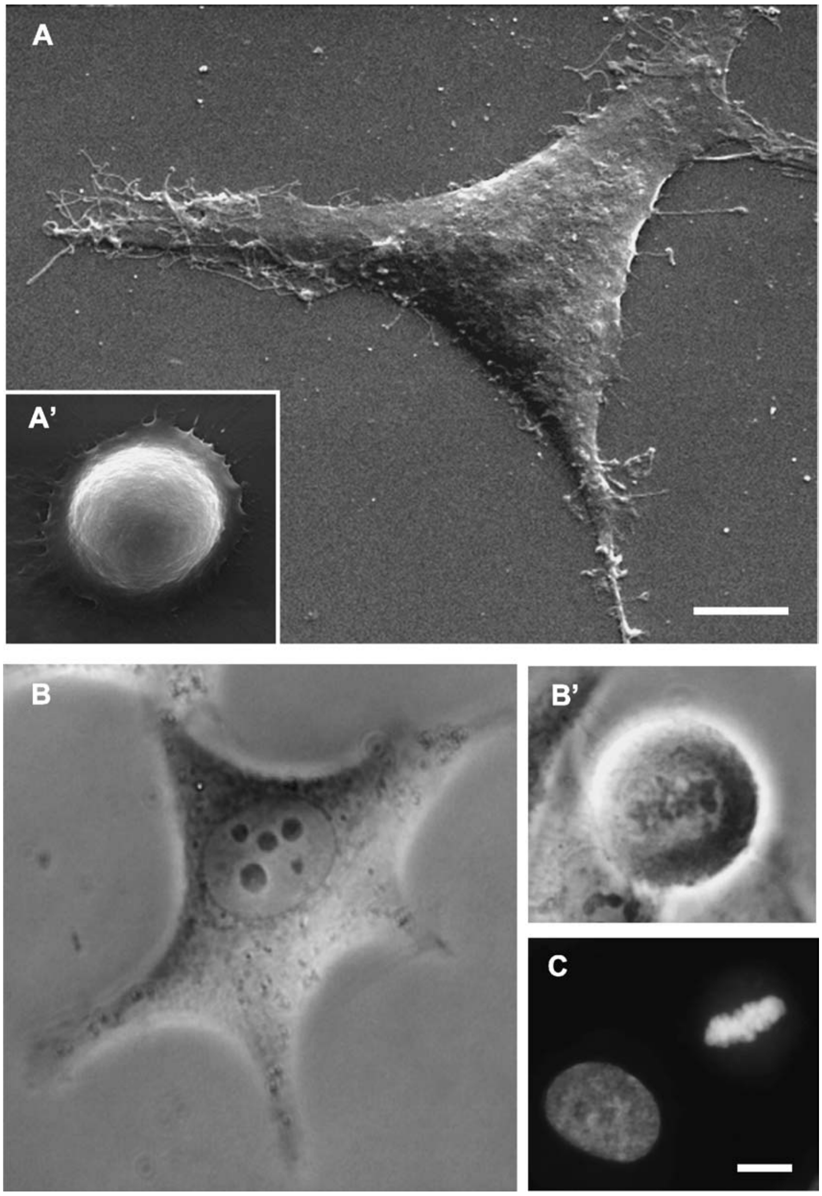

surface, which were entirely similar to those observed after etoposide treatment or serum deprivation. Cells appeared shrunk and rounded, showing numerous plasma membrane deformations which were specially evident by SEM (Figure 2A′), although the integrity of the plasma membrane was well preserved. The nucleus of apoptotic cells appeared also affected and showed structural rearrangements consisting in cup-shaped margination and/or fragmentation of chromatin (Figure 2C).

Likewise, it is important to note that in SEM images, early apoptotic cells lose plasma membrane connections with neighbour cells before the detaching process (Figures 2A and A′). Most apoptotic treatments used in this work produced loss of cellular adhesion to the substrate and, therefore, detached cells appeared floating in the culture medium.

Morphological necrotic changes

Cell death via necrosis was scored on the basis of a typical sequence of morphological alterations affecting fundamentally the plasma membrane. HeLa cells subjected to the different necrotic treatments started the process with an immediate and massive production of small surface evaginations (bubbles) clearly visible by both phase contrast optics (Figure 3B) and SEM (Figure 3A). Such evaginations are caused by the loss of control of the water

Figure 2. Apoptotic HeLa cells after photodynamic treatment with CF3 (right) and etoposide (left), showing the severe surface changes that characterize this type of death mechanism. Surface alterations are easily visible under phase contrast (B, B′), but they appear especially conspicuous when observed by SEM (A, A′). The condensation and fragmentation of apoptotic chromatin are evident in fluorescence microscopy after H-33258 staining (C, C′). Scale bar: 5 μm.

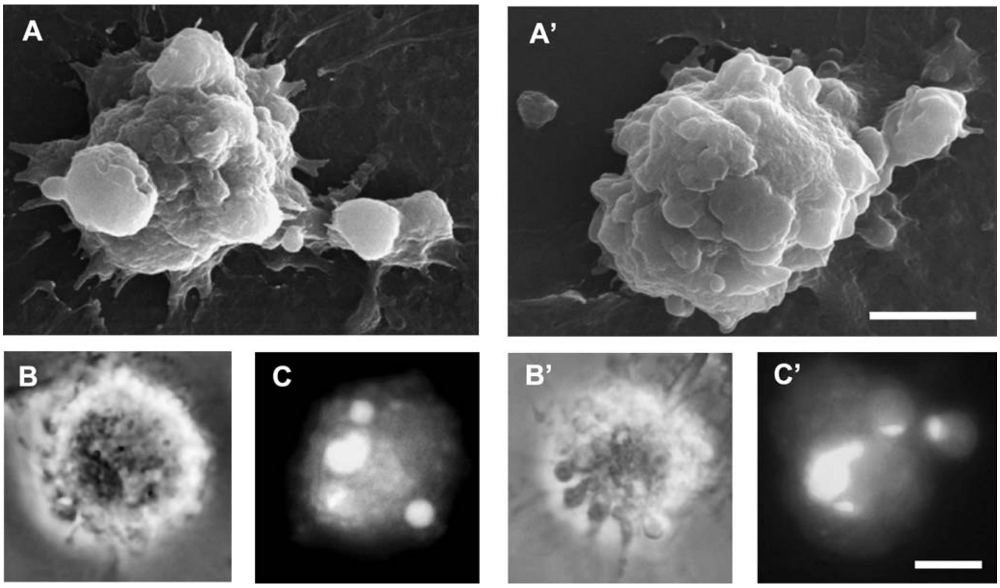

Figure 3. HeLa cells immediately after receiving a necrotic photodynamic treatment with ZnPc. Important changes of the cell surface (bubbles) are observed by SEM (A). Phase contrast microscopy also allows the visualization of the typical necrotic morphology (B), and a big, single bubble that is formed some minutes after the necrotic photodynamic treatment (B′). Cell nuclei stained with H-33258 show a similar morphology to that of control cells (C). Scale bar: 5 μm.

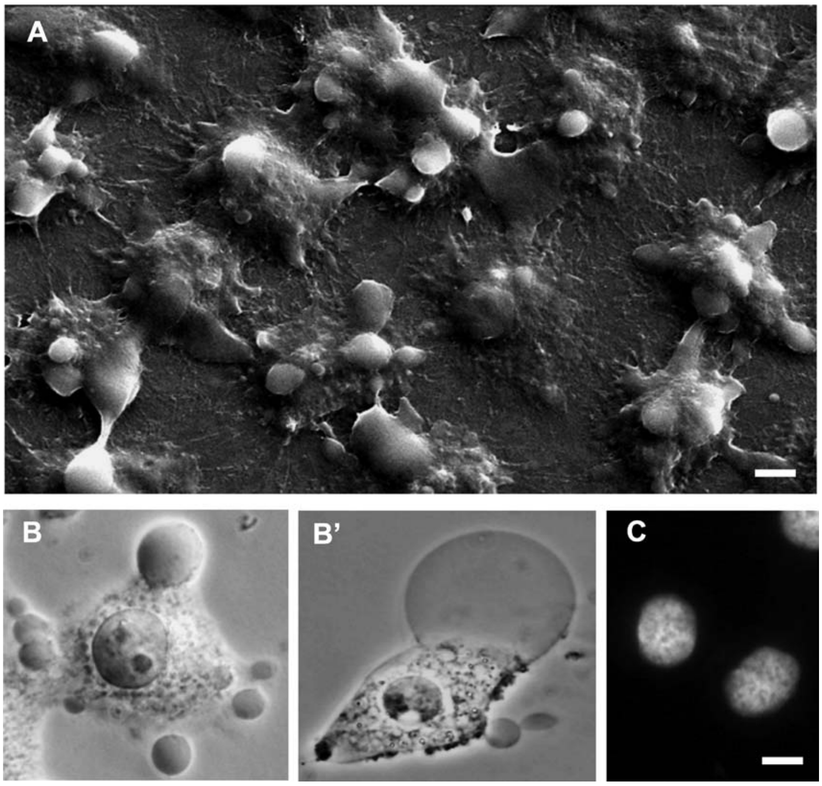

influx through the plasma membrane but do not cause membrane disruption. A few minutes later, these surface deformations converge into a big, single bubble which finally detaches from the cell, whereas the cell body still remains firmly attached to the substrate (Figure 3B′). In contrast, the nuclear morphology is not affected immediately after necrotic treatments, photodynamic or not and, therefore, nuclei show a rather normal aspect (Figure 3C).

Some hours later, all the cells subjected to the necrotic treatments used in this study presented a succession of similar morphological alterations that began with the rupture of the plasma membrane after the detachment of the giant bubble, with gradual liberation of the cytoplasmic content. After necrotic treatments, the loss of integrity of the plasma membrane was clearly visualised by SEM as a common morphological alteration (Figure 4, top). Cytoplasmic damage appeared along variable times following necrotic conditions. Several hours after treatments, there was an uniform condensation of the chromatin leading to pyknotic nuclei that were clearly observed under phase contrast microscopy (Figure 4, middle). Later, cells

Figure 4. Microphotographs of HeLa cells showing the evolution of the common morphological alterations that characterize the cell death in early (top, middle) and late necrosis (bottom). Cell necrosis was caused by photodynamic treatment with CF3 (A, B, C), freezing-thawing (A′, B′, C′), and H_2O_2 (A″, B″, C″). Scale bar: 5 μm.

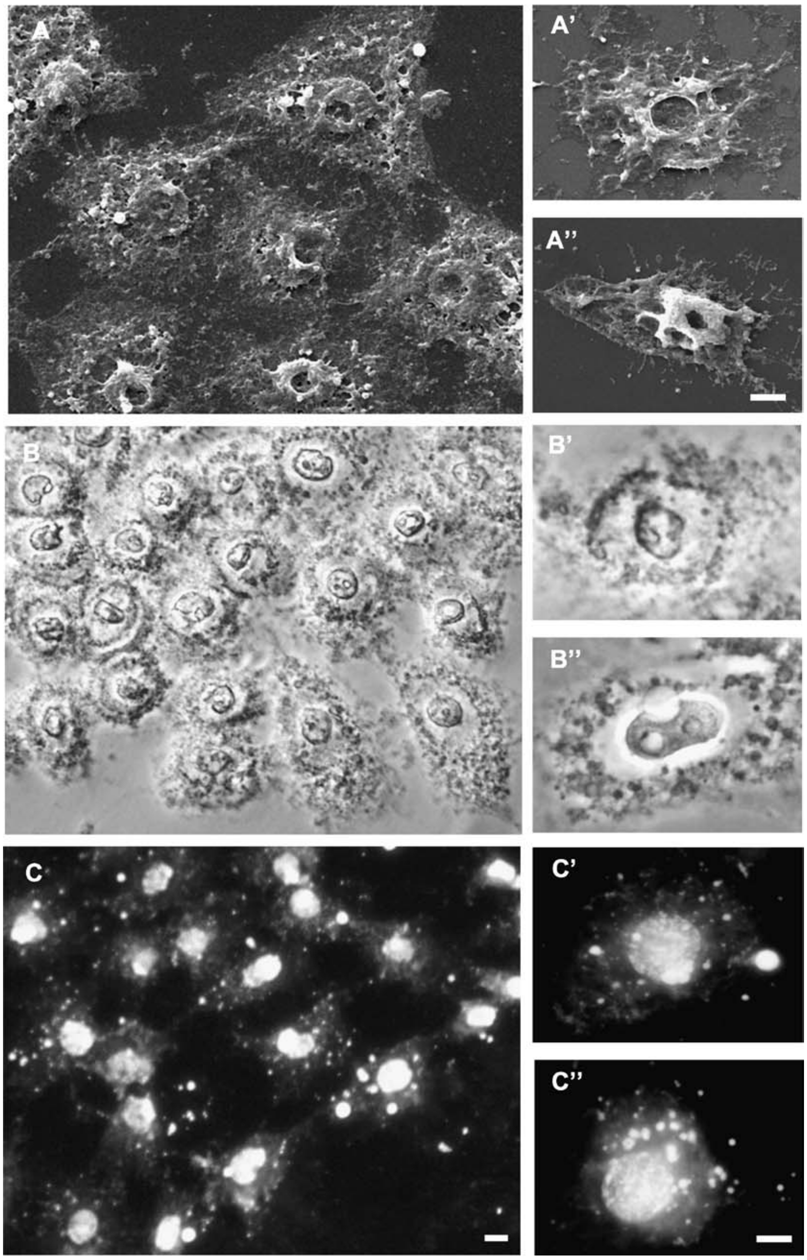

stained with H-33258 showed the chromatin broken in fragments of different size, some of which appeared dispersed within the cytoplasm remnants still attached to the substrate (Figure 4, bottom). The morphological evolution was quicker after non-photodynamic treatments, since these necrotic images were observed as early as 3 h after the treatment with H_2O_2. However, necrotic photodynamic treatments with ZnPc and CF3 induced similar chromatin degradation only 24 h later.

In this succession of necrotic alterations, it is interesting to note that the basic polygonal morphology of undamaged cells was also recognisable in necrotic cells at early stages (Figure 3). Later, the polygonal shape could be still identified by the occurrence of some cell debris that remained attached to the substrate (Figure 4). All these features clearly differentiate the apoptotic and necrotic cell death, the former being characterised by cell rounding and detachment (Figure 2) and the later by flattening and occurrence of attached cell remnants (Figure 4).

Discussion

Different methods are currently employed on cell cultures in order to differentiate between apoptosis and necrosis, the most important being morphological analysis, flow cytometry, TUNEL assay, annexin V labelling and DNA gel electrophoresis. However, each of them separately is considered unable to identify unambiguously the type of cell death. In addition, morphological differences in tissue sections can be detected by staining with hematoxylin-eosin or DNA fluorochromes, but the use of phase contrast or SEM is thought to be unsuitable due to the processing of samples (paraffin embedding, sectioning). In the last years, new methods developed for cell cultures (assays for DNA fragmentation, immunohistochemical detection of apoptotic proteins) have been applied to paraffin sections.[10]

Some studies indicate that features considered characteristic of apoptosis can also take place during necrosis. According to Lecoeur *et al*.[11] the apoptotic external exposure of phosphatidylserine also occurs in the early phase of necrosis, and thus flow cytometry analysis using the annexin V/propidium iodide assay does not distinguish between apoptosis and necrosis, although this technique could be now improved by combining it with a caspase activation assay.[12] Likewise, the TUNEL assay detects both apoptotic and necrotic cells and therefore it can not be considered as a specific marker for apoptosis.[13]

The internucleosomal break of DNA is a characteristic feature of apoptotic cell death, whereas DNA cleavage during necrosis is at random. This fact is reflected in different electrophoretic patterns of DNA: a ladder pattern for apoptosis and a diffuse smear for necrosis. However, this technique is also not definitive, since if the number of apoptotic cells is small there is no detection of DNA ladder.[14] Likewise, although internucleosomal DNA cleavage seems to be typical of apoptosis, several reports show that some cells with apoptotic characteristics do not show the ladder pattern, and therefore DNA electrophoresis can not be considered the only assay to identify apoptosis.[15–18]

The morphological changes that characterise apoptosis are mainly cell shrinkage and rounding. However, cells do not respond at the same time to apoptotic conditions, and therefore it is necessary to determine the time interval where the greater amount of cells undergoes some of the stages that define this type of cell death. The cell shrinkage and a highly refringent aspect are very easy to evaluate, and thus a simple observation using an inverted phase contrast microscope can give a right idea of the intensity of the treatment used. In addition, the sample can be observed repeated times after treatment. Obviously, the confirmation of the precise mechanism of cell death and the specific identification of apoptosis will require additional assays, which should complement the necessary morphological observation.

Our results indicate that in addition to conserving the plasma membrane initially intact, all cells that enter into apoptosis present the same pattern of membrane blebbing. This apoptotic pattern (termed zeiosis) has been described as a typical feature in many cell types.[19] In this sense, SEM analysis justly allows detailed examination of cell surface changes including blebbing and thus it is a very useful tool to assess the type of induced cell death.

Cells in necrosis are unable to repair the caused damage and rapidly lose their viability. It is worth noting that the succession of morphological events that characterise necrosis has been described with lesser details than those of apoptosis, and therefore its microscopical features must be further analysed.

We have previously found that using photodynamic treatments on HeLa cells with the phthalocyanine ZnPc and the porphyrin derivative CF3, either apoptotic or necrotic cell death can be induced depending on light doses.[1,2] This fact is not surprising since similar dose-dependent responses have been described for other non photodynamic damaging conditions.[20,21]

In the present work we show that, as in the case of apoptosis, all the necrotic treatments (photosensitisation, H_2O_2, freezing) also induce a similar succession of typical events. The morphology of the irreversibly damaged cells presented the following time-dependent alterations: (i) small deformations (bubbles) of the plasma membrane and underlying cytoplasm material that converge into a single macrobubble; this structure finally breaks producing the loss of the plasma membrane integrity and the liberation of cell components to the medium; (ii) an initial uniform chromatin condensation with reduction of the nuclear size; (iii) necrotic cells remain attached to the substrate and therefore it is still possible to recognise their polygonal shape as well as severely altered nuclei, (iv) finally, chromatin DNA becomes disorganised appearing as dispersed fragments among the cytoplasmic remnants.

It is interesting to note that these necrotic modifications were observed in cells at different time intervals as a function of the nature of the damaging conditions. Whereas H_2O_2 and freezing induced all these changes after 1–3 h, necrotic photodynamic treatments with ZnPc[1] and CF3[2] required 18–24 h to complete the whole process, the most delayed stage being the appearance of dispersed chromatin fragments.

Similar results related to the necrotic alteration of the plasma membrane have been previously described by other authors.[22] Using video microscopy, Herman *et al.*[23] showed stepwise changes in the cell surface of rat hepatocytes subjected to anoxia for 1–3 h, which they divided in three stages. Stage I was defined by the formation of membrane protrusions followed in stage II by their coalescence and fusion to form a large terminal bubble, which is ruptured in stage III, producing a rapid increase of cell permeability. Stages I and II are reversible if reoxygenation takes place, but the rupture of the terminal bubble is an irreversible process which causes the cell death. Recently, Nieminen[24] has described an increased permeability of the plasma membrane by monitoring with SEM and confocal microscopy the necrotic cell death in cultured rat hepatocytes exposed to hypoxia. Interestingly, the break of the terminal bubble in damaged hepatocytes is correlated with the loss of cell viability as revealed by dye exclusion tests using trypan blue and propidium iodide.

In response to damaging conditions of high intensity, the alteration of the homeostatic balance is reflected by the rapid appearance of bubbles on the surface of most cultured cells. Our results show that the formation of cell bubbles is a feature that occurs immediately after severe damage, affecting all cells in a practically simultaneous way, indicating an imminent and irreversible loss of the membrane integrity. If the treatment is not so severe, cells show no morphological changes immediately, but some hours later they present the apoptotic pattern (shrinkage, blebbing, and detaching from the substrate). In this way it is possible to determine, from the first evaluation, the timescale along which apoptosis can occur and if it is necessary to wait for cell detachment in order to quantify apoptosis accurately.

It is important to emphasise that the use of light microscopy and SEM allows identifying in a precise way the type of cell death which is taking place, not only after a photodynamic treatment, but also under any other experimental condition causing cell damage. Keeping in mind that structural changes of the plasma membrane and chromatin of the injured cell are clearly visible and relevant parameters for the identification of the type of cell death, we consider it very useful to perform the morphological analysis after apoptotic and necrotic treatments by means of SEM, phase contrast and fluorescence microscopy.

Conclusion

Using HeLa cells we have shown that apoptosis and necrosis can be identified by morphological criteria independently of the damaging agent. Severe shrinkage, rounding and blebbing of highly refringent cells followed by chromatin condensation and fragmentation, as well as detaching from the substrate, were the main morphological features of apoptosis. In addition, immediate formation of membrane bubbles followed by coalescence and rupture were typical of early necrosis; disorganization of cytoplasm, homogeneous nuclear condensation and final chromatin disintegration within flattened polygonal cell remnants still attached to the substrate characterised late necrosis. Independently of the damaging agents, these morphological criteria allow recognising the type of death mechanism of cultured cells in a rapid and precise way.

Acknowledgments

We thank Esperanza Salvador and Laura Tormo (Servicio de Microscopía Electrónica de Barrido, Universidad Autónoma de Madrid) for their valuable collaboration. This work was supported by a grant from the Dirección General de Investigación Científica y Técnica (SAF2002-04034-C02-01), Spain. JCS is a scientific member of the Consejo Superior de Investigaciones Científicas (CSIC), Spain.

References

1. Villanueva A, Domínguez V, Polo S, *et al*. Photokilling mechanisms induced by zinc(II)-phthalocyanine on cultured tumor cells. *Oncol Res* 1999; **11**: 447–453.
2. Villanueva A, Durantini EN, Stockert JC, *et al*. Photokilling of cultured tumour cells by the porphyrin derivative CF3. *Anticancer Drug Des* 2001; **16**: 279–290.
3. Joza N, Susin SA, Daugas E, *et al*. Essential role of the mitochondrial apoptosis-inducing factor in programmed cell death. *Nature* 2001; **410**: 549–554.
4. Colombaioni L, Frago LM, Varela-Nieto I, Pesi R, García-Gil M. Serum deprivation increases ceramide levels and induces apoptosis in undifferentiated HN9.10e cells. *Neurochem Int* 2002; **40**: 327–336.
5. Negri C, Bernardi R, Braghetti A, Riccotti GC, Scovassi AI. The effect of the chemoterapeutic drug VP-16 on poly(ADP-ribosylation) in apoptotic HeLa cells. *Carcinogenesis* 1993; **14**: 2559–2564.
6. Kressel M, Groscurth P. Distinction of apoptotic and necrotic cell death by in situ labelling of fragmented DNA. *Cell Tissue Res* 1994; **278**: 549–556.

7. Didenko VV, Ngo H, Baskin DS. Early necrotic DNA degradation: Presence of blunt-ended DNA breaks, 3′ and 5′ overhangs in apoptosis, but only 5′ overhangs in early necrosis. *Am J Pathol* 2003; **162**: 1571–1578.
8. Palomba L, Sestili P, Columbaro M, Falcieri E, Cantoni O. Apoptosis and necrosis following exposure of U937 cells to increasing concentrations of hydrogen peroxide: The effect of the poly(ADP-ribose)polymerase inhibitor 3-aminobenzamide. *Biochem Pharmacol* 1999; **58**: 1743–1750.
9. McKeague AL, Wilson DJ, Nelson J. Staurosporine-induced apoptosis and hydrogen peroxide-induced necrosis in two human breast cell lines. *Br J Cancer* 2003; **88**: 125–131.
10. Stadelmann C, Lassmann H. Detection of apoptosis in tissue sections. *Cell Tissue Res* 2000; **301**: 19–31.
11. Lecoeur H, Prévost MC, Gougeon ML. Oncosis is associated with exposure of phosphatidylserine residues on the outside layer of the plasma membrane: A reconsideration of the specificity of the annexin V/propidium iodide assay. Cytometry 2001; 44: 65–72.
12. Darzynkiewicz Z, Juan G, Li X, Gorczyca W, Murakami T, Traganos F. Cytometry in cell necrobiology: Analysis of apoptosis and accidental cell death (necrosis). *Cytometry* 1997; **27**: 1–20.
13. Frankfurt OS, Krishan A. Identification of apoptotic cells by formamide-induced DNA denaturation in condensed chromatin. *J Histochem Cytochem* 2001; **49**: 369–378.
14. Stolzenberg I, Wulf S, Mannherz HG, Paddenberg R. Different sublines of Jurkat cells respond with varying susceptibility of internucleosomal DNA degradation to different mediators of apoptosis. *Cell Tissue Res* 2000; **301**: 273–278.
15. Herrmann M, Lorenz HM, Voll R, Grunke M, Woith W, Kalden JR. A rapid and simple method for the isolation of apoptotic DNA fragments. *Nucleic Acids Res* 1994; **22**: 5506-5507.
16. Cohen GM, Sun XM, Snowden RT, Dinsdale D, Skilleter DN. Key morphological features of apoptosis may occur in the absence of internucleosomal DNA fragmentation. *Biochem J* 1992; **286**: 331–334.
17. Collins RJ, Harmon BV, Gobé GC, Kerr JFR. Internucleosomal DNA cleavage should not be the sole criterion for identifying apoptosis. *Int J Radiat Biol* 1992; **61**: 451–453.
18. Zhang Y, Wu LJ, Tashiro S, Onodera S, Ikejima T. Evodiamine induces tumor cell death through different pathways: Apoptosis and necrosis. *Acta Pharmacol Sin* 2004; **25**: 83–89.
19. Estacion M, Schilling WP. Blockade of maitotoxin-induced oncotic cell death reveals zeiosis. *BMC Physiol* 2002; **2**: 2.
20. Renvoize C, Biola A, Pallardy M, Breard J. Apoptosis: Identification of dying cells. *Cell Biol Toxicol* 1998; **14**: 111–120.
21. Formigli L, Papucci L, Tani A, *et al*. Aponecrosis: Morphological and biochemical exploration of a syncretic process of cell death sharing apoptosis and necrosis. *J Cell Physiol* 2000; **182**: 41–49.
22. Collins JA, Schandl CA, Young KK, Vesely J, Willingham MC. Major DNA fragmentation is a late event in apoptosis. *J Histochem Cytochem* 1997; **45**: 923–934.
23. Herman B, Nieminen AL, Gores GJ, Lemasters JJ. Irreversible injury in anoxic hepatocytes precipitated by an abrupt increase in plasma membrane permeability. *FASEB J* 1988; **2**: 146–151.
24. Nieminen AL. Apoptosis and necrosis in health and disease: Role of mitochondria. *Int Rev Cytol* 2003; **224**: 29–55.

Artículo 4:

Parada metafásica y muerte celular inducidas por etopósido en células HeLa

The International Journal of Biochemistry & Cell Biology 38: 2183-2195 (2006)

El etopósido (VP-16) es un fármaco ampliamente estudiado en los últimos años por su empleo como agente quimioterapéutico. Actúa como veneno de la topoisomerasa II, causando roturas de la doble cadena del ADN que desencadena la apoptosis. Existen en la literatura infinidad de protocolos distintos de administración, con resultados diversos.

Trabajando con la línea celular HeLa (proveniente de un tumor de útero humano y carente de p53 funcional), aplicamos un tratamiento corto, un "pulso", de 3 h de incubación con VP-16 a una concentración de 50 µM. Este tratamiento provoca una amplia respuesta apoptótica a las 72 h de haber retirado el fármaco (supervivencia del 37,5 %), que cae hasta el 1 % a las 96 h.

Haciendo observaciones al microscopio óptico invertido se apreció un marcado incremento de células refringentes a partir de las 48 h después del tratamiento (ΔT=48 h), por lo que se decidió estudiar la posible existencia de alteraciones del ciclo celular.

Análisis del contenido de ADN, marcado con yoduro de propidio (PI) y medido por citometría de flujo, determinaron una acumulación de células en el pico G2/M del 26,2 % (frente a un valor control del 6,6 %). Este valor se confirmó mediante un recuento de fases del ciclo celular, posible gracias al inmunomarcaje de la tubulina (lo que dio un valor del 19,8 % de índice mitótico, frente al 4,6 % del control).

Estos recuentos permitieron, además, identificar que la parada del ciclo celular normal se verificaba en metafase (el 86,2 % de las células en mitosis) y que era debido a graves alteraciones en la disposición del huso mitótico (presentes en el 89,8 % de las metafases). Estas alteraciones consistían fundamentalmente en la presencia de polos supernumerarios en los husos (de tres a seis).

Por otra parte, estudios más detallados, que implicaron el uso de la microscopía electrónica de barrido, confirmaron que las células aumentan de tamaño tras el tratamiento. Este dato es indicativo de la aparición de fenómenos de poliploidía y aneuploidía. La presencia además de alteraciones morfológicas también en las células interfásicas (como la presencia de núcleos multifragmentados con puentes cromatínicos entre ellos) sustentan el dato anterior.

En busca del origen de estas células poliploides se analizaron, mediante inmunofluorescencia para tubulina, muestras a ΔT=24 h y se encontraron células con metafases alteradas en las que se aprecia claramente la fragmentación de los cromosomas: la acumulación en un margen de la célula de los fragmentos acéntricos, que no se unen al huso mitótico, causa una distorsión en el huso mitótico.

Todo este conjunto de datos suponen una secuencia de eventos que se corresponden con los procesos denominados de "catástrofe mitótica": (i) las células sufren roturas de los cromosomas por acción del VP-16 (que no causan apoptosis al encontrarnos en un sistema sin p53 funcional); (ii) las células no pueden dividirse con éxito y sufren un fenómeno de "restitución" a interfase poliploide; (iii) las células poliploides intentan volver a dividirse, bloqueándose en metafase por las severas alteraciones (fundamentalmente la presencia de polos supernumerarios); (iv) la acumulación de alteraciones desencadena finalmente la apoptosis de las células dañadas.

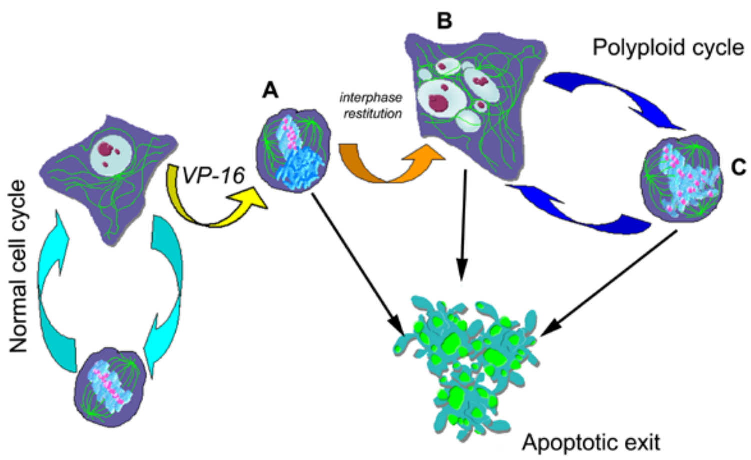

Figure 13 VP-16 induces cell death upon mitotic catastrophe in HeLa cells. Using a short, pulsed, etoposide incubation in HeLa cells we obtain a sequence of milestones that begins 24 h after etoposide retirement with the appearance of abnormal metaphases with the spindle moved by the accumulation of acentrinc chromosomal fragments (A). 48 h after the treatment (24 h after abnormal metaphases first detection) the number of cells in mitosis rises the highest value, showing that a metaphase arrest is established. The arrested metaphases show a typical configuration with extra poles in the mitotic spindle (C). The presence of aneuploid micronucleated giant cells (resulting from mitotic slippage and interphase restitution) is also increased (B). Delayed exit to death is possible from each step, but the largest amount of cell death is detected 72 h after the treatment and is thought to be triggering from the cells in B and C.

Esta secuencia se confirmó mediante el análisis del contenido de ADN de las células apoptóticas, identificadas por reacción de TUNEL, que mostraron valores generales por encima del contenido "G1" (lo que implicaría un contenido de partida de las células apoptóticas entre los rangos de "G2/M" y "Poliploidía"). Asimismo se realizaron grabaciones de videomicroscopía que mostraron la aparición de eventos morfológicos típicos de la apoptosis (el "blebeo" o *zeiosis*) en células detenidas en metafase durante varias horas (sin regreso previo a interfase).

Available online at www.sciencedirect.com
ScienceDirect
ELSEVIER
IJBCB
The International Journal of Biochemistry & Cell Biology 38 (2006) 2183–2195
www.elsevier.com/locate/biocel

Metaphase arrest and cell death induced by etoposide on HeLa cells

Santiago Rello-Varona, Angelo Gámez, Vanessa Moreno, Juan Carlos Stockert, Javier Cristóbal, María Pacheco, Magdalena Cañete, Ángeles Juarranz, Ángeles Villanueva*

Departamento de Biología, Facultad de Ciencias, Universidad Autónoma de Madrid, C/ Darwin 2, Citología A-115, E-28049 Madrid, Spain

Received 3 May 2006; received in revised form 22 June 2006; accepted 25 June 2006
Available online 18 July 2006

Abstract

DNA damage, cell cycle and apoptosis form a network with important implications for cancer chemotherapy. Dysfunctions of the cycle checkpoints can allow cancer cells to acquire drug resistance. Etoposide is a well-known inducer of apoptosis, which is widely used in cell biology and in clinical practice. In this work we report that a pulse of 50 μM etoposide (incubation for only 3 h) on HeLa cells causes a sequence of events that leads to abnormal mitotic figures that could be followed either by cell death or, more commonly, by interphase restitution and endocycle. The endocycling polyploid cells enter immediately into mitosis and suffer metaphase blockage with multiple spindle poles, which were generally followed by a direct triggering of apoptosis from metaphase (mitotic catastrophe), or by a new process of endocycling, until surviving cells finally became apoptotic (96 h after the treatment).

Keywords: Etoposide; HeLa cells; Metaphase arrest; Mitotic catastrophe; Apoptosis

1. Introduction

Apoptosis is a mechanism of cell death of vital importance to target tumoral cells by anti-neoplastic treatments, and also because of its implication in carcinogenesis, as well as in its resistance to chemotherapy. The cell cycle checkpoints conform a system to regulate the correct sequence of events that allows a cell to reproduce itself in a proper manner (Kastan & Bartek, 2004). Taken together, the knowledge of the relationships between proliferation, apoptosis and their regulation mechanisms constitutes a high-priority objective in cell biology studies (Makin & Dive, 2003; Pommier, Sordet, Antony, Hayward, & Kohn, 2004).

Chemotherapeutic drugs interfere with cell viability and proliferation at multiple levels (Boldt, Weidle, & Kolch, 2002). Many of the commonly used agents act interfering with the basic machinery of DNA synthesis and cell division (Evan & Vousden, 2001). In response to DNA damage, the cellular decision between life versus death involves an intricate network of factors that play critical roles in the regulation of DNA repair, cell cycle and cell death. DNA-damage checkpoint proteins are crucial for maintaining DNA integrity and normal cellular functions, but they may reduce the effectiveness of cancer treatments (Jiang, Luo, & Li, 2005). Often they can avoid apoptosis because these proteins are inactivated or can bypass checkpoints that control the cell

* Corresponding author. Tel.: +34 91497 8236; fax: +34 91497 8344.
E-mail address: angeles.villanueva@uam.es (Á. Villanueva).

1357-2725/$ – see front matter
doi:10.1016/j.biocel.2006.06.013

cycle progression (Erenpreisa & Cragg, 2001; Kastan & Bartek, 2004).

DNA topoisomerases are nuclear enzymes which are essential for DNA replication, transcription, DNA decatenation, chromosomal segregation and DNA recombination (Fortune & Osheroff, 2000; Skoufias, Lacroix, Andreassen, Wilson, & Margolis, 2004). There are two isoforms of the human topoisomerase II (α and β) with different expression along the cell cycle. Some studies *in vitro* and *in vivo* have found a relationship between the level of expression of both topo II types and cellular inactivation. While topo II β remains relatively constant during the cell cycle, topo II α expression increases from G1 to G2-M phase (Woessner, Mattern, Mirabelli, Johnson, & Drake, 1991). Apoptosis induction in cell cultures seems related to high levels of topo I or topo II expression (Isaacs et al., 1998). Some clinical studies have also found a favourable tumoral response to the treatment when the expression level of topo II is high (Coon et al., 2002).

Topoisomerase inhibitors are divided into two groups: (i) drugs able to stabilize the covalent DNA-topo II complex (also known as the "cleavable complex") and to induce DNA strand breaks (topo II poisons), and (ii) agents acting on any of the other steps in the catalytic cycle (catalytic inhibitors), that do not produce clastogenic effects. The chromosomes of cells treated with etoposide or other "cleavable complex" inducers are extensively fragmented, whereas chromosomes from cells treated with the catalytic topo II inhibitors (merbarone, ICRF-187, and aclarubicin) are intact but elongated and/or entangled (Larsen, Escargueil, & Skladanowski, 2003a).

Etoposide (also known as VP-16) is a semisynthetic derivative of podophyllotoxin, which has been used for over 20 years in the treatment of a variety of neoplasias, including small cell lung cancer, testicular cancer and lymphomas (Meresse, Dechaux, Monneret, & Bertounesque, 2004). VP-16 is a member of topo II poisons (Boldt et al., 2002) and acts by stabilizing a normally transient DNA-topo II cleavable complex and inhibiting the religation of DNA double-strand breaks, through DNA unwinding, during replication or transcription (Godard, Deslandes, Sichel, Poul, & Gauduchon, 2002; Hande, 1998; Kamesaki et al., 1993; Kropotov et al., 2004; Meresse et al., 2004).

Since its introduction in 1971, VP-16 has been widely used as a powerful apoptosis inductor in numerous experimental protocols *in vitro* (Bartova, Jirsova, Fojtova, Soucek, & Kozubek, 2003). The studies carried out with VP-16 have demonstrated that numerous biochemical routes are implied in the cellular response to this drug (Ayene, Ford, & Koch, 2005; Bartling, Lewensohn, & Zhivotovsky, 2004; Kim et al., 2005; Larsen, Escargueil, & Skladanowski, 2003b).

On the other hand, cell cultures are an important tool to analyze the precise action mechanism of chemotherapeutic drugs. In this sense, the HeLa cell line (established from a human cervix carcinoma) is one of the best known and most used cell models *in vitro*. HeLa cells lack a functional p53 due to a papillomavirus 16 infection, which encodes the oncoprotein E6 responsible of p53 degradation via the ubiquitin in proteasome, thus rendering them insensitive to apoptosis induced by many conventional chemotherapeutic agents (Fletcher, Yen, & Muschel, 2003; Godard et al., 2002; Makin & Dive, 2001; Scheffner, Werness, Huibregtse, Levine, & Howley, 1990).

Taking into account that different responses have been described after treatment of cell cultures with VP-16, the aim of the present study is to determine the alterations in the cell cycle of HeLa cells, as well as to analyze the possible implications of cell cycle blockage for cell inactivation induced by means of an apoptotic mechanism.

2. Materials and methods

2.1. Cell culture

HeLa cells were grown in Dulbecco's modified Eagle's medium (DMEM) with 50 units/mL penicillin, 50 μg/mL streptomycin and supplemented with foetal bovine serum (FBS) at a final concentration of 10%. All the media, sera and antibiotics were provided by Gibco, Paisley, Scotland, UK.

Cell cultures were performed in a 5% CO_2 atmosphere at 37 °C and maintained in a SteriCult 200 (Hucoa-Erloss) incubator. Depending on the experiments, the cells were seeded either in 25 cm^2 flasks or on 22 mm square coverslips placed into 33 mm Petri dishes (both from Corning Inc, Corning, NY, USA). The incubation with VP-16 was initiated using cultures at 50% of confluence to avoid contact inhibition along the post-incubation time due to effects of the treatment on the mitotic rate and the cell size.

2.2. Preparation and incubation of VP-16

Stock solutions of 10^{-2} M VP-16 (Sigma, St. Louis, MO, USA) were prepared in dimethyl sulfoxide (DMSO, Panreac Química, Montcada i Reixac, Spain). Work solutions were 50 μM VP-16 in DMEM with 10% FBS. The final concentration of DMSO was 0.5% (v/v) and the lack of toxicity of this DMSO concentration for HeLa cells was tested and confirmed.

2.3. Cell cycle analysis

For flow cytometry measurement of the DNA content, flasks were trypsinised (saving also the detached cells), centrifuged at 1200 rpm (rotor radius: 7 cm) for 5 min and fixed 15 min in cold ethanol. After centrifugation, the cells were resuspended in 1 mL of fresh PBS and 50 μL of 100 μg/mL RNase (Sigma) was added. Cells were incubated for 30 min with the RNase solution. Immediately prior to measurement, DNA was stained by adding 25 μL of 1 mg/mL propidium iodide (PI, Sigma). Measurements were taken on a Coulter Epics XL-MCL flow cytometer with an argon laser line at 488 nm and complemented with the appropriate filters.

2.4. Mitotic cell morphology

2.4.1. Fluorescence and confocal microscopy

We performed a combined immunofluorescence analysis of microtubules and centromeres for assessing both, the mitotic index and the morphology of mitotic cells. For this purpose, cells on coverslips were fixed in cold methanol and permeabilised with 0.5% Triton X-100 (v/v). Primary antibodies were monoclonal mouse anti-α-tubulin (Sigma) and purified human anti-centromere proteins (Antibodies Inc., Davis, CA, USA). The secondary antibodies were goat anti-mouse FITC-labelled IgG (Fab specific) and goat anti-human IgG (Fc specific) TRITC-labelled antibody (both from Sigma). For a more complete study using fluorescence microscopy, cells on coverslips were also stained with 5 μL/mL Hoechst-33258 (H-33258, Sigma) in distilled water for 3 min and mounted with ProLong Gold antifade reagent (Molecular Probes, Eugene, OR, USA). Photographs were taken using an Olympus BX61 epifluorescence microscope equipped with an Olympus DP50 digital camera, and a Leica TCS SP2 confocal microscope, operating with the 543 nm (Argon–Helium–Neon), 488 nm (Argon), and 351 and 364 nm (Argon-UV) laser lines.

2.4.2. Scanning electron microscopy

A morphological analysis of cells was also performed using scanning electron microscopy. For this purpose, cells were seeded on 12 mm round coverslips, fixed in 3% glutaraldehyde for 1 h, and post-fixed in 1% osmium tetroxide for 1 h (both fixatives from Taab Labs., Aldermaston, England, UK). After fixation, cells were dehydrated in ethanol solutions, critical-point dried and gold-coated using a Sputter Coater SC502. Samples were visualised with a Hitachi S-3000N scanning electron microscope at an accelerating voltage of 20 kV.

2.4.3. Videomicroscopy recording

Movies were taken using a Leica TCS SP2 confocal microscope equipped with a 5% CO_2 chamber thermostated at 37 °C. For this experiment, cells were seeded on 35 mm glass bottom culture dishes (from Mattek, Ashland, MA, USA). Control slides were used to assess that the recording conditions were absolutely innocuous to the cells.

2.5. Cell viability

Thiazolyl blue (MTT, Sigma) was used for cell viability studies. A stock solution (1 mg/mL) in PBS was prepared immediately prior to use. One hundred microliters of this solution were added to each culture dish (containing 2 mL of the whole medium; final concentration of MTT: 47.6 μg/mL). Cells were incubated for at least 3 h for formazan production, after which formazan precipitates were dissolved in 1.5 mL DMSO and the absorbance was measured at 540 nm on a Tecan Spectra Fluor spectrophotometer. Cell survival was expressed as the percentage of absorption of treated cells in comparison with that of control cells. The results obtained are the mean value and standard deviation from at least six experiments.

2.6. Assessment of apoptosis

2.6.1. Flow cytometry

The DNA content of the subpopulation of apoptotic cells was determined by combining the above flow cytometry protocol with the TUNEL assay (Roche, Barcelona, Spain). Briefly, floating and trypsinised cells were fixed in 3.5% paraformaldehyde (BDH, Poole, England, UK) for 20 min at room temperature. Then cells were permeabilised with 0.1% Triton X-100 (Sigma), incubated with RNase and subjected to the TUNEL reaction. Prior to measurement, PI was added as described.

2.6.2. Fluorescence microscopy

Changes in the nuclear morphology of treated cells were principally studied by means of H-33258 staining as described above. Following morphological criteria (Rello et al., 2005), cells were classified as living (control-like interphases), mitotic or apoptotic. At least six experiments for cell counting were made.

For the study of the cytochrome *c* release, cells on coverslips were fixed in 3.5% paraformaldehyde and permeabilised with 1% Triton X-100 and 0.02% Tween

20 (Sigma). The primary antibody used was sheep anti-cytochrome *c* antibody; the secondary antibody was rabbit anti-sheep IgG (whole molecule)-FITC (both from Sigma). Cells were mounted with ProLong Gold antifade reagent (Molecular Probes).

3. Results

3.1. Cell cycle analysis

The treatment of HeLa cells with VP-16 not only caused the expected triggering of an apoptotic response, but also a severe alteration of the cell cycle. Flow cytometry analysis of the effects of our pulse (3 h incubation with 50 μM VP-16) showed that, in contrast with the DNA content of control (untreated) cells measured by PI, cell cycle profiles of treated cells were changed by the accumulation of cells at the G2-M peak (Fig. 1). This effect was quite evident before the amount of apoptotic cells reached its maximum value. The highest G2-M peak was found 48 h after incubation with the drug ($\Delta T = 48$ h), when apoptosis was not yet a massive phenomenon.

As seen in Fig. 1, flow cytometry measurements showed that at $\Delta T = 48$ h the G2-M blockage reached the 26.2% of cell population. Moreover, microscopic visualisation of cells showed that 48 h after VP-16 treatment there was an important increase of the number of rounded and refringent cells (Fig. 1); this result suggested a mitotic arrest.

Cell counting of immunofluorescent tubulin-labelled samples on slides resulted in a mitotic index of 19.8%, versus 4.6% in the controls (Table 1). This difference between flow cytometry and direct microscopy counting data might be due to methodological aspects: numerous mitotic cells are lost during the immunofluorescence labelling process, as well as part of G2-M cells measured at $\Delta T = 48$ h may be endocycling polyploid cells or cells already in apoptosis triggered from a polyploid state.

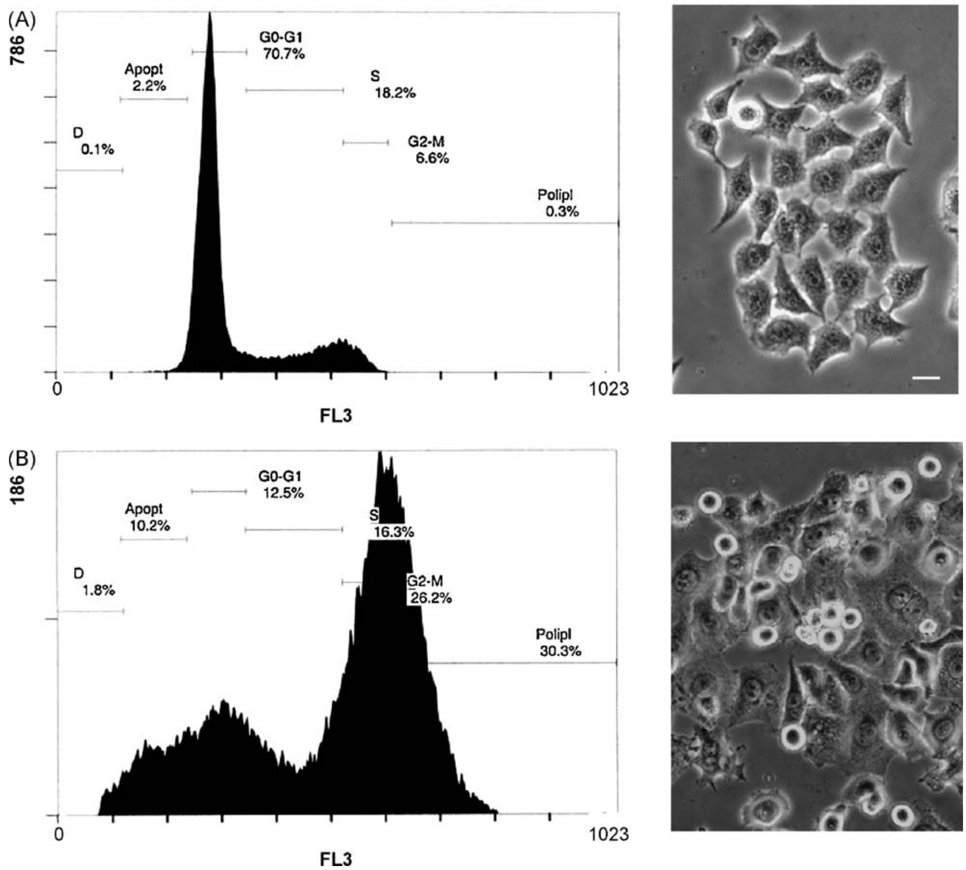

Fig. 1. Flow cytometry analysis of DNA content (measured using propidium iodide) and morphology of HeLa cells. Scale bar: 10 μm. (A) DNA content profile of a control HeLa population; right: control HeLa cells observed by phase contrast microscopy. (B) DNA content profile of HeLa cells 48 h after 3 h incubation with 50 μM VP-16. The peak pattern is clearly shifted towards G2-M and polyploid areas; right: phase contrast microscopy shows the increase of the number of round and refringent mitotic cells.

Table 1
Effects produced in HeLa cells, by 50 μM VP-16 pulse, on mitotic index (MI) and the ratios of total metaphases (TM) and abnormal metaphases (AM)

	MI (% ± S.D.)	TM (% ± S.D.)	AM (% ± S.D.)
Control	4.6 ± 0.1	61.25 ± 1.5	2 ± 0.2
$\Delta T = 24$ h	5 ± 3.7	70.6 ± 9.2	82.8 ± 7.5
$\Delta T = 48$ h	19.8 ± 2.5	86.2 ± 8.1	89.8 ± 7.4
$\Delta T = 72$ h	2.6 ± 1.6	80.5 ± 5.7	98.2 ± 3

Data correspond to mean values ± standard deviation (S.D.) from six different experiments.

The mitotic arrest decreased rapidly and at $\Delta T = 72$ h it was difficult to observe mitotic cells (Table 1). At this time there was a higher amount (27.9%, see Fig. 4) of G2-M cells according to their DNA content profile measured by flow cytometry. However, this result should not be considered in contradiction with direct cell counting, as almost all of them were polyploid cells that became apoptotic (revealed by the TUNEL assay, as explained below).

Another relevant phenomenon after VP-16 treatment was the high number of polyploid cells (Fig. 1). At $\Delta T = 48$ h the percentage of polyploid cells (with a DNA content higher than 4C) was 30.3%, versus 0.3% in control samples. This is in agreement with the appearance of interphase and metaphase cells bigger than those of control cultures (see Figs. 1 and 2A). Taken altogether, these data support the idea that our experimental conditions cause relevant alterations on the HeLa cell cycle, involving metaphase blockage and polyploidy.

3.2. Effects on mitotic cells

To improve our knowledge on the action mechanisms of the drug, and to test the hypothesis according to which VP-16 causes mitotic rather than G2 phase arrest, we performed additional immunofluorescence studies. Cell counting after immunofluorescence detection of tubulin revealed that the mitotic arrest was principally the consequence of a metaphase blockage due to abnormal mitotic spindle configurations (see Table 1). After VP-16 treatment, the ratio of metaphases over mitotic cells increased, and those metaphases were mainly abnormal (reaching 89.8% of metaphases at $\Delta T = 48$ h, when the metaphase blockage is more evident).

At $\Delta T = 48$ h there was a majority of multipolar metaphase cells (Fig. 2A). These multipolar metaphases were also immunolabelled for human centromeres, showing that the number of fluorescent spots was considerably higher in comparison with control cells (Fig. 2B). This increased number of centromeres clearly evidenced that the multipolar metaphases corresponded to polyploid cells. Moreover, a scanning electron microscope analysis confirmed that at $\Delta T = 48$ h, treated metaphases were almost double-sized with respect to control ones (Fig. 3).

Besides, these multipolar metaphases also showed chromosome disruption and fragmentation (Fig. 2B and C). It is important to remark that only few of the chromosome fragments seemed to be joined to the spindle, as well as the majority of fragments did not show any centromeric signal. The number of poles was rather variable, the most common mitotic configuration being that with three poles; however, metaphases with four to six poles could be also seen.

For further understanding of the process, a microscopic analysis of metaphases at $\Delta T = 24$ h was made. At this time the mitotic index appeared almost the same as that of control cells (5% versus 4.6%, see Table 1), still far from the highest value. But at $\Delta T = 24$ h, altered metaphases showing a disturbance of the spindle were found in a significant amount (see Table 1). Analysis of the organization of chromatin and centromeres (Fig. 2B) demonstrated that the disturbance was caused by the accumulation of acentromeric fragments of chromosomes (because only the centromeric fragments succeeded to join the spindle).

Experiments using higher doses of VP-16 (100 μM) and increased incubation times (24 h) caused direct cell death by apoptosis without a previous step of metaphase blockage (data not shown).

3.3. Polyploid cells

Flow cytometry analysis showed that at prolonged ΔT (48 h after treatment and later) all the surviving cells had a polyploid condition. These polyploid cells were easy to identify due to their big size. Treatment also caused a dramatic morphological alteration of giant interphase cells, which showed typical morphological features.

Some giant cells appeared with multiple nuclei of different sizes (Fig. 2C), some of which did not present any centromeric signal. The origin of these polyploid interphase cells could be the wrong resolution of abnormal metaphases. It is easy to find cells joined by chromatin and tubulin bridges in microscopic preparations (Fig. 2C); these bridges can be also seen between the nuclei of multinucleated cells and they could be remnants of aberrant mitotic processes.

3.4. Assessment of cell death

Under our experimental conditions, HeLa cell death measured with the MTT assay (see Table 2) was evident

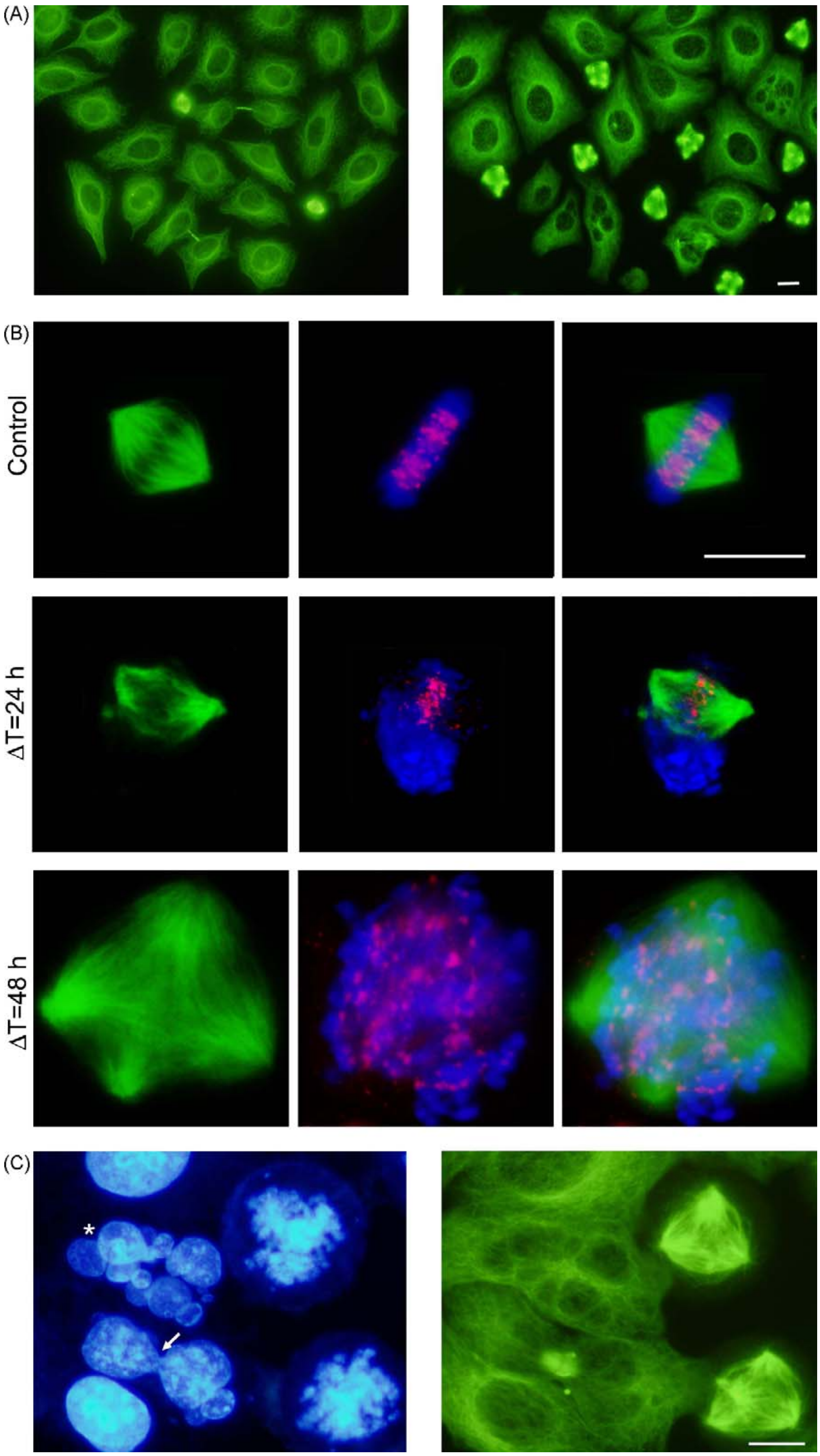
(A)
(B)
Control
ΔT=24 h
ΔT=48 h
(C)
*

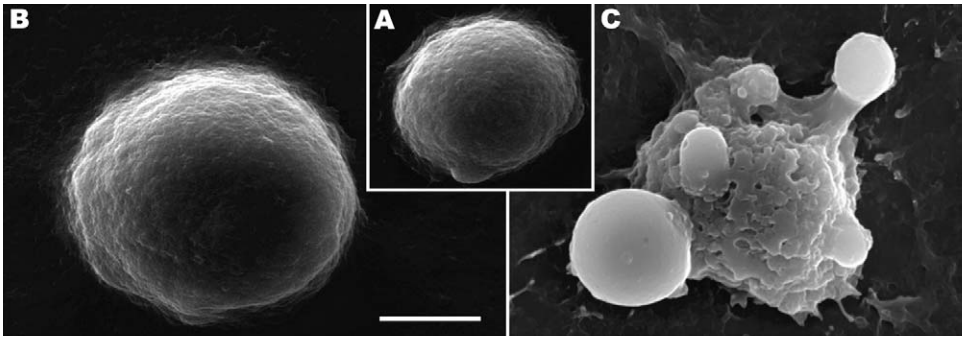

Fig. 3. HeLa cells observed by scanning electron microscopy. Scale bar: 5 μm. (A) Control metaphase cell showing a smooth surface and spherical shape. (B) Metaphase cell at $\Delta T = 48$ h after the VP-16 pulse. Both cells are morphologically almost identical but the treated cell is double-sized, suggesting its polyploidy. (C) Apoptotic HeLa cell at $\Delta T = 72$ h after treatment. The smooth surface and the spherical morphology are lost by the appearance of apoptotic bodies. Note that this apoptotic cell is also a giant cell.

Table 2
Cell survival after 50 μM VP-16 pulse, measured by the MTT assay

	Surviving fraction (% ± S.D.)
Control cells	100 ± 2.6
$\Delta T = 48$ h	81.6 ± 4.8
$\Delta T = 72$ h	37.5 ± 5.9
$\Delta T = 96$ h	1 ± 0.5

Data correspond to mean values ± standard deviation (S.D.) from six different experiments.

48 h after a 50 μM VP-16 pulse, followed by complete cell death 96 h later (cell survival of 1%). Cell death was also confirmed by direct counting of cells stained with H-33258, which also allowed us to identify apoptosis, under morphological criteria, as the unique cell death mechanism (data not shown). At $\Delta T = 72$ and 96 h, the great majority of the cells detached from the culture surface and showed the typical morphological features of apoptosis after H-33258 staining (cell rounding and blebbing, chromatin condensation, fragmentation and packing into apoptotic bodies; see Figs. 3 and 4A).

We also studied the cell death mechanism using the TUNEL assay measured by flow cytometry. This assay showed that 64.3% of HeLa cells were already in apoptosis at $\Delta T = 72$ h (Fig. 4B). This result was consistent with previous MTT assay data (see Table 2). We also performed a combined analysis with TUNEL assay and PI staining, aimed to identify the origin of apoptotic cells. This study, carried out at $\Delta T = 72$ h, showed that this 64.3% of apoptotic cells was distributed on all the sections of the DNA content histogram (G0–G1, S and G2-M, see Fig. 4C). In the course of the apoptotic process, it is well known that cells modify their DNA content. The high amount of PI signal seen at $\Delta T = 48$ h, suggests that this high DNA-containing apoptotic cells probably were the former metaphase-arrested and polyploid ones.

Cytochrome *c* exit from the mitochondria is a specific and characteristic event related to apoptosis triggering. Using immunofluorescence we confirmed the cytochrome *c* translocation to the cytoplasm in almost all cells with apoptotic nuclear morphology at $\Delta T = 48$ h and 72 h after VP-16 treatment (Fig. 4D and D′, arrows).

As a final confirmation of the sequence of described events, a living cell videomicroscopy study was made. In a time lapse from 55 to 72 h after the treatment, round metaphases failed to divide and became directly apoptotic cells, as shown by their typical blebbing behaviour (see Fig. 5 and Supplementary Information). We can conclude that the treatment of HeLa cells with VP-16 causes a sequence of events, starting with chromosome breaks, which prevent a proper joining of chromosomes to microtubules during mitosis, which could be followed by restitution. Next, resti-

Fig. 2. Mitotic arrest, alteration of the mitotic spindles and polyploidy caused by VP-16 pulse. Scale bar: 10 μm. (A) Tubulin immunolabelled cells observed by fluorescence microscopy; left: control cells; right: cells 48 h after treatment ($\Delta T = 48$ h) showing cell size increase and metaphase blockage with multiple spindle's poles. (B) Metaphase cells labelled for tubulin (green), chromatin (blue) and centromeres (red), observed by confocal microscopy, and complete merged image; up: control metaphase; middle: metaphase disrupted by extensive chromosome breakage (the centromeric fragments join the spindle but acentric ones accumulate in the cell periphery) observed at $\Delta T = 24$ h; below: tetrapolar mitotic spindle in which centromeric fragments adopt a disperse disposition ($\Delta T = 48$ h). (C) Forty-eight hours after VP-16 treatment, cells stained with H-33258 (left) and immunolabelled for tubulin (right). One interphase cell shows the presence of a chromatin bridge joining the daughter nuclei (identified by an arrow). A giant multinucleated cell is identified with an asterisk. The fluorescence of the chromatin is reduced in several micronuclei. Note that the tubulin fluorescence is very bright in an area between the micronuclei suggesting the presence of bridges.

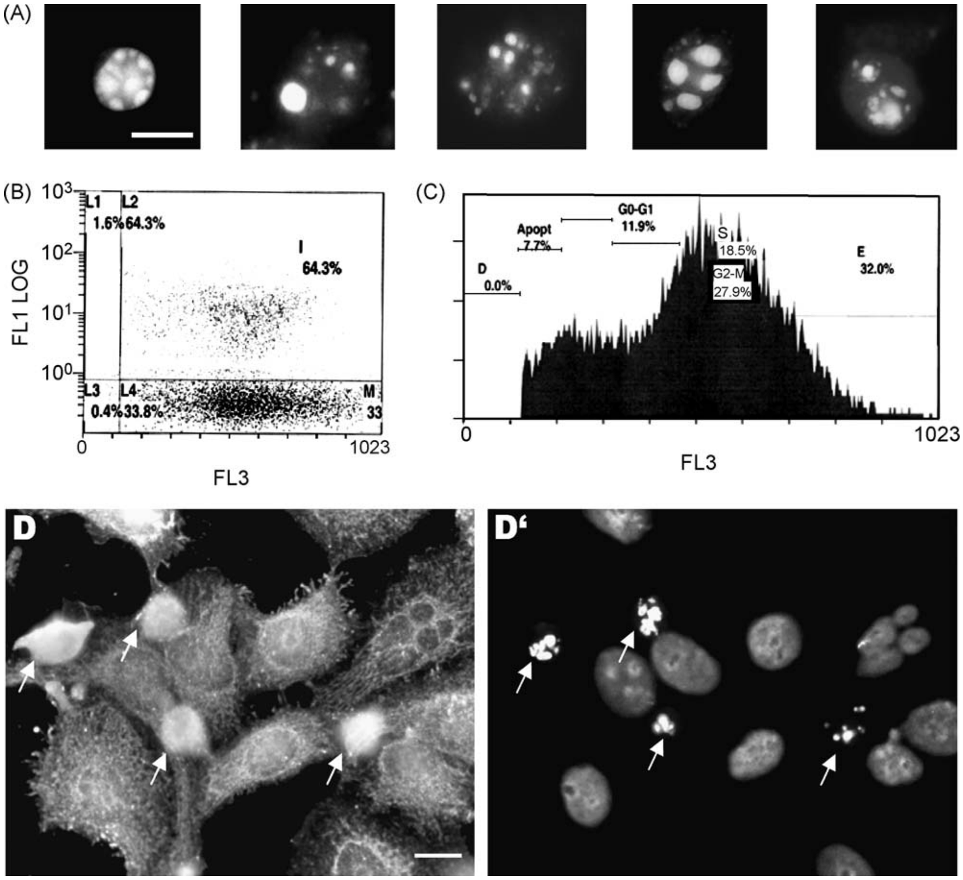

Fig. 4. Cell death caused by 50 μM VP-16 pulse. Scale bar: 10 μm. (A) Details of apoptotic HeLa cells (H-33258 staining) detached from the cell culture 72 h after VP-16 pulse. (B) Flow cytometry diagram showing the percentage of apoptosis (area L2) and the surviving fraction (area L4) measured with TUNEL assay at $\Delta T = 72$ h. (C) Flow cytometry diagram showing the DNA content of the apoptotic cells of the area L2. Apoptosis starts from G2-M or polyploid state, because of the high DNA content. (D and D′) Immunofluorescence for cytochrome *c* (D) and H-33258 staining (D′) of HeLa cells at $\Delta T = 72$ h. Note that apoptotic cells show both diffuse cytoplasmic cytochrome *c* signal and DNA condensation (arrows).

tuted cells enter into a new mitotic cycle with multipolar spindles, causing metaphase blockage and finally apoptosis.

4. Discussion

Inhibitors of topo II have been the object of intense study, because this enzyme is the target for several chemotherapy drugs against cancer (Andoh & Ishida, 1998; Fortune & Osheroff, 2000; Wang et al., 2001; Wilstermann & Osheroff, 2003). VP-16 inhibits the activity of topo II and induces single- and double-strand DNA breaks (Hande, 1998; Kamesaki et al., 1993), but it can only be used for inhibiting DNA decatenation during the S phase (triggering the apoptotic process at the spindle checkpoint) (Skoufias et al., 2004). In response to this genotoxic effect, cells can alter their cell cycle and die by apoptosis, although cancer cells usually have mutations that allow them to survive (Kastan & Bartek, 2004; Kaufmann, 1998).

In the present study we have shown that under our experimental conditions, VP-16 is able to induce the arrest of HeLa cells in metaphase, followed by cell death. These effects do not take place immediately. Instead, they are observed after a considerable time delay after VP-16 treatment.

In this sense, at $\Delta T = 24$ h (50 μM VP-16, 3 h), mitotic cells often showed bipolar spindles, but with the chromosomes not being well positioned in the equator (see Fig. 2). Presumably these cells would be able to restitute to "primary" polyploid cells. However, at $\Delta T = 48$ h, a G2-M arrest was observed by flow cytometry. The analysis of microtubules by immunofluorescence evidenced that the mitotic index increased 4 times over the controls (19.8% versus 4.6%, respectively). Cell counting indicated that most of the mitosis corresponded to

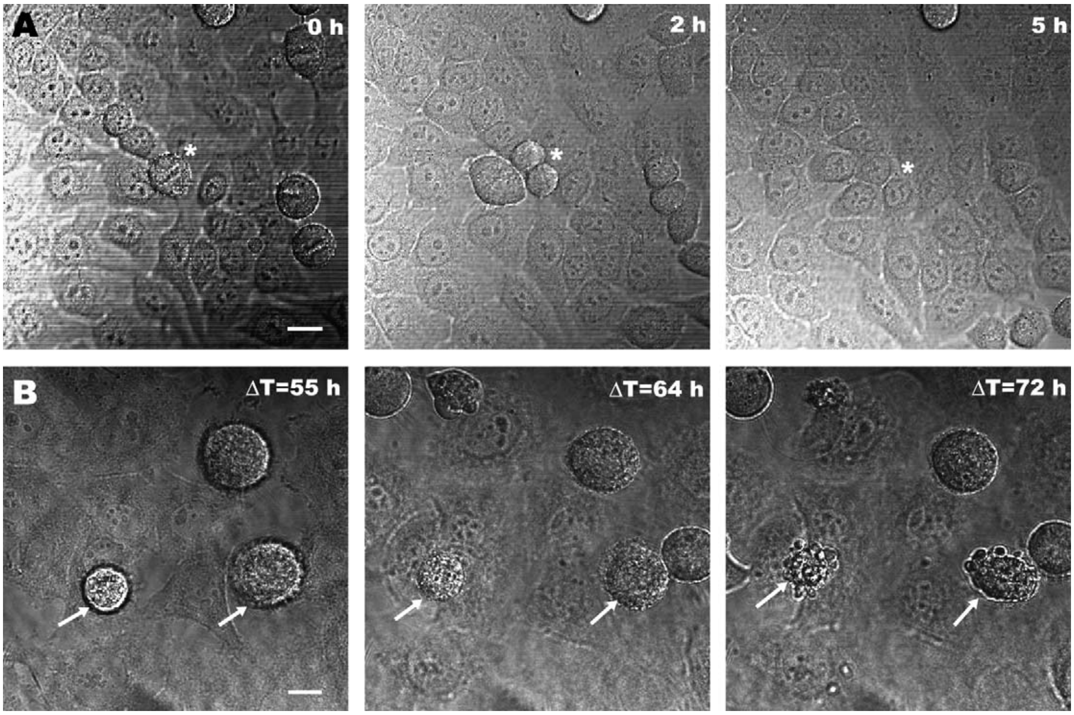

Fig. 5. Images of HeLa cells extracted from videomicroscopy records. Scale bar: 10 μm. (A) Control cells sequence of 5 h showing normal mitosis resolution. (B) The 50 μM VP-16 treated cells showing metaphase blocked cells entering directly into apoptosis, identified by the characteristic surface blebbing (sequence recorded in 17 h from $\Delta T = 55$ to 72 h).

abnormal, mainly multipolar metaphases, with several chromosomes scattered around the mitotic spindle. Likewise, interphase cells with chromatin bridges, as well as giant and/or multinucleated cells were also observed. Between 48 and 72 h after the incubation with VP-16, HeLa cells gradually entered in apoptosis, with complete cell inactivation 96 h after VP-16 treatment.

Our results indicate that a pulse of VP-16 requires a prolonged time to trigger apoptosis in HeLa cells. During the first 24 h after treatment, some cells can survive in spite of the incorrect positioning of the chromosomes and their incapacity to join the mitotic spindle. Forty-eight hours after treatment, cells were arrested in G2-M, due to the formation of multiple spindle's poles and the absence of chromosomes joining to microtubules. Finally 72 h after treatment, 64.3% of cells were positive to the TUNEL assay. Apoptotic cell death of the rounded and detached cells was confirmed by H-33258 staining and by immunofluorescence. The first method evidenced the characteristic condensation and fragmentation of the apoptotic nuclei and the second, the cytochrome *c* release from the mitochondria to the cytosol.

Previous results using VP-16 in HeLa cells showed that the experimental conditions were quite different. In many cases, lower concentrations and higher incubation times than in our present protocol, have been used. As an example, Bartling et al. (2004) employed 2.5 μM VP-16 for 48 h to trigger apoptosis in HeLa cells, and Elliott, Stribinskiene, and Lock (1998) reached the complete cell inactivation with 1 μM VP-16 for 24 h. On the other hand, higher concentrations combined with reduced incubation times, have also been assayed. HeLa cells apoptosis was induced using 50 μM VP-16 for up to 12 h by Kim et al. (2005) and Boldt et al. (2002) used 70 μM VP-16 for 18 h incubation time. In other cell culture models than HeLa, different experimental protocols with etoposide have also been used (Ayene et al., 2005; Clifford, Beljin, Stark, & Taylor, 2003; Facompre, Wattez, Kluza, Lansiaux, & Bailly, 2000; Sleiman & Stewart, 2000).

The time delay of the cytotoxic effects after treatment is also variable. Martins et al. (1997) have reported apoptosis in HL60 and K562 cells induced by VP-16. Both leukaemia cell lines have a negligible expression of p53 (Law, Ritke, Yalowich, Leder, & Ferrell, 1993; Prokocimer et al., 1986). However, they differ in the expression of the tyrosine kinase protein bcr/abl, being positive for K562 and negative for HL60. Apoptotic changes appeared in each cell line at different time intervals after VP-16 (17 μM, 1 h). HL60 cells showed the morphological and biochemical apoptotic changes 6 h after treatment. On the contrary, the same treatment of K562 cells provoked an arrest of the cell cycle in G2 and an apparently normal behaviour of cells, during 3–4 days before developing apoptotic signs. An increase in VP-16 concentration (68 μM) induced an apoptotic response after 2–3 h in HL60 cells, while a similar response in K562 cells was reached after 3–4 days. The authors showed in the same work that the apoptotic delay in K562 cells was not specific for etoposide, as other stimuli, including staurosporine, cisplatin and ionizing radiation, provoked similar apoptosis kinetics. They suggested that bcr/abl tyrosine kinase played an important role in delaying apoptosis rather than preventing it. This is in contrast to previous belief, in that K562 cells were described to be resistant to apoptosis induced by etoposide and other antitumoral agents. This resistance was indeed attributed to K562 being a cell line expressing the bcr/abl tyrosine kinase for apoptosis suppression, as apoptosis appeared again upon treatment with antisense oligonucleotides that inhibit bcr/abl kinase (McGahon et al., 1994, 1997). Martins et al. (1997) propose that the discrepancy on the apoptosis induction by etoposide in K562 cells is due to the short time elapsed after treatment with the inducing stimulus (4–24 h) before cell survival assessment. We agree with these authors in the sense that rapid apoptotic assessments (often used for drug-screening studies) could underestimate the true effectiveness of the tested agents in killing cells.

It is well known that apoptosis is a cell death mechanism involved in the development and progression of cancer, as well as in the cytotoxicity or resistance induced by anticancer drugs. Recent reviews include significant progress in the understanding of the molecular pathways of apoptosis (or defective apoptosis) involved in these processes (Gerl & Vaux, 2005; Johnstone, Ruefli, & Lowe, 2002; Kim, 2005; Tsuruo et al., 2003). In this context, the role of the tumour suppressing gene p53 raised a special interest. In addition to its link to apoptotic signalling, it is the most commonly mutated gene in human cancers. Therefore, the activation state of the p53 protein could be related to tumour cell sensitivity to anticancer agents (Brown & Wouters, 1999; Johnstone et al., 2002; Sun, 2006; Vousden, 2002).

Numerous studies suggest that some chemotherapeutic drugs, including etoposide, are able to provoke apoptotic cell death through pathways other than p53-mediated apoptosis. Recently, Karpinich, Tafani, Schneider, Russo, and Farber (2006) have demonstrated that etoposide is able to induce apoptosis in Jurkat T-cells, a leukaemia cell line characterized by a loss of both p53 and Bax. These authors propose that the etoposide-induced DNA damage is linked to Bid activation. In the same way, the nuclear caspase-2 activation seems to be related to the engagement of the mitochondrial apoptotic pathway induced by etoposide in wild-type Jurkat T-lymphocytes (Robertson, Enoksson, Suomela, Zhivotovsky, & Orrenius, 2002). Moreover, the proapoptotic BH3-only protein ITM2Bs is able to induce apoptosis in both $p53^{+/+}$ and $p53^{-/-}$ cellular models including HeLa cells (Fleischer & Rebollo, 2004). These results seem to indicate that the knowledge of the p53 status of a cancer cell might not be sufficient to predict the efficiency of potentially chemotherapeutic drugs in treated cells. They also indicate that there are other ways for cell death in the case of tumour cells with p53 null or mutated.

Besides, numerous and discrepant results have been reported on the blockage of the cell cycle progression induced by VP-16 in several cell lines. Some reports indicate that cells accumulate in the G1-S phase of the cell cycle (Blass, Kronfeld, Kazimirsky, Blumberg, & Brodie, 2003), while other authors have proposed cell arrest in the G2-M phase (Clifford et al., 2003; Facompre et al., 2000; Fletcher et al., 2003; Ridd, Alexander, & Reed, 2004; Sleiman & Stewart, 2000). It is widely accepted that activation of checkpoints in response to DNA damage leads to cell cycle arrest, but when severe damage occurs, arrested cells result in apoptotic death (Singh et al., 2004).

To the best of our knowledge, apoptotic cell death preceded by metaphase blockage of HeLa cells by etoposide has not yet been described. However, low concentrations (10 nM for 20 h) of paclitaxel (Taxol) induce metaphase blockage in HeLa cells leading to apoptotic cell death at 48-72 h after drug removal, which is related to the stabilization of the spindle-microtubule dynamics (Jordan et al., 1996).

Keeping in mind that our treatment with VP-16 is able to induce the formation of aberrant mitosis and multinucleated/giant cells, it seems that the mitotic catastrophe could be involved in HeLa cell death. The same cellular alterations described have been identified as characteristic of the mitotic catastrophe (also known as mitotic death); a form of cell death different from apoptosis and necrosis (Erenpreisa et al., 2000). Although its molecular mechanism is not completely known, this type of death process can explain cell death induced by treatments that cause aberrant mitosis, when the G2 checkpoint is defective and cells enter in mitosis before DNA damage has been repaired. Moreover, mitotic catastrophe could represent a “survival phenotype” as cells with damaged DNA do not suffer immediate apoptosis in G2 and continue their cycle upon metaphase blockage and restitution as polyploid cells (endocycle). These polyploid cells have more time for DNA repair using homologous recombination and somatic reduction processes (multipolar spindles could act as a mechanism to recover diploid cells), allowing the generation of new resistant clones (Erenpreisa & Cragg, 2001). Likewise, mitotic catastrophe seems also to be involved in cell damage by drugs that affect the mitotic spindle, like taxol-derived compounds (see review from Okada & Mak, 2004).

Morphological features similar to those described 48 h after VP-16 treatment can be induced by other drugs. The histone-deacetylase inhibitor azelaic bishydroxamic acid (ABHA) induces an abnormal disjunction of chromosomes around the mitotic spindle in three different cell lines, including HeLa cells (Qiu et al., 2000). Cells can enter in mitosis without the appropriate alignment of replicated chromosomes, originating multiple nuclei and micronuclei. In some cases, cells undergo cytokinesis with an incomplete separation of the chromosomes, giving place to cell images similar to that of Fig. 2, which these authors (Qiu et al., 2000) denominate 'cut' phenotype. The authors have proposed that a dysfunction of the G2 checkpoint can also disrupt the mitotic spindle checkpoint, therefore ensuring that cells with a significant DNA damage finally die.

Likewise, micronucleation, DNA bridges coming from incomplete cytokinesis, and progression to mitotic catastrophe, has also been described in human colon carcinoma cells (HCT116) after 12 Gy of γ-radiation (Andreassen, Lacroix, Lohez, & Margolis, 2001). Recently, exposure of human colon carcinoma cells HT-29 to the antitumour drug imidazoacridone C-1311 (another inhibitor of topo II in phase I clinical trials), induces cell death by mitotic catastrophe (Hyzy, Bozko, Konopa, & Skladanowski, 2005).

Eukaryotic cells respond to genome-damaging agents by activating checkpoints that stop the cell cycle reversibly or, in certain cases, induce cell death. Potter and Rabinovitch (2005) have demonstrated that the extent of DNA damage (e.g., strand breakage) is related to the cell cycle phase in which DNA damage is initiated. HeLa and A549 (human lung adenocarcinoma) cells treated with topo II targeting drugs (including VP-16) showed the highest level of strand breakage in G2-M, followed by S and G1. Likewise, they have found a different response of both cell types to the drugs; DNA damage being significantly greater in HeLa than in A549 cells.

In summary, VP-16 induces a metaphase arrest in HeLa cells, which seems to contribute to the cell inactivation by mitotic catastrophe and by triggering of death pathways without p53 participation. Clearly, further investigations on HeLa cells, as well as in other cell lines, are required in order to understand the molecular mechanisms underlying the described processes.

Acknowledgements

We thank Sylvia Gutiérrez (Cytometry Facility, Centro Nacional de Biotecnología, Madrid), Marta Furió and Esperanza Salvador (Scanning Electron Microscopy Laboratory, Universidad Autónoma de Madrid), and Dolores Morales and Lucía Sánchez (Confocal Microscopy Laboratory, Universidad Autónoma de Madrid). JCS is a scientific member of the Consejo Superior de Investigaciones Científicas (CSIC), Spain. Contract grant sponsor: Comunidad de Madrid, Spain. Contract grant number: GR/SAL/0213/2004.

Appendix A. Supplementary data

Supplementary data associated with this article can be found, in the online version, at doi:10.1016/j.biocel.2006.06.013.

References

Andoh, T., & Ishida, R. (1998). Catalytic inhibitors of DNA topoisomerase II. *Biochimica et Biophysica Acta*, *1400*, 155–171.

Andreassen, P. R., Lacroix, F. B., Lohez, O. D., & Margolis, R. L. (2001). Neither p21WAF1 nor 14-3-3sigma prevents G2 progression to mitotic catastrophe in human colon carcinoma cells after DNA damage, but p21WAF1 induces stable G1 arrest in resulting tetraploid cells. *Cancer Research*, *61*, 7660–7668.

Ayene, I. S., Ford, L. P., & Koch, C. J. (2005). Ku protein targeting by Ku70 small interfering RNA enhances human cancer cell response to topoisomerase II inhibitor and gamma radiation. *Molecular Cancer Therapeutics*, *4*, 529–536.

Bartling, B., Lewensohn, R., & Zhivotovsky, B. (2004). Endogenously released Smac is insufficient to mediate cell death of human lung carcinoma in response to etoposide. *Experimental Cell Research*, *298*, 83–95.

Bartova, E., Jirsova, P., Fojtova, M., Soucek, K., & Kozubek, S. (2003). Chromosomal territory segmentation in apoptotic cells. *Cellular and Molecular Life Sciences*, *60*, 979–990.

Blass, M., Kronfeld, I., Kazimirsky, G., Blumberg, P. M., & Brodie, C. (2002). Tyrosine phosphorylation of protein kinase Cdelta is essential for its apoptotic effect in response to etoposide. *Molecular and Cellular Biology*, *22*, 182–195.

Boldt, S., Weidle, U. H., & Kolch, W. (2002). The role of MAPK pathways in the action of chemotherapeutic drugs. *Carcinogenesis*, *23*, 1831–1838.

Brown, J. M., & Wouters, B. G. (1999). Apoptosis, p53, and tumor cell sensitivity to anticancer agents. *Cancer Research*, *59*, 1391–1399.

Clifford, B., Beljin, M., Stark, G. R., & Taylor, W. R. (2003). G2 arrest in response to topoisomerase II inhibitors: The role of p53. *Cancer Research*, *63*, 4074–4081.

Coon, J. S., Marcus, E., Gupta-Burt, S., Seelig, S., Jacobson, K., Chen, S., Renta, V., Fronda, G., & Preisler, H. D. (2002). Amplification and overexpression of topoisomerase II alpha predict response to anthracycline-based therapy in locally advanced breast cancer. *Clinical Cancer Research*, *8*, 1061–1067.

Elliott, M. J., Stribinskiene, L., & Lock, R. B. (1998). Expression of Bcl-2 in human epithelial tumor (HeLa) cells enhances clonogenic survival following exposure to 5-fluoro-2′-deoxyuridine or staurosporine, but not following exposure to etoposide or doxorubicin. *Cancer Chemotherapy and Pharmacology*, *41*, 457–463.

Erenpreisa, J. E., & Cragg, M. S. (2001). Mitotic death: A mechanism of survival? A review. *Cancer Cell International*, *1*, 1.

Erenpreisa, J. E., Ivanov, A., Dekena, G., Vitina, A., Krampe, R., Freivalds, T., Selianova, G., & Roach, H. I. (2000). Arrest in metaphase and anatomy of mitotic catastrophe: Mild heat shock in two human osteosarcoma cell lines. *Cell Biology International*, *24*, 61–70.

Evan, G. I., & Vousden, K. H. (2001). Proliferation, cell cycle and apoptosis in cancer. *Nature*, *411*, 342–348.

Facompre, M., Wattez, N., Kluza, J., Lansiaux, A., & Bailly, C. (2000). Relationship between cell cycle changes and variations of the mitochondrial membrane potential induced by etoposide. *Molecular Cell Biology Research Communications*, *4*, 37–42.

Fleischer, A., & Rebollo, A. (2004). Induction of p53-independent apoptosis by the BH3-only protein ITM2Bs. *FEBS Letters*, *557*, 283–287.

Fletcher, L., Yen, T. J., & Muschel, R. J. (2003). DNA damage in HeLa cells induced arrest at a discrete point in G2 phase as defined by CENP-F localization. *Radiation Research*, *159*, 604–611.

Fortune, J. M., & Osheroff, N. (2000). Topoisomerase II as a target for anticancer drugs: When enzymes stop being nice. *Progress in Nucleic Acid Research and Molecular Biology*, *64*, 221–253.

Gerl, R., & Vaux, D. L. (2005). Apoptosis in the development and treatment of cancer. *Carcinogenesis*, *26*, 263–270.

Godard, T., Deslandes, E., Sichel, F., Poul, J. M., & Gauduchon, P. (2002). Detection of topoisomerase inhibitor-induced DNA strand breaks and apoptosis by the alkaline comet assay. *Mutation Research*, *520*, 47–56.

Hande, K. R. (1998). Etoposide: Four decades of development of a topoisomerase II inhibitor. *European Journal of Cancer*, *34*, 1514–1521.

Hyzy, M., Bozko, P., Konopa, J., & Skladanowski, A. (2005). Related antitumour imidazoacridone C-1311 induces cell death by mitotic catastrophe in human colon carcinoma cells. *Biochemical Pharmacology*, *69*, 801–809.

Isaacs, R. J., Davies, S. L., Sandri, M. I., Redwood, C., Wells, N. J., & Hickson, I. D. (1998). Physiological regulation of eukaryotic topoisomerase II. *Biochimica et Biophysica Acta*, *1400*, 121–137.

Jiang, H., Luo, S., & Li, H. (2005). Cdk5 activator-binding protein C53 regulates apoptosis induced by genotoxic stress via modulating the G2/M DNA damage checkpoint. *The Journal of Biological Chemistry*, *280*, 20651–20659.

Johnstone, R., Ruefli, A., & Lowe, S. (2002). Apoptosis: A link between cancer genetics and chemotherapy. *Cell*, *108*, 153–164.

Jordan, M. A., Wendell, K., Gardiner, S., Derry, W. B., Copp, H., & Wilson, L. (1996). Mitotic block induced in HeLa cells by low concentrations of paclitaxel (Taxol) results in abnormal mitotic exit and apoptotic cell death. *Cancer Research*, *56*, 816–825.

Kamesaki, S., Kamesaki, H., Jorgensen, T. J., Tanizawa, A., Pommier, Y., & Cossman, J. (1993). Bcl-2 protein inhibits etoposide-induced apoptosis through its effects on events subsequent to topoisomerase II-induced DNA strand breaks and their repair. *Cancer Research*, *53*, 4251–4256.

Karpinich, N. O., Tafani, M., Schneider, T., Russo, M. A., & Farber, J. L. (2006). The course of etoposide-induced apoptosis in Jurkat cells lacking p53 and Bax. *Journal of Cellular Physiology*, *208*, 55–63.

Kastan, M. B., & Bartek, J. (2004). Cell-cycle checkpoints and cancer. *Nature*, *432*, 316–323.

Kaufmann, S. H. (1998). Cell death induced by topoisomerase-targeted drugs: More questions than answers. *Biochimica et Biophysica Acta*, *1400*, 195–211.

Kim, R. (2005). Recent advances in understanding the cell death pathways activated by anticancer therapy. *Cancer*, *103*, 1551–1560.

Kim, Y., Koo, K. T., Choi, J. S., Jin, Y. H., Yim, H., Oh, Y. T., & Lee, S. K. (2005). Analysis of cyclin-dependent kinase 2-regulated phosphorylation of stathmin in etoposide-induced apoptotic HeLa cells by two-dimensional electrophoresis and mass spectrometry. *Journal of Health Science*, *51*, 224–232.

Kropotov, A. V., Grudinkin, P. S., Pleskach, N. M., Gavrilov, B. A., Tomilin, N. V., & Zhivotovsky, B. (2004). Downregulation of peroxiredoxin V stimulates formation of etoposide-induced double-strand DNA breaks. *FEBS Letters*, *572*, 75–79.

Larsen, A. K., Escargueil, A. E., & Skladanowski, A. (2003a). Catalytic topoisomerase II inhibitors in cancer therapy. *Pharmacology and Therapeutics*, *99*, 167–181.

Larsen, A. K., Escargueil, A. E., & Skladanowski, A. (2003b). From DNA damage to G2 arrest: The many roles of topoisomerase II. *Progress in Cell Cycle Research*, *5*, 295–300.

Law, J. C., Ritke, M. K., Yalowich, J. C., Leder, G. H., & Ferrell, R. E. (1993). Mutational inactivation of the p53 gene in the human erythroid leukemic K562 cell line. *Leukemia research*, *17*, 1045–1050.

Makin, G., & Dive, C. (2001). Apoptosis and cancer chemotherapy. *Trends in Cell Biology*, *11*, S22–S26.

Makin, G., & Dive, C. (2003). Recent advances in understanding apoptosis: New therapeutic opportunities in cancer chemotherapy. *Trends in Molecular Medicine*, *9*, 251–255.

Martins, L. M., Mesner, P. W., Kottke, T. J., Basi, G. S., Sinha, S., Tung, J. S., Svingen, P. A., Madden, B. J., Takahashi, A., McCormick, D. J., Earnshaw, W. C., & Kaufmann, S. H. (1997). Comparison of caspase activation and subcellular localization in HL-60 and K562 cells undergoing etoposide-induced apoptosis. *Blood*, *90*, 4283–4296.

McGahon, A., Bissonnette, R., Schmitt, m., Cotter, K. M., Green, D. R., & Cotter, T. G. (1994). BCR-ABL maintains resistance of chronic myelogenous leukemia cells to apoptotic cell death. *Blood*, *83*, 1179–1187.

McGahon, A. J., Brown, D. G., Martin, S. J., Amarante-Mendes, G. P., Cotter, T. G., Cohen, G. M., & Green, D. R. (1997). Downregulation of Bcr-Abl in K562 cells restores susceptibility to apoptosis: Characterization of the apoptotic death. *Cell Death and Differentiation*, *4*, 95–104.

Meresse, P., Dechaux, E., Monneret, C., & Bertounesque, E. (2004). Etoposide: Discovery and medicinal chemistry. *Current Medicinal Chemistry*, *11*, 2443–2446.

Okada, H., & Mak, T. W. (2004). Pathways of apoptotic and non-apoptotic death in tumour cells. *Nature Reviews Cancer*, *4*, 592–603.

Pommier, Y., Sordet, O., Antony, S., Hayward, R. L., & Kohn, K. W. (2004). Apoptosis defects and chemotherapy resistance: Molecular interaction maps and networks. *Oncogene*, *23*, 2934–2949.

Potter, A. J., & Rabinovitch, P. S. (2005). The cell cycle phases of DNA damage and repair initiated by topoisomerase II-targeting chemotherapeutic drugs. *Mutation Research*, *572*, 27–44.

Prokocimer, M., Shaklai, M., Ben Bassat, H., Wolf, D., Goldfinger, N., & Rotter, V. (1986). Expression of p53 in human leukemia and lymphoma. *Blood*, *68*, 113–118.

Qiu, L., Burgess, A., Fairlie, D. P., Leonard, H., Parsons, P. G., & Gabrielli, B. G. (2000). Histone deacetylase inhibitors trigger a G2 checkpoint in normal cells that is defective in tumor cells. *Molecular Biology of the Cell*, *11*, 2069–2083.

Rello, S., Stockert, J. C., Moreno, V., Gámez, A., Pacheco, M., Juarranz, A., Cañete, M., & Villanueva, A. (2005). Morphological criteria to distinguish cell death induced by apoptotic and necrotic treatments. *Apoptosis*, *10*, 201–208.

Ridd, K., Alexander, D. J., & Reed, C. J. (2004). Foetal rat lung epithelial (FRLE) cells: Alterations in cellular homeostasis and gene expression in response to etoposide, hydrogen peroxide and sodium butyrate. *Toxicology*, *195*, 209–220.

Robertson, J. D., Enoksson, M., Suomela, M., Zhivotovsky, B., & Orrenius, S. (2002). Caspase-2 acts upstream of mitochondria to promote cytochrome *c* release during etoposide-induced apoptosis. *The Journal of Biological Chemistry*, *277*, 29803–29809.

Scheffner, M., Werness, B. A., Huibregtse, J. M., Levine, A. J., & Howley, P. M. (1990). The E6 oncoprotein encoded by human papillomavirus types 16 and 18 promotes the degradation of p53. *Cell*, *63*, 1129–1136.

Singh, S. V., Herman-Antosiewicz, A., Singh, A. V., Lew, K. L., Srivastava, S. K., Kamath, R., Brown, K. D., Zhang, L., & Baskaran, R. (2004). Sulforaphane-induced G2/M phase cell cycle arrest involves checkpoint kinase 2-mediated phosphorylation of cell division cycle 25C. *The Journal of Biological Chemistry*, *279*, 25813–25822.

Skoufias, D. A., Lacroix, F. B., Andreassen, P. R., Wilson, L., & Margolis, R. L. (2004). Inhibition of DNA decatenation, but not DNA damage, arrests cells at metaphase. *Molecular Cell*, *15*, 977–990.

Sleiman, R. J., & Stewart, B. W. (2000). Early caspase activation in leukemic cells subject to etoposide-induced G2-M arrest: Evidence of commitment to apoptosis rather than mitotic cell death. *Clinical Cancer Research*, *6*, 3756–3765.

Sun, Y. (2006). p53 and its downstream proteins as molecular targets of cancer. *Molecular Carcinogenesis*, *45*, 409–415.

Tsuruo, T., Naito, M., Tomida, A., Fujita, N., Mashima, T., Sakamoto, H., & Haga, N. (2003). Molecular targeting therapy of cancer: Drug resistance, apoptosis and survival signal. *Cancer Science*, *94*, 15–21.

Vousden, K. H. (2002). Activation of the p53 tumor suppressor protein. *Biochimica et Biophysica Acta*, *1602*, 47–59.

Wang, H., Mao, Y., Zhou, N., Hu, T., Hsieh, T. S., & Liu, L. F. (2001). ATP-bound topoisomerase II as a target for antitumor drugs. *The Journal of Biological Chemistry*, *276*, 15990–15995.

Wilstermann, A. M., & Osheroff, N. (2003). Stabilization of eukaryotic topoisomerase II-DNA cleavage complexes. *Current Topics in Medicinal Chemistry*, *3*, 321–338.

Woessner, R. D., Mattern, M. R., Mirabelli, C. K., Johnson, R. K., & Drake, F. H. (1991). Proliferation- and cell cycle-dependent differences in expression of the 170 kilodalton and 180 kilodalton forms of topoisomerase II in NIH-3T3 cells. *Cell Growth and Differentiation*, *2*, 209–214.

Artículo 5:

Catástrofe mitótica inducida en células HeLa por un tratamiento fotodinámico con ftalocianina de zinc (II)

Enviado para su publicación (2007)

La Terapia Fotodinámica del cáncer puede desencadenar distintos tipos de muerte celular, en función de la intensidad del daño producido. El fotosensibilizador ftalocianina de zinc (ZnPc) es uno de los más prometedores entre los llamados "fotosensibilizadores (PSs) de segunda generación". La PDT basa su toxicidad en la producción de ROS, que se disipan muy rápidamente de manera que el daño que causan por su alta reactividad queda circunscrito a las cercanías del punto de producción (que es el de acumulación subcelular del PS).

Nuestro grupo lleva años trabajando con ZnPc vehiculizada en liposomas de DPPC. En publicaciones previas hemos mostrado cómo la PDT con ZnPc puede causar distintos niveles de daño en los elementos del citoesqueleto en células HeLa. Entre esos daños se encontraba la inducción de bloqueos en metafase y, en la presente publicación, se pretende analizar la evolución de las células tras la inducción de dicho bloqueo para determinar si se está produciendo un verdadero proceso de catástrofe mitótica.

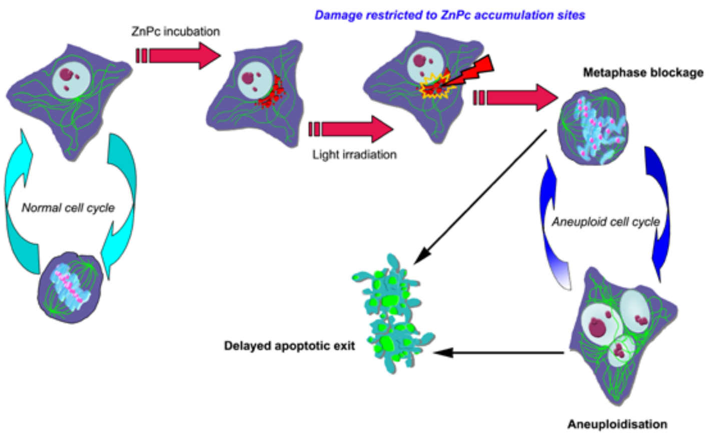

Figure 14 ZnPc-PDT can induce cell death by means of mitotic catastrophe. As PDT is not a genotoxic therapy, it is not clearly established it's potential to induce mitotic catastrophe. We show that, in sub-lethal conditions, ZnPc-PDT induces a quick metaphase arrest (evident 6 h after light irradiation and still present in a lesser form 24 h after treatment). The presence of restituted aneuploid interphases with multinucleation rather micronucleation is also confirmed. A delayed exit to death, starting 24 h after treatment and arising its maximum 72 h after light exposure, connects the reproductive abnormalities with cell inactivation in a typical sequence of mitotic catastrophe processes.

Asimismo, se han realizado pruebas experimentales pendientes para confirmar la incorporación del PS en las células HeLa y su localización subcelular. Se ha evaluado la cinética de penetración de la ZnPc en las células, que ha demostrado ser dependiente de la concentración y del tiempo de incubación, de manera análoga a lo descrito en la literatura para otros tipos celulares. Igualmente, hemos obtenido imágenes de la localización subcelular de la ZnPc en células HeLa, que muestran una acumulación del fotosensibilizador en un área concreta cercana al núcleo, claramente distinta del conjunto de mitocondrias, y que se corresponde perfectamente con el aparato de Golgi (mediante comparación con marcadores específicos de dichos orgánulos).

Las células fueron incubadas con ZnPc a una concentración de 10^{-7} M durante sólo una hora, permitiendo una acumulación intracelular de ZnPc de 4,8 ng ZnPc/mg proteína. Posteriormente, las células fueron sometidas a irradiación durante 15 min con una lámpara de LEDs (*light-emitting diodes*, λ=640 nm, con una potencia de 4 mW/cm^2). De esta manera se obtuvo un bloqueo de células en metafase que se evidencia a las 6 h de la irradiación (17,8 % de células detenidas en G2/M y un 11,7 % de células poliploides de acuerdo a las lecturas del contenido en yoduro de propidio en las células mediante citometría de flujo).

El análisis morfológico, mediante inmunodetección de la tubulina y el marcaje de la cromatina, mostró que la mayoría de las células bloqueadas en metafase presentaban claras anomalías en la disposición del huso mitótico. Particularmente, se observó la multiplicación de los polos del huso (en una conformación típica de tres polos, aunque se contabilizaron metafases con hasta seis polos) y la presencia de cromosomas retrasados en su progresión (cercanos a los polos). La inmunodetección de los centrómeros, con el suero ACA, permitió comprobar que, como se esperaba, no había fragmentos acéntricos (diagnósticos de daño genético). Las células poliploides identificadas presentaban típicamente dos-tres núcleos de tamaño equivalente entre ellos (frente a la multiplicación de micronúcleos que se observa con fármacos genotóxicos).

La detención del ciclo en la metafase es evidente hasta las 24 h desde la exposición a la luz; en ese momento se verifica la creciente acumulación de células despegadas que se correlaciona con la pérdida de la viabilidad celular (medida a través del método del MTT y del ensayo de exclusión del Azul Tripán). Pasadas 72 h desde la irradiación, la viabilidad se ha reducido hasta un 60 %, aproximadamente, respecto de la de los cultivos control. Estos resultados se correlacionan bien con los provenientes del recuento directo de células con caracteres morfológicos, diagnósticos de la apoptosis (35,7 %, visualizadas mediante tinción con H-33258), y presentan una buena correspondencia con el total de células bloqueadas o poliploides a las 6 h (29,7 %). En los recuentos realizados a 72 h de la irradiación se siguen detectando células bloqueadas en metafase, con cromosomas retrasados (3,11 %).

La apoptosis como proceso último de la muerte celular en nuestro sistema experimental, se comprobó mediante el análisis de la ruptura de la proteína PARP (poli-(ADP-ribosa) polimerasa) por acción de las caspasas empleando la técnica de *Western blotting*. Con esta técnica se puede apreciar la coexistencia de dos subpoblaciones (viva y apoptótica) a partir de las 24 h y cómo la subpoblación de células despegadas se corresponde totalmente con la de las células con PARP fragmentado. De igual manera se visualizó la translocación de Bax a la mitocondria en las células apoptóticas, que no se verifica en las células detenidas en metafase.

Bloqueo metafásico, aneuploidía y muerte celular “retrasada” temporalmente son los caracteres diagnósticos de los procesos de catástrofe mitótica. Este tipo de muerte celular se ha relacionado fundamentalmente con terapias inductoras de daño genético, mientras que la PDT no produce genotoxicidad. La falta del sistema de regulación gobernado por p53 (como en nuestro modelo) ha sido relacionada con permisividad para la formación de polos supernumerarios. Por el momento, sin embargo, no existe evidencia suficiente en la literatura acerca de los mecanismos por los que la fotosensibilización induce alteraciones del huso y bloqueo metafásico. Sin embargo, la constatación por primera vez de la capacidad de la PDT, en este caso con ZnPc como PS, para inducir muerte celular por un mecanismo de catástrofe mitótica, abre no sólo nuevas posibilidades terapéuticas para esta terapia, sino que también permitirá profundizar en el estudio de los estímulos inductores de dicho tipo de muerte celular.

Mitotic catastrophe and cell death induced in HeLa cells by photodynamic treatment with Zn(II)-phthalocyanine

Santiago Rello-Varona[1]*, Juan Carlos Stockert[2], Magdalena Cañete[1], Pilar Acedo[1] & ÁngelesVillanueva[1]

[1]Departamento de Biología, Facultad de Ciencias, Universidad Autónoma de Madrid.

C/ Darwin 2, Citología A-115, E-28049 Madrid, Spain

[2] Centro de Investigaciones Biológicas, Consejo Superior de Investigaciones Científicas,

C/ Ramiro de Maeztu 9, E-28040 Madrid, Spain

* Santiago Rello-Varona. Departamento de Biología-UAM. C/ Darwin 2, Citología A-115; E-28049 Madrid; Spain. E-mail: santiago.rello@uam.es Telephone: +34 91497 2821. Fax: +34 91497 8344.

SUMMARY

Photodynamic therapy (PDT) is a growing tool against neoplastic and non-neoplastic diseases. PDT is known to be capable to induce different cell death mechanisms *in vitro*, triggered in a dose-dependent manner. Relationships between PDT and apoptosis or necrosis induction are well-known, but other cell death mechanisms triggered after PDT are less understood. Here we present our results in p53-deficient human cervix carcinoma HeLa cells subjected to sublethal PDT treatments (mortality about 40%) using Zn(II)-phthalocyanine (ZnPc) incorporated into liposomes. We obtained a rapid metaphase blockage (6 h after light exposure) of cells that also showed clearly altered configurations of the mitotic spindle. Cell cycle arrest was followed by aneuploidisation and cell death with apoptotic morphology. Apoptosis was also confirmed by occurrence of PARP cleavage and Bax translocation to mitochondria. These features are components of the cell death mechanism known as mitotic catastrophe and represent, to our knowledge, the first description of this cell death modality after PDT with ZnPc.

INTRODUCTION

Zinc(II)-phthalocyanine (ZnPc) is one of the so-called second generation agents for photodynamic therapy (PDT), which is a useful treatment of neoplasic and non-neoplasic diseases (Dolmans et al., 2003; Triesscheijn et al., 2006). It is based on the appropriate combination of oxygen, light and a photosensitiser compound (PS), which becomes excited and mediates the production of cytotoxic reactive oxygen species (ROS) (Triesscheijn et al., 2006).

Approved PDT protocols are mainly related with first generation photosensitisers (i.e. Photofrin®), while basic research is most centred in second generation PSs with improved photophysical characteristics (Konan et al., 2002). Among them, phthalocyanines are high-lightened by their increased absorbance coefficient at wavelengths with optimal tissue penetration (in the 630-800 nm spectral region). ZnPc has particular interest on account of its long-lived triplet state and good capacity for localisation in tumours (Konan et al., 2002).

However, in spite of their interesting properties, the extreme hydrophobicity of phthalocyanines makes necessary the use of specific carriers for delivery into biological systems (Konan et al., 2002). At present, several ZnPc formulations are used for experimental purposes, examples being nanoparticles (Ricci-Júnior and Marchetti, 2006), dispersions (Alexandratou et al., 2005), micelles (Sibata et al., 2004) and different types of liposomes (Nunes et al., 2004).

Mitotic catastrophe is a specific cell death process intimately related with defective mitosis behaviour causing cell cycle arrest, evident alterations in the spindle and chromosomes disposition, aneuploidy, and finally cell death (Galluzzi et al., 2007; Kroemer et al., 2005). Mitotic catastrophe and subsequent aneuploidy are also linked with genomic instability, tumour progression, development of drug resistance, and aging and senescence (Baker et al., 2005; Castedo et al., 2006). Those processes indicate several alterations in checkpoint regulation, principally related with p53 abrogation or dysfunction (Castedo et al., 2006; Castedo et al., 2004; Chen et al., 2003), as the signalling cascades regulated by p53 keep the genome integrity and trigger cell death when a severe damage occurs (Kastan and Bartek, 2004).

Several chemicals cause cell death preceded by different events of the so-called mitotic catastrophe program, especially spindle aberrations that lead to metaphase arrest (Jackson et al., 2007; Jordan et al., 1996; Rello-Varona et al., 2006). They are, mainly, chemotherapeutic agents targeted against the microtubule system (Jordan and Wilson, 2004; Mollinedo and Gajate, 2003). Paclitaxel (Taxol®) is the most known microtubule interfering agents but, nowadays, other compounds are also used in different trial phases (i.e. *Vinca* alkaloids, colchicine derivatives, etc.) (Mollinedo and Gajate, 2003).

The Bcl-2 family proteins are targets of p53 activity and there is evidence connecting them with different cell death processes compressing mitotic catastrophe (Castedo et al., 2004; Ferri and Kroemer, 2001). Bcl-2 family proteins regulate the integrity of the mitochondrial membranes as a result of a complex hierarchical behaviour (Kim et al., 2006), releasing cytochrome c and inducing apoptosis with the activation of caspases (van Delft and Huang, 2006). The role of Bcl-2 family proteins in

PDT has the maximum interest, as mitochondria are now considered the principal target of this therapeutical approach (Almeida et al., 2004; Srivastava et al., 2001).

ZnPc photosensitisation produces ROS that are responsible for cell damage (Alexandratou et al., 2005). As ROS have a very little action radius, photodamage was traditionally considered to be restricted to subcellular areas where the PS is accumulated (Triesscheijn et al., 2006; Villanueva et al., 1999).

Previously, we have described dramatic cytoskeletal alterations (mainly compressing microtubules, MTs) after ZnPc-PDT treatments of p53-deficient HeLa cells (Juarranz et al., 2001). These alterations included spindle aberrations that lead to metaphase arrest, but no longer-experiments were made at that time. The aim of the present work is to determine if ZnPc-PDT can inactivate HeLa cells by means of a mitotic catastrophe response.

RESULTS

Uptake and localisation of ZnPc in HeLa cells

The incorporation of ZnPc was studied by fluorimetric analysis of lysates from cells previously incubated with different PS concentrations for short and long time intervals. Results are summarized in Table 1.

As it is shown, the amount of ZnPc in cells is increased in function of the concentration and the time interval employed. In our experimental conditions, using a short incubation period with a very low concentration, the presence of ZnPc is enough to be detected (4.8 ng of ZnPc/mg of protein).

Once confirmed the presence of the PS, we studied its precise accumulation site inside the cells, using the red fluorescence of ZnPc under ultraviolet excitation. Under our PDT treatment conditions the amount of intracellular ZnPc was too low to allow imaging; but we succeed using the largest uptake conditions assayed (2.5 μM ZnPc for 24 h, 233.7 ng ZnPc/mg protein). In Fig. 1 we show the localisation of ZnPc in HeLa cells. The red signal of the PS is constrained to a single area near the nucleus. In no cases there was any co-localisation between the red ZnPc signal and the blue autofluorescence of the mitochondria (Fig. 1B and C). The ZnPc signal diverged from the typical morphology of the mitochondrial network (shown in Fig 1E by cytochrome c immunostaining) but is quite similar to that of the Golgi apparatus (shown in Fig. 1D after golgin 58 immunolabelling).

In summary, liposomally-driven ZnPc success to penetrate in HeLa cells and it accumulates into the Golgi apparatus.

Cell cycle arrest

The first effect caused by our treatment conditions (10^{-7} M ZnPc for 1 h, 15 min light exposure) is evident 6 h after the irradiation (ΔT=6 h). Cells start to become blocked at metaphase as visualised under fluorescence microscopy with tubulin immunolabelling (Fig. 2A and B, right panels).

This metaphase blockage was quantified using PI labelling of DNA and flow cytometry (Fig. 2A and B, left panels); the G2/M peak increases from 9.7 % (in the control culture) to 17.8 %, and a new area of polyploid cells reaches the 11.7 % of the total cell population. In general, the PI profile suffered a movement towards the right, indicating processes of aneuploidisation.

Alterations in metaphase morphology

A more detailed analysis of the metaphase-blocked cells revealed several abnormalities both in microtubule and chromosome arrangement (Fig. 3). A great amount of mitotic cells showed alterations of the mitotic spindle, but the most frequent modifications were the presence of extra poles (Figs. 3B-D). The commonest mitotic morphology had three poles but cells with more poles were also seen. The disruption of the normal equilibrium between the forces on the spindle by these extra poles, caused abnormalities in the chromosome disposition in the metaphase plate with dispersed and delayed chromosomes (Figs. 3B and C). The total absence of a regular congregation of chromosomes into a plate resulted in a "cloud disposition" of chromosomes (Fig. 3D). By mean of centromere immunolabelling, we also observed that no chromosomal fragmentation occurred: dispersed and delayed chromosomes did not represent acentric fragments and, even in metaphases with a "cloud disposition", regular centromeric signals were clearly visible (Fig. 3D).

Aneuploidy

Metaphase blockage is closely linked to aneuploidy. In our experimental conditions, a significant increase of cells placed in the "polyploid" sector of the flow cytometry profile was shown (reaching 11.7 % 6 h after light exposition, see Fig. 2B). Aneuploid cells were microscopically recognisable due to size increase and typical morphological abnormalities. In our experimental conditions, aneuploid cells showed a round-like outline (rather than polygonal), with multiple microtubule organizing centres and chromosomes disposed within two or three nuclei of similar size (Fig. 3E).

Cell death

The metaphase blockage was still recognizable 24 h after irradiation, but the total amount of cells stopped at mitosis decreased from $\Delta T=6$ h. At $\Delta T=24$ h it was possible to notice for the first time the presence of an important number of detached cells, which increased with time.

We performed two different assays to determine cell death after PDT treatment: MTT and trypan blue assays. Both results (summarized in Table 2) were consistent and showed the cell death progression after PDT treatments.

Cell viability decreased with time until levels about the 60 % at $\Delta T=72$ h after treatment. As shown in Figure 4 after H-33258 DNA staining, cells trypsinised from the flasks (saving also the detached ones) could be divided in two groups (Fig. 4A). One group were living cells with apparently normal nuclei; the other group included death cells showing chromatin condensation, marginalization and fragmentation (see also Fig. 4B).

These morphological features and detachment from substrate are typical of cell death by apoptosis. Using these microscopical criteria for direct cell counting in samples stained only with H-33258 the amount of apoptotic cells 48 h after light exposure was 30.50 % ± 2.02. At 72 h after treatment the apoptotic counting reached the 35.47 % ± 0.86.

The involvement of apoptosis as the main cell death mechanism was also confirmed using the cleavage of PARP protein as visualised by western blotting (Fig. 4C). Cleaved PARP was visible at the same time when the first detached cells occurred (24 h after irradiation) and continued 48 and 72 h after light exposure. Using purified samples of detached cells at 72 h, the cleavage of PARP became more evident (Fig. 4C), showing that this population was formed by apoptotic cells exclusively. The behaviour of the pro-apoptotic Bcl-2 family protein Bax confirmed this apoptotic mechanism. By immunostaining and microscope imaging of Bax we observed that death cells showed an increased signal intensity, which appeared concentrated in structures corresponding to mitochondria instead of having a diffuse cytosolic pattern typical of living HeLa cells (Fig. 4D left panel).

It is important to remark that, several hours after light exposure, it was still possible to find mitotic cells with diffuse Bax signal, clearly distinguishable from apoptotic ones showing mitochondrial Bax localisation (Fig. 4D right panel). The total amount of mitosis is, however, reduced (mitotic index = 3.11% ± 0.97 at ΔT= 72 h), and most mitotic cells showed aberrant chromosome configurations (mainly delayed chromosomes).

Taking together, all the above features (metaphase blockage, spindle's abnormalities, appearance of aneuploid and polyploid cells, apoptotic cell death and survival of a considerable amount of cells) allow us to consider that ZnPc photosensitization of HeLa cells induced the mitotic catastrophe.

DISCUSSION

Cell death triggering is the main objective of oncological therapy. Several chemotherapeutical drugs have been developed in the last decades with different success rates (Varmus, 2006). In the last years the knowledge about the action of the anti-tumour agents has increased and several cell death mechanisms have been proposed (Kroemer et al., 2005). The Nomenclature Committee on Cell Death reviewed them in 2005 for clarify the concepts, promoting three main processes: apoptosis (type 1), autophagy (type 2) and necrosis (type 3), and also admitting the presence of other particular phenomena in specific models (Kroemer et al., 2005).

Mitotic catastrophe is one of these particular phenomena and, until present, it lacks an adequate definition; it is often described simply as a cell death resulting of aberrant mitosis (Mansilla et al., 2006; Stevens et al., 2007). Mitotic catastrophe is often related closely with sublethal conditions of different treatments that triggers a delayed cell death response (Castedo et al., 2004; Erenpreisa and Cragg, 2001). It has been contradictorily linked with both apoptotic and non-apoptotic processes (Stevens et al., 2007). The molecular mechanisms that lead to morphological features used to describe the mitotic catastrophe (metaphase blockage, interphase restitution, aneuploidy and cell death) are not clearly known (Blagosklonny, 2007; Galluzzi et al., 2007). Several studies indicate that the abrogation of functional p53 is required for this response to treatments (Andreassen et al., 2001; Castedo et al., 2004; Pantic et al., 2006) but, depending on the model or the timing of the process, the activation of some p53-regulated genetic pathways is also important (Castedo et al., 2006; Castedo et al., 2004; Chen et al., 2003).

PDT constitutes an appropriate tool for studying cell death mechanisms as the injury intensity is easily monitored (Almeida et al., 2004). Although it was early considered that necrosis was the main cell death process induced by PDT (Kessel et al., 2006), now it is well known that PDT treatments induce apoptosis (Almeida et al., 2004; Villanueva et al., 2003). In the last few years there are published studies connecting PDT and autophagy, as a consequence of apoptosis inhibition or as the main cell death mechanism (Buytaert et al., 2006; Kessel et al., 2006). Hovewer, the precise mechanism of cell death in PDT treatments remains elusive due to the variability of the conditions employed.

Upon appropriate light irradiation, PSs act in the cell as sources of ROSgenerated by the photochemical reaction type II (Dolmans et al., 2003), which cause important macromolecular damage to regions where they are produced and in its proximities (Almeida et al., 2004). However, ROS can also act as messengers triggering different signalization pathways either leading to death (by Ca^{2+} release) or resistance (stimulating different kinases) responses (Almeida et al., 2004). The molecular cascades concerned in the cell death triggering are complex, and often different mechanisms share the same pathway (Danial and Korsmeyer, 2004).

ZnPc is one of the most promising PDT agents due to the diversity of their delivery systems (Ricci-Júnior and Marchetti, 2006; Rodal et al., 1998; Sibata et al., 2004). As other PSs, ZnPc induces different death responses on cell cultures, examples being the classical necrosis and apoptosis (Fabris et al., 2001; Villanueva et al., 1999) and other mechanisms like detachment-linked cell death ("anoikis") (Galaz et al., 2005). Recently, Alexadratou and co-workers have revealed, using confocal microscopy, the events activated in the very first minutes after non-lethal ZnPc-PDT treatment of human foetal foreskin fibroblasts HFF2 cells at a single-cell scale. They verify transitory increased ROS levels, which lead to transient acidification, loss of the mitochondria membrane potential and pH gradients, and Ca^{2+} influx (Alexandratou et al., 2005).

On account of the reduced life time of ROS, the specific subcellular localisation of PSs will be the most damaged site of the cell (Rodal et al., 1998). In the case of ZnPc, the precise subcellular accumulation site seems to be dependent on the cell line (as occurs with other PSs). Fabris and co-workers have proposed a localisation of ZnPc in the Golgi apparatus of 4R rat fibroblasts (Fabris et al., 2001). This result was consequent with previous observations in NHIK 3025 cells (Rodal et al., 1998) showing a rapid damage both in Golgi apparatus and mitochondria. On the other hand, more recent data using a computer algorithm to analyse confocal microphotographs, indicated a mitochondrial localisation of ZnPc in human HFFF2 cells (Alexandratou et al., 2005). Besides, there is also evidence, using hydrosoluble derivatives of ZnPc, of PS re-localisation (from plasma membrane to Golgi and cell nucleus) after light irradiation (Wood et al., 1997).

In the present work, we have observed that in HeLa cells ZnPc accumulated within a single wide area near the nucleus that did not correspond to mitochondria. By comparison with organelle specific markers (golgin 58 and cytochrome c), the accumulation site of ZnPc strongly resembles to the pattern of the Golgi apparatus in this cell line (see Fig. 1).

Our results show that the uptake of ZnPc-DPPC by HeLa cells depends of both concentration and incubation time, in agreement with previous reports (Fabris et al., 2001; Rodal et al., 1998; Valduga et al., 1996). We found no references similar to our experimental conditions (very short incubation with low doses of ZnPc) as uptake studies were usually performed at higher concentrations and increased time intervals. Despite this, our results using the largest incubation time with the highest concentration (24 h incubation with 2.5 μM ZnPc, see Table 1) are within the magnitude order showed previously by Valduga and co-workers in 4R transformed fibroblasts (Valduga et al., 1996) and indicate that the uptake kinetics in HeLa cells may not differ heavily from other models.

Previously we have described that in HeLa cells both apoptosis and necrosis, as well as characteristic cytoskeleton alterations and accumulation of mitotic cells with abnormal spindles were produced by ZnPc (Juarranz et al., 2001; Villanueva et al., 1999). Photodamage to microtubules was also described either with ZnPc or other PSs (Juarranz et al., 2001; Rodal et al., 1998; Villanueva et al., 2003). The tubulin photodamage resulted from the disappearance of tubulin in soluble protein fractions after lethal treatments, but no diminution was observed in sublethal treatments inducing altered mitotic cells which show the typical morphology of the mitotic catastrophe (Juarranz et al., 2001).

The origin of the alterations of the mitotic spindle, mainly the appearance of supernumerary poles is far of being completely understood, but deficiencies in p53 signalling seem to be related with that process (Tsou and Stearns, 2006). As mentioned above, there is a broad consensus on the fact that p53 abrogation allows the cells to survive after mitotic slippage and appearance of aneuploidy (Castedo et al., 2004). In this sense, it is important to remark that HeLa cells constitutes one of the best known models of cell lines that lack functional p53 protein due to the activity of the host HPV16 viruses (May et al., 1991). There are very few reports about the relationship between p53, cell cycle blockage and sensitivity to PDT treatments. The results seem to be confusing as they are highly dependent on the cell model employed. Thus Photofrin®-mediated cell photokilling can occur either without correlation with p53 abrogation in colon cancer cells (Fisher et al., 1999) or with p53 dependency in Li-Fraumeni syndrome cells (Tong et al., 2000). In this example it is important to notice that p53 absence was positively linked with resistance development meanwhile G2/M blockage and delayed apoptosis (Tong et al., 2000). More recently, Lee and co-workers stated that the p53 status does not interfere at all, in terms of survival rates, in the response of U2OS osteosarcoma cells to hypericin (Lee et al., 2006).

Here we have shown that ZnPc induced metaphase blockage of HeLa cells followed by apoptotic death of the arrested cells. Six hours after treatment, about a 29.5 % of cells were either blocked in metaphase or became aneuploid (see Fig. 2). The metaphase blockage was clearly correlated with the presence of abnormal mitotic spindles, mainly by the presence of supernumerary poles (see Fig. 3). At 24 h after the treatment, cells started to detach from surface, and 72 h later, cell counting revealed 35.7 % of apoptosis, these values corresponding with those from MTT and TB survival assays (see Table 2). At this time some mitotic cells were observed, although the mitotic index was reduced to 3.11 %. Death cells showed morphological features (rounding, shrinkage, chromatin condensation and fragmentation) that are typical of apoptotic cells. We also confirmed apoptosis as the cell death mechanism by PARP cleavage and Bax translocation (from cytosol to mitochondria) in dying cells (see Fig. 4). To our knowledge, this is the first reference of Bax translocation to mitochondria supported by immunolabelling images using ZnPc, and confirms previous data obtained with other PSs and chemotherapeutic agents (Chiu et al., 2003; Sarkar et al., 2003). Bax translocation must be not considered strictly p53-dependent as there are also observations describing it, in mitotic catastrophe, as a process partially independent of p53 (Castedo et al., 2006; Castedo et al., 2004).

In summary, our results indicate that after ZnPc-PDT apoptotic HeLa cells were first blocked in metaphase and some of those evolved to aneuploid ones. Metaphase blockage, aneuploidy and delayed apoptosis are the main features of mitotic catastrophe. PDT can cause cell death by mitotic catastrophe under sublethal conditions. Obviously, further research is needed to clarify the biochemical processes underlying this morphological process. As mitotic catastrophe is observed normally in sublethal or delayed-lethality conditions, it is often considered as an “open gate” to resistance and survival by means of aneuploidy-linked genomic instability (normally caused by p53 deficiency) (Erenpreisa and Cragg, 2001; Merlo et al., 2006). In this sense, we consider that mitotic catastrophe requires more attention in cancer research because it can be really useful to better characterise the action mechanism of chemotherapeutic drugs.

MATERIALS AND METHODS

The p53-deficient HeLa cell line (May et al., 1991) was grown in Dulbecco's modified Eagle's medium (DMEM) with 50 units/mL penicillin, 50 μg/mL streptomycin and supplemented with foetal bovine serum (FBS) at a final concentration of 10 % (whole medium). All the media, sera and antibiotics were provided by Gibco (Paisley, UK). Cell cultures were performed in a 5 % CO_2 atmosphere at 37 ºC and maintained in a SteriCult 200 (Hucoa-Erloss) incubator.

Depending on the experiment, cells were seeded in 25 cm^2 flasks (90,000 cells) or in 35 mm Petri dishes (20,000 cells) with or without 22 mm square coverslip. All sterile plastics were from Corning Inc (Corning, USA). Cells were grown for 72 h and treated when cultures were in exponential growing.

ZnPc supply and treatment conditions

Zinc(II) phthalocyanine was acquired from Sigma-Aldrich (St. Louis, USA). A stock 0.5 mg/mL solution was prepared in pyridine (Panreac Química, Montcada i Reixac, Spain) and stored at 4 ºC until use. ZnPc was incorporated into dipalmitoyl-phosphatidylcholine (DPPC) liposomes (Sigma) according to the injection procedure of Ginevra and co-workers (Ginevra et al., 1990). Liposome solution was sterilized by filtration with a 0.22 μm diameter filter (Millipore Corp., Bedford, USA). Afterwards, the concentration of the ZnPc-DPPC stock solution was measured using a Shimadzu UV-1601 spectrophotometer (Kyoto, Japan); for working, ZnPc was diluted in phosphate buffered saline (PBS) or in 1 % FBS medium to desired concentrations, within the first 48 h after stock preparation.

Cellular uptake of ZnPc was measured, using different incubation conditions, with a Perkin-Elmer 650-10S Fluorescence Spectrophotometer (Waltham, USA), after 2 % sodium dodecyl sulphate (SDS) lysis of the cells. Lysate fractions were preserved for protein quantification by the BCA assay (Pierce, Rockford, USA). ZnPc localisation within cells was analysed after 24 h incubation with 2.5 μM ZnPc-DPPC solution in DMEM. Microphotographs were taken with an Olympus BX61 epifluorescence microscope equipped with an Olympus DP50 digital camera under ultraviolet (UV, 365 nm) excitation.

For PDT treatments, cells were incubated with 10^{-7} M ZnPc-DPPC solution in PBS for one hour, washed three times with fresh PBS and maintained in whole medium during irradiation and post-treatment time. Red light irradiation for 15 min was performed using a LED source ($\lambda = 640 \pm 20$ nm) with a mean intensity of 4 mW/cm^2, measured with a M8 Spectrum Power Energymeter.

Cell survival

Thiazolyl blue (MTT, Sigma) was used for the assessment of cell survival. A stock solution (1 mg/mL) in PBS was prepared immediately prior to use. 100 μL of this solution were added to each culture dish (containing 2 mL of whole medium; final MTT concentration: 47.6 μg/mL). Cells were incubated for 3 h; formazan precipitates were dissolved in 1.5 mL DMSO and the absorbance was measured at 540 nm in a Tecan

Spectra Fluor spectrophotometer. Cell survival was expressed as the percentage of absorption of treated cells in comparison with that of control cells. The results presented were the mean value and standard deviation from at least six different experiments.

MTT procedure results were confirmed using also the trypan blue (TB, Sigma) exclusion test. Briefly, treated and untreated cells were trypsinised (harvesting also the detached ones) and mixed 50 % (v/v) with 300 μL of a 0.2 % TB solution in PBS. Cell counting of death (blue) or alive (white and bright cells) was performed using a Neubabuer haemocytometer chamber (Marienfeld GmbH, Lauda-Königshofen, Germany).

Microscopical analysis

The effects of PDT treatments were studied mainly by microscopical observations. Cells were routinely observed at different time intervals using an inverted microscope. Further analysis was performed by α-tubulin FITC-fluorescence immunostaining on cold-methanol fixed cells (permeabilised with 0.5 % Triton X-100 in PBS); nuclei were counterstained using 0.5 mg/mL Hoechst-33258 (H-33258, Sigma) solution in distilled water. Centromeres were immunolabelled using purified human anti-centromere proteins (Antibodies Inc., Davis, CA, USA) as primary antibody and goat anti-human IgG (Fc specific) TRITC-labelled antibody. Bcl-2 family protein Bax was immunolabelled with mouse anti-Bax (2D2) primary antibody (Santa Cruz Biotech., Santa Cruz, USA). For comparison purposes, immunostaining of the Golgi apparatus and mitochondria was performed using antibodies against the proteins golgin 58 and cytochrome c (respectively) as targets and, in these cases, cells were fixed in 3.5 %

paraformaldehyde (BDH, Poole, England, UK). All fixatives, stains, antibodies, etc. were from Sigma.

Microscopical analysis was also used for assessing cell death. Apoptotic cells were identified using morphological criteria (mainly chromatin condensation and packing into apoptotic bodies) (Rello et al., 2005). Cell counting was performed from samples fixed in paraformaldehyde for 20 min at 4 ºC and stained with 0.5 mg/mL H-33258.

Observations were made with an Olympus BX61 microscope/Olympus DP50 digital camera; all photographs were taken using Photoshop CS software (Adobe Systems, San Jose, USA).

Flow cytometry analysis

Analysis of the cell cycle was performed by measurement of propidium iodide (PI) labelling of DNA cell content. Flasks were trypsinised (harvesting also the detached cells) and centrifuged at 1200 rpm (rotor radius: 7 cm) for 5 min for pelleting prior to fixing with cold 70 % ethanol solution (15 min, on ice). After centrifugation, the pellet was resuspended in 1 mL of fresh PBS with 50 µL of a 100 µg/mL solution of RNase and incubated for 0.5 h at 37 ºC. Immediately prior to measurement, DNA was stained by adding 25 µL of 1 mg/mL PI solution. All reactives were from Sigma. Measurements were performed with a Coulter Epics XL-MCL flow cytometer with an argon laser line at 488 nm and complemented with the appropriate filters.

Western blot analysis

For protein analysis by western blotting techniques, samples from ZnPc-PDT treatments were obtained. Whole protein content was extracted by lysis using RIPA buffer [50 mL of distilled water with 50 mM Tris-HCl at pH=8; 150 mM NaCl; 1 % (v/v) Igepal CA630 (all from Sigma) and 0.1 % (v/v) SDS; complemented with a tablet of complete EDTA-free protease inhibitors (Roche)].

Protein concentration was determined using a BCA assay kit and samples were loaded and separated on 10 % SDS-PAGE and transferred to nitrocellulose membranes using Mini-Protean 3 equipment, with the appropriate reactives, according to manufacturer instructions (Bio-Rad, Hercules, USA).

The chemoluminescent detection of proteins was performed using mouse monoclonal anti-β-actin (clone AC-15), as control, and mouse monoclonal anti-PARP (clone C-2-10). The secondary antibody employed was sheep ECL anti-mouse horseradish peroxidase conjugate (Amersham Biosciences, Bucks, UK). Bands were revealed in Curix CP-G Plus paper (AGFA, Barcelona, Spain) with Western Blotting Luminol Reagent (Santa Cruz).

ACKNOWLEDGEMENTS

The authors recognise the valuable contribution of Sylvia Gutierrez (Confocal Microscopy and Flow Cytometry Service, Centro Nacional de Biotecnología, Madrid) and Dolores Morales (Confocal Microscopy Laboratory, Interdepartmental Research Service, Universidad Autónoma de Madrid). This work was supported by grants from Comunidad Autónoma de Madrid (S-0505 MAT-0194) and Ministerio de Educación y Ciencia (CTQ2007-67763-C03-02/BQU), Spain.

REFERENCES

Alexandratou, E., Yova, D. and Loukas, S. (2005). A confocal microscopy study of the very early cellular response to oxidative stress induced by zinc phthalocyanine sensitization. *Free Radical Biology & Medicine* **39**, 1119-1127.

Almeida, R. D., Manadas, B. J., Carvalho, A. P. and Duarte, C. B. (2004). Intracellular signaling mechanisms in photodynamic therapy. *Biochimica et Biophysica Acta* **1704**, 59-86.

Andreassen, P. R., Lacroix, F. B., Lohez, O. D. and Margolis, R. L. (2001). Neither $p21^{WAF1}$nor 14-3-3σ prevents G_2 progression to mitotic catastrophe in human colon carcinoma cells after DNA damage, but $p21^{WAF1}$ induces stable G_1 arrest in resulting tetraploid cells. *Cancer Research* **61**, 7660-7668.

Baker, D. J., Chen, J. and van Deursen, J. M. A. (2005). The mitotic checkpoint in cancer and aging: what have mice taught us? *Current Opinion in Cell Biology* **17**, 583-589.

Blagosklonny, M. V. (2007). Mitotic arrest and cell fate. *Cell Cycle* **6**, 70-74.

Buytaert, E., Callewaert, G., Hendrickx, N., Scorrano, L., Hartmann, D., Missiaen, L., Vandenheede, J. R., Heirman, I., Grooten, J. and Agostinis, P. (2006). Role of endoplasmic reticulum depletion and multidomain proapoptotic BAX and BAK proteins in shaping cell death after hypericin-mediated photodynamic therapy. *FASEB Journal* **20**, 756-758.

Castedo, M., Coquelle, A., Vivet, S., Vitale, I., Kauffmann, A., Dessen, P., Pequignot, M. O., Casares, N., Valent, A., Mouhamad, S. et al. (2006). Apoptosis regulation in tetraploid cancer cells. *The EMBO Journal* **25**, 2584-2595.

Castedo, M., Perfettini, J. L., Roumier, T., Andreau, K., Medema, R. and Kroemer, G. (2004). Cell death by mitotic catastrophe: a molecular definition. *Oncogene* **23**, 2825-2837.

Chen, J. G., Yang, C. P. H., Cammer, M. and Horwitz, S. B. (2003). Gene expression and mitotic exit induced by microtubule stabilizing drugs. *Cancer Research* **63**, 7891-7899.

Chiu, S. M., Xue, L. Y., Usuda, J., Azizuddin, K. and Oleinick, N. L. (2003). Bax is essential for mitochondrion-mediated apoptosis but not for cell death caused by photodynamic therapy. *British Journal of Cancer* **89**, 1590-1597.

Danial, N. N. and Korsmeyer, S. J. (2004). Cell death: critical control points. *Cell* **116**, 205-219.

Dolmans, D. E. J., Fukumura, D. and Jain, R. K. (2003). Photodynamic therapy for cancer. *Nature Reviews Cancer* **3**, 380-387.

Erenpreisa, J. E. and Cragg, M. S. (2001). Mitotic death: a mechanism of survival? A review. *Cancer Cell International* **1**, 1.

Fabris, C., Valduga, G., Miotto, G., Borsetto, L., Jori, G., Garbisa, S. and Reddi, E. (2001). Photosensitization with zinc (II) phthalocyanine as a switch in the decision between apoptosis and necrosis. *Cancer Research* **61**, 7495-7500.

Ferri, K. F. and Kroemer, G. (2001). Organelle-specific initiation of cell death pathways. *Nature Cell Biology* **3**, E255-E263.

Fisher, A. M. R., Ferrario, A., Rucker, N., Zhang, S. and Gomer, C. J. (1999). Photodynamic therapy sensitivity is not altered in human tumor cells after abrogation of p53 function. *Cancer Research* **59**, 331-335.

Galaz, S., Espada, J., Stockert, J. C., Pacheco, M., Sanz-Rodríguez, F., Arranz, R., Rello, S., Cañete, M., Villanueva, A., Esteller, M. et al. (2005). Loss of E-cadherin mediated cell-cell adhesion as an early trigger of apoptosis induced by photodynamic treatment. *Journal of Cellular Physiology* **205**, 86-96.

Galluzzi, L., Maiuri, M. C., Vitale, I., Zischka, H., Castedo, M., Zitvogel, L. and Kroemer, G. (2007). Cell death modalities: classification and pathophysiological implications. *Cell Death and Differentiation* **14**, 1237-1266.

Ginevra, F., Biffanti, S., Pagnan, A., Biolo, R., Reddi, E. and Jori, G. (1990). Delivery of the tumour photosensitizer zinc(II)-phthalocyanine to serum proteins by different liposomes: studies *in vitro* and *in vivo*. *Cancer Letters* **49**, 59-65.

Jackson, J. R., Patrick, D. R., Dar, M. M. and Huang, P. S. (2007). Targeted anti-mitotic therapies: can we improve on tubulin agents? *Nature Reviews Cancer* **7**, 107-117.

Jordan, M. A., Wendell, K., Gardiner, S., Derry, W. B., Copp, H. and Wilson, L. (1996). Mitotic block induced in HeLa cells by low concentrations of paclitaxel (taxol) results in abnormal mitotic exit and apoptotic cell death. *Cancer Research* **56**, 816-825.

Jordan, M. A. and Wilson, L. (2004). Microtubules as a target for anticancer drugs. *Nature Reviews Cancer* **4**, 253-265.

Juarranz, A., Espada, J., Stockert, J. C., Villanueva, A., Polo, S., Domínguez, V. and Cañete, M. (2001). Photodamage induced by zinc(II)-phthalocyanine to microtubules, actin, alpha-actinin and keratin of HeLa cells. *Photochemistry and Photobiology* **73**, 283-289.

Kastan, M. B. and Bartek, J. (2004). Cell-cycle checkpoints and cancer. *Nature* **432**, 316-323.

Kessel, D., Vicente, M. G. H. and Reiners, J. J. (2006). Initiation of apoptosis and autophagy by photodynamic therapy. *Autophagy* **2**, 289-290.

Kim, H., Rafiuddin-Shah, M., Tu, H. C., Jeffers, J. R., Zambetti, G. P., Hsieh, J. J. D. and Cheng, E. H. Y. (2006). Hierarchical regulation of mitochondrion-dependent apoptosis by BCL-2 subfamilies. *Nature Cell Biology* **8**, 13481358.

Konan, Y. N., Gurny, R. and Allémann, E. (2002). State of the art in the delivery of photosensitizers for photodynamic therapy. *Journal of Photochemistry and Photobiology, B: Biology* **66**, 89-106.

Kroemer, G., El-Deiry, W. S., Golstein, P., Peter, M. E., Vaux, D., Vandenabeele, P., Zhivotovsky, B., Blagosklonny, M. V., Malorni, W., Knight, R. A. et al. (2005). Classification of cell death: recommendations of the Nomenclature Commitee on Cell Death. *Cell Death and Differentiation* **12**.

Lee, H. B., Ho, A. S. H. and Teo, S. H. (2006). p53 status does not affect photodynamic cell killing induced by hypericin. *Cancer Chemotherapy and Pharmacology* **58**, 91-98.

Mansilla, S., Priebe, W. and Portugal, J. (2006). Mitotic catastrophe results in cell death by caspase-dependent and caspase-independent mechanisms. *Cell Cycle* **5**, 53-60.

May, E., Jenkins, J. R. and May, P. (1991). Endogenous HeLa p53 proteins are easily detected in HeLa cells transfected with mouse deletion mutant p53 gene. *Oncogene* **6**, 1363-1365.

Merlo, L. M. F., Pepper, J. W., Reid, B. J. and Maley, C. C. (2006). Cancer as an evolutionary and ecological process. *Nature Reviews Cancer* **6**, 924-935.

Mollinedo, F. and Gajate, C. (2003). Microtubules, microtubule-interfering agents and apoptosis. *Apoptosis* **8**, 413-450.

Nunes, S. M. T., Sguilla, F. S. and Tedesco, A. C. (2004). Photophysical studies of zinc phthalocyanine and chloroaluminum phthalocyanine incorporated into liposomes in the presence of additives. *Brazilian Journal of Medical and Biological Research* **37**, 273-284.

Pantic, M., Zimmermann, S., El Daly, H., Opitz, O. G., Popp, S., Boukamp, P. and Martens, U. M. (2006). Telomere dysfunction and loss of p53 cooperate in defective mitotic segregation of chromosomes in cancer cells. *Oncogene* **25**, 4413-4420.

Rello-Varona, S., Gámez, A., Moreno, V., Stockert, J. C., Cristóbal, J., Pacheco, M., Cañete, M., Juarranz, A. and Villanueva, A. (2006). Metaphase arrest and cell death induced by etoposide on HeLa cells. *The International Journal of Biochemistry and Cell Biology* **38**, 2183-2195.

Rello, S., Stockert, J. C., Moreno, V., Gámez, A., Pacheco, M., Juarranz, A., Cañete, M. and Villanueva, A. (2005). Morphological criteria to distinguish cell death induced by apoptotic and necrotic treatments. *Apoptosis* **10**, 201-208.

Ricci-Júnior, E. and Marchetti, J. M. (2006). Zinc(II)phthalocyanine loaded PLGA nanoparticles for photodynamic therapy use. *International Journal of Pharmaceutics* **310**, 187-195.

Rodal, G. H., Rodal, S. K., Moan, J. and Berg, K. (1998). Liposome-bound Zn(II)-phthalocyanine. Mechanisms for celular uptake and photosensitization. *Journal of Photochemistry and Photobiology, B: Biology* **45**, 150-159.

Sarkar, F. H., Rahman, K. M. W. and Li, Y. (2003). Bax translocation to mitochondria is an important event in inducing apoptotic cell death by Indole-3-carbinol (I3C) treatment of breast cancer cells. *The Journal of Nutrition* **133**, 2434S-2439S.

Sibata, M. N., Tedesco, A. C. and Marchetti, J. M. (2004). Photophysicals and photochemicals studies of zinc(II) phthalocyanine in long time circulation micelles for Photodynamic Therapy use. *European Journal of Pharmaceutical Sciences* **23**, 131-138.

Srivastava, M., Ahmad, N., Gupta, S. and Mukhtar, H. (2001). Involvement of Bcl-2 and Bax in photodynamic therapy-mediated apoptosis. *Journal of Biological Chemistry* **276**, 15481-15488.

Stevens, J. B., Liu, G., Bremer, S. W., Ye, K. J., Xu, W., Xu, J., Sun, Y., Wu, G. S., Savasan, S., Krawetz, S. A. et al. (2007). Mitotic cell death by chromosome fragmentation. *Cancer Research* **67**, 7686-7694.

Tong, Z., Singh, G. and Rainbow, A. J. (2000). The role of the p53 tumor suppressor in the response of human cells to Photofrin-mediated photodynamic therapy. *Photochemistry and Photobiology* **71**, 201-210.

Triesscheijn, M., Baas, P., Schellens, J. H. M. and Stewart, F. A. (2006). Photodynamic therapy in oncology. *The Oncologist* **11**, 1034-1044.

Tsou, M. F. B. and Stearns, T. (2006). Controlling centrosome number: licenses and blocks. *Current Opinion in Cell Biology* **18**, 74-78.

Valduga, G., Bianco, G., Csik, G., Reddi, E., Masiero, L., Garbisa, S. and Jori, G. (1996). Interaction of hydro- or lipophilic phthalocyanines with cells of different metastatic potential. *Biochemical Phamacology* **51**, 585-590.

van Delft, M. F. and Huang, D. C. S. (2006). How the Bcl-2 family of proteins interact to regulate apoptosis. *Cell Research* **16**, 203-213.

Varmus, H. (2006). The new era in cancer research. *Science* **312**, 1162-1165.

Villanueva, A., Domínguez, V., Polo, S., Vendrell, V. D., Sanz, C., Cañete, M., Juarranz, A. and Stockert, J. C. (1999). Photokilling mechanisms induced by zinc(II)-phthalocyanine on cultured tumor cells. *Oncology Research* **11**, 447-453.

Villanueva, A., Vidania, R., Stockert, J. C., Cañete, M. and Juarranz, A. (2003). Photodynamic effects on cultured tumor cells. Cytoskeleton alterations and cell death mechanisms. In *Handbook of Photochemistry and Photobiology*., vol. 4 (ed. H. S. Nalwa), pp. 79-117. Los Ángeles: American Scientific Publishers.

Wood, S. R., Holroyd, J. A. and Brown, S. B. (1997). The subcellular localization of Zn(II) phthalocyanines and their redistribution on exposure to light. *Photochemistry and Photobiology* **65**, 397-402.

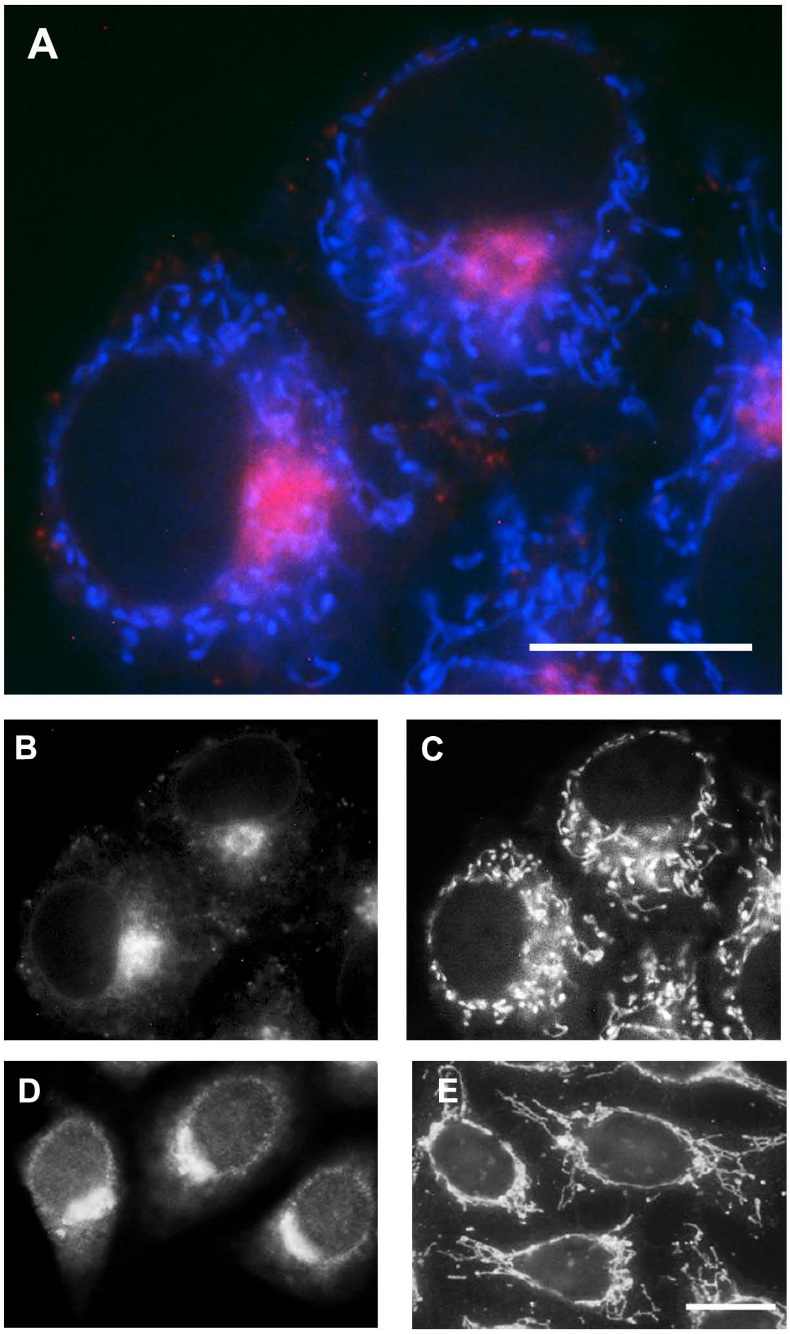
A
B
C
D
E

A

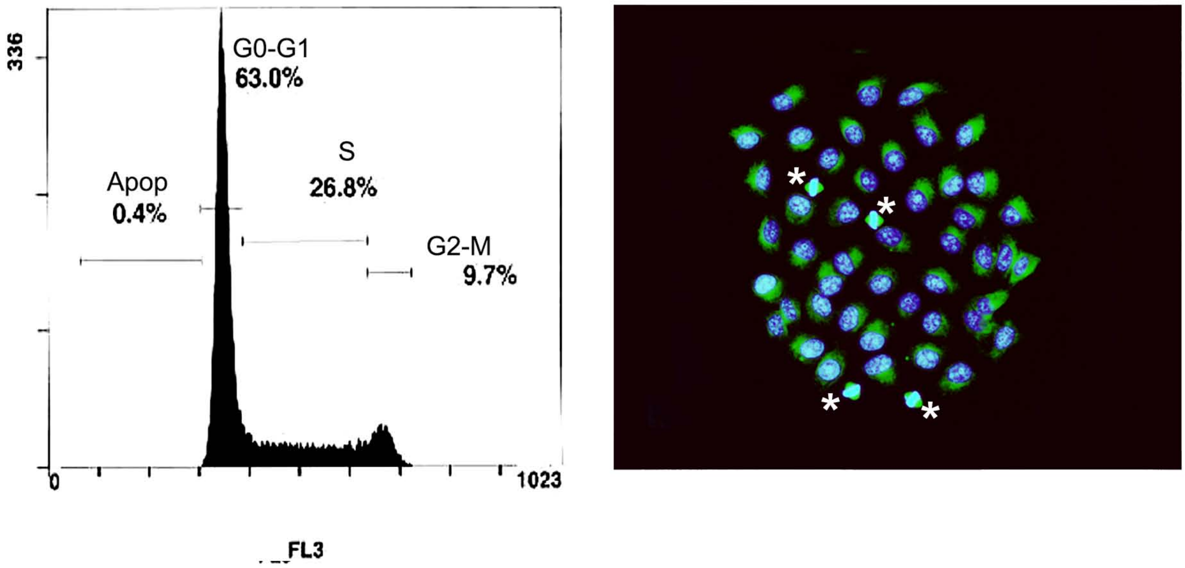
336
G0-G1
63.0%
S
26.8%
Apop
0.4%
G2-M
9.7%
0
1023
FL3

B

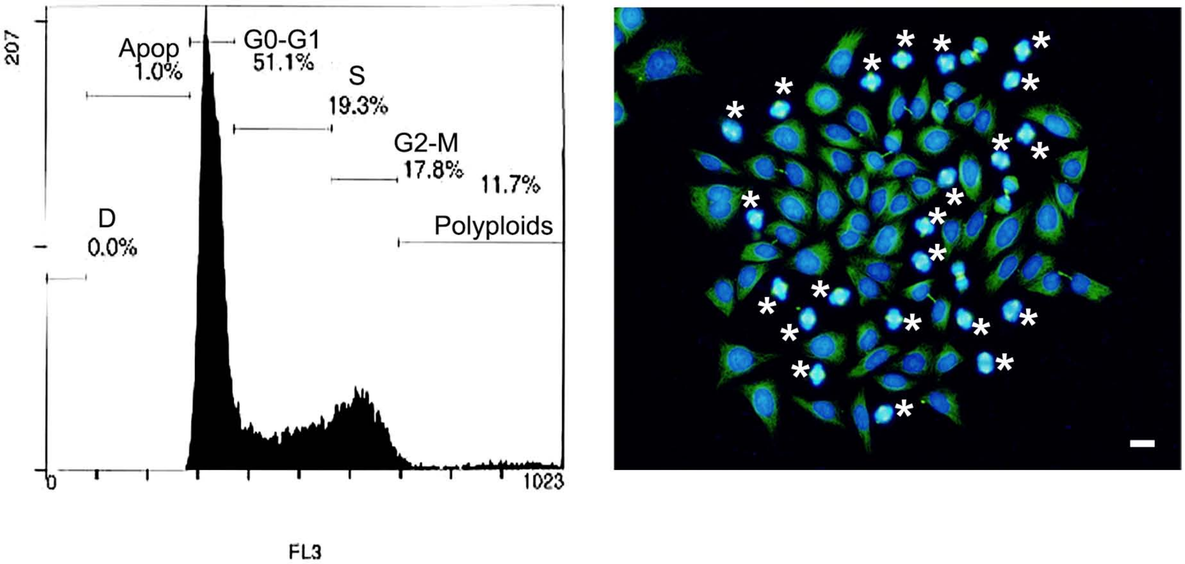
207
Apop
1.0%
G0-G1
51.1%
S
19.3%
G2-M
17.8%
11.7%
D
0.0%
Polyploids
0
1023
FL3

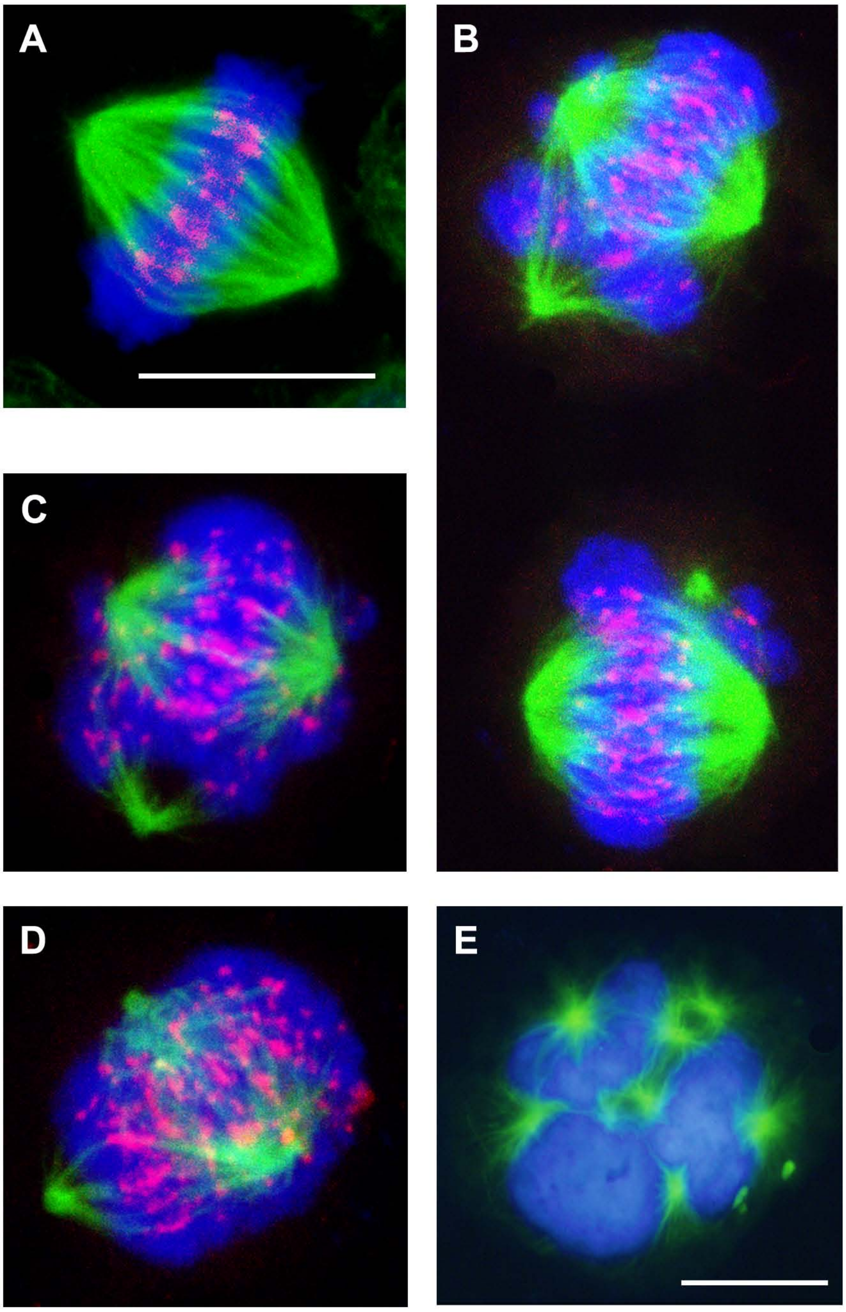
A
B
C
D
E

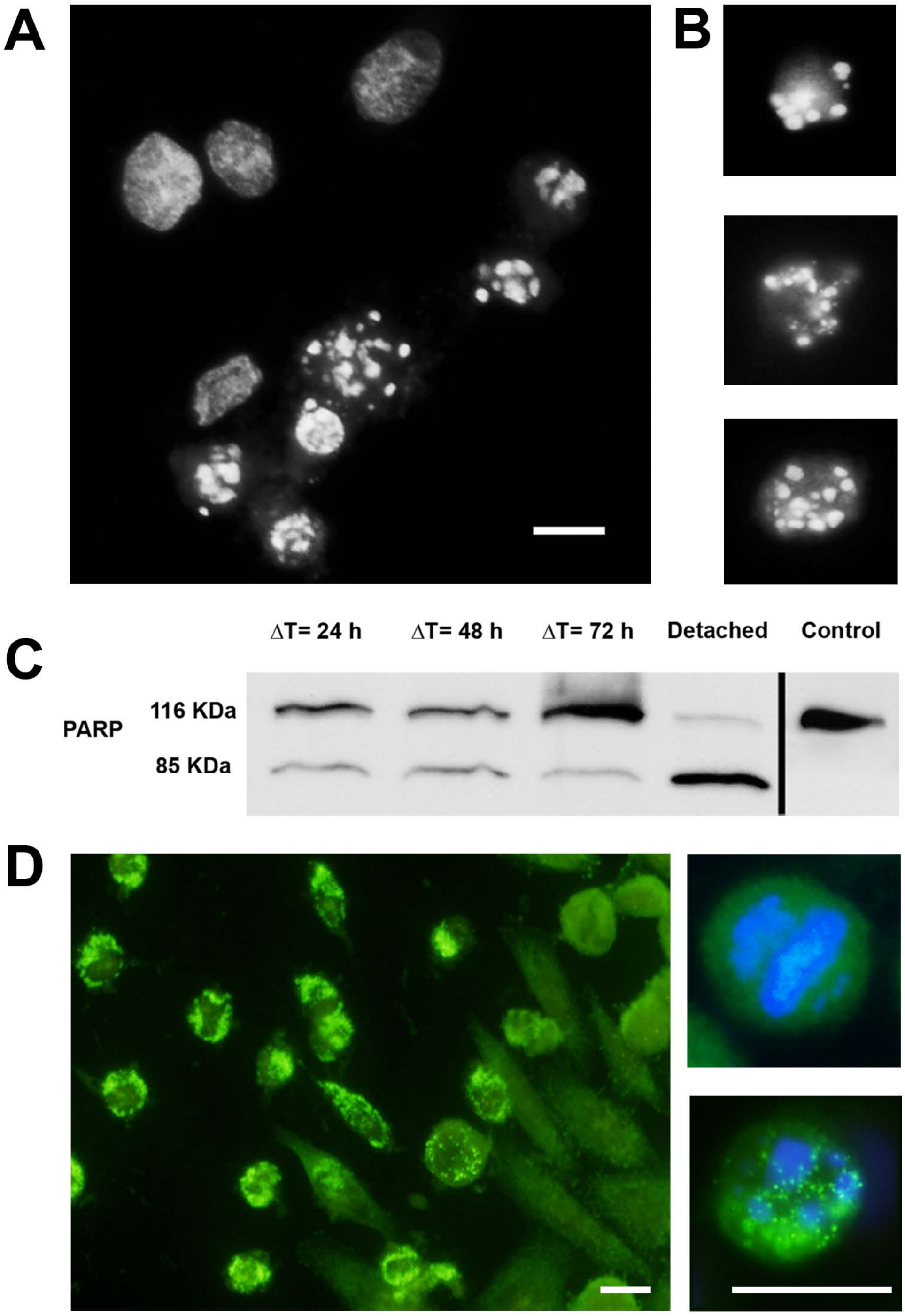

A
B
C
ΔT= 24 h
ΔT= 48 h
ΔT= 72 h
Detached
Control
PARP
116 KDa
85 KDa
D

FIGURE LEGENDS

Fig. 1. Subcellular localisation of ZnPc in HeLa cells. Scale bar: 10 µm. **A:** Photograph obtained by fluorescence microscopy under UV excitation showing the red signal of ZnPc in a Golgi apparatus-like area near the nucleus. **B to E:** Isolating the red and blue channels of the above photograph clearly emphasises that the red signal of ZnPc (**B**) does not co-localise with the blue signal of mitochondria (**C**). The site of ZnPc accumulation strongly resembles that of the Golgi apparatus (**D:** golgin 58 immunostaining), and is very different to the mitochondria (**E:** cytochrome c immunostaining).

Fig. 2. ZnPc-PDT treatment of HeLa cells rapidly causes dramatic alterations of cell cycle. Scale bar: 10 µm. **A, left:** Flow cytometry of DNA content (measured by PI) of control cells; **right:** a colony of control cells visualized by tubulin immunolabelling (green) and H-33258 staining of nuclei (blue). **B, left:** PI profile of HeLa cells 6 h after 10^{-7} M ZnPc-PDT (1 h incubation, 15 min red light irradiation), G2/M and polyploid areas are clearly increased; **right,** a HeLa colony 6 h after this PDT treatment showing numerous cells blocked at metaphase (marked with asterisks).

Fig. 3. Details of the abnormalities of mitotic HeLa cells 6 h after ZnPc-PDT. Confocal microscopy: DNA in blue, α-tubulin in green, centromeres in red. Scale bars 10 µm. **A:** Control metaphase. **B:** Two metaphases showing the emergence of a third spindle pole disturbing the convergence of some chromosomes. **C:** Tripolar metaphase showing a greater dispersion of chromosomes. **D:** Abnormal metaphase showing irregularly dispersed chromosomes; metaphase abnormalities (**B to D**) do not correlate with chromosome fragmentation and dispersed or delayed chromosomes always show

centromere signal. **E:** HeLa aneuploid cell from a culture 24 h after light exposure, showing gigantism, three size-equivalent nuclei and multiplication of microtubule organizing centres.

Fig. 4. ZnPc-PDT induced cell death. Scale bar: 10 μm. **A:** Cells trypsinised from flasks 72 h after light exposure and visualised by H-33258 staining. There are clearly two groups: living cells with normal round nuclei and death ones with pycnotic and condensed nuclei. **B:** details of some death cells showing chromatin condensation and marginalization (typical morphology of apoptosis). **C:** Cleavage of PARP revealed by western blotting shows both the coexistence of living and apoptotic cells from 24 h after irradiation and the apoptotic nature of the detached cells (collected at ΔT=72 h). **D:** Dying cells also show Bax translocation to mitochondria 48 h after light irradiation (**left panel**). At this time, mitotic cells (despite abnormal configuration) are still living and show a diffuse Bax pattern (**right-upper panel**); in contrast, apoptotic cells show the Bax signal concentrated in several discrete spots (**right-lower panel**).

TABLE 1. Cellular uptake of ZnPc incorporated into DPPC liposomes. The results are presented as ng of ZnPc/mg of total proteins.

Incubation	ng ZnPc/mg prot.
10^{-7} M - 1 h	4.8 ± 1.6
10^{-7} M - 24 h	17.1 ± 0.5
2.5 µM - 1 h	35.7 ± 7.6
2.5 µM - 24 h	233.7 ± 47.0

Data correspond to mean values ± standard deviation (SD) from six different experiments.

TABLE 2. Cell survival after 10^{-7} M ZnPc-PDT treatment, measured by MTT and trypan blue assays. The results are presented as the surviving fraction in percentage.

	MTT	**Trypan blue**
Control cells	100 ± 2.6	98.7 ± 1.0
ΔT=24 h	86.5 ± 4.3	86.4 ± 4.3
ΔT=48 h	70.1 ± 0.7	74.3 ± 4.8
ΔT=72 h	60.7 ± 9.0	62.0 ± 1.3

Data correspond to mean values ± standard deviation (SD) from six different experiments. ΔT= elapsed time after PDT treatment.

DISCUSIÓN

Discusión

En esta Tesis Doctoral se presentan resultados de variada procedencia en forma de una serie de publicaciones científicas, con contenidos diferentes pero interrelacionados unos con otros. Por lo tanto, en este apartado de la Tesis Doctoral no se pretende analizar pormenorizadamente los resultados obtenidos en cada una de ellas (en los correspondientes artículos figuran discusiones específicas), sino que se intenta ponerlos en contexto a través de los Objetivos específicos de esta Tesis Doctoral.

OBJETIVO A:
Cuantificar el potencial citotóxico (sobre líneas celulares en cultivo) de tratamientos antitumorales de distinta naturaleza.

- The cytotoxic potential of a therapy is not only a function of inactivation records but also of cell death type specific triggering.
- *In vitro* protocols provide, as main advantages, the increased control of the experimental conditions and the possibility of obtain samples or observations for each desired time lapse. Proper time lapse selection can have a high influence in results' evaluation.

Para el desarrollo de nuevos fármacos en Oncología, la eficacia en términos de inactivación celular es un concepto de capital importancia (Johnstone y col., 2002; Cozzi y col., 2004; Jackson y col., 2007). Los estudios aquí presentados se han realizado fundamentalmente *in vitro*, empleando diversas líneas celulares establecidas de origen generalmente tumoral. La experimentación en estas condiciones presenta evidentes ventajas a la hora del análisis de las respuestas ante tratamientos antitumorales. La principal es el elevado nivel de control tanto en las condiciones de cultivo como en las de tratamiento; esto posibilita obtener el número necesario de réplicas de un experimento para las pruebas y procedimientos que nos permitan extraer el mayor número posible de datos. Empleando técnicas microscópicas se pueden hacer observaciones en una ilimitada serie de tiempos intermedios, y así evaluar cuales son los intervalos que proporcionarán una mayor cantidad de información acerca de los efectos inducidos. La correcta elección de los tiempos a los que se llevarán a cabo los distintos análisis tiene una importancia fundamental para el estudio de cualquier agente quimioterapéutico, ya que una inadecuada elección puede determinar pérdidas significativas de información.

La **Terapia Fotodinámica (PDT)** es una modalidad terapéutica con un largo recorrido en investigación básica que va creciendo en el mundo clínico (Dolmans y col., 2003; Triesscheijn y col., 2006). Los resultados presentados aquí prueban el gran potencial fotoinactivador de la PDT. Nuestras experiencias con el derivado porfirínico **CF3** demuestran que este agente es capaz de alcanzar elevados niveles de fotoinactivación celular en combinación con luz azul-violeta. En nuestras condiciones experimentales se alcanzó una inactivación celular muy elevada tanto para las condiciones experimentales más intensas (LD_{96}) como para condiciones de tratamiento menos extremas (LD_{85}). Como se comenta en el correspondiente artículo, estos elevados niveles de inducción de la apoptosis son marcadamente distintos a los comúnmente obtenidos con esta modalidad terapéutica. Todos estos datos evidencian el gran potencial de desarrollo que posee este PS de nueva síntesis. La que podría ser considerada su única desventaja (la dependencia de luz de longitud de onda con un bajo nivel de penetración tisular) es menos decisiva en el tratamiento de tumores pequeños y, para tumores de mayor tamaño, se han desarrollado sondas de fibra óptica capaces de introducir la luz en las proximidades e incluso el interior del tumor (Triesscheijn y col., 2006).

Por otra parte, la **ZnPc** es uno de los más prometedores PSs de segunda generación (Bonnet, 1999; Triesscheijn y col., 2006). Los datos aquí presentados se centran en los procesos desencadenados en condiciones de tratamiento subletales (un 40 % de fotoinactivación celular a las 72 h); pero existen diversos estudios (tanto provenientes de nuestro laboratorio como de otros centros) que muestran su efectividad, tanto *in vitro* como *in vivo* (Villanueva y col., 1999; Fabris y col., 2001; Galaz y col., 2005; Cristóbal y col., 2006; Magaraggia y col., 2006).

- Second generation PSs are improving the therapeutic possibilities of PDT.
- CF3 is capable to induce high records of cell inactivation (reaching the 96 %), even in the defined condition LD_{38}: cell death goes up until the 76.8 % if we take the data from 48 h after the treatment instead of the 24 h.
- Although work presented here with ZnPc was made in sub-lethal conditions (40 % death 72 h after light exposure), literature shows that this PS also has a high inactivation potential.

La **Terapia Fototérmica (PTT)** ha demostrado, en los resultados aquí presentados, su buen rendimiento como posible terapia anticancerígena. Empleando el PS naftalocianina de níquel (NiNc) obtuvimos porcentajes de supervivencia celular de plena inactivación en líneas de melanoma tanto humanas (C32) como murinas (B78H1). De igual manera conseguimos retrasos claramente significativos (de más de un mes) en el desarrollo de tumores *in vivo*, con muy poca afectación del tejido no tumoral circundante, aunque no se observó en ningún caso la completa regresión tumoral. Es necesario indicar que nuestro trabajo experimental con la PTT no se ha circunscrito a la NiNc, sino que en este momento, y en colaboración con la Universidad de Padua, se están estudiando otros sensibilizadores fototérmicos (naftalocianinas de platino, de paladio etc.) que están mostrando asimismo un buen comportamiento *in vitro*.

El **etopósido (VP-16)** es un agente quimioterapéutico muy conocido y empleado tanto en investigación básica como en clínica por su capacidad para inducir apoptosis (revisada por Meresse y col., 2004). Como se analiza en la discusión del correspondiente artículo, frente a los protocolos clásicos con VP-16 (con concentraciones y tiempos de incubación elevados) decidimos ensayar otras condiciones de tratamiento. Estas condiciones experimentales consistieron en una incubación relativamente corta (3 h) con una concentración no muy alta (50 µM) en comparación a las habitualmente empleadas, y periodos de observación post-incubación elevados (hasta 96 h) para poder estudiar la evolución de las alteraciones producidas y comprobar que se alcanzan elevados índices de inactivación celular. Los resultados obtenidos mostraron la práctica inactivación de las células HeLa a las 96 h tras la retirada del fármaco. En experimentos posteriores (no incluidos en la publicación) se ha trabajado con VP-16 en otras líneas celulares humanas (la tumoral MCF7 y la no tumoral HaCaT) y se han analizado, asimismo, la evolución a tiempos post-incubación superiores.

OBJETIVO B:
Relacionar el tipo de muerte celular inducida en función de la intensidad del estímulo aplicado.

El tipo de muerte celular inducido en terapia antitumoral es un elemento del máximo interés en las investigaciones oncológicas. Se han descrito conexiones entre la intensidad del estímulo causado (generalmente como concentración del agente quimioterapéutico) y el tipo de muerte desencadenado como respuesta para distintos fármacos con propiedades antineoplásicas (Schellens y col., 2005; Kim y col., 2006; Ricci y Zong, 2006).

Por acción de la **Terapia Fotodinámica** se inducen daños en las estructuras membranosas donde se retiene el PS (tanto membrana plasmática como las endomembranas de los orgánulos diana) y sus proximidades, particularmente en el citoesqueleto (Moor, 2000; Oleinick y col., 2002; Villanueva y col., 2003). La PDT genera un estrés oxidativo en las células que es procesado por todo el sistema de transducción de señales hasta las distintas respuestas de muerte y/o supervivencia (Almeida y col., 2004). Recientemente Alexandratou y colaboradores (2005) han evidenciado que, en condiciones subletales, la ZnPc desencadena varios procesos de señalización (como la liberación de Ca^{2+}) en las proximidades del área subcelular de acumulación del PS.

- Literature shows that cytotoxic activity of PDT is due to ROS generation in the PS location area. As levels of induced ROS are depending on PS amount and irradiation time, PDT-induced damage is easily to modulate, leading in different cell death type triggering.
- Despite the most common mitochondrial localisation, our PSs show in HeLa cells localisation patterns that closely resemble to the Golgi apparatus.
- The links between ROS generation, cellular injure and death induction at the Golgi are not well established. Effector caspase 2 (related with mitotic catastrophe process) is being active at this point and the neighbouring centrosome may be a good target for cytoskeletal damage.

Todos los resultados obtenidos mediante PDT indican que, dependiendo de la intensidad del tratamiento, la cantidad de especies reactivas de oxígeno (ROS) producida varía, lo que se traduce no sólo en distintos porcentajes de inactivación total, sino también en el disparo específico de tipos de muerte celular (fundamentalmente apoptosis en intensidades de daño bajas y necrosis en tratamientos comparativamente más intensos) (Fabris y col., 2001; Villanueva y col., 2003; Almeida y col., 2004; Stockert y col., 2007).

Nuestras experiencias, aquí mostradas con el derivado porfirínico CF3, evidencian claramente esa capacidad de la PDT de ejercer un daño modulable, en el que los niveles de supervivencia y los mecanismos de muerte descritos (necrosis, apoptosis y parada en metafase seguida de muerte) pueden relacionarse con los protocolos experimentales de distinta intensidad. Esta capacidad se ha descrito también con otros PS tanto de primera como de segunda generación, incluyendo a la ZnPc (Villanueva y col., 1999; Fabris y col., 2001; Juarranz y col., 2001; Morgan y Oseroff, 2001; Oleinick y col., 2002).

Como se ha comentado anteriormente, la localización subcelular del PS es de especial importancia a la hora de la activación de las distintas rutas de señalización de muerte celular, ya que las ROS tienen un muy limitado radio de acción (Triesscheijn y col., 2006). En base a la preferente localización en la mitocondria de diversos PSs, se ha venido considerando que dicho orgánulo actuaría como la principal diana en PDT (Granville y col., 2001; Morgan y Oseroff, 2001; Oleinick y col., 2002). La decisión entre apoptosis y necrosis como mecanismo principal de muerte celular se basaría en la capacidad de las mitocondrias dañadas para producir el ATP necesario para alimentar las rutas apoptóticas (Desagher y Martinou, 2000; Oleinick y col., 2002). Sin embargo, es creciente la opinión de que otros orgánulos están directamente implicados en los procesos de fotoinactivación mediante PDT (Villanueva y col., 2003; Almeida y col., 2004). En este sentido, los dos PSs empleados en la presente Tesis Doctoral presentan unos patrones de localización subcelular similares (en células HeLa): en el caso de la CF3 incluye el conjunto de lisosomas (y probablemente también el aparato de Golgi); en el caso de la ZnPc se muestran imágenes que evidencian su acumulación en un área perinuclear que se corresponde con el Golgi. Es importante recordar que la localización subcelular de un mismo PS puede variar entre distintos tipos celulares e incluso se pueden dar relocalizaciones como respuesta a la irradiación, tal y como se ha comentado en el quinto artículo en relación a la ZnPc (Wood y col., 1997; Oleinick y Evans, 1998).

La localización de los PSs (sobre todo de los que necesitan ser vehiculizados en los medios acuosos mediante liposomas) ha de ser entendida de una manera menos exclusivista, que tenga en cuenta el papel del aparato de Golgi (organizador de gran parte del tráfico vesicular en las células) como mediador de las respuestas desencadenadas por la PDT. En el ya mencionado trabajo de Alexandratou y colaboradores (empleando ZnPc en fibroblastos fetales humanos HFFF 2), la generación de ROS y los procesos de señalización derivados de ella se producen en un área perinuclear que incluye al aparato de Golgi. Los experimentos llevados a cabo en nuestro laboratorio con células A-549 y ZnPc han mostrado la activación localizada de caspasa-2 en el aparato de Golgi (Cristóbal y col., 2006). La caspasa-2 se localiza fundamentalmente en dicha zona del Golgi y es, probablemente, el miembro de la familia de las caspasas del que menos información se ha obtenido hasta el momento (Bao y Shi, 2007; Kumar, 2007). Esta caspasa se activa en los procesos de catástrofe mitótica, pero los mecanismos que determinan su activación y la identidad de los principales objetivos de su actividad proteolítica permanecen desconocidos (Castedo y col., 2004; Jackson y col., 2007).

Por otra parte, se ha documentado el daño a distintas estructuras del citoesqueleto por acción de las ROS (revisado por Villanueva y col., 2003). Tradicionalmente, las relaciones entre PDT y las alteraciones del citoesqueleto se habían interpretado como resultado de daños directos causados por la producción de ROS en las mitocondrias (Rodal y col., 1998; Juarranz y col., 2001). La generación de ROS en el área del aparato de Golgi puede ampliar el conjunto de estructuras del citoesqueleto susceptibles de ser dañadas.

La capacidad de inducir distintos tipos de muerte celular no ha sido observada aún en **Terapia Fototérmica**. La PTT desemboca siempre en la lisis celular, no habiéndose podido documentar ninguna otra alteración morfológica en las muestras analizadas. Nuestros experimentos, pioneros en este campo, han mostrado la súbita expulsión de toda el área donde se acumula la NiNc inmediatamente después de la irradiación. De igual modo, hemos confirmado que la agregación del PS en un área perinuclear, consistente con la posición del aparato de Golgi (confirmada, en experimentos no incluidos en la publicación, por comparación con el patrón obtenido con el marcador específico para Golgi NBD-C_6-ceramida), está relacionada con una mayor respuesta a la terapia, en términos de menor supervivencia.

- PTT is a pioneer therapeutics approach with a very high capability for inducing almost complete cell inactivation in melanoma cell lines from mice and human origins. *In vivo* experiences also show a significant delay in tumour progression.
- There is little literature about PTT-induced cell death at present. Our results clearly prove that the unique cell death mechanism is the physical ejection of the PS accumulation area due to thermal shockwave and leading in plasma membrane disruption. PS accumulation in a Golgi-like area correlates with an increased death induction.

La muerte que causa el tratamiento de PTT es prácticamente instantánea (el proceso culmina en pocos minutos tras la irradiación con el láser) y ello es otro punto a favor a encuadrar el tipo de muerte celular inducido como una necrosis: la muerte, al producirse de forma casi inmediata, no da lugar a la participación activa de ningún componente intrínseco de la célula. Como se ha comentado anteriormente, existe una literatura muy escasa acerca de los efectos de la PTT en células en cultivo, pero se ha descrito la pérdida de ciertas actividades enzimáticas, tanto en el citoplasma como en las mitocondrias, por acción de la PTT con NiNc (Busetti y col., 1999).

En relación con los mecanismos de muerte celular inducidos por tratamientos con **etopósido** hay que tener en cuenta que, al ser considerado un inductor típico de apoptosis (Meresse y col., 2004), la mayoría de estudios sobre él se han centrado en la cuantificación de la mortalidad celular (por lo común empleando exclusivamente citometría de flujo) sin realizar análisis morfológicos detallados (Facompré y col., 2000).

- The chemotherapeutic agent VP-16 is subject of several studies. We decided to work in new conditions characterised by a short incubation period of a low concentration dosage of VP-16. We prolong the observation time until 96 h after VP-16 removal, confirming that cell death induction reaches the almost complete inactivation.
- The analysis of the samples obtained at different sub-times in the observation period, allows us to identify a more complex process of death than classic apoptosis. Although the presence of cell cycle blockages or mitotic catastrophe process was cited previously, our work represents the first extended study of this cell death mechanism in cultured cell lines inactivated by VP-16.

Alteraciones del ciclo celular debidas a VP-16 han sido previamente descritas como detenciones genéricas con acumulación de células en el pico G2/M del perfil de contenido de ADN sin complementarlo con análisis morfológicos (Andreassen y col., 2001). La catástrofe mitótica inducida por etopósido ha sido vinculada , en una ocasión, a la aparición de resistencias a la apoptosis en un modelo muy específico de células sometidas a una transformación genética para sobrexpresar Bcl-2 (Castedo y col., 2004). Por todo ello, nuestros resultados (sobre células HeLa sin alterar) en los que se verifica la presencia de un bloqueo metafásico con acumulación de formas aberrantes, como paso previo a la muerte con características apoptóticas, representan una clara novedad en el estudio de este fármaco. La verificación de que pueden desarrollarse respuestas de muerte celular distinta a la apoptosis clásica amplía nuestro conocimiento acerca de los mecanismos que las células tumorales pueden utilizar en respuesta a la terapia con VP-16.

Es interesante destacar que mecanismos de catástrofe mitótica han sido descritos recientemente para otros venenos de la topo II (Vogel y col., 2005; Stevens y col., 2007). Asimismo, hay creciente evidencia de la efectividad de condiciones de incubación cortas (pulsos) como inductoras de esta modalidad de muerte celular (Michalakis y col., 2005).

OBJETIVO C:

Ampliar los criterios (morfológicos y/o bioquímicos) existentes para identificar los distintos tipos de muerte celular observados, profundizando en aquellos procesos que están menos clarificados.

- Morphology is the main criteria used for identifying cell death mechanisms, as the proposed biochemical probes fail to discriminate with accuracy in several occasions. Apoptosis descriptors (blebbing, shrinkage, chromatin marginalisation, condensation and fragmentation and final cell detachment) are well defined and our experiences only serve as confirmation. Instead, we propose here a sequence of well-characterised morphological milestones that, in our opinion, permits to widen our knowledge about necrotic process in adherent cells.

La presente Tesis Doctoral se basa en la premisa de que la morfología permite estudiar los tipos de muerte celular con una fiabilidad suficiente como para evaluar su importancia relativa en la capacidad citotóxica de una selección de tratamientos antitumorales. Pretendemos contribuir a ampliar y clarificar el conjunto de descriptores morfológicos existentes para los distintos tipos de muerte celular. Este énfasis por el desarrollo de los criterios morfológicos, se debe al creciente consenso entre los investigadores acerca de la incapacidad de los criterios basados en marcadores bioquímicos para discriminar fiablemente, por sí solos, entre los distintos tipos de muerte celular (Darzynkiewicz y col., 1997; Otsuki y col., 2003; Kroemer y col., 2005; Galluzzi y col., 2007). Creemos que, tomados en su conjunto, nuestros resultados permiten confirmar que el análisis morfológico es lo suficientemente eficaz a la hora de estudiar y clasificar con éxito los procesos de muerte celular producidos por los nuevos agentes antitumorales aquí analizados.

La **muerte celular apoptótica** (tipo 1) ha estado desde el principio unida a una serie muy bien definida de caracteres morfológicos (Kerr y col., 1972; Kroemer y col., 2005; Galluzzi y col., 2007). Nuestras experiencias han confirmado la bien conocida secuencia de acontecimientos ("blebeo" o *zeiosis* de la membrana plasmática, retracción celular, marginación, condensación y fragmentación cromatínica y pérdida final de adhesión al sustrato) que desembocan en la disgregación de la célula en cuerpos apoptóticos.

Ninguno de nuestros tratamientos ha generado respuestas que pertenezcan a la secuencia de la muerte celular de tipo 2 (autofagia), por lo que este tipo de muerte ha quedado fuera de nuestro análisis.

Sobre la **necrosis** (muerte celular de tipo 3) existe una cierta carencia de marcadores morfológicos específicos. El principal carácter (en ocasiones el único) empleado para definir e identificar la necrosis es la pérdida de la integridad de membrana, de forma más o menos dramática (Darzynkiewicz y col., 1997). A este carácter se le suma la ausencia de participación directa de la célula en el proceso, aunque últimamente se esté sugiriendo la presencia de ciertas actividades enzimáticas en el proceso (Kroemer y col., 2005; Galluzzi y col., 2007). Nuestros resultados (analizados con detalle en el tercer artículo) contribuyen de manera significativa a aportar una secuencia descriptiva clara de los eventos que conforman el proceso necrótico, un campo en el que aún hoy es muy poco lo publicado (Galluzzi y col., 2007).

- Necrosis was often described and defined only by plasma membrane rupturing. Our sequence starts prior with the loss of plasma membrane function as osmotic barrier, which is morphologically visualised as the growing of hyaline bubbles in cell surface. Bubbles coalesce into one giant bubble (that can reach a similar size of the rest of the cell) which finally detaches causing plasma membrane rupturing. The necrotic process do not finish here, as the cell remnants forms a precipitate as "cellular phantom" in which it could be observed nuclear shrinkage and random fragmentation of chromatin.

En el artículo publicado en la revista *Apoptosis*, trabajamos sobre células adheridas a la superficie de cultivo con tratamientos de muy distinta naturaleza: PDT con CF3 y ZnPc en intensidades inductoras de necrosis; incubaciones con concentraciones elevadas de H_2O_2 y procesos de congelación y descongelación. El primer evento morfológico necrótico que se comprueba es la pérdida del control osmótico de la membrana plasmática. Esa pérdida se manifiesta morfológicamente en la aparición de grandes burbujas hialinas, producidas por la entrada incontrolada de agua (que consideramos típicas y definitorias para predecir una respuesta necrótica). Las burbujas se pueden visualizar inmediatamente, o pocos minutos después de finalizado el tratamiento, mucho antes de que se observe la ruptura de la membrana. Observaciones anteriores, revisadas por Nieminen (2003), muestran que dichas burbujas están compuestas por elementos del citosol y trazas del retículo endoplásmico, en vez de ser macizas como los cuerpos apoptóticos. La ruptura de la membrana plasmática representa el final de la viabilidad celular pero no marca el final de la secuencia de eventos de la necrosis.

Al realizar observaciones más prolongadas en el tiempo hemos podido identificar otros dos caracteres morfológicos definitorios de los procesos de necrosis en cultivos adherentes. El más evidente es la conformación de un "fantasma celular" por la precipitación de todo el contenido insoluble de la célula (que no se libera al medio al romperse la membrana) y que permanece adherido al sustrato. Este "fantasma" degenera muy lentamente y permite, incluso en tiempos de observación muy prolongados, reconocer la forma y disposición de las células muertas por necrosis. El segundo implica al núcleo celular y comienza con una evidente retracción y condensación uniforme del núcleo (visible cuando se verifica la pérdida de la integridad de membrana) seguida de un proceso de degradación aleatoria de la cromatina, que queda dispersa por los restos del cuerpo celular.

Como se comenta ampliamente en la discusión del segundo artículo, la rapidez, la ruptura de la integridad de membrana y la ausencia de control celular en todo el proceso incluyen dentro del tipo necrótico a la muerte celular producida por PTT. A la hora de su descripción morfológica debe tenerse en cuenta que dichas células se irradiaban en suspensión, lo que nos dificulta la observación de estos marcadores morfológicos.

Se ha venido considerando generalmente que la necrosis es sólo una consecuencia debida a la imposibilidad de completar el desarrollo apoptótico por falta de energía en forma de ATP (Desagher y Martinou, 2000; Nieminen, 2003; Laporte y col., 2007). La no aparición de burbujas acuosas en respuesta a los tratamientos que conducen a la apoptosis, y su rápida presencia en los tratamientos necróticos, nos indicarían que la pérdida de los procesos de control osmótico es un proceso primordial en el disparo necrótico.

En resumen, si la apoptosis es un proceso controlado por la célula (en base a una red de dispositivos que monitorizan la homeostasis interna y las señales del exterior), la necrosis es un proceso de muerte en el que la célula no puede ejercer ningún mecanismo de control (lo que no quiere decir que varios procesos activables ante daños celulares no funcionen también en la necrosis). Una vez detectado un estímulo conducente a la muerte celular, la apoptosis se desarrolla a través de una compleja red de señales que determinan variaciones de poca importancia a nivel de las características finales del proceso (implicación diferencial de las distintas rutas, orden de activación de proteasas etc.). A la vista de nuestros resultados, la necrosis se estructura a través de una rápida pérdida de la función de la membrana plasmática como barrera osmótica (y que la compromete a una definitiva pérdida de su integridad física).

Aunque no entraba en nuestro planteamiento inicial, los resultados obtenidos a lo largo del periodo investigador conducente a la presente Tesis Doctoral, nos han permitido estudiar las características morfológicas de la **catástrofe mitótica** en muestras de diferentes orígenes.

Hay disponibles en la literatura referencias dedicadas a organizar los descriptores de este proceso (Erenpreisa y col., 2000; Erenpreisa y col., 2005; Kroemer y col., 2005; Galluzzi y col., 2007). Estos descriptores principales incluyen: parada en metafase (con conformaciones anómalas), salida en falso de la mitosis y restitución a interfase aneuploide (frecuentemente multi o micronucleada) y finalmente muerte celular. Igualmente ha sido descrito un fenómeno de formación de puentes cromatínicos entre los subnúcleos de las células aneuploides, que representa un estado intermedio en el proceso de restitución a interfase: estos puentes permiten explicar por qué no siempre los procesos de catástrofe mitótica incluyen la presencia de células aneuploides con micronúcleos o varios núcleos de similar tamaño (Erenpreisa y col., 2005; Galluzzi y col., 2007). En experimentos con VP-16 (posteriores a la publicación) hemos observado por videomicroscopía como los "subnúcleos" que presentan estos puentes tienden a reunirse en un solo núcleo.

Además de la confirmación de todos estos eventos citados en la literatura, hemos podido señalar la importancia de la correcta evaluación del tamaño celular para identificar interfases, mitosis y células en apoptosis provenientes de células previamente detenidas en metafase y que han sufrido aneuploidización (fenómeno que es especialmente evidente en los experimentos con VP-16).

- Our experiments also allow us to study the morphological features of the mitotic catastrophe process. Literature cited a series of morphological events, like abnormal spindle configuration that leads in cell cycle arrest or the presence of multi- or micro-nuclei in the aneuploid cells. The presence of more that one nucleus is not an absolute character as often sub-nuclei have chromatin bridges that permits nuclei fusion.
- Besides confirming these morphological features, we noticed that the size increasing in aneuploid cells is a major character that is clearly visible and conserved even in mitosis blockage or after cell death triggering.
- Cell death exits in mitotic catastrophe show the main characters of apoptotic cell death both morphological (blebbing, chromatin condensation etc.) and biochemical (cytochrome c release and caspase activation). We consider that is enough evidence for a definitive positioning of mitotic catastrophe into type 1 (apoptotic) cell death.

Acerca de la caracterización de las células muertas generadas en los procesos de catástrofe mitótica dentro de los tipos ya descritos, existen datos contradictorios que mantienen abierto hoy en día el debate (Michalakis y col., 2005; Mansilla y col., 2006; Blagosklonny, 2007; Galluzzi y col., 2007). En todos nuestros modelos experimentales con células HeLa hemos podido verificar que en dicho proceso de muerte están implicados eventos característicos de la apoptosis: relocalización de Bax en las mitocondrias, liberación del citocromo c, activación de las caspasas (mediante la ruptura de la proteína PARP), fragmentación y condensación de la cromatina y la formación de cuerpos apoptóticos. En los experimentos con VP-16 mediante técnicas de videomicroscopía se evidenció además que el disparo apoptótico (entendido por el "blebeo" o *zeiosis* de la superficie celular) se puede producir directamente desde células detenidas en metafase.

A nuestro entender, los datos mostrados en la presente Tesis Doctoral aportan suficientes evidencias para proponer la integración de la catástrofe mitótica dentro de la apoptosis. La apoptosis definida en sentido clásico se ha considerado ligada a la presencia de señales disparadoras específicas, tanto externas a la célula (típicas de los procesos de desarrollo) como provenientes de la actividad de los *checkpoints* que regulan el correcto funcionamiento de la célula (en respuesta a daños, fundamentalmente a través del *checkpoint* de daño genético). En ambos casos se ha venido considerando que el proceso apoptótico monitoriza la homeostasis celular con el objetivo de permitir, en condiciones óptimas, tanto el inicio de los procesos de replicación del material genético (entre G1 y S) como el de división celular (entre G2 y M) (Kastan y Bartek, 2004; Perona y Sánchez-Pérez, 2004). De esta manera, los fenómenos de muerte celular que se inician ante fallos durante la mitosis se consideraban fuera del proceso apoptótico. En nuestra opinión, incluir los procesos de catástrofe mitótica dentro de la apoptosis supone ampliar el rango de estímulos (más allá de la entrada en mitosis e, incluso, de su salida en falso) ante los que una célula puede reaccionar desencadenando dicho tipo de muerte celular. Por todo ello, consideramos que los datos aportados en la presente Tesis Doctoral se suman a otros presentes en la literatura (Erenpreisa y Cragg, 2001; Castedo y col., 2004; Vogel y col., 2007) para mostrar que, una vez iniciada la muerte por catástrofe mitótica, esta finaliza con la manifestación de los caracteres morfológicos (salvo la diferencia de tamaño en las células aneuploides) y con el concurso de, al menos, parte de las rutas bioquímicas de la apoptosis (incluyendo la activación de las caspasas).

OBJETIVO D:
Analizar las diferencias que puedan presentarse entre los patrones de muerte observados, con particular atención a los intervalos de tiempo post-tratamiento en los que se manifiestan los eventos que conforman la respuesta a los tratamientos.

El empleo de descriptores morfológicos nos proporciona la posibilidad de comparar los fenotipos de muerte (y su secuencia de desarrollo) inducidos por los distintos tratamientos empleados. Los análisis morfológicos nos permiten, por lo tanto, estudiar las semejanzas y diferencias entre los procesos de muerte celular obtenidos con nuestros tratamientos. A lo largo del texto se ha podido comprobar como nuestros distintos protocolos de tratamiento (en base a agentes de muy distinta naturaleza y comportamiento) nos han permitido alcanzar los mismos resultados finales a nivel de fenotipo de muerte, tal y como esperábamos. El correcto conocimiento de las diferencias a nivel del tiempo de respuesta (puede haber retrasos entre unas y otras) entre los distintos tratamientos es de capital importancia, ya que permite obtener la información más útil y significativa a través de la selección de los intervalos de tiempo más adecuados.

- Studying cell death induced by a number of different agents and processes allows us to establish both resemblances and differences between them.
- All the three main cell death mechanisms studied here (apoptosis, necrosis and mitotic catastrophe) showed the same morphological sequences of events, independently of the nature of the agent. But they showed also specific differences in the response times that lead on the precise processes triggered for each agent at that damage intensity. These differences are quite important for experimental planning as they determine the correct selection of observation and sample collection times.
- PDT procedures were faster inductors of apoptosis than serum withdrawal and VP-16 but the final steps of necrosis were seen later in comparison with H_2O_2 or freezing. PTT causes a necrotic death, fast and without cell control but some specific features described above couldn't be seen as irradiation was performed with cell suspensions.
- Response time's differences in studied mitotic catastrophe processes reveal that in VP-16 cell cycle arrest is a secondary event after a previous mitotic slippage suffered by the cells (24 h prior to metaphase blockage). In PDT metaphase blockage is a fast phenomenon due to direct damage to microtubule architecture.
- Relationships between cell death type triggering and whole inactivation records permits to build a "cellular damage scale".

En este apartado de la investigación, cobra un especial interés la naturaleza de la principal línea celular del estudio. El carcinoma de cérvix uterina humano HeLa fue la primera línea celular en establecerse (Scherer y col., 1953). HeLa se distingue de otras líneas por la integración en su genoma del virus del papiloma humano, HPV-18, que se encarga de eliminar p53 (y de interferir en otras señales) del sistema de regulación de estas células (Scherer y col., 1953; May y col., 1991). Como se ha comentado en la Introducción, la ausencia funcional de p53 se ha venido considerando como un requisito imprescindible tanto en los procesos de tumorigénesis como en los procesos de resistencia a la terapia (Hanahan y Weinberg, 2000; Kastan y Bartek, 2004; Vousden y Lane, 2007). A escala celular, la falta de p53 proporciona a las células HeLa capacidad de resistir, en determinadas ocasiones, a estímulos apoptóticos (Brown y Wouters, 1999) sin impedir el desencadenamiento de la muerte celular: de manera que se favorecen la aparición de respuestas tanto necróticas (por falta del disparo apoptótico) como de "apoptosis retrasada" a través de mecanismos de catástrofe mitótica (Chen y col., 2003; Almeida y col., 2004; Castedo y col., 2004).

En el artículo tercero se discuten extensamente los principales descriptores y criterios empleados para **apoptosis y necrosis**, por lo que aquí sólo haremos una referencia resumida a los mismos. Hemos conseguido inducir porcentajes de muerte de características apoptóticas muy elevados con la PDT empleando CF3 (LD_{85}). La morfología de las células así inactivadas se corresponde bien con la obtenida a través de condiciones de trabajo previamente publicadas para ZnPc (Villanueva y col., 1999), de procesos de deprivación de suero y de incubación con el agente VP-16. La PDT con CF3 puede ser asimismo empleada para producir muerte celular con características morfológicas de la necrosis (LD_{96}), de igual manera a las que se obtienen con ZnPc (Villanueva y col., 1999), mediante incubación con H_2O_2 o los resultantes de procesos de congelación y descongelación repetidos (en el caso de los eventos más tardíos). La muerte celular conseguida mediante PTT con NiNc es igualmente evaluada como una necrosis, pero sus particulares condiciones de experimentación (en suspensión) inducen comprensibles variaciones en los resultados. Las claras semejanzas que se observan entre los tipos apoptóticos y necróticos de muerte se comprueban también en cada una de las morfologías intermedias que conforman dichos patrones (como se comenta en la discusión del tercer artículo). Sin embargo, tal y como se muestran en las figuras de dicho artículo, se observa un claro desfase entre los protocolos de PDT y los empleados como control a nivel de los tiempos de respuesta: los tratamientos de PDT son más rápidos inductores de la apoptosis (se observa con un adelanto de unas 24 h), pero son más lentos cuando hablamos de las fases finales de la necrosis (la fragmentación nuclear y la conformación del "fantasma celular").

Tanto trabajando con VP-16 como en protocolos de PDT empleando los dos PSs, hemos conseguido inducir una respuesta subletal en el cultivo que se ha desarrollado, como corresponde a procesos de **catástrofe mitótica**, a través de bloqueos metafásicos que, finalmente, se resuelven en un desencadenamiento retrasado de la apoptosis. En estos procesos también se verifican diferencias con respecto a los tiempos de respuesta. Los procesos de catástrofe mitótica causados por la PDT son significativamente más rápidos que los que se observan con el VP-16. En PDT los bloqueos de las células en metafase se observan a las pocas horas (generalmente dentro de las primeras 24 h tras la irradiación) mientras que con el tratamiento con un "pulso" de VP-16 es necesario esperar 48 h, tras retirarse el fármaco, para verificar el proceso.

Las diferencias en los tiempos de respuesta nos señalan aspectos que están ligados al tipo de daño específico que genera cada agente antineoplásico, en función de su naturaleza. El VP-16 es un agente genotóxico: en su presencia las células sufren fragmentación cromosómica. Debido a esta fragmentación durante el proceso mitótico, en el primer ciclo tras la exposición, parte del material genético está formado por fragmentos acéntricos que no se unen al huso. Las células restituyen a interfase poliploide y es en el posterior ciclo de división (48 h tras el tratamiento) cuando se produce el bloqueo de células multipolares en metafase. A partir de ahí el proceso de catástrofe deriva hacia la conformación de un ciclo celular aneuploide y/o la salida a muerte celular. Sin embargo, las células detenidas en metafase tras un tratamiento de PDT, lo hacen en las primeras horas subsiguientes al tratamiento (dentro de las primeras 24 h, aunque en el caso de la ZnPc es ya evidente a las 6 h). La parada de las células sometidas a PDT viene acompañada por graves alteraciones en el huso mitótico (fundamentalmente polos supernumerarios) sin que se haya verificado la presencia previa de daños en el citoesqueleto y sin que se haya observado ninguna alteración clara en la morfología cromosómica (ya que en este caso conservan funcionales sus áreas centroméricas y no se ha detectado ningún fragmento acéntrico).

A partir de estas diferencias, podemos suponer que con el VP-16 las metafases bloqueadas, por acumulación de polos supernumerarios, son secundarias en su proceso de respuesta a la terapia, resultado de la no progresión de las metafases previas con cromosomas fragmentados (que son el producto de la actividad del fármaco). Por otra parte, la rápida aparición de husos con polos supernumerarios en la catástrofe mitótica producida por PDT ha de responder a daños atribuibles directamente a las ROS. En este sentido es importante indicar que la presencia de centrosomas supernumerarios no es sólo típica de células aneuploides, sino que la falta de p53 funcional se ha relacionado con la amplificación anómala del número de centrosomas (Tsou y Stearns, 2006).

Vistos en su conjunto, podríamos ordenar los tratamientos antitumorales aquí revisados, a lo largo de una **escala de daño celular** (ver **Figura 15**). Los experimentos de PTT, y todos los otros conducentes a una respuesta de muerte necrótica, se encuentran en un extremo de la gradación del daño producido, y se caracterizan por la velocidad en la que se verifica el proceso de muerte; en el otro extremo de dicha gradación se encontrarían los obtenidos con la PDT con ZnPc (que presentan una mortalidad más baja) y los de CF3 a LD_{38}. En relación con estos últimos, deberíamos colocar los resultados obtenidos con el VP-16, ya que tiene un efecto letal sobre el cultivo pero por el mismo mecanismo de catástrofe mitótica (que se caracteriza particularmente por el elevado tiempo necesario para lograr la inactivación celular). Entre ambos extremos en nuestra escala de modulación del daño, se situarían los resultados obtenidos con la PDT con CF3 que se desarrollan a través de la inducción de un tipo de muerte celular claramente apoptótico (LD_{85}). Ordenando de esta manera nuestros resultados, resulta evidente la gran utilidad que presenta la PDT a la hora de producir distintos tipos de muerte mediante la modulación precisa de los protocolos de tratamiento.

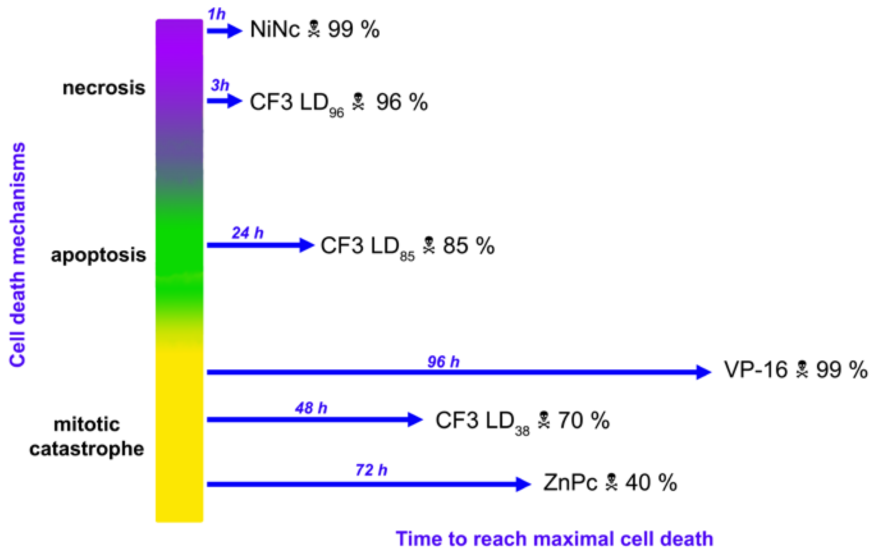

Figure 15 Anti-tumour treatments employed in the present PhD Thesis can be displayed as functions of cell death mechanisms that they trigger (due to the induction of graded doses of damage). As it could be seen, Photodynamic therapy (exemplified here in the experiences with the novel porphyrin derivative CF3) could be easily modulated for obtaining different levels of damage correlated with distinct cell death types.

En resumen, los datos aportados por los trabajos conducentes a esta Tesis Doctoral nos llevan a concluir que, ante la enorme variedad de agentes quimioterapéuticos, de líneas celulares y de modelos animales, el estudio sobre los mecanismos de muerte celular debe tener como prioridad inicial la información morfológica (asequible al experimentador y fácilmente interpretable). El estudio de la regulación bioquímica debe hacerse simultáneamente, para que estas dos fuentes de

- The study of cell death mechanisms in anti-tumour therapy will allow establishing the best manner of combine agents that induce different sources of damage in order to improve the response. Morphological data provides a first step of knowledge about cell death type and response times that links with biochemical research about the precise pathway stimulation.

datos complementarias puedan contribuir al esclarecimiento de los procesos que se dan tras un tratamiento antitumoral, y ser empleados en el desarrollo de terapias más eficaces y con reducidas posibilidades de inducción de resistencia celular. En este sentido, la tendencia entre los investigadores se está moviendo hacia una creciente revalorización de los análisis morfológicos y hacía el estudio de las cepas resistentes a la terapia (frente a la mera cuantificación de los niveles de supervivencia).

CONCLUSIONES

Conclusiones

Las conclusiones de la presente Tesis Doctoral se presentan referenciadas a los Objetivos específicos que se han enumerado anteriormente (A-E).

- A1.- La Terapia Fotodinámica (PDT) del cáncer es una modalidad terapéutica con elevada capacidad citotóxica. No está dirigida contra la integridad genómica de las células tumorales sino contra el correcto funcionamiento fisiológico y metabólico de los orgánulos. Proporciona, por tanto, un amplio abanico de nuevas dianas para actuar contra tumores resistentes a las terapias genotóxicas convencionales.

- A2.- Derivada de la PDT, la Terapia Fototérmica (PTT) puede convertirse en una alternativa terapéutica contra tumores especialmente resistentes (como los melanomas), proporcionando un daño celular masivo.

- B1.- La PDT proporciona la posibilidad de modular el daño celular para obtener la inactivación tumoral mediante distintos tipos y mecanismos de muerte. El papel del aparato de Golgi (y de otros orgánulos subcelulares distintos de la mitocondria) en la muerte celular generada por PDT necesita de una mayor atención, ya que puede ayudar a entender el disparo de señales de muerte específicas.

- B2.- La PTT genera, a través de ondas de choque térmico, alteraciones que conducen físicamente a la muerte celular por necrosis (mediante la ruptura de la membrana plasmática por la eyección de parte de la masa celular).

- B3.- La respuesta de muerte celular inducida por el etopósido (VP-16) puede desarrollarse, al menos en células HeLa, por procesos de catástrofe mitótica además de por la apoptosis clásica.

- C1.- La necrosis es un tipo de muerte celular carente de control interno celular. La pérdida de la integridad de la barrera osmótica de la membrana plasmática es un hecho fundamental. Morfológicamente, en células adherentes, se identifican una serie de eventos destacados: aparición y convergencia de burbujas en la superficie celular, ruptura de la membrana plasmática al desprenderse la burbuja, fragmentación aleatoria del núcleo y formación de un "fantasma" al precipitar componentes celulares.

- C2.- La catástrofe mitótica es un proceso en el que la muerte celular se desencadena con un significativo retraso temporal con respecto a la apoptosis clásica. En nuestros modelos experimentales se verifica que las células que mueren muestran características morfológicas (blebeo, formación de cuerpos y desprendimiento del sustrato) y bioquímicas (relocalización de Bax, liberación de citocromo c, ruptura de PARP y fragmentación cromatínica internucleosomal) claramente apoptóticas. Aquellas células que hubiesen sufrido aneuploidización pueden mostrar un marcado incremento del tamaño incluso tras la adopción del fenotipo apoptótico.

- D1.- A pesar de la diversidad de los agentes antitumorales y de los modelos de experimentación disponibles, los procesos de muerte celular que inducen se pueden agrupar en pocos tipos atendiendo fundamentalmente a sus características morfológicas. Modulando las condiciones de tratamiento hemos conseguido reproducir secuencias equivalentes de apoptosis, necrosis y catástrofe mitótica con distintos agentes antineoplásicos.

- D2.- Entre los distintos tratamientos analizados con similares respuestas existen claras diferencias en los tiempos de respuesta. Este dato ha de ser tenido en cuenta a la hora de la correcta evaluación de los resultados. Las diferencias revelan los distintos mecanismos de inducción de daño entre cada uno de los agentes, y pueden ser muy valiosas a la hora de diseñar terapias combinadas.

Conclusions

For making them more accessible, conclusions are presented related to the Main Objectives of the Thesis.

- A1. - Photodynamic therapy (PDT) is a therapeutic approach with high cytotoxic potential. It is not driven against the genomic integrity, instead is targeted to the physiological and metabolic activities of cell organelles. PDT gives a wide spectrum of new possible targets for tumours resistant to classic genotoxic therapies.

- A2. - Branched from PDT, Photothermal therapy (PTT) provides massive dell damage and could develop into an alternative therapeutic tool against highly resistant tumours (like melanomas).

- B1. - PDT provides the opportunity to modulate cell damage to obtain cell inactivation with different cell death types and mechanisms. The role of the Golgi apparatus (and other non-mitochondrion organelles) in cell death triggering by PDT needs more attention as it could contribute to correct understanding of specific death signals activation.

- B2. - PTT causes, upon thermal shockwaves, an alteration that leads to the physical rupture of the plasma membrane by the ejection of part of the cellular mass. The whole process can be classified as a necrosis.

- B3. - Cellular response to VP-16 treatments could be performed, at least in HeLa cells, by means of mitotic catastrophe instead of classic apoptosis.

- C1. - Necrosis is a cell death type without any cell's internal control. The loss of the osmotic barrier at plasma membrane is a main event in this process. Morphologically, in adherent cells, we have proposed a series of events: development and coalescence of bubbles in cell surface, plasma membrane rupture caused by bubble's detachment, random nuclear fragmentation and persistence of a cellular phantom conformed by cell remnants.

- C2. - Mitotic catastrophe is characterised by a delayed death response in comparison to classic apoptosis. Once triggered, mitotic catastrophe's death cells show the phenotypical features of apoptosis (both morphological and biochemical). Those cells that suffer previous aneuploidisation prior to death can show a marked size increase, even after the acquisition of the apoptotic morphology.

- D1. - Despite the diversity of anti-tumour agents and research models, cell death processes can be successfully gathered in a few types attending its morphological characteristics. Modulating our treatment conditions we can reproduce similar series of apoptosis, necrosis and mitotic catastrophe events using different anti-neoplasic agents.

- D2. - Although the patterns obtained were quite similar, there are significant differences in response times between the treatments. This is an important feature in order to a proper evaluation of experimental data. Differences reveal the different mechanisms of damage induction among the agents and they are also highly informative in order to develop combined therapies.

BIBLIOGRAFÍA

Bibliografía

Adams, J. M., y Cory, S. (2002). *Apoptosomes: engines for caspase activation*. Current Opinion in Cell Biology **14**, 715-720.

Aguirre-Ghiso, J. A. (2007). *Models, mechanisms and clinical evidence for cancer dormancy*. Nature Reviews Cancer **7**, 834-846.

Alexandratou, E., Yova, D., y Loukas, S. (2005). *A confocal microscopy study of the very early cellular response to oxidative stress induced by zinc phthalocyanine sensitization.* Free Radical Biology & Medicine **39**, 1119-1127.

Almeida, R. D., Manadas, B. J., Carvalho, A. P., y Duarte, C. B. (2004). *Intracellular signaling mechanisms in photodynamic therapy.* Biochimica et Biophysica Acta **1704**, 59-86.

Ameisen, J. C. (2004). *Looking for death at the core of life in the light of evolution.* Cell Death and Differentiation **11**, 4-10.

Anderson, A. R. A., Weaver, A. M., Cummings, P. T., y Quaranta, V. (2006). *Tumor morphology and phenotypic evolution driven by selective pressure from the microenvironment.* Cell **127**, 905-915.

Andreassen, P. R., Lacroix, F. B., Lohez, O. D., y Margolis, R. L. (2001). *Neither $p21^{WAF1}$ nor 14-3-3σ prevents G_2 progression to mitotic catastrophe in human colon carcinoma cells after DNA damage, but $p21^{WAF1}$ induces stable G_1 arrest in resulting tetraploid cells.* Cancer Research **61**, 7660-7668.

Baker, D. J., Chen, J., y van Deursen, J. M. A. (2005). *The mitotic checkpoint in cancer and aging: what have mice taught us?* Current Opinion in Cell Biology **17**, 583-589.

Bao, Q., y Shi, Y. (2007). *Apoptosome: a platform for the activation of initiator caspases.* Cell Death and Differentiation **14**, 56-65.

Blagosklonny, M. V. (2007). *Mitotic arrest and cell fate.* Cell Cycle **6**, 70-74.

Bonnet, R. (1999). *Photodynamic therapy in historical perspective.* Reviews in Contemporary Pharmacotherapy **10**, 1-17.

Borner, C. (2003). *The Bcl-2 protein family: sensors and checkpoint for life-or-death decisions.* Molecular Immunology **39**, 615-647.

Boyce, M., Degterev, A., y Yuan, J. (2004). *Caspases: an ancient cellular sword of Damocles.* Cell Death and Differentiation **11**, 29-37.

Bröker, L. E., Kruyt, F. A. E., y Giaccone, G. (2005). *Cell death independent of caspases: a review.* Clinical Cancer Research **11**, 3155-3162.

Brown, J. M., y Wouters, B. G. (1999). *Apoptosis, p53, and tumor cell sensitivity to anticancer agents.* Cancer Research **59**, 1391-1399.

Burden, D. A., Kingma, P. S., Froelich-Ammon, S. J., Bjornstii, M. A., Patchan, M. W., Thompson, R. B., y Osheroff, N. (1996). *Topoisomerase II·Etoposide Interactions Direct the Formation of Drug-induced Enzyme-DNA Cleavage Complexes.* Journal of Biological Chemistry **271**, 29238-29244.

Busetti, A., Soncin, M., Reddi, E., Rodgers, M. A. J., Kenney, M. E., y Jori, G. (1999). *Photothermal sensitization of amelanotic melanoma cells by Ni(II)-octabutoxy-naphthalocyanine.* Journal of Photochemistry and Photobiology, B: Biology **53**, 103-109.

Camerin, M., Rodgers, M. A. J., Kenney, M. E., y Jori, G. (2005). *Photothermal sensitisation: evidence for the lack of oxygen effect on the photosensitising activity.* Photochemical and Photobiological Sciences **4**, 251-253.

Castano, A. P., Mroz, P., y Hamblin, M. R. (2006). *Photodynamic therapy and anti-tumour immunity.* Nature Reviews Cancer **6**, 535-545.

Castedo, M., Coquelle, A., Vivet, S., Vitale, I., Kauffmann, A., Dessen, P., Pequignot, M. O., Casares, N., Valent, A., Mouhamad, S., Schmitt, E., Modjtahedi, N., Vainchenker, W., Zitvogel, L., Lazar, V., Garrido, C., y Kroemer, G. (2006). *Apoptosis regulation in tetraploid cancer cells.* The EMBO Journal **25**, 2584-2595.

Castedo, M., Perfettini, J. L., Roumier, T., Andreau, K., Medema, R., y Kroemer, G. (2004). *Cell death by mitotic catastrophe: a molecular definition.* Oncogene **23**, 2825-2837.

Castedo, M., Perfettini, J. L., Roumier, T., y Kroemer, G. (2002). *Cyclin-dependent kinase-1: linking apoptosis to cell cycle and mitotic catastrophe.* Cell Death and Differentiation **9**, 1287-1293.

Cortes, J., y Baselga, J. (2007). *Targetting the microtubules in breast cancer beyond taxanes: the epothilones.* The Oncologist **12**, 271-280.

Cozzi, P., Mongelli, N., y Suarato, A. (2004). *Recent anticancer cytotoxic agents.* Current Medicinal Chemistry. Anti-cancer Agents. **4**, 93-121.

Cristóbal, J., Stockert, J. C., Villanueva, A., Rello-Varona, S., Juarranz, A., y Cañete, M. (2006). *Caspase-2: A possible trigger of apoptosis induced in A-549 cells by ZnPc photodynamic treatment.* International Journal of Oncology **28**, 1057-1063.

Chang, H. Y., y Yang, X. (2000). *Proteases for cell suicide: functions and regulation of caspases.* Microbiology and Molecular Biology Reviews **64**, 821-846.

Chen, J. G., Yang, C. P. H., Cammer, M., y Horwitz, S. B. (2003). *Gene expression and mitotic exit induced by microtubule stabilizing drugs.* Cancer Research **63**, 7891-7899.

Chen, W. R., Adams, R. L., Higgins, A. K., Bartels, K. E., y Nordquist, R. E. (1996). *Photothermal effects on murine mammary tumors using indocyanine green and 808-nm diode laser: an in vivo efficacy study.* Cancer Letters **98**, 169-173.

Danial, N. N., y Korsmeyer, S. J. (2004). *Cell death: critical control points.* Cell **116**, 205-219.

Darzynkiewicz, Z., Juan, G., Li, X., Gorczyca, W., Murakami, T., y Traganos, F. (1997). *Cytometry in cell necrobiology: analysis of apoptosis and accidental cell death (necrosis).* Cytometry **27**, 1-20.

Desagher, S., y Martinou, J. C. (2000). *Mitochondria as the central control point of apoptosis.* Trends in Cell Biology **10**, 369-377.

Deveraux, Q. L., y Reed, J. C. (1999). *IAP family proteins-suppressors of apoptosis.* Genes and development **13**, 239-252.

Diddens, H., Fischer, F., y Pottier, R. (2003). *In vivo investigations on dye enhanced photothermal tumor therapy with a naphthalocyanine derivative.* Oftalmologia **1**, 59-61.

Diven, D. G., Pohl, J., y Motamendi, M. (1996). *Dye-enhanced diode laser photothermal ablation of skin.* Journal of the American Academy of Dermatology **35**, 211-215.

Dolmans, D. E. J., Fukumura, D., y Jain, R. K. (2003). *Photodynamic therapy for cancer.* Nature Reviews Cancer **3**, 380-387.

Dougherty, T. J. (2002). *An update on photodynamic therapy applications.* Journal of Clinical Laser Medicine & Surgery **20**, 3-7.

Eccles, S. A., y Welch, D. A. (2007). *Metastasis: recent discoveries and novel treatment strategies.* The Lancet **369**, 1742-1757.

Edinger, A. L., y Thompson, C. B. (2003). *Defective autophagy leads to cancer.* Cancer Cell **4**, 422-424.

Edinger, A. L., y Thompson, C. B. (2004). *Death by design: apoptosis, necrosis and autophagy*. Current Opinion in Cell Biology **16**, 663-669.

Erenpreisa, J. E., y Cragg, M. S. (2001). *Mitotic death: a mechanism of survival? A review.* Cancer Cell International **1**, 1.

Erenpreisa, J. E., Ivanov, A., Dekena, G., Vitina, A., Krampe, R., Freivalds, T., Selivanova, G., y Roach, H. I. (2000). *Arrest in metaphase and anatomy of mitotic catastrophe: mild heat shock in two human osteosarcoma cell lines.* Cell Biology International **24**, 61-70.

Erenpreisa, J. E., Kalejs, M., y Cragg, M. S. (2005a). *Mitotic catastrophe and endomitosis in tumour cells: An evolutionary key to a molecular solution.* Cell Biology International **29**, 1012-1018.

Erenpreisa, J. E., Kalejs, M., Ianzini, F., Kosmacek, E. A., Mackey, M. A., Emzinsh, D., Cragg, M. S., Ivanov, A., y Illidge, T. M. (2005b). *Segregation of genomes in polyploid tumour cells following mitotic catastrophe.* Cell Biology International **29**, 1005-1011.

Fabris, C., Valduga, G., Miotto, G., Borsetto, L., Jori, G., Garbisa, S., y Reddi, E. (2001). *Photosensitization with zinc (II) phthalocyanine as a switch in the decision between apoptosis and necrosis.* Cancer Research **61**, 7495-7500.

Facompré, M., Wattez, N., Kluza, J., Lansiaux, A., y Baily, C. (2000). *Relationship between cell cycle changes and variations of the mitocondrial membrane potential induced by etoposide.* Molecular Cell Biology Research Communications **4**, 37-42.

Ferri, K. F., y Kroemer, G. (2001). *Organelle-specific initiation of cell death pathways.* Nature Cell Biology **3**, E255-E263.

Festjens, N., van Gurp, M., van Loo, G., Saelens, X., y Vandenabeele, P. (2004). *Bcl-2 family members as sentinels of cellular integrity and role of mitochondrial intermembrane space proteins in apoptotic cell death.* Acta Haematologica **111**, 7-27.

Fulda, S., y Debatin, K. M. (2004). *Apoptosis signaling in tumor therapy.* Annals of the New York Academy of Sciences **1028**, 150-156.

Galaz, S., Espada, J., Stockert, J. C., Pacheco, M., Sanz-Rodríguez, F., Arranz, R., Rello, S., Cañete, M., Villanueva, A., Esteller, M., y Juarranz, A. (2005). *Loss of E-cadherin mediated cell-cell adhesion as an early trigger of apoptosis induced by photodynamic treatment.* Journal of Cellular Physiology **205**, 86-96.

Galluzzi, L., Maiuri, M. C., Vitale, I., Zischka, H., Castedo, M., Zitvogel, L., y Kroemer, G. (2007). *Cell death modalities: classification and pathophysiological implications.* Cell Death and Differentiation **14**, 1237-1266.

Garrido, C., Galluzzi, L., Brunet, M., Puig, P. E., y Kroemer, G. (2006). *Mechanisms of cytochrome c release from mitochondria.* Cell Death and Differentiation **13**, 1423-1433.

Garrido, C., y Kroemer, G. (2004). *Life's smile, death's grin: vital functions of apoptosis-executing proteins.* Current Opinion in Cell Biology **16**, 639-646.

Gozuacik, D., y Kimchi, A. (2007). *Autophagy and Cell Death*. Current Topics in Developmental Biology **78**, 217-245.

Granville, D. J., McManus, B. M., y Hunt, D. W. C. (2001). *Photodynamic therapy: shedding light on the biochemical pathways regulating porphyrin-mediated cell death.* Histology and Histopathology **16**, 309-317.

Greaves, M. (2002). *Cáncer, el legado evolutivo.* (**Barcelona**: Editorial Crítica).

Hanahan, d., y Weinberg, R. A. (2000). *The hallmarks of cancer.* Cell **100**, 57-70.

Harrington, K. J., Syrigos, K. N., y Vile, R. G. (2002). *Liposomally targeted cytotoxic drugs for the treatment of cancer.* Journal of Pharmacy and Pharmacology **54**, 1573-1600.

Huang, Z. (2002). *The chemical biology of apoptosis: exploring protein-protein interactions and the life and death of cells with small molecules.* Chemistry and Biology **9**, 1059-1072.

Huettenbrenner, S., Maier, S., Leisser, C., Polgar, D., Strasser, S., Grusch, M., y Krupitza, G. (2003). *The evolution of cell death programs as prerequisites of multicellularity.* Mutation Research **543**, 235-249.

Ito, A., Shinkai, M., Honda, H., y Kobayashi, T. (2005). *Medical application of funcionalized magnetic nanoparticles.* Journal of Bioscience and Bioengineering **100**, 1-11.

Jackson, J. R., Patrick, D. R., Dar, M. M., y Huang, P. S. (2007). *Targeted anti-mitotic therapies: can we improve on tubulin agents?* Nature Reviews Cancer **7**, 107-117.

Johnstone, R. W., Ruefli, A. A., y Lowe, S. W. (2002). *Apoptosis: a link between cancer genetics and chemotherapy.* Cell **108**, 153-164.

Jordan, M. A., y Wilson, L. (2004). *Microtubules as a target for anticancer drugs.* Nature Reviews Cancer **4**, 253-265.

Jori, G., y Spikes, J. D. (1990). *Photothermal sensitizers: possible use in tumor therapy.* Journal of Photochemistry and Photobiology, B: Biology **6**, 93-101.

Juarranz, A., Espada, J., Stockert, J. C., Villanueva, A., Polo, S., Domínguez, V., y Cañete, M. (2001). *Photodamage induced by zinc(II)-phthalocyanine to microtubules, actin, alpha-actinin and keratin of HeLa cells.* Photochemistry and Photobiology **73**, 283-289.

Kastan, M. B., y Bartek, J. (2004). *Cell-cycle checkpoints and cancer.* Nature **432**, 316-323.

Kerr, J. F., Wyllie, A. H., y Currie, A. R. (1972). *Apoptosis: a basic biological phenomenon with wide-ranging implications in tissue kinetics.* British Journal of Cancer **26**, 239-256.

Kessel, D., Castelli, M., y Reiners, J. J. (2005). *Ruthenium red-mediated suppression of Bcl-2 loss and* $Ca^{(2+)}$ *release initiated by photodamage to the endoplasmic reticulum: scavenging of reactive oxygen species.* Cell Death and Differentiation **12**, 502-511.

Kim, H., Rafiuddin-Shah, M., Tu, H. C., Jeffers, J. R., Zambetti, G. P., Hsieh, J. J. D., y Cheng, E. H. Y. (2006). *Hierarchical regulation of mitochondrion-dependent apoptosis by BCL-2 subfamilies.* Nature Cell Biology **8**, 13481358.

Kim, R., Emi, M., y Tanabe, K. (2005). *Caspase-dependent and -independent cell death pathways after DNA damage (Review).* Oncology Reports **14**, 595-599.

Kim, R., Emi, M., Tanabe, K., Uchida, Y., y Arihiro, K. (2006). *The role of apoptotic or nonapoptotic cell death in determining cellular response to anticancer treatment.* European Journal of Surgical Oncology **32**, 269-277.

Klarsfeld, A., y Revah, F. (2002). *Biología de la muerte.* (**Madrid**: Editorial Complutense).

Klionsky, D. J. (2007). *Autophagy: from phenomenology to molecular understanding in less than a decade*. Nature Reviews Molecular Cell Biology **8**, 931-937.

Kroemer, G., El-Deiry, W. S., Golstein, P., Peter, M. E., Vaux, D., Vandenabeele, P., Zhivotovsky, B., Blagosklonny, M. V., Malorni, W., Knight, R. A., Piacentini, M., Nagata, S., y Melino, G. (2005). *Classification of cell death: recommendations of the Nomenclature Commitee on Cell Death.* Cell Death and Differentiation **12**, 1463-1467.

Kumar, S. (2007). *Caspase function in programmed cell death.* Cell Death and Differentiation **14**, 32-43.

Laporte, C., Kosta, A., Klein, G., Aubry, L., Lam, D., Tresse, E., Luciani, M. F., y Golstein, P. (2007). *A necrotic cell death model in a protist.* Cell Death and Differentiation **14**, 266-274.

Lawen, A. (2003). *Apoptosis - an introduction.* BioEssays **25**, 888-896.

Leist, M., y Jäättelä, M. (2001a). *Four deaths and a funeral: from caspases to alternative mechanisms.* Nature Reviews Molecular Cell Biology **2**, 1-10.

Leist, M., y Jäättelä, M. (2001b). *Triggering of apoptosis by cathepsins*. Cell Death and Differentiation **8**, 324-326.

Liu, V. G., Cowan, T. M., Jeong, S. W., Jacques, S. L., Lemley, E. C., y Chen, W. R. (2002). *Selective photothermal interaction using an 805 nm diode laser and indocyanine green in gel phantom and chicken breast tissue*. Lasers in Medical Science **17**, 272-279.

Liu, Z., y Lenardo, M. J. (2007). *Reactive oxygen species regualte autophagy through redox-sensitive proteases.* Developmental Cell **12**, 484-485.

Magaraggia, M., Visonà, A., Furlan, A., Pagnan, A., Miotto, G., Tognon, G., y Jori, G. (2006). *Inactivation of vascular smooth muscle cells photosensitised by liposome-delivered Zn(II)-phthalocyanine.* Journal of Photochemistry and Photobiology, B: Biology **82**, 53-58.

Mansilla, S., Priebe, W., y Portugal, J. (2006). *Mitotic catastrophe results in cell death by caspase-dependent and caspase-independent mechanisms.* Cell Cycle **5**, 53-60.

Marchal, C., Anghileri, L. J., Escanye, M. C., y Robert, J. (1986). *Hyperthermia and cytotoxic drugs. Possible use of lanthanum as a potentiator of hyperthermia.* International Journal of Hyperthermia **2**, 83-92.

Markman, M. (2007). *New, expanded, and modified use of approved antineoplastic agents in ovarian cancer.* The Oncologist **12**, 186-190.

May, E., Jenkins, J. R., y May, P. (1991). *Endogenous HeLa p53 proteins are easily detected in HeLa cells transfected with mouse deletion mutant p53 gene.* Oncogene **6**, 1363-1365.

Meresse, P., Dechaux, E., Monneret, C., y Bertounesque, E. (2004). *Etoposide: discovery and medicinal chemistry.* Current Medicinal Chemistry **11**, 2443-2446.

Merlo, L. M. F., Pepper, J. W., Reid, B. J., y Maley, C. C. (2006). *Cancer as an evolutionary and ecological process.* Nature Reviews Cancer **6**, 924-935.

Michalakis, J., Georgatos, S. D., Romanos, J., Koutala, H., Georgoulias, V., Tsiftsis, D., y Thoeodoropoulos, P. A. (2005). *Micromolar taxol, with or without hyperthermia, induces mitotic catastrophe and cell necrosis in HeLa cells.* Cancer Chemotherapy and Pharmacology **56**, 615-622.

Moan, J., y Berg, K. (1991). *The photodegradation of porphyrins in cells can be used to estimate the lifetime of singlet oxygen.* Photochemistry and Photobiology **53**, 549-553.

Mollinedo, F., y Gajate, C. (2003). *Microtubules, microtubule-interfering agents and apoptosis.* Apoptosis **8**, 413-450.

Moor, A. C. E. (2000). *Signaling pathways in cell death and survival after photodynamic therapy.* Journal of Photochemistry and Photobiology, B: Biology **57**, 1-13.

Morgan, J., y Oseroff, A. R. (2001). *Mitochondria-based photodynamic anti-cancer therapy.* Advanced Drug Delivery Reviews **49**, 71-86.

Nicholson, D. W. (2000). *From bench to clinic with apoptosis-based therapeutic agents.* Nature **407**, 810-816.

Nieminen, A. L. (2003). *Apoptosis and necrosis in health and disease: role of mitochondria.* International Review of Citology **224**, 29-55.

Okada, H., y Mak, T. W. (2004). *Pathways of apoptotic and non-apoptotic death in tumour cells.* Nature Reviews Cancer **4**, 592-603.

Oleinick, N. L., y Evans, H. H. (1998). *The photobiology of photodynamic therapy: cellular targets and mechanisms.* Radiation Research **150**, S146-S156.

Oleinick, N. L., Morris, R. L., y Belichenko, I. (2002). *The role of apoptosis in response to photodynamic therapy: what, where, why, and how.* Photochemical and Photobiological Sciences **1**, 1-21.

Otsuki, Y., Li, Z., y Shibata, M. A. (2003). *Apoptotic detection methods - from morphology to gene.* Progress in Histochemistry and Cytochemistry **38**, 275-340.

Perona, R., y Sánchez-Pérez, I. (2004). *Control of oncogenesis and cancer therapy resistance.* British Journal of Cancer **90**, 573-577.

Reiners, J. J., Caruso, J. A., Mathieu, P., Chelladurai, B., Yin, X. M., y Kessel, D. (2002). *Release of cytochrome c and activation of pro-caspase 9 following lysosomal photodamage involves Bid cleavage.* Cell Death and Differentiation **9**, 934-944.

Ricci, M. S., y Zong, W. X. (2006). *Chemotherapeutic approaches for targeting cell death pathways.* The Oncologist **11**, 342-357.

Robertson, J. D., Orrenius, S., y Zhivotovsky, B. (2000). *Review: Nuclear events in apoptosis.* Journal of Structural Biology **129**, 346-358.

Rodal, G. H., Rodal, S. K., Moan, J., y Berg, K. (1998). *Liposome-bound Zn(II)-phthalocyanine. Mechanisms for celular uptake and photosensitization.* Journal of Photochemistry and Photobiology, B: Biology **45**, 150-159.

Rozan, L. M., y El-Deiry, W. S. (2007). *p53 downstream target genes and tumor suppression: a classical view in evolution.* Cell Death and Differentiation **14**, 3-9.

Rupinder, S. K., Gurpreet, A. K., y Manjeet, S. (2007). *Cell suicide and caspases*. Vascular Pharmacology **46**, 383-393.

Schellens, J. H. M., Newell, D. R., y McLeod, H. L. (2005). *Cancer Clinical Pharmacology* (**Oxford**: Oxford University Press).

Scherer, W. F., Syverton, J. T., y Gey, G. O. (1953). *Studies on the propagation in vitro of poliomyelitis viruses IV. Viral multiplication in a stable strain of human malignant epithelial cells (strain HeLa) derived from a epidermoid carcinoma of the cervix.* The Journal of Experimental Medicine **5**, 695-718.

Schimmer, A. D. (2004). *Inhibitor of Apoptosis Proteins: traslating basic knowledge into clinical practice.* Cancer Research **64**, 7183-7190.

Segovia, M., Haramaty, L., Berges, J. A., y Falkowski, P. G. (2003). *Cell death in the unicellular chlorophyte Dunaliella tertiolecta. A hypothesis on the evolution of apoptosis in higher plants and metazoans.* Plant Physiology **132**, 99-105.

Sieber, O. M., Heinimann, K., y Tomlinson, P. M. (2003). *Genomic instability - the engine of tumorigenesis?* Nature Reviews Cancer **3**, 701-708.

Soncin, M. (1999) **Tesis Doctoral:** *Fotosensibilizzazione di melanociti mediante processi fotodinamici e fototermici.*, **Università degli studi di Roma, "La Sapienza"**, Roma.

Soncin, M., Busetti, A., Fusi, F., Jori, G., y Rodgers, M. A. J. (1999). *Irradiation of amelanotic melanoma cells with 532 nm high peak power pulsed laser radiation in the presence of photothermal sensitizer Cu(II)-hematoporphyrin: a new approach to cell photoinactivation*. Photochemistry and Photobiology **69**, 708-712.

Srivastava, M., Ahmad, N., Gupta, S., y Mukhtar, H. (2001). *Involvement of Bcl-2 and Bax in photodynamic therapy-mediated apoptosis.* Journal of Biological Chemistry **276**, 15481-15488.

Stevens, J. B., Liu, G., Bremer, S. W., Ye, K. J., Xu, W., Xu, J., Sun, Y., Wu, G. S., Savasan, S., Krawetz, S. A., Ye, C. J., y Heng, H. H. Q. (2007). *Mitotic cell death by chromosome fragmentation*. Cancer Research **67**, 7686-7694.

Stiewe, T. (2007). *The p53 family in differentiation and tumorigenesis.* Nature Reviews Cancer **7**, 165-168.

Stockert, J. C., Cañete, M., Juarranz, A., Villanueva, A., Horobin, R. W., Borrell, J. I., Teixidó, J., y Nonell, S. (2007). *Porphycenes: facts and prospects in photodynamic therapy of cancer.* Current Medicinal Chemistry **14**, 997-1026.

Stone, R. M. (2007). *Novel therapeutic agents in acute myeloid leukemia.* Experimental Hematology **35**, 163-166.

Sullivan, M., y Morgan, D. O. (2007). *Finishing mitosis, one step at a time*. Nature Reviews Molecular Cell Biology **8**, 894-903.

Triesscheijn, M., Baas, P., Schellens, J. H. M., y Stewart, F. A. (2006). *Photodynamic therapy in oncology.* The Oncologist **11**, 1034-1044.

Tsou, M. F. B., y Stearns, T. (2006). *Controlling centrosome number: licenses and blocks.* Current Opinion in Cell Biology **18**, 74-78.

van Doorn, W. G., y Woltering, E. J. (2005). *Many ways to exit? Cell death categories in plants.* Trends in Plant Science **10**, 117-122.

Varmus, H. (2006). *The new era in cancer research.* Science **312**, 1162-1165.

Villanueva, A., Domínguez, V., Polo, S., Vendrell, V. D., Sanz, C., Cañete, M., Juarranz, A., y Stockert, J. C. (1999). *Photokilling mechanisms induced by zinc(II)-phthalocyanine on cultured tumor cells.* Oncology Research **11**, 447-453.

Villanueva, A., Vidania, R., Stockert, J. C., Cañete, M., y Juarranz, A. (2003). *Photodynamic effects on cultured tumor cells. Cytoskeleton alterations and cell death mechanisms.*, In Handbook of Photochemistry and Photobiology., H. S. Nalwa, ed. (**Los Ángeles**: American Scientific Publishers), pp. 79-117.

Vogel, C., Hager, C., y Bastians, H. (2007). *Mechanisms of mitotic cell death induced by chemotherapy-mediated G2 checkpoint abrogation*. Cancer Research **67**, 339-345.

Vogel, C., Kienitz, A., Müller, R., y Bastians, H. (2005). *The mitotic spindle checkpoint is a critical determinant for topoisomerase-based chemotherapy.* Journal of Biological Chemistry **280**, 4025-4028.

Vousden, K. H., y Lane, D. P. (2007). *p53 in health and disease.* Nature Reviews Molecular Cell Biology **8**, 275-283.

Weaver, B. A. A., Silk, A. D., Montagna, C., Verdier-Pinard, P., y Cleveland, D. W. (2007). *Aneuploidy acts both oncogenically and as a tumor suppressor.* Cancer Cell **11**, 25-36.

Willis, S. N., y Adams, J. M. (2005). *Life in the balance: how BH3-only proteins induce apoptosis.* Current Opinion in Cell Biology **17**, 617-625.

Wood, S. R., Holroyd, J. A., y Brown, S. B. (1997). *The subcellular localization of Zn(II) phthalocyanines and their redistribution on exposure to light.* Photochemistry and Photobiology **65**, 397-402.